Synthesis of Mechanically Interlocked Oligomacrocyclic Systems

Marius Matthias Kroll

Doctor of Philosophy
University of Edinburgh
2010

To my dear Parents. Without you I would not have been able to pursue my passion for science.

Declaration

The scientific work described in this Thesis was carried out in the School of Chemistry at the University of Edinburgh between February 2006 and July 2010. Unless otherwise stated, it is the work of the author and has not been submitted in whole or as part of an application for another degree or qualification at this or any other university or institute of learning.

(*Marius Matthias Kroll*)

Abstract

This thesis presents a modular palladium(II) template-directed synthetic strategy towards mechanically interlocked polymacrocyclic architectures, such as a Borromean link and linear [n]-catenanes. Central to the synthetic strategy is the use of the Huisgen-Meldal-Sharpless Cu(I)-catalysed 1,3-cycloaddition of azides to terminal alkynes (CuAAC) as a ring-closure procedure between complementary pairs of building blocks. The amalgamation of the palladium(II) [3+1]-template and CuAAC reaction is without methodological precedent and represents both an efficient and versatile procedure for the construction of interlocked architectures.

Thematically, this thesis consists of three parts arranged in chronological order. Beginning with the synthesis towards a Borromean link, where the first successful palladium(II) template-directed double CuAAC ring-closure is documented. This is followed by the application of the "double-click" strategy to form a [3]catenane - the first such structure generated using metal ions other than Cu(I). Finally, the development of a modular CuAAC building block library is described, which was used to construct a [2]catenane and [3]catenane as well as later developments towards higher oligocatenanes .

Contents

Acknowledgments

First and foremost, I must thank my supervisor professor David Leigh for giving me the opportunity to explore my passion for science in such a nourishing environment. I also have to thank Paul Lusby for the valuable advice he gave me at the beginning of my endeavours in the field of template directed synthesis.

I also want to express my gratitude to the university staff, who are doing a great job in supplying the science crowd with everything they need. Especially the girls from upstairs, namely Annette and Amanda. Furthermore, I'd like to thank the glassblower who made fabulous pieces of art so I could satisfy my needs for exotic glassware, the boys from the mechanical workshop who responded a bit quicker then usual, Alan Taylor who entrusted me with the key to the inner sanctum, Juraj Bella for helping out with NMR troubles and John Millar who was always both friendly and helpful.

However, a chemist never walks alone... So I want to thank the brave soldiers that have accompanied me on the way (in alphabetical order): Monica Alvaraz Perez, Vincent Aucagne, Jonathon Beves, Barry Blight, Mike Barrell, José Berná-Cánovas, Armando Carlone, James Crowley, Romen Carrillo, Max von und zu Delius, Raul Garcia Rodriguez, Edzard Geertseema, Paul McGonigal, Philipp Gramlich, Kevin Hänni, David Howgego, Bartosz Lewandowski, Urszula Lewandowska, Tao Long, Christiane Petzold, Vicki Ronaldson, David Schultz, Mark Deee Symes, Takeshi Umehara, Aurelien Viterisi.

And last but not least, I want to express my deepest gratitude to my parents. Without you this would not have been possible. The support I received from you cannot be measured in any scale and is priceless. I owe you.

List of Abbreviations

δ	Chemical shift
μL	Microlitre(s)
Å	Angstrom
BPU	Pyridine-2,6-dicarboxylic acid bis-(4-hydroxy-benzylamide)
$CDCl_3$	Deuterochloroform
dec	Decomposed
DIAD	Diisopropylazodicarboxylate
DIPEA	Diisopropylethylamine
DMF	N,N'-dimethylformamide
EDTA	Ethylenediamine tetraacetic acid
Et	Ethyl
Et_2O	Diethyl ether
EtOAc	Ethyl acetate
FAB	Fast Atom Bombardment
g	Gram(s)
h	Hour(s)
HRMS	High Resolution Mass Spectrometry
HV	High Vacuum
J	Coupling constant
L	Litre
LRMS	Low Resolution Mass Spectrometry
Me	Methyl
MeOH	Methanol
MHz	Mega hertz
min	Minute(s)
mL	Millilitre(s)
mmol	Millimole(s)
m/z	Mass-to-charge ratio
N_2	Nitrogen

n-BuLi	n-Butyl lithium
NBSH	2-Nitrobenzenesulfonylhydrazide
NEt_3	Triethylamine
NMR	Nuclear Magnetic Resonance
NMP	N-Methylpyrrolidone
PCy_3	Tricyclohexylphosphine
PEPPSI	(1,3-Diisopropylimidazol-2-ylidene)(3-chloropyridyl) palladium(II) dichloride
PPh_3	Triphenylphosphine
ppm	Part per million
RCM	Ring Closing Metathesis
RT	Room Temperature
THF	Tetrahydrofuran
TiPS	Triisopropylsilyl
TiPSCl	Chlorotriisopropylsilane
TLC	Thin Layer Chromatography
TM	Transition Metal
TMS	Trimethylsilyl
TMSCl	Chlorotrimethylsilane
TPS	Tripropylsilyl
TPSCl	Chlorotripropylsilane
TBTA	Tris[(1-benzyl-1H-1,2,3-triazol-4-yl)methyl] amine
TsCl	p-Toluenesulfonyl chloride
TsOH	p-Toluenesulfonic acid

General Remarks on Experimental Data

Unless otherwise stated, all reagents and solvents were purchased from Aldrich Chemicals and used without further purification. Tetrahydrofuran, dichloromethane, chloroform, toluene, acetonitrile and *N,N'*-dimethylformamid were dried using a solvent purification system PureSolv manufactured by Innovative Technology Inc. ESI and EI mass spectrometry was performed either by the departmental mass spectrometry service of the University of Edinburgh or the EPSRC National Mass Spectrometry Service, Swansea. HPLC analysis was performed on Agilent Technologies Series 1200 with diode array detector and LC-MS was carried out on Agilent Technologies Series 1200 with single wavelength UV-detector coupled with a single quadrupol mass spectrometer Series 6130. Column chromatography was carried out using DAVISIL 60Å (purchased from Fisher) as stationary phase, and TLC was performed on silica gel coated aluminium plates (0.25 mm thick, $60F_{254}$, Merck Germany) and observed under UV light or stained with $KMNO_4$ (0.5% in water). ^{1}H-NMR and ^{13}C-NMR spectra were recorded on a Bruker AV 400 or AV 500 instrument at a constant temperature of 300 K (AV 400) or 298 K (AV 500). Chemical shifts are reported in parts per million from low to high field and referenced to TMS. Coupling constants (J) are reported in Hertz (Hz). Standard abbreviations indicating multiplicity were used as follows: s = singlet, d = doublet, t = triplet, q = quartet, p = pentet, m = multiplet.

Chapter 1

Introduction

Synopsis

Within the last 25 years, TM template-directed synthesis of mechanically interlocked structures flourished and brought about some of the most intriguing examples of molecular art. Knots and links and the synthesis thereof are from the intellectual as well as the aesthetical viewpoint a worthwhile occupancy that bears challenges on a multitude of different levels. In this chapter, the general concept of knots and links is introduced and brought together in the context of prominent examples with emphasis on copper(I) and palladium(II) template directed synthesis.

1.1 Knots and Links

Knots and links are integral constituents of our every day life. They are used in mechanical, naval, cultural or social context. For example the tie, which is a pseudo-knot, can be tied in 85 different ways.[1] Carl Friedrich Gauss studied knots and was probably the first who tried to conquer this field of topology using mathematics. During the evolution of the knot theory, Peter Guthrie Tait, a Scottish scientist, developed tables of knots and what is known as Tait conjectures on alternating knots.[2]

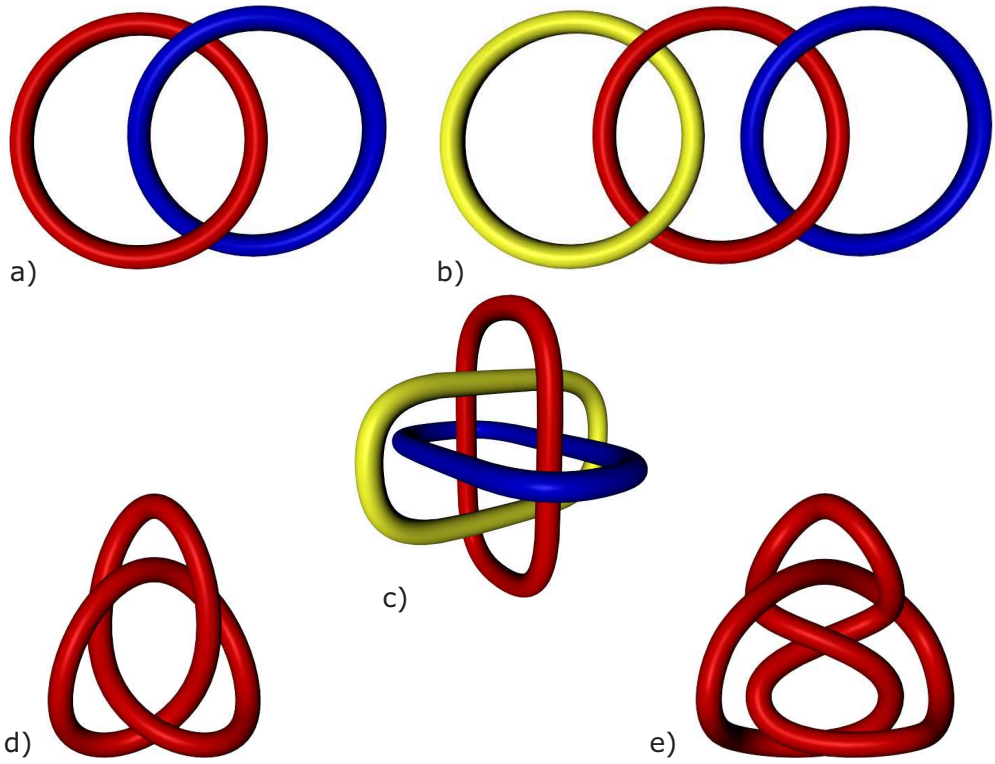

Figure 1.1. Selection of links and knots: a) Hopf link, b) Chain link, c) Borromean link, d) Trefoil knot, e) Figure-of-eight knot.

Tait defined a knot to be a simple closed curve in 3D-space.[3] To be considered a knot, the curve must have at least three crossover points, which prohibit it from being transformed into a planar ring shape, as can be seen in the example of the trefoil knot (simplest representative of a knot). A trivial knot (a simple closed curve which can be deformed into a planar ring) is called an unknot. A link is, *per definitionem*, two or more disjointed curves in 3D-space.[3] The Hopf link, or in chemistry terms a [2]catenane, is simply a interlocked combination of two

unknots or simple closed curves (rings), which cannot be deformed to a planar arrangement due to the two crossover points, which cannot be displayed in a 2-dimensional representation. A trivial link (a collection of simple closed curves which can be transformed into a plane) is called an unlink. To find out if two knots or links are topological equivalent, it has to be shown that one can be deformed to the other, where the definition of a knot or link does not permit the curve to pass through itself.

1.2 Transition Metal Templates in the Synthesis of Molecular Interlocked Architectures

In the 1960s Curtis and co-workers reported the first templated synthesis of a macrocycle.[4] Soon it became apparent, that this methodology could be used to generate complex structures. The potential of this methodology was shown by Sauvage and co-workers, with the first transition metal (TM) templated synthesis of a catenane.[5]

1.2.1 Definition

According to Busch's definition, a chemical template organises an assembly of atoms with respect to one or more geometric loci in order to achieve a particular linking.[6] With many different forms of templates, it became necessary to classify them; therefore Sanders introduced a classification system which consists of three main classes of template:[7]

- A Cyclisation template in which the two reactive ends of the substrate are brought close together, so that the formation of the cyclic compound is preferred over polymerisation.
- A Linear template is used as a template for the synthesis of the complementary linear substrate (e.g. DNA).
- An Interweaving template forces the components to be aligned perpendicularly (interwoven), while carrying out an intra-component or intermolecular reaction (e.g. catenation).

The majority of TM template systems that are used to synthesise mechanically interlocked architectures, are interweaving templates. Despite the incredible number of templates that have emerged in the last 20 years, only the most prominent TM templates which are relevant to the thesis will be discussed here.

1.2.2 Terminology

'*In any chemical template, an anchor constitutes the first component (a metal ion, ion pair complement, partial charge complement, or hydrogen bonded partner); this anchor holds an appropriate conjugate component, or components.*'[8]

In TM templates, the metal ion or anchor defines the arrangement of the template constituents through its preferred coordination geometry. Many different metals have been utilised in TM template directed synthesis, but only a few possible metal-ligand coordination geometries have been used to construct mechanically interlocked structures (Figure 1.2).

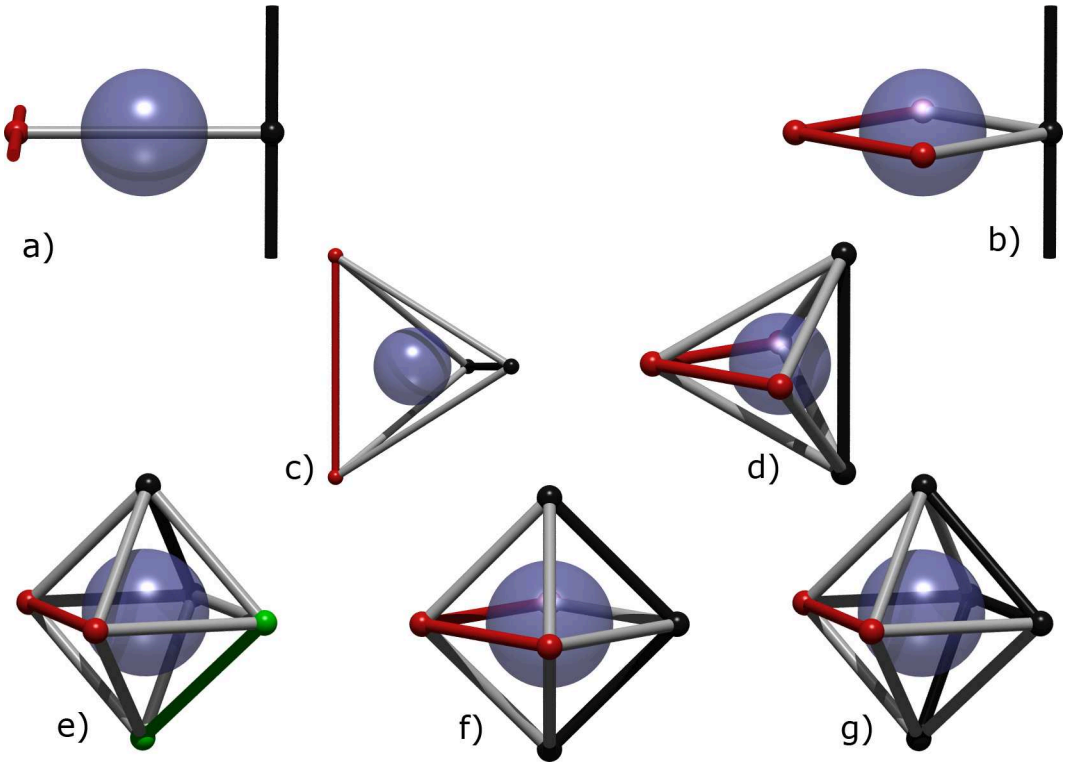

Figure 1.2. Possible template arrangements around a central metal: a) linear template; b) square planar; c) tetrahedral; d) trigonal bipyramidal; e) [2+2+2] octahedral; f) [3+3] octahedral; g) [2+4] octahedral.

Although the anchor plays a major role in the assembly of the TM template, the role of the ligands is as important. The ligands, being part of the backbone of the chemical structures that shall be interlocked, play the role of twisting or threading the backbone structure it is attached to through cavities or around preexisting parts of the complementary backbone structure. To achieve that, the twist or turn is intrinsically incorporated into the ligand structure, as can be seen

in Figure 1.3. Ligands which encircle the anchor are called convergent turns; if they bind to the anchor at an exo-position they are called divergent turns. The opening angle can be given to specify the geometrical properties of the turn (e.g. a 90° turn.)

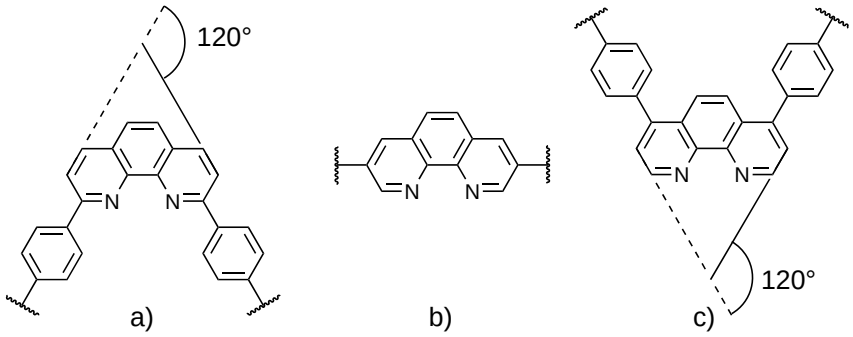

Figure 1.3. A selection of turns: a) 120° convergent turn; b) linear thread; c) 120° divergent turn.

1.3 The Sauvage System

Since his first publication of a catenane synthesis using a transition metal template,[5] Sauvage pursued the possibilities that this particular motif offers and synthesised numerous compounds in the form of knots and links. The main components of this template system are the copper(I) anchor, which delivers a well defined tetrahedral coordination geometry, and the bidentate 1,10-phenantroline derivatives, which represent convergent turns, thus encapsulating the metal when a complex is formed. This system has been extensively used and, since its discovery, the amount of successful metal template systems increased, giving modern supramolecular chemists a versatile toolbox to choose from.

1.3.1 [2]Catenanes

The original strategy (Scheme 1.1, Route B) introduced by the Sauvage group comprised the use of the tetrahedral coordination sphere of Cu(I), which orthogonally arranged a phenantroline macrocycle **3** and bisphenol-containing phenantroline ligand **1** perpendicularly around the TM anchor.[5,9] Subsequent reaction of the bisphenol complex **2** with 1,14-diiodo-3,6,9,12-tetraoxatetradecane in DMF at high dilution afforded the catenate **5** in 42% yield. One year later Sauvage and co-workers successfully employed Route A to generate catenane **5** and the non-interlocked macrocycle **3** in 27% and 20% yield, respectively.

The afore mentioned [2]catenand **6** is topologically achiral and can be described as a Hopf link. Upon the introduction of one phenyl substituent to the backbone of the phenantroline ligand, Sauvage and co-workers were able to obtain a topological chiral [2]catenate **7** (Figure 1.4) (Topologial chirality is defined as the inability to continually deform a graph into its mirror image)[10] .[11] The catenate **7** can therefore be described as topologically chiral Hopf link.

All of the previous approaches relied on a double Williamson ether forming reaction with the bis-iodo-oligo-ethylene-glycol counterpart and by-product formation could not be suppressed effectively. Applying ring closing metathesis (RCM), in place of the Williamson ether formation as the cyclisation step, tremendously improved the yield as the reaction could be conducted at room

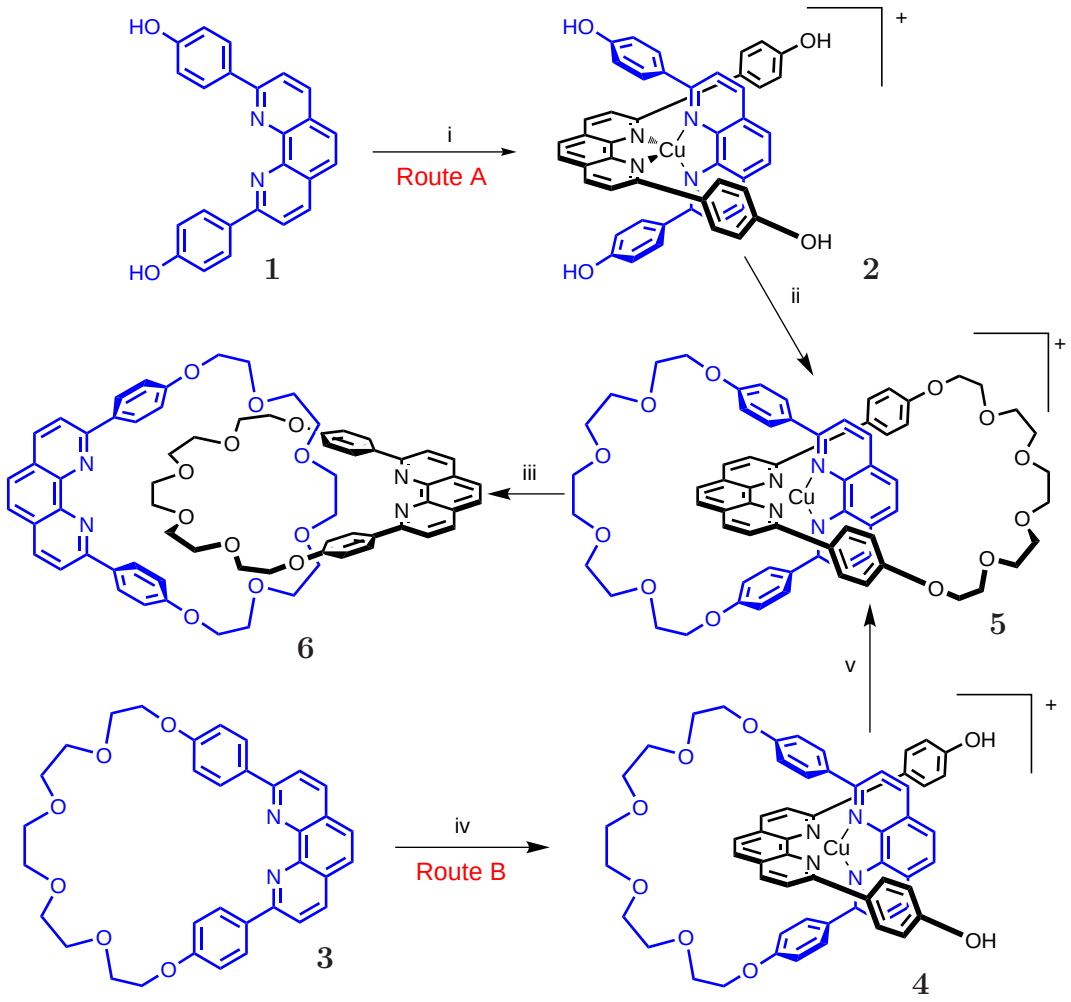

Scheme 1.1. Sauvage's original Cu(I) templated [2]catenane synthesis. Reagents and conditions: i, iv) $[Cu(MeCN)_4]PF_6$; ii, v) Cs_2CO_3, $ICH_2CH_2(OCH_2CH_2)_4I$; iii) Me_4NCN.

temperature in a non-coordinating solvent with a high yielding intramolecular reaction (Scheme 1.2).[12,13]

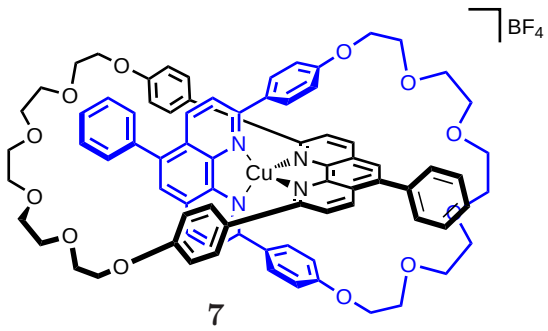

Figure 1.4. A topologically chiral [2]catenate.

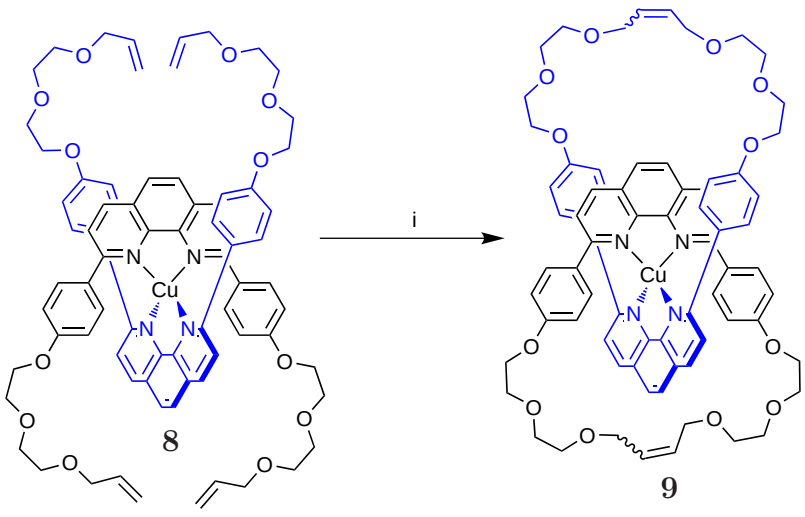

Scheme 1.2. Synthesis of a [2]catenate using RCM. Reagents and conditions: i) Grubbs' $1^{st.}$ generation catalyst, CH_2Cl_2, c = 0.01 M, 92%.

1.3.2 Synthesis of a Trefoil Knot

Inspired by the early attempts of Schill,[14] Sauvage announced the successful synthesis of the first molecular trefoil knot in 1989.[15] The structure with its intertwined topology was irrefutably confirmed by X-ray crystallography one year later.[16]

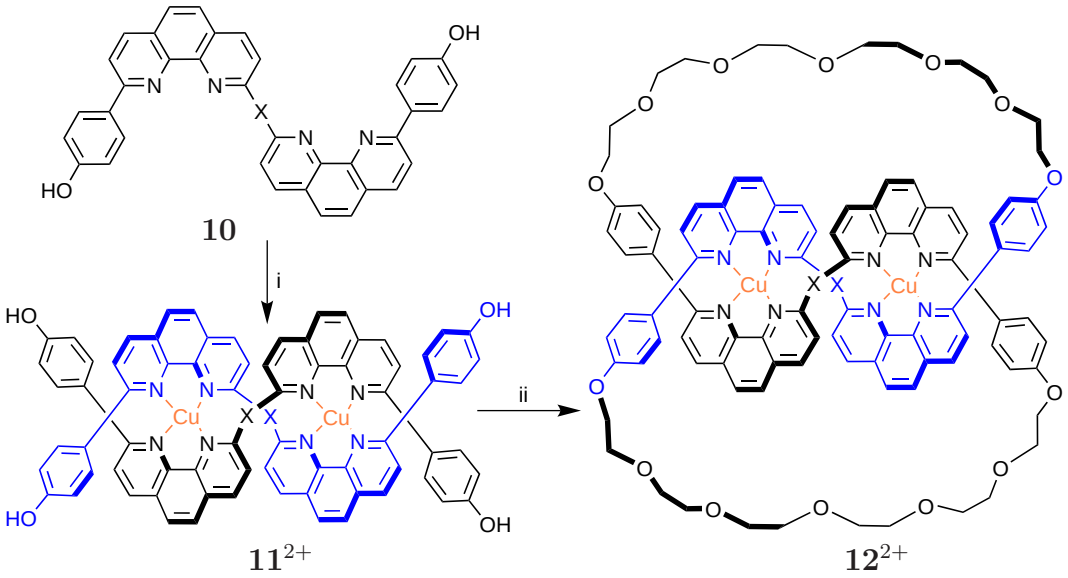

Scheme 1.3. Synthesis of a trefoil knot. Reagents and conditions: i) $[Cu(MeCN)_4]^+$; ii) Cs_2CO_3, $IEt(OEt)_4I$, **12a** = 3%, **12b** = 29%.

Sauvage's trefoil knot was initially synthesised using the n-butyl linked bisphenantroline ligand **10a** (Scheme 1.3). This short linker should keep the two phenantroline units away from each other, allowing them to adopt a helical structure and prevent the formation of an intramolecular complex. Complex $\mathbf{11a}^{2+}$ did not efficiently prevent the formation of the intramolecular complex and therefore led to a poor yield of 3% for the cyclisation step. Replacing the n-butyl linker by a 1,3-phenylene, increased the yield to 29%.[17] Utilising RCM as cyclisation step further increased the yield to 74%.[18] Furthermore, Sauvage and co-workers were able to replace one copper(I) ion from the homodimetallic trefoil knot $\mathbf{12b}^{2+}$ with a silver(I) ion, creating the heterodimetallic trefoil knot $\mathbf{14}^{2+}$ (Scheme 1.4).[19]

In contrast to links, knots are intrinsically chiral molecules. The trefoil as the simplest knot possesses this property and has two topological enantiomers. The original synthesis of the knots afforded a topological racemic mixture, for

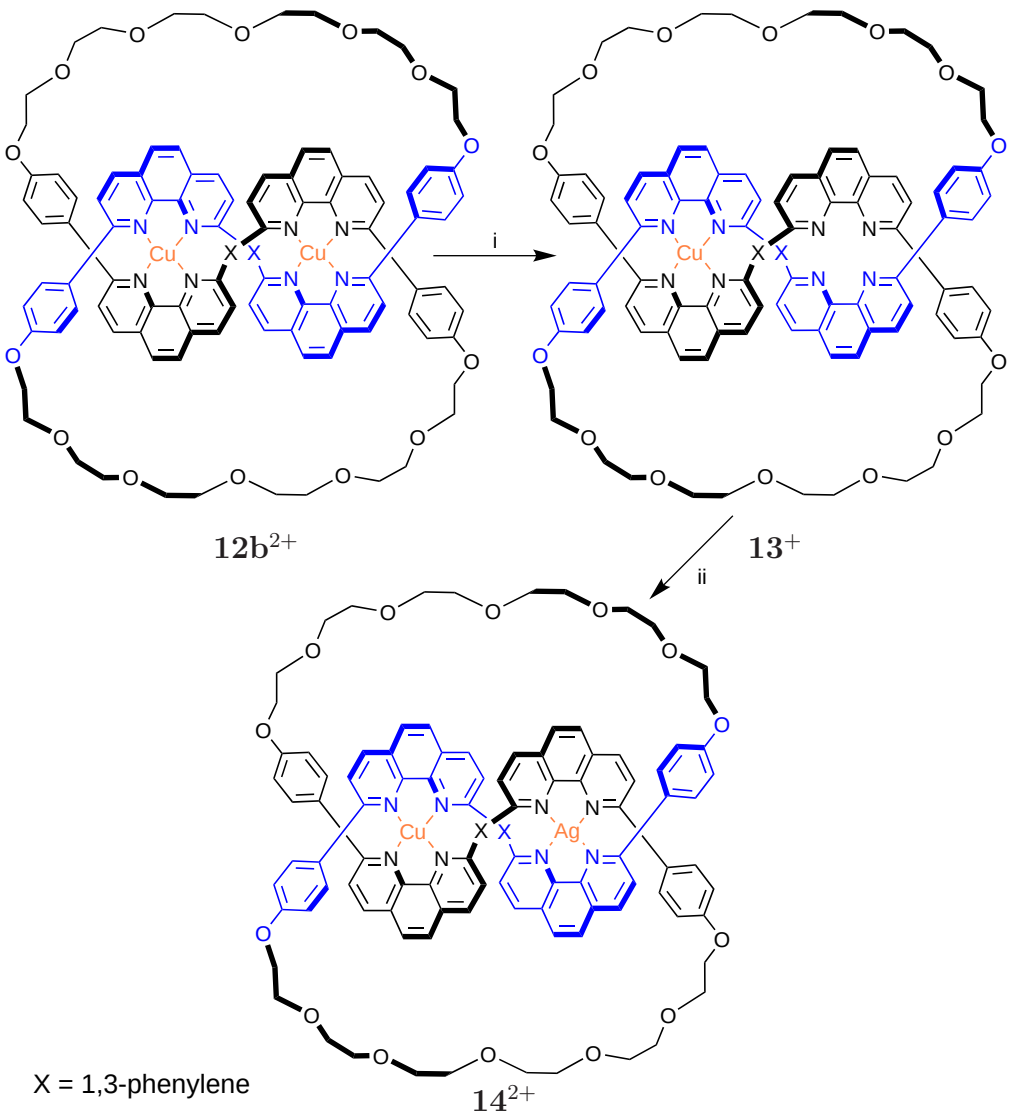

Scheme 1.4. Mono-demetalation of a trefoil knot followed by generation of a heterodimetalic complex. Reagents and conditions: i) KCN; ii) AgBF4.

which separation methods were subsequently developed.[20] Furthermore, in 2004 Sauvage and co-workers announced the stereoselective synthesis of a trefoil knot, which they achieved by using chiral bipyridine ligands to induce chirality on a topologial level.[21]

1.3.3 Rotaxanes

In 1991, Gibson reported the first rotaxane synthesis using the TM template system introduced by Sauvage (Scheme 1.5).[22] The rotaxane **16** was produced by reacting the copper ring-and-thread complex $\mathbf{15}^{+}$ with a bulky iodo compound (stopper). The stopper prevents dethreading after subsequent demetallation.

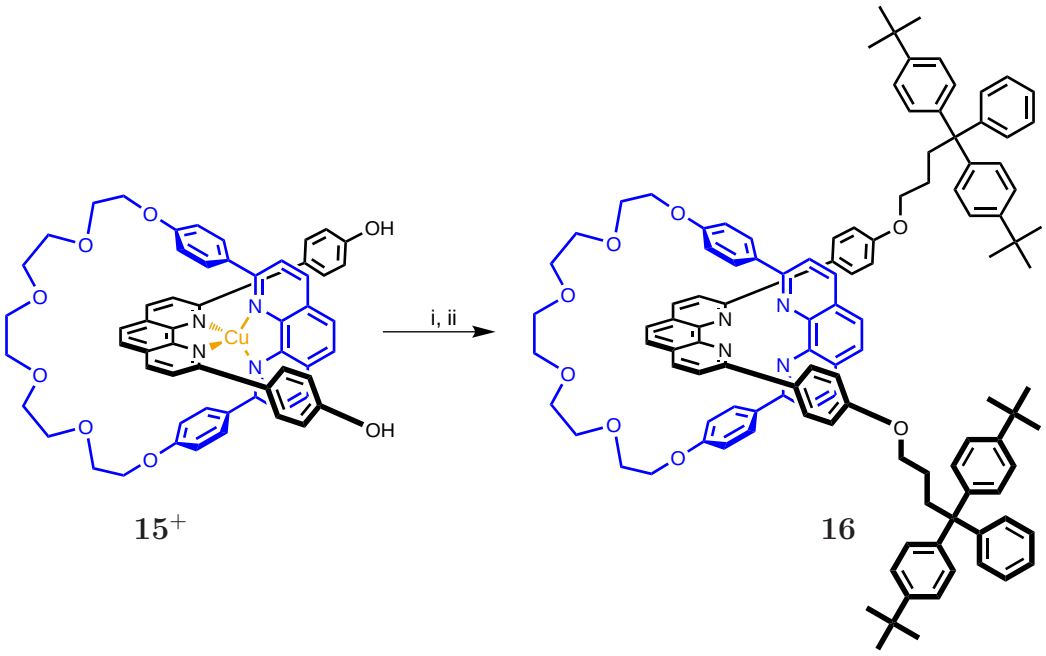

$\mathbf{15}^{+}$ **16**

Scheme 1.5. Gibson's Cu(I)-phenantroline based rotaxane synthesis. Reagents and conditions: i) $I(CH_2)_3CAr_3$, K_2CO_3, DMF / MeCN; ii) Amberlite-CN, 48%.

1.3.4 Redox Active Molecular Machine Prototypes

Controlling molecular motion of mechanically interlocked molecules has always been a major objective of supramolecular chemists. With the introduction of Sauvage's switchable catenate, whose motion is controlled by a reversible redox process, a bistable switching system was established (Scheme 1.6).[23]

In this switchable catenate the copper(I) anchor prefers the tetrahedral coordination geometry, which is saturated by the two orthogonally arranged phenantroline ligands. Upon oxidation of the copper(I) to copper(II) the geometric preference of the copper changes from tetrahedral to trigonal bipyramidal. Consequently, the system relaxes to its stable co-conformation $\mathbf{18}^{2+}$, where the terpyridine ligand occupies the equatorial and the phenantroline ligand the axial

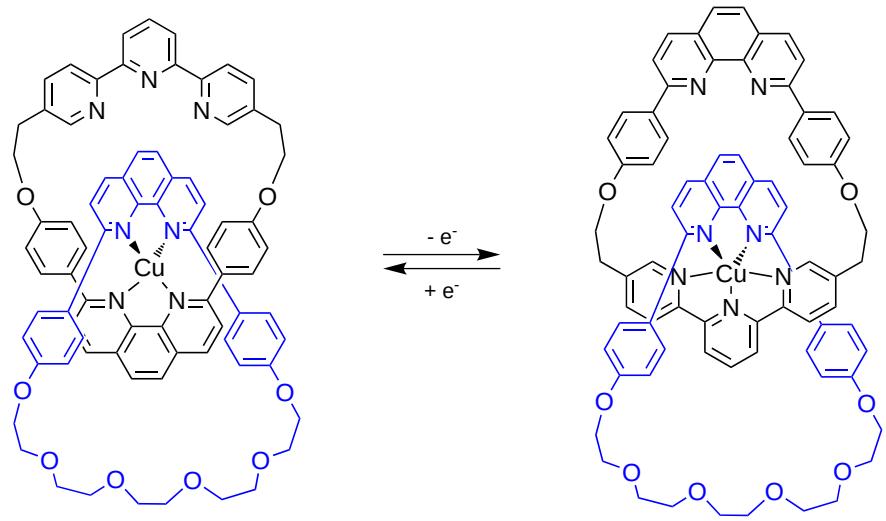

$\mathbf{17}^{+}$ $\mathbf{18}^{2+}$

Scheme 1.6. Sauvage's original redox switchable [2]catenate.

positions. Reduction of the copper(II) anchor resets the system to its initial state. This system has also been successfully applied to rotaxanes (Figure 1.5).[24]

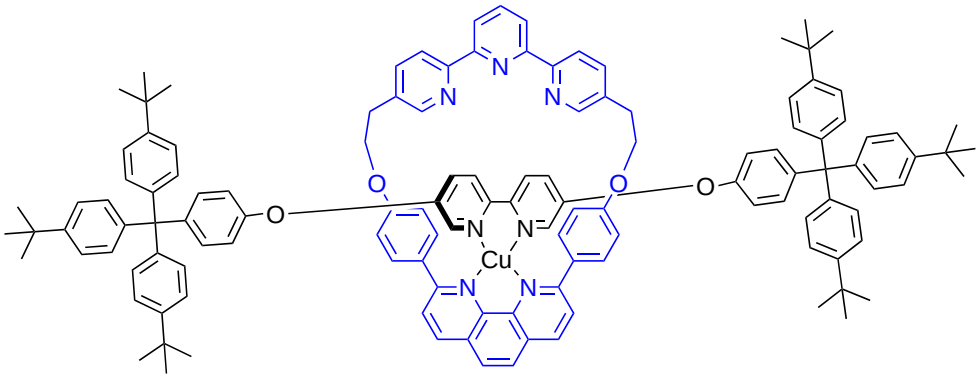

$\mathbf{19}^{+}$

Figure 1.5. A redox controlled [2]rotaxane where addition/removal of 1 e^{-} induces a co-conformational change.

The first artificial molecular muscle represented one of the most impressive TM-directed synthetic achievements at that time.[25] This particular system is controlled by a metal-exchange reaction, which contracts or expands the artificial muscle (Scheme 1.7). When two copper(I) ions are coordinated, they form the homoleptic, dimetallic bisphenantroline complex, thus giving the expanded state $\mathbf{20}^{2+}$. Upon demetallation and insertion of two zinc(II) anchors, the heteroleptic terpyridine phenantroline complex is formed; zinc prefers a trigonal bipyramidal

coordination and therefore the system adopts the contracted state $\mathbf{21}^{4+}$. The process can be reversed by extraction of the zinc(II) anchors and reinsertion of two copper(I) anchors.

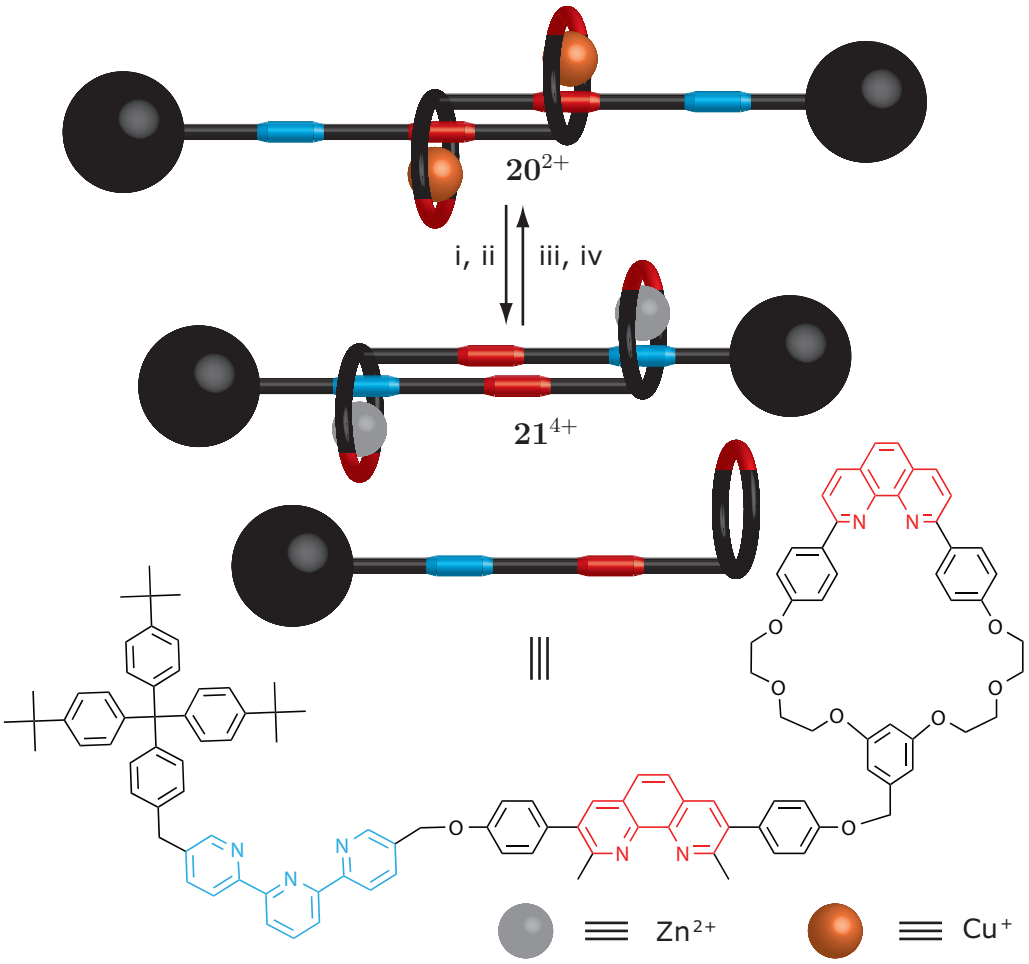

Scheme 1.7. Schematic representation of the operation of Sauvage's artificial muscle. Reagents and conditions: i) KCN; ii) $Zn(NO_3)_2$; iii) KCN; iv) $[Cu(MeCN)_4]BF_4$.

1.4 6-Coordinate TM Template Systems

1.4.1 Rhodium and Ruthenium Templated Synthesis of Interlocked Molecules

The first catenate synthesis, using an octahedral coordination geometry TM anchor was reported in 1991.[26] This was achieved by employing a Ru(II) complex formed with two terpyridine derivatives and subsequent cyclisation. Changing the metal anchor to Fe(II) and applying RCM as the cyclisation step afforded an figure-of-eight complex, but not the desired catenane.[27] This finally led to the [4+2] approach, where two linked phenantroline units act as κ^4-ligand, whereas the bipyridine counterpart establishes the cross over point (Scheme 1.8).[28] The latter system has been successfully exercised to afford Ru(II)[29,30] and Rh(II)[31]] containing catenates. Taking advantage of the well established photochemistry of

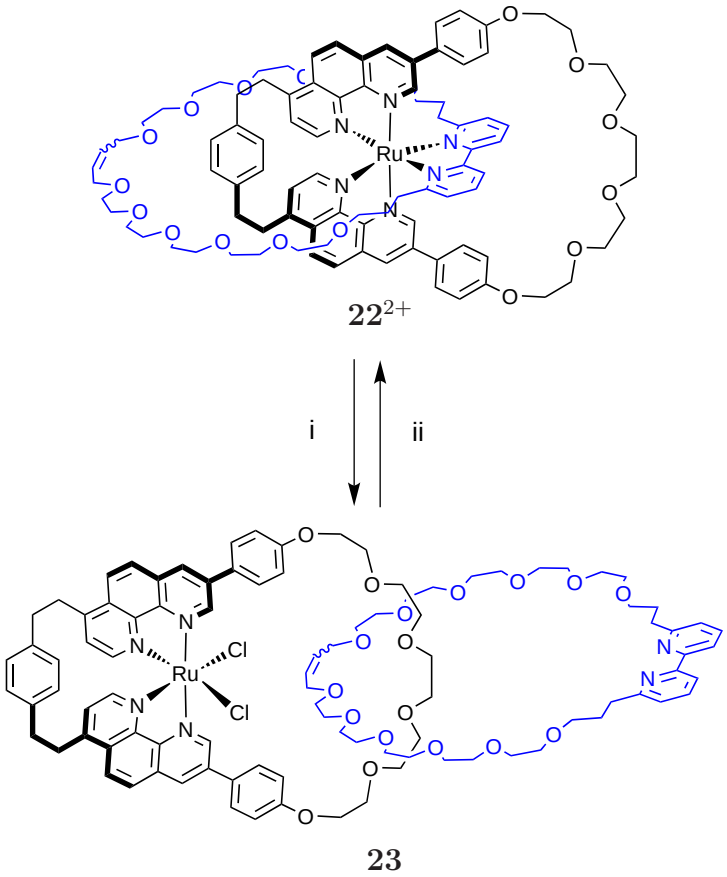

22^{2+}

23

Scheme 1.8. Sauvage's light switchable Ru(II) [2]catenate and its operation. Reagents and conditions: i) Et_4Cl, hν (470 nm); ii) ΔT.

Ru(II), Sauvage and co-workers were able to show that photoinduced labilisation of the bipyridine ligand can be achieved when a Ru(II) containing catenate is irradiated in presence of Cl^- anions. The bidentate ligand can then be displaced by two Cl^- anions inducing a revolving motion of 180° **23**. The process can be reversed by heating, so that the thermodynamically stable $\kappa^4\kappa^2$-complex is formed again **22**.

1.4.2 A Simple General Ligand System for the Assembly of Catenates and Rotaxanes

In 2001, Leigh and co-workers published a template system for the synthesis of catenanes around a range of divalent TM ions (Scheme 1.9).[32] The 2,6-bisimino pyridine motif **24** the used, ensures a 180° convergent turn that also aligns the benzyl substituents parallel to each other, so that π-stacking with an orthogonally bound guest can occur **25**. This arrangement strongly favours intracomponent RCM cyclisation of the terminal olefins **26**.

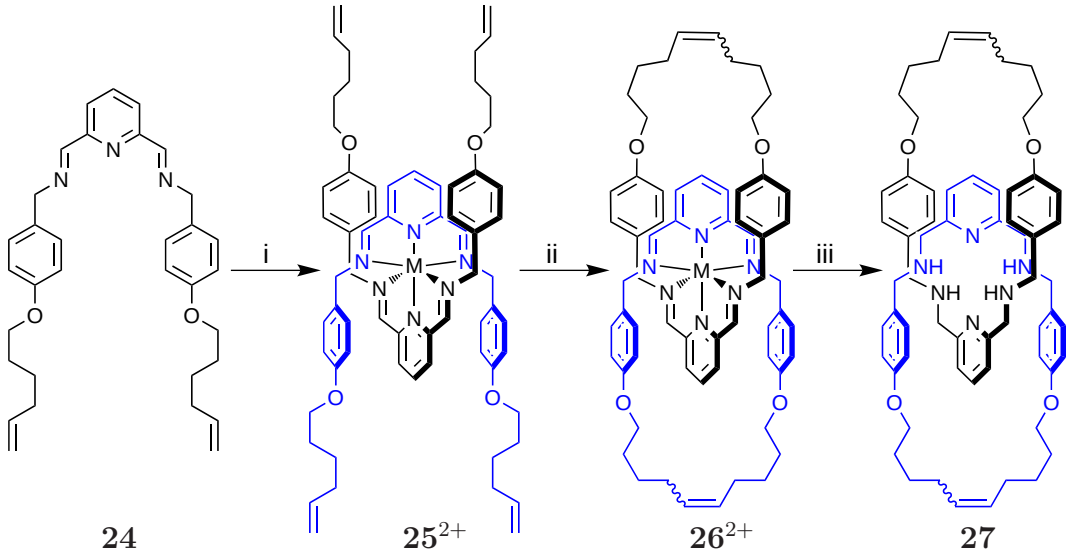

24 **25**$^{2+}$ **26**$^{2+}$ **27**

Scheme 1.9. Synthesis of [2]catenates around a range of divalent TM ions. Reagents and conditions: i) M^{2+}, ii) Grubbs' ^{1st} generation catalyst; yields: $Mn(ClO_4)_2$: 63%; $FeBr_2$: 75%; $Co(ClO_4)_2$: 36%; $Co(BPh_4)_2$: 41%; $Ni(ClO_4)_2$: 32%; CuI_2: 61%; $Zn(ClO_4)_2$: 73%; $Zn(BPh_4)_2$: 81%; $Cd(ClO_4)_2$: 70%; $Hg(ClO_4)_2$: 5%; iii) a) $NaBH_4$; b) Na_2EDTA.

The synthesis of catenane **27** started from the free Schiff-base ligand **24**, which was coordinated to a metal anchor, giving the homoleptic complex $\mathbf{25}^{2+}$. RCM of $\mathbf{25}^{2+}$ with Grubbs' $1^{st.}$ generation catalyst afforded the desired catenate $\mathbf{26}^{2+}$ in modest to good yields. Upon treatment of the catenate with $NaBH_4$ the imines were converted into sec. amines, that allowed the extraction of the metal ion with EDTA to afford catenane **27**. The synthesis a rotaxane employing

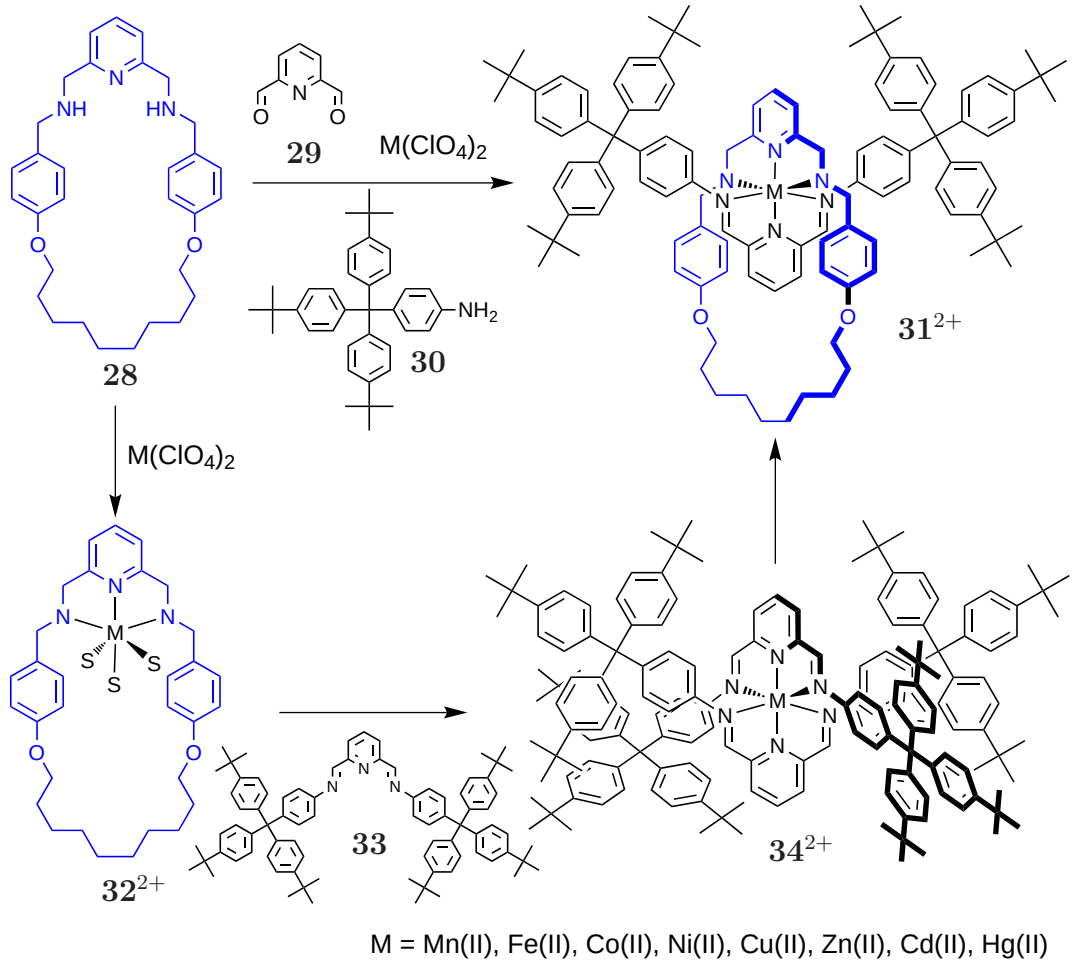

Scheme 1.10. Synthesis of [2]rotaxanes by metal templation under thermodynamic control. Reagents and conditions: **28**, **29**, **30**, $M(ClO_4)_2$, CH_2Cl_2/MeCN (2:5), RT (Fe 50 °C), 24 h (Fe; 2 weeks), Mn: 83%, Fe: 57%, Co: 99%, Ni: 94%, Cu: 87%, Zn: 92%, Cd: 73%, Hg: 79%.

the afore mentioned methodology, required the use of the preformed bisamine macrocycle **28** (Scheme 1.10). This eliminates the possibility of the formation of crossover products that might be encountered as a consequence of the reversible nature of the imine formation. The preformed amine macrocycle **28**, pyridine 2,6-dialdehyde **29**, metal salt and amine bearing stopper **30** were reacted to give the

desired rotaxane $\mathbf{31}^{2+}$ under thermodynamic control. To prove that the rotaxane is the thermodynamic product, a control experiment using the pre-complexed macrocycle $\mathbf{32}^{2+}$ and preformed thread **33** was carried out. At first, the *bis*-thread complex $\mathbf{34}^{2+}$ was formed, which reacted to the rotaxane $\mathbf{31}^{2+}$ within 24 hours.[33]

1.4.3 Cobalt Directed Synthesis of Catenanes and Rotaxanes

Deprotonated amide (carboxamido) ligands can bind to 'hard' TM ions like Fe(III) and Co(III).[34–40] This feature was successfully exploited by Leigh and co-workers, who were able to obtain a figure-of-eight complex, [2]catenane and rotaxane utilising a bis-carboxamide pyridine ligand set to generate the necessary crossover geometries.[41] The initial attempt to synthesise a catenane started from the biscarboxamide pyridine ligand **35**, which was deprotonated with NaH and treated with a cobalt(II) salt without excluding air and afforded the homoleptic cobalt(III) complex **36**$^-$. Subsequent double RCM of two macrocycle precursors that were aligned in an orthogonal manner (Scheme 1.11) led to the figure-of-eight complex **37**$^-$, which was hydrogenated leading to compound **38**$^-$. In order

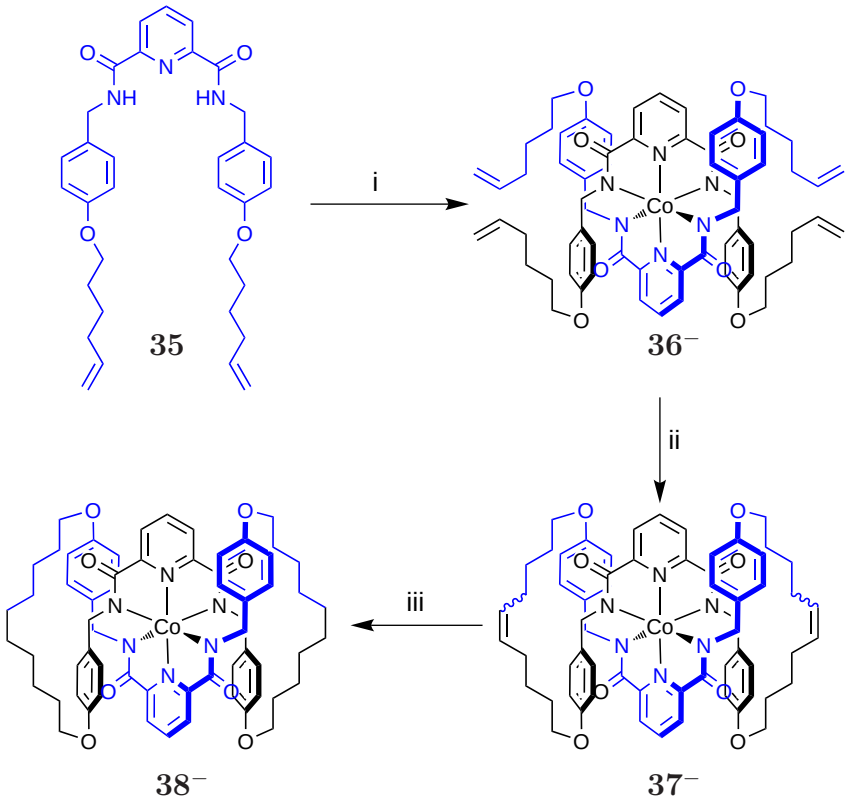

Scheme 1.11. Cobalt^{3+} template directed synthesis of a figure-of-eight shaped complex. Reagents and conditions: i) $Co(OAc)_2$, NaH, Et_4NOAc, air, MeOH, 91%; ii) Grubbs' 1$^{st.}$ generation catalyst, CH_2Cl_2, 80%; iii) H_2, Pd/C, THF, 85%.

to obtain [2]catenate **42**$^-$, an alternative strategy was chosen (Scheme 1.12). To exclude intercomponent cyclisation, a preformed macrocycle was deprotonated and metallated prior to complex-formation with ligand **35**. RCM of the macro-

cycle bis-alkene complex led to catenate $\mathbf{41}^-$, which was hydrogenated to afford the catenate $\mathbf{42}^-$. The catenand **43** was obtained upon reductive demetallation of $\mathbf{42}^-$ with zinc and acetic acid.

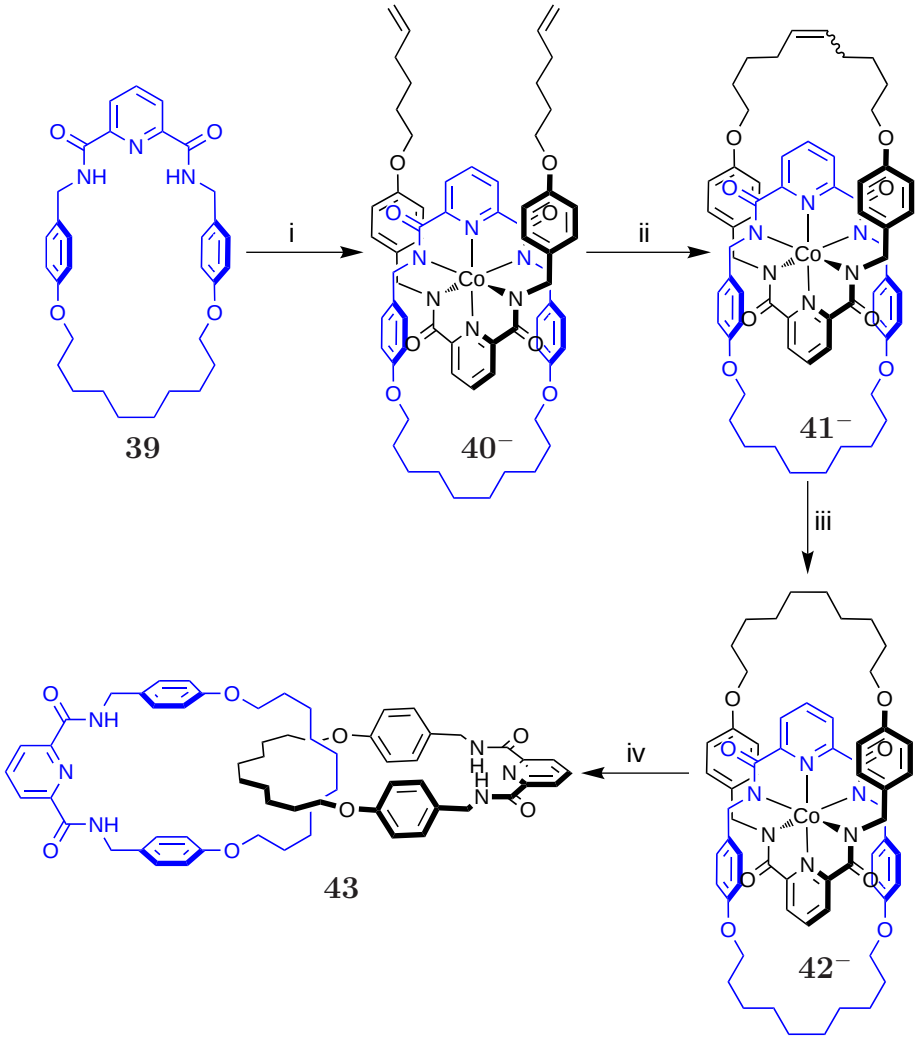

Scheme 1.12. Cobalt(III) template directed synthesis of a [2]catenane. Reagents and conditions: i) $Co(OAc)_2$, NaH, **35**, Et_4NOAc, air, MeOH, 87%; ii) Grubbs' $1^{st.}$ generation catalyst, CH_2Cl_2, 66%; iii) H_2, Pd/C, THF; iv) Zn, HOAc, MeOH, 64% (over 2 steps).

1.5 Square Planar Metal Template Motif

1.5.1 Palladium(II) Template Directed Synthesis of a [2]Rotaxane

The first synthesis of a rotaxane using a square planar metal template system was reported by Leigh and co-workers in 2004.[42] The design, based on the palladium chemistry developed by Hirao,[43] consists of a 2,6-di(benzylamid)pyridine moiety **35** (tridentate ligand) and either a 2,6- or 3,5- disubstituted pyridine counterpart **45** (monodentate ligand) (Scheme 1.13). In either case, the heteroleptic complex formed constitutes a crossover point, where the monodentate ligand is aligned orthogonally to the plane, which is defined by the three nitrogen atoms of the tridentate ligand. This is the consequence of the two benzyl groups attached to the amide function, which are able to flank the electron deficient pyridine monodentate ligand, thus establishing π-stacking and granting the orthogonal arrangement. The π-stacking can be observed in the ^{1}H-NMR spectra, where the two doublets of the benzylic positions shift significantly, indicating a strong interaction.

The synthesis of rotaxane **48a** commenced by reacting tridentate ligand **35** with $Pd(OAc)_2$ in acetonitrile. This generated complex, where the labile acetonitrile ligand can be exchanged with a suitable monodentate ligand, namely **37a-d**. This was followed by a RCM reaction, which generated the macrocyclic tridentate ligand and consequently [2]rotaxane **48a**.

The X-ray structure of **48a** (Figure 1.6) confirms the interlocked architecture and the pseudo-square planar geometry of the palladium, with a tridentate ligand bite angle of 160°. Although the π-stacking between macrocycle and pyridine of the thread is apparent in solution, the ^{1}H-NMR signals of the phenyl rings shift significantly, it is not present in the solid state structure; the phenyl rings are twisted out of the plane, defined by the four nitrogen atoms. This may also be the reason why RCM of 3,5-disubstituted thread complexes can lead to non interlocked products; with the conformation adopted by the macrocycle and thread, cyclisation of **46b/d** can readily occur without encircling. Furthermore,

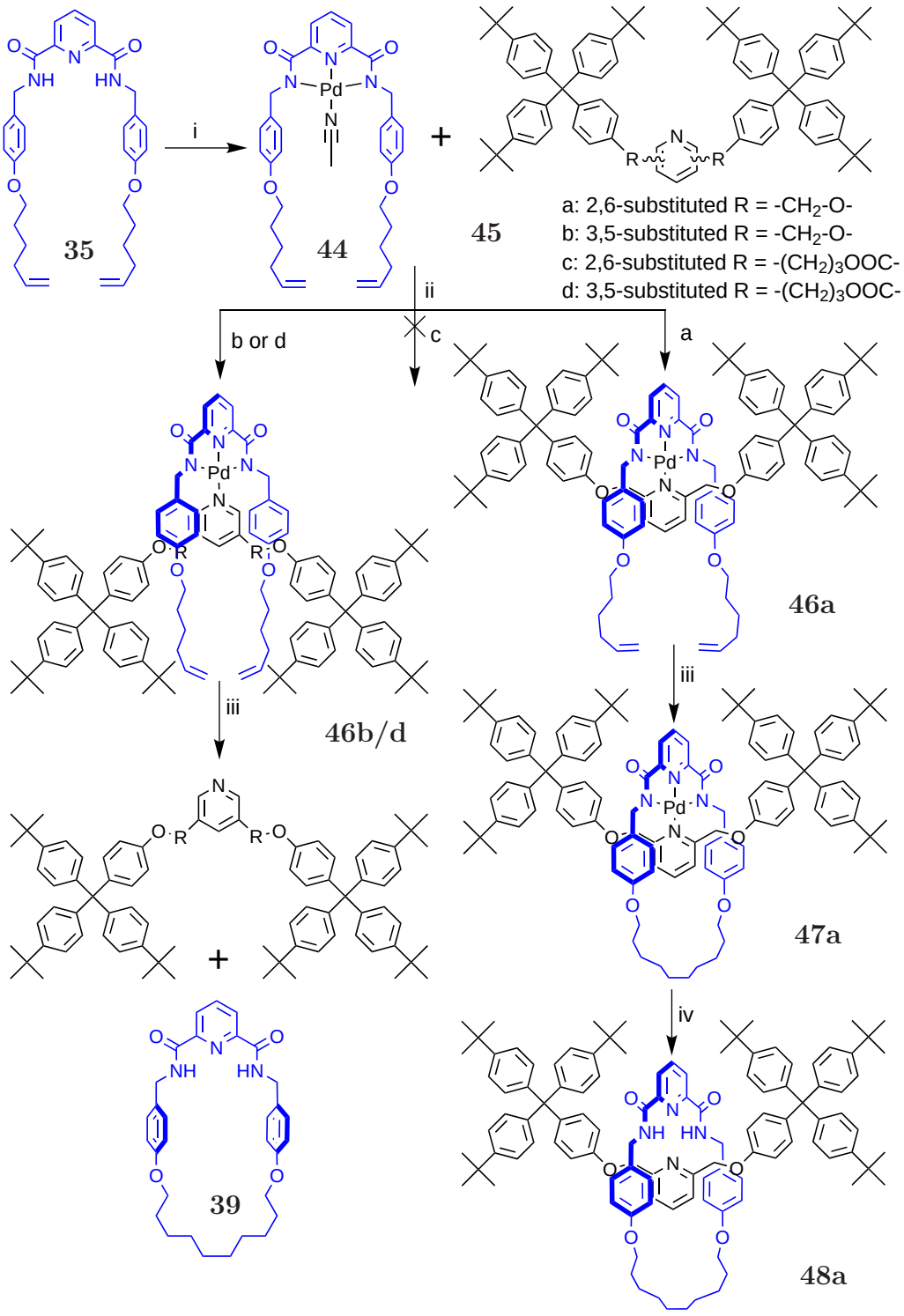

Scheme 1.13. Palladium(II) template directed synthesis of rotaxane **48a**. Reagents and conditions: i) $Pd(OAc)_2$, MeCN, 76%; ii) $CHCl_3$, 50 °C, **46a** = 63%, **46b** = 96%, **46c** = 0%, **46d** = 97%; iii) 1. Grubbs 1st Gen. Catalyst, CH_2Cl_2; 2. H_2, Pd/C, THF, **47a** = 98%, **45b** + **39** = 63%, **45d** + **39** = 69% (over 2 steps); iv) KCN, CH_2Cl_2, 20 °C, 1 h and then 40 °C, 0.5 h, 97%.

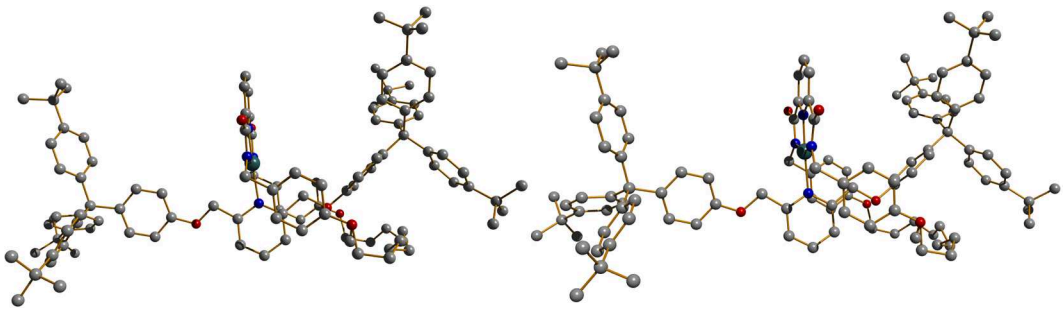

Figure 1.6. Two views of the crystal structure of [2]rotaxane **48a**.[42]

the conformation of the thread - the electron-rich oxygen atoms are pointing away from the central metal - could explain why the formation of rotaxane **48c** does not take place; the ester oxygen would point towards the d_{z^2}-orbital of the palladium and therefore experience a repulsive interaction which makes this arrangement unstable.

1.5.2 Palladium(II) Template Directed Synthesis of a [2]Catenane

One year after the publication of the palladium(II) template directed synthesis of a rotaxane, Leigh and co-workers were able to announce the first [2]catenane synthesis using this methodology (Scheme 1.14).

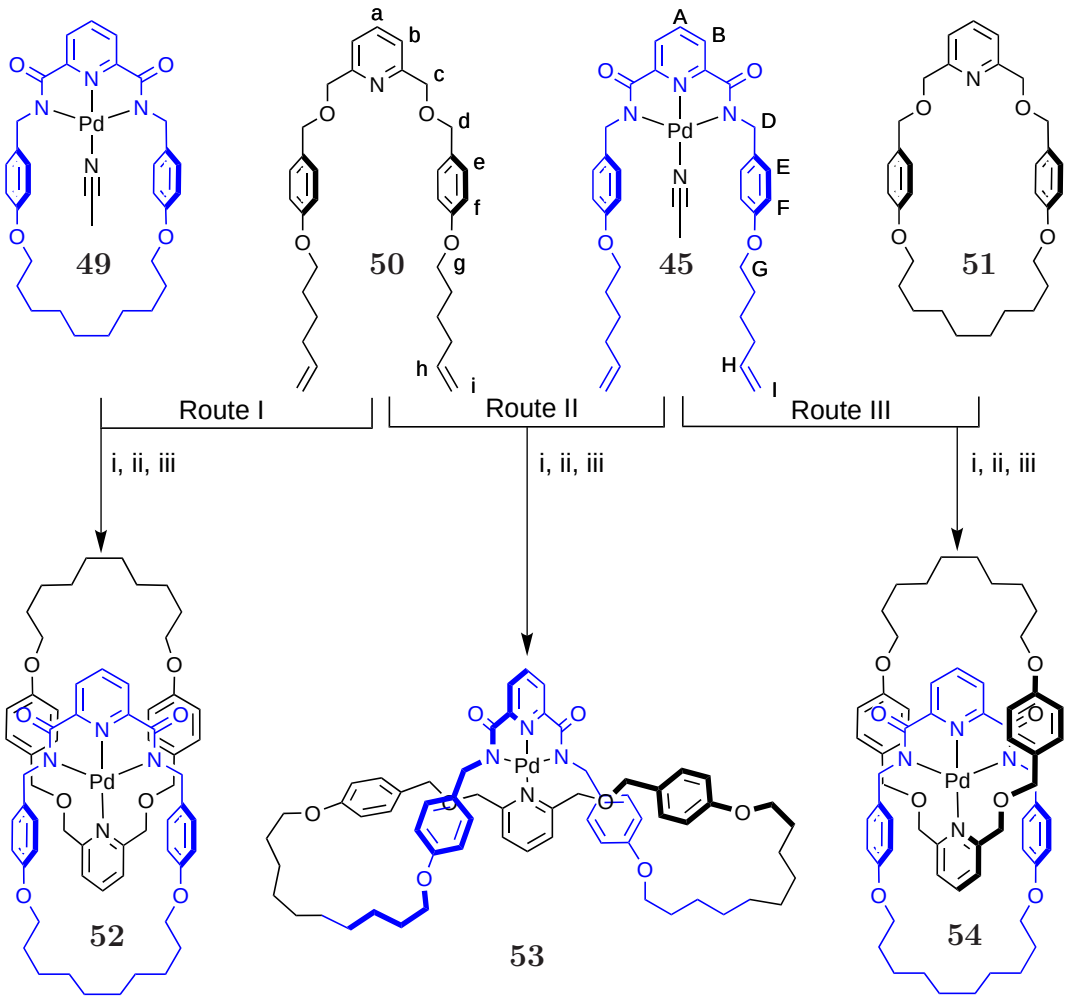

Scheme 1.14. Three isomers that result from the synchronous or simultaneous metal-directed cyclisation of two acyclic building blocks. Reaction sequence and yields: i) ligand exchange; ii) RCM; iii) hydrogenation; Route I = 75%; Route II = 57%; Route III = 78%.

This was achieved by synthesising two different tridentate and monodentate ligand sets - one macrocyclic and one bis-alkene form of each. The "pre-metallated" macrocyclic tridentate ligand **49** (palladium(II) is inserted into the tridentate ligand and the vacant coordination site is occupied by a labile solvent

ligand; here acetonitrile) was reacted in a ligand exchange reaction with monodentate ligand **50** (Scheme 1.14 Route I). Surprisingly this reaction yielded a mixture of exo-/endo-coordinated species in a ratio of 3:2. Subjecting this exo-/endo complex mixture to RCM conditions, hydrogenation and demetallation afforded a mixture of free ligands **39**, **51** (from exo-coordinated species) and the desired [2]catenane (from the endo-coordinated species). The demetallation step was necessary due to the poor chromatographic separation between **52** and **54**. Re-insertion of the metals into the separated compounds confirmed the existence of **52** and **54** as their superimposed spectra reflected the spectrum of the obtained mixture from step (iii). A figure-of-eight complex was obtained when **45** was reacted with **50** in a ligand exchange reaction, followed by RCM and hydrogenation of the cis/trans product mixture (Scheme 1.14 Route II). Finally, a route that exclusively produces the [2]catenane was devised (Scheme 1.14 Route III). This comprised the use of the acyclic tridentate **45** and the monodentate macrocycle **51**, which were reacted in a ligand exchange reaction by simply stirring the components in CH_2Cl_2. Subsequent RCM followed by hydrogenation completed the synthesis of [2]catenane **54**. Comparing the ^{1}H-NMR spectra of the trivial

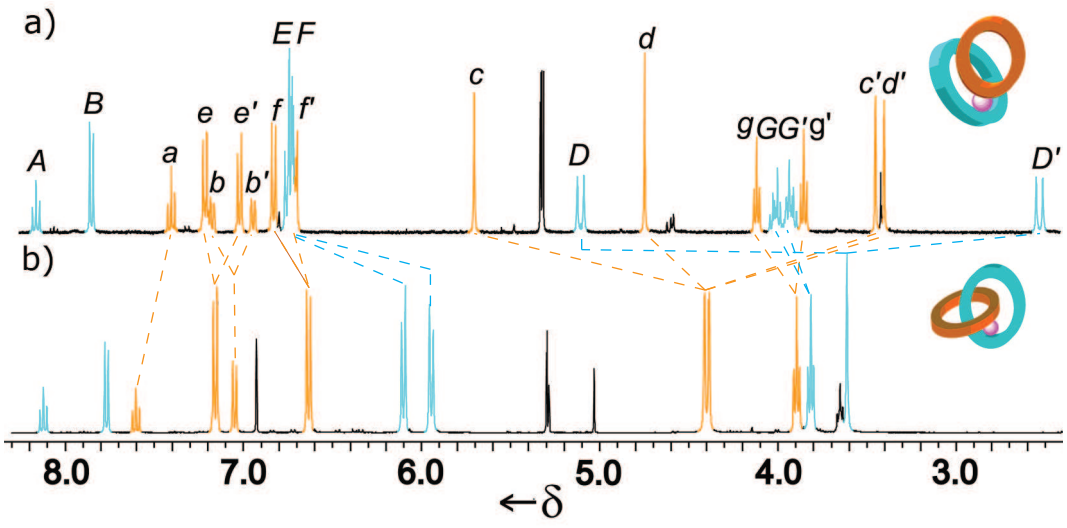

Figure 1.7. ^{1}H-NMR spectra of a) trivial link **52**; b) [2]catenane **54**The lettering corresponds to the assignment in Scheme 1.14; tridentate signals are coloured in cyan and monodentate ligand signals in orange. Reproduced from the PhD thesis of D. Barney Walker.[44]

link **52** and the corresponding [2]catenane **54**, one can see that the reduced sym-

metry of **52** comes with a drastic increase of signal complexity. Most signals of the monodentate ligand split up, due to the different environments they experience. Regarding the proton signals of the tridentate ligand, proton H_D changes from a singlet in the [2]catenane spectrum to a doublet of doublets indicating a diastereotopic environment. This proton signal can be used as a NMR-probe to distinguish between exo and endo conformations of the palladium [3+1] template.

1.5.3 Palladium(II)-Complexed Stimulus Responsive Shuttle and its Metastable Positional Isomers

On the way towards developing molecular machinery, molecular stimulus responsive shuttles mark the first step. Usually, these shuttles are mechanically interlocked molecules with one or more intercomponent recognition sites, which can be addressed by a defined stimulus, so that the preferred co-conformation, representing the thermodynamic minimum, is altered resulting in large amplitude motion of the components relative to one another. As a consequence, the overall chemical and physical behavior changes and the two co-conformers become distinguishable. Leigh and co-workers used the palladium(II) template directed synthesis together with covalent capture to obtain two co-conformational isomers of a [2]rotaxane (Scheme 1.15).[45] The rotaxane consisted of a palladium(II) containing bis-carboxamide pyridine macrocycle and a thread with a DMAP and a pyridine station. The thread was synthesised from **55** and **57** in a series of Sonogashira cross-coupling and Mitsunobu reactions. The thread **61** was then reacted with **49** in a ligand exchange reaction, leading to the kinetically trapped macrocycle thread complex, which was subsequently subjected to Mitsunobu reaction conditions to stopper the thread and complete the synthesis of rotaxane positional isomer **62**. For comparison, Leigh and co-workers also synthesised the other positional isomer, with the macrocycle residing over the pyridine station. Furthermore, they were able to apply selective stimuli to switch between the co-conformers with a high degree of discrimination between the two stations. Recently Leigh and co-workers were able to improve the dynamics and positional bias of the palladium(II) rotaxane system, by introducing a new macrocycle with

a wider cavity.[46]

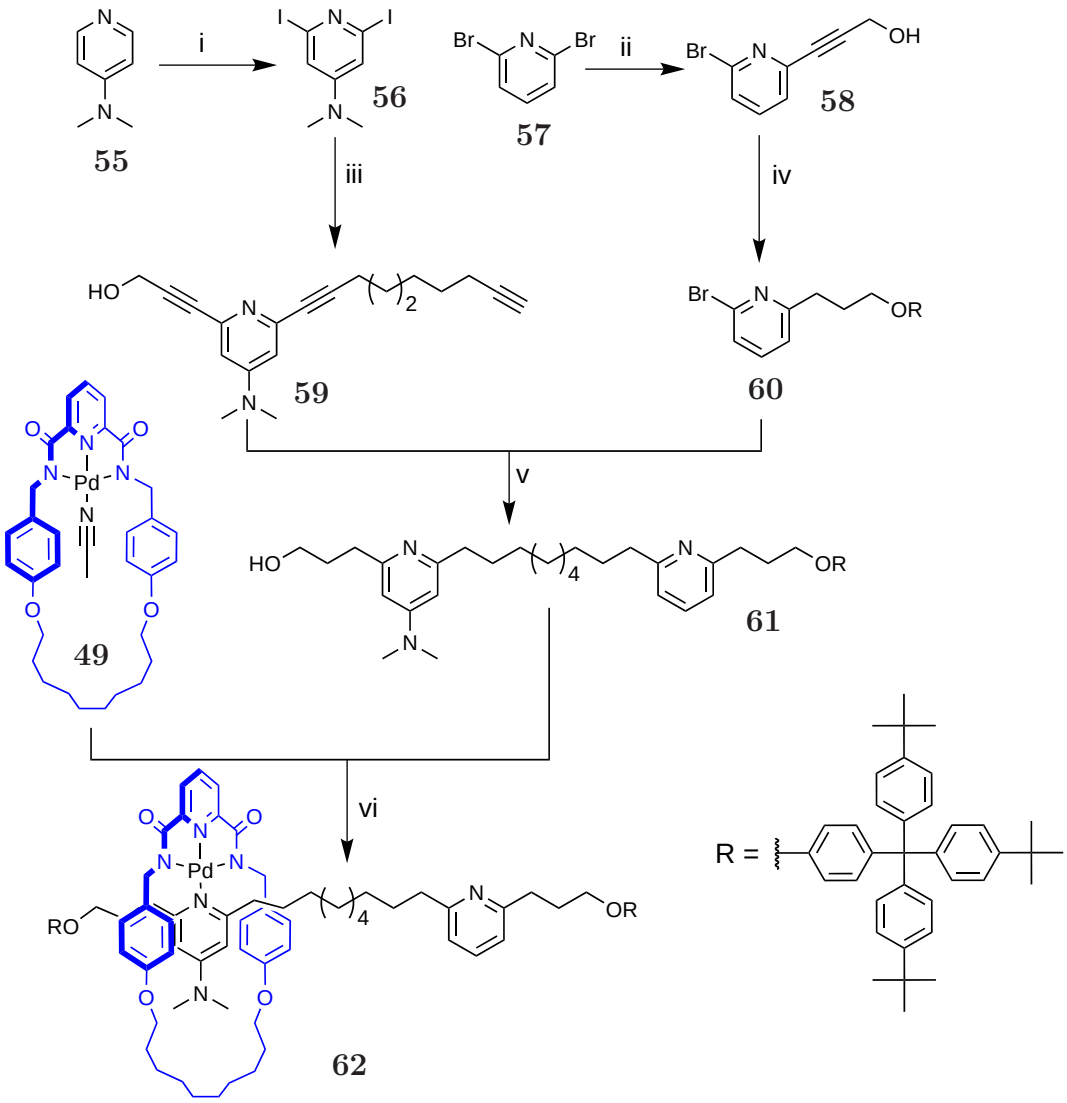

Scheme 1.15. Leigh's switchable palladium complexed molecular Shuttle and synthesis of one of its positional isomers. Reagents and conditions: i) $BF_3{\cdot}Et_3N$, LDA, I_2, THF 40%; ii) propargyl alcohol, $Pd(PPh_3)_4$, CuI, Et_3N/THF (1:2), 60%; iii) propargyl alcohol, $Pd(PPh_3)_4$, CuI, Et_3N/THF, 75%; 1,9-decadiyne (5 eq.), $Pd(PPh_3)_4Et_3N$/THF, 77%; iv) H_2, PtO_2, EtOH/Et_3N, 94%; ROH, DIAD, PPh_3, THF, 61%; v) $Pd(PPh_3)_4$, CuI, Et_3N/THF, 66%, H_2, $Pd(OH)_2$/C, THF, 88%; vi) **49**, CH_2Cl_2, 90%; ROH, DIAD, PPh_3, THF, 26%.

1.5.4 Sequence Isomerism in Palladium(II) Template Directed Synthesis of a [3]Rotaxane

Mechanically interlocked architectures exhibit, due to the arrangement of their components, many different forms of isomerism. One type of isomerism - se-

quential isomerism - was selectively addressed by Leigh and co-workers. They were able to construct a [3]rotaxane with an asymmetric thread and two different macrocycles, controlling the order of sequence in which the macrocycles are arranged on the thread (Scheme 1.16).[47]

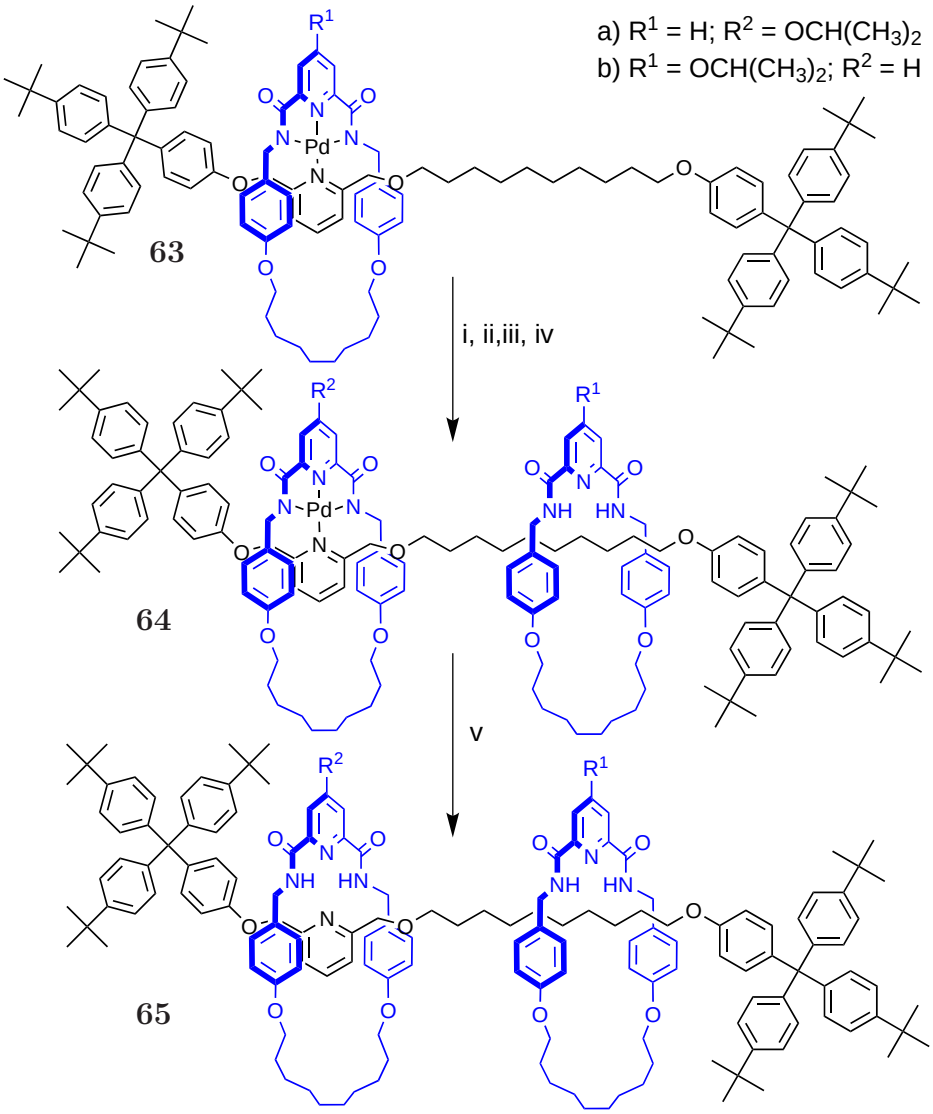

Scheme 1.16. Leigh's [3]rotaxane sequence isomers and their synthesis. Reagents and conditions: i) KCN, CH_2Cl_2/MeOH; ii) **45** or **45**-$OCH(CH_3)_2$, CH_2Cl_2; iii) Grubbs' $1^{st.}$ generation catalyst, CH_2Cl_2; iv) NBSH, NEt_3, CH_2Cl_2; KCN, CH_2Cl_2/MeOH. Yields: a) 67% (over 5 steps); b) 74% (over 5 steps).

This was done by following the methodology published in a proceeding article, where a stoppered 2,6-disubstituted pyridine containing thread (same thread as in rotaxane **63**) was sequentially loaded with pre-metallated macrocyclic precursor **45** and subjected to RCM, hydrogenation and demetallation, thus yielding a

[4]rotaxane.[48] Here (Scheme 1.16), the macrocycle precursor **45** or its derivative **45**-$OCH(CH_3)_2$ are loaded on the thread via ligand exchange reaction, followed by RCM, hydrogenation and extraction of the metal using KCN. This causes the macrocycle to leave the pyridine station and to predominantly reside close to the opposite stopper. Repeating the loading process with a different macrocycle precursor creates a [3]rotaxane exhibiting the sequential isomerism.

1.5.5 Anion Switchable Palladium(II)-Based Molecular Shuttle

With the introduction of an anion switchable molecular shuttle, Leigh and co-workers established another example of a multiple stimulus responsive bistable molecular switch based on a palladium(II)-containing [2]rotaxane (Scheme 1.17).[49]

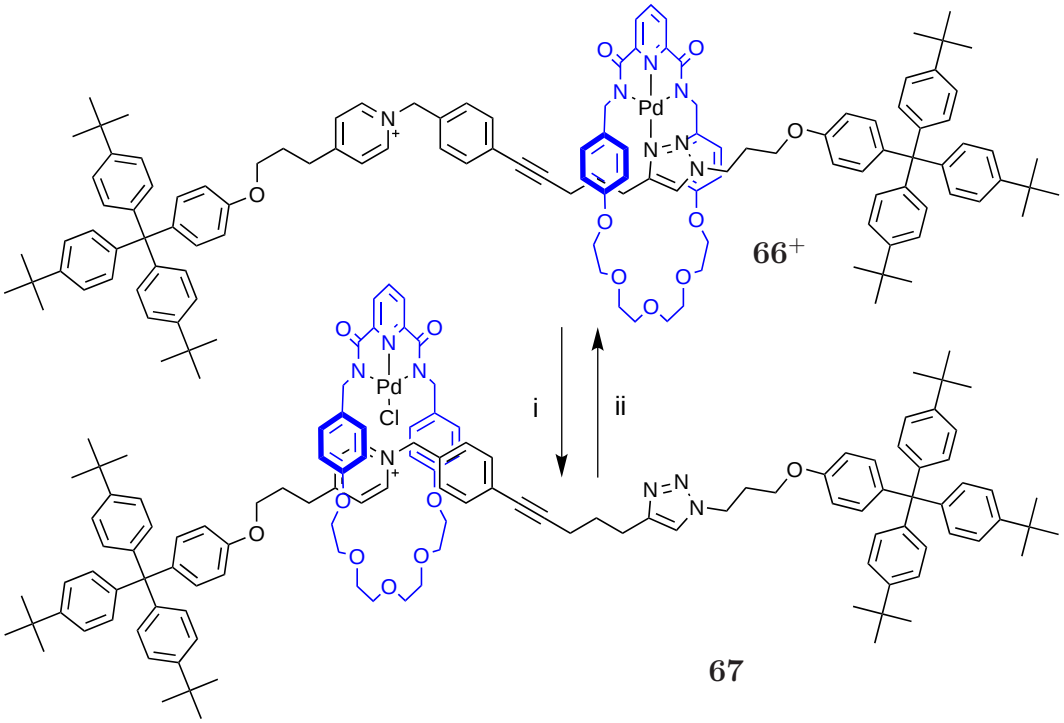

Scheme 1.17. Operation of the chloride switchable shuttle. Reagents and conditions: i) Bu_4NCl, $CHCl_3$, quantitative; ii) $AgPF_6$, acetone, 18 h, quantitative.

Up to this point, the palladium(II) played the role of prearranging the subcomponents of the rotaxanes or catenanes for the interlocking step. Here, the rotaxane **67** was covalently captured using the Huisgen-Meldal-Sharpless 1,3-cycloaddition

of azides to terminal alkynes, whilst the palladium-chloro macrocycle complex was residing over the benzyl-pyridinium position of the track due to ion pairing and secondary interactions of the macrocycle with the track components. To switch to the other station, the chloride anion was removed with a silver(I) salt, and the coordinative unsaturated palladium macrocycle translocated to the triazole. The process could be reversed upon addition of Bu_4NCl.

References

[1] T. Fink, Y. Mao, *The 85 Ways to Tie a Tie: The Science and Aesthetics of Tie Knots*, Fourth Estate Ltd, **2001**.

[2] P. G. Tait, *On Knots I, II, III, Vol. I*, Cambridge University Press, London, **1898**.

[3] J.-P. Sauvage, C. O. Dietrich-Buchecker (Eds.), *Catenanes, Rotaxanes, and Knots*, Wiley-VCH, **1999**.

[4] N. F. Curtis, D. A. House, *Chemistry & Industry* **1961**, 1708–1709.

[5] C. O. Dietrich-Buchecker, J.-P. Sauvage, J. P. Kintzinger, *Tetrahedron Lett.* **1983**, *24*, 5095–5098.

[6] D. H. Busch, *J. Inclusion Phenom. Mol. Recognit. Chem.* **1992**, *12*, 389–395.

[7] S. Anderson, H. L. Anderson, J. K. M. Sanders, *Acc. Chem. Res.* **1993**, *26*, 469–475.

[8] T. J. Hubin, D. H. Busch, *Coord. Chem. Rev.* **2000**, *200-202*, 5 – 52.

[9] C. O. Dietrich-Buchecker, J.-P. Sauvage, J. M. Kern, *J. Am. Chem. Soc.* **1984**, *106*, 3043–3045.

[10] E. Flapan, *When Topology Meets Chemistry: A Topological Look at Molecular Chirality (Outlooks)*, Cambridge University Press, **2000**.

[11] D. K. Mitchell, J.-P. Sauvage, *Angew. Chem., Int. Ed. Engl.* **1988**, *27*, 930–931.

[12] B. Mohr, M. Weck, J.-P. Sauvage, R. H. Grubbs, *Angew. Chem., Int. Ed. Engl.* **1997**, *36*, 1308–1310.

[13] M. Weck, B. Mohr, J.-P. Sauvage, R. H. Grubbs, *J. Org. Chem.* **1999**, *64*, 5463–5471.

[14] G. Schill, *Catenanes, Rotaxanes, Knots (Organic Chemistry Monographs)*, Academic Press Inc.,U.S., **1971**.

[15] C. O. Dietrich-Buchecker, J.-P. Sauvage, *Angew. Chem., Int. Ed. Engl.* **1989**, *28*, 189–192.

[16] C. O. Dietrich-Buchecker, J. Guilhem, C. Pascard, J.-P. Sauvage, *Angew. Chem., Int. Ed. Engl.* **1990**, *29*, 1154–1156.

[17] C. O. Dietrich-Buchecker, J. F. Nierengarten, J.-P. Sauvage, N. Armaroli, V. Balzani, L. De Cola, *J. Am. Chem. Soc.* **1993**, *115*, 11237–11244.

[18] C. O. Dietrich-Buchecker, G. Rapenne, J.-P. Sauvage, *Chem.Commun.* **1997**, 2053–2054.

[19] C. O. Dietrich-Buchecker, J.-P. Sauvage, N. Armaroli, P. Ceroni, V. Balzani, *Angew. Chem., Int. Ed. Engl.* **1996**, *35*, 1119–1121.

[20] G. Rapenne, C. O. Dietrich-Buchecker, J.-P. Sauvage, *J. Am. Chem. Soc.* **1996**, *118*, 10932–10933.

[21] L.-E. Perret-Aebi, A. von Zelewsky, C. O. Dietrich-Buchecker, J.-P. Sauvage, *Angew. Chem., Int. Ed.* **2004**, *43*, 4482–4485.

[22] C. Wu, P. R. Lecavalier, Y. X. Shen, H. W. Gibson, *Chem. Mater.* **1991**, *3*, 569–572.

[23] A. Livoreil, C. O. Dietrich-Buchecker, J.-P. Sauvage, *J. Am. Chem. Soc.* **1994**, *116*, 9399–9400.

[24] I. Poleschak, J. M. Kern, J.-P. Sauvage, *Chem.Commun.* **2004**, 474–476.

[25] M. C. Jimenez, C. O. Dietrich-Buchecker, J.-P. Sauvage, *Angew. Chem., Int. Ed.* **2000**, *39*, 3284–3287.

[26] J.-P. Sauvage, M. Ward, *Inorg. Chem.* **1991**, *30*, 3869–3874.

[27] N. Belfrekh, C. O. Dietrich-Buchecker, J.-P. Sauvage, *Inorg. Chem.* **2000**, *39*, 5169–5172.

[28] J. C. Chambron, J. P. Collin, V. Heitz, D. Jouvenot, J. M. Kern, P. Mobian, D. Pomeranc, J.-P. Sauvage, *Eur. J. Org. Chem.* **2004**, 1627–1638.

[29] F. Arico, P. Mobian, J. M. Kern, J.-P. Sauvage, *Org. Lett.* **2003**, *5*, 1887–1890.

[30] P. Mobian, J. M. Kern, J.-P. Sauvage, *J. Am. Chem. Soc.* **2003**, *125*, 2016–2017.

[31] P. Mobian, J. M. Kern, J.-P. Sauvage, *Inorg. Chem.* **2003**, *42*, 8633–8637.

[32] D. A. Leigh, P. J. Lusby, S. J. Teat, A. J. Wilson, J. K. Y. Wong, *Angew. Chem., Int. Ed.* **2001**, *40*, 1538–1543.

[33] L. Hogg, D. A. Leigh, P. J. Lusby, A. Morelli, S. Parsons, J. K. Y. Wong, *Angew. Chem., Int. Ed.* **2004**, *43*, 1218–1221.

[34] F. A. Chavez, P. K. Mascharak, *Acc. Chem. Res.* **2000**, *33*, 539–545.

[35] F. A. Chavez, J. M. Rowland, M. M. Olmstead, P. K. Mascharak, *J. Am. Chem. Soc.* **1998**, *120*, 9015–9027.

[36] D. S. Marlin, P. K. Mascharak, *Chem. Soc. Rev.* **2000**, *29*, 69–74.

[37] J. C. Noveron, M. M. Olmstead, P. K. Mascharak, *Inorg. Chem.* **1998**, *37*, 1138–1139.

[38] J. C. Noveron, M. M. Olmstead, P. K. Mascharak, *J. Am. Chem. Soc.* **1999**, *121*, 3553–3554.

[39] J. C. Noveron, M. M. Olmstead, P. K. Mascharak, *J. Am. Chem. Soc.* **2001**, *123*, 3247–3259.

[40] L. A. Tyler, J. C. Noveron, M. M. Olmstead, P. K. Mascharak, *Inorg. Chem.* **2000**, *39*, 357–362.

[41] D. A. Leigh, P. J. Lusby, R. T. McBurney, A. Morelli, A. M. Z. Slawin, A. R. Thomson, D. B. Walker, *J. Am. Chem. Soc.* **2009**, *131*, 3762–3771.

[42] A.-M. L. Fuller, D. A. Leigh, P. J. Lusby, I. D. H. Oswald, S. Parsons, D. B. Walker, *Angew. Chem., Int. Ed. Engl.* **2004**, *43*, 3914–3918.

[43] T. Moriuchi, S. Bandoh, M. Miyaishi, T. Hirao, *Eur. J. Inorg. Chem.* **2001**, 651–657.

[44] D. B. Walker, Ph.D. thesis, School of Chemistry University of Edinburgh, **2005**.

[45] J. D. Crowley, D. A. Leigh, P. J. Lusby, R. T. McBurney, L.-E. Perret-Aebi, C. Petzold, A. M. Z. Slawin, M. D. Symes, *J. Am. Chem. Soc.* **2007**, *129*, 15085–15090.

[46] D. A. Leigh, P. J. Lusby, R. T. McBurney, M. D. Symes, *Chem.Commun.* **2010**, *46*, 2382–2384.

[47] A.-M. L. Fuller, D. A. Leigh, P. J. Lusby, *J. Am. Chem. Soc.* **2010**, *132*, 4954–4959.

[48] A.-M. L. Fuller, D. A. Leigh, P. J. Lusby, *Angew. Chem., Int. Ed.* **2007**, *46*, 5015–5019.

[49] M. J. Barrell, D. A. Leigh, P. J. Lusby, A. M. Z. Slawin, *Angew. Chem., Int. Ed.* **2008**, *47*, 8036–8039.

Chapter 2

Studies Towards the Stepwise Synthesis of a Borromean Link

Acknowledgements and Declaration

Dr. D. Barney Walker conducted preliminary studies towards the Borromean link (not described here). Dr. José Berná-Cánovas conducted preliminary studies on the ring closure of the second ring of the Borromen link (not described here) and also synthesised compounds **11b**, **12b**, **15b** and **35**. The content of this chapter is the result of a joint effort of Dr. José Berná-Cánovas and the author.

2.1 Synopsis

This chapter describes the topological analysis, the conceptual design and the synthetic attempt of a stepwise synthesis towards one of the topologlically most challenging und intriguing structures synthesised to date - the Borromean link. At first, different strategic starting points are identified and presented in context with relevant examples. The topological analysis is employed to identify valid precursor geometries and synthetic routes, followed by the description of the envisaged design and its features. The synthetic attempt towards the Borromean link is reported up to the synthesis of the primary ring, which is centerpiece of the synthetic strategy.

2.2 Introduction

'*The molecular Borromean link is one of the most challenging synthetic targets generated from molecular graphs of complex topology. Its structural complexity stems from the interweaving of three macrocycles such that no two of the macrocycles are concatenated nor covalently connected, yet collectively they form an integral molecular unit.*'[1]

Since the publication of the first successful synthesis of a molecular DNA-based Borromean link by Seeman and co-workers in 1997,[2] this target has fueled the imagination of many chemists. In 2003, Siegel and co-workers presented a ring-in-ring two-core ruthenium(II) complex, which they claimed, would be the perfect precursor towards the stepwise synthesis of the Borromean link.[1] However, one year later, Stoddart and co-workers were able to announce the second example of a molecular Borromean link, using the reversible imine formation in conjunction with metal templated alignment of the ring constituents in a thermodynamically controlled self-assembly process.[3]

According to Siegel, there are three distinct representations of the Borromean link that inspire targets for the molecular design and synthesis (Venn rings, chain rings, and orthogonal rings).[1] These topologically equivalent representations of a Borromean link constitute valuable starting points for a retrosynthetic analysis, as depicted in Figure 2.1. The Venn rings representation (Figure 2.1), was chosen by Seeman and co-workers to construct their version of the Borromen link. The chain rings (Figure 2.1) approach was used by Whitesides and co-workers for their fabrication of metallic microknots, which were produced via a micro-pattern printing procedure and subsequent welding.[4] The orthogonal rings (Figure 2.1) approach was proposed by Siegel *et al.* . In contrast to the afore mentioned approaches, Stoddart and co-workers employed a self-assembly process, in which all rings are formed in a concerted manner. However, the resulting product closely resembles the orthogonal rings and therefore could be counted as such.

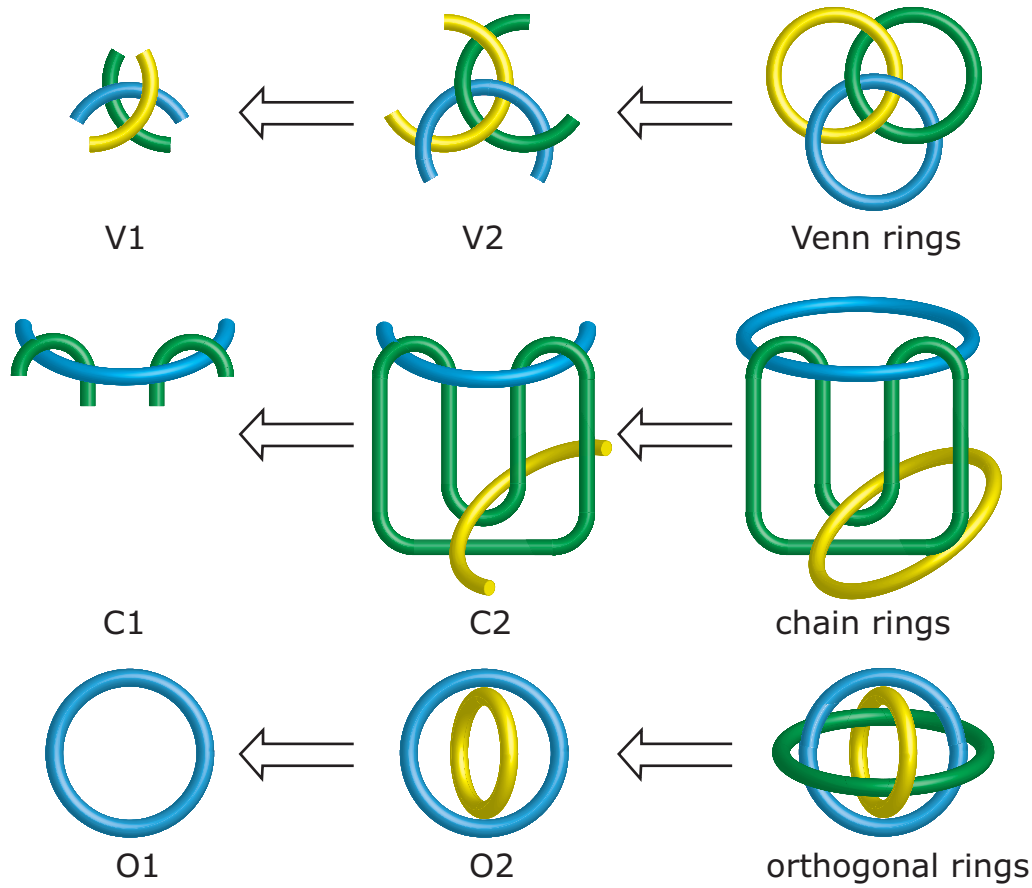

Figure 2.1. Retrosynthetic representations of the Borromean link (Venn rings, chain rings, orthogonal rings).[1]

2.2.1 Borromean Links from Single-Stranded DNA

The first successful synthesis of a molecular Borromean link was reported 1997 by Seeman and co-workers, using single stranded DNA.[2] This was accomplished by assembling each macrocycle of two complementary strands, which consist of 196, 206 or 216 residues. Therefore, six different strands of DNA were synthesised, each of which bearing hairpin regions at one ends and two crossing point domains.

The hairpin regions' sequence was designed to recognize their half-macrocycle counterpart and also contain a sequence to allow restricted digestion with an appropriate nuclease. The crossing nodes (B-DNA[5] and Z-DNA[6]) are separated by a dT_4 (oligo-desoxythymidine) spacer and separated from the hairpins by dT10 spacer. To ensure the right topology, each strand contained either two negative (B-DNA; right handed) or two positive crossing points (Z-DNA; left-handed) which were uniquely encoded to guarantee the specific entanglement.

Three strands which either contain B-DNA nodes or Z-DNA nodes were annealed individually to give the two "hemispheres" of the globular Borromean link assembly (Figure 2.2). These two complementary building blocks were ligated under Z-DNA promoting conditions, which gave the desired Borromean link after purification on 2-D denaturing gel electrophoresis.

In the case of the Borromean link, cleavage of one of the rings leads to the whole assembly falling apart. Thus applying this method, using three restricton nucleases which are able to selectively cleave one of the rings, the other two rings could be obtained and hence their different weight, identified by gel electrophoresis.

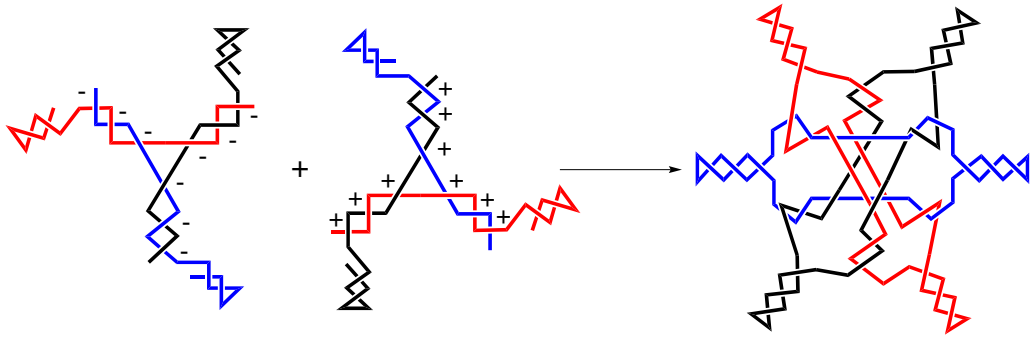

Figure 2.2. Synthesis of Borromean links from three strands of B-DNA (left), three strands of Z-DNA (middle) and after ligation (right).

2.2.2 Borromean Links Precursor Ring-in-Ring Complex

In 2002 Schmittel and co-workers reported the synthesis of a ring-in-ring complex, based on Sauvage's template, using convergent turns for the outer ring and divergent turns for the inner ring.[7] However, one year later, Siegel and co-workers published the synthesis of a ring-in-ring complex, which was bearing additional coordination sites and therefore constitutes a possible precursor for the synthesis of a Borromean link.[1] The ring-in-ring complex was synthesised from a preformed macrocycle **1**, containing two terpyridine moieties in a convergent turn configuration, linked by a 12 atom long spacer ($(CH_2)_2O(CH_2)_6O(CH_2)_2$). Through the cavity of this macrocycle two divergent turn terpyridine units were threaded, giving rise to the two core ruthenium complex **4**. The synthesis of the ring-in-ring complex was completed by a Williamson ether formation of the phenolic

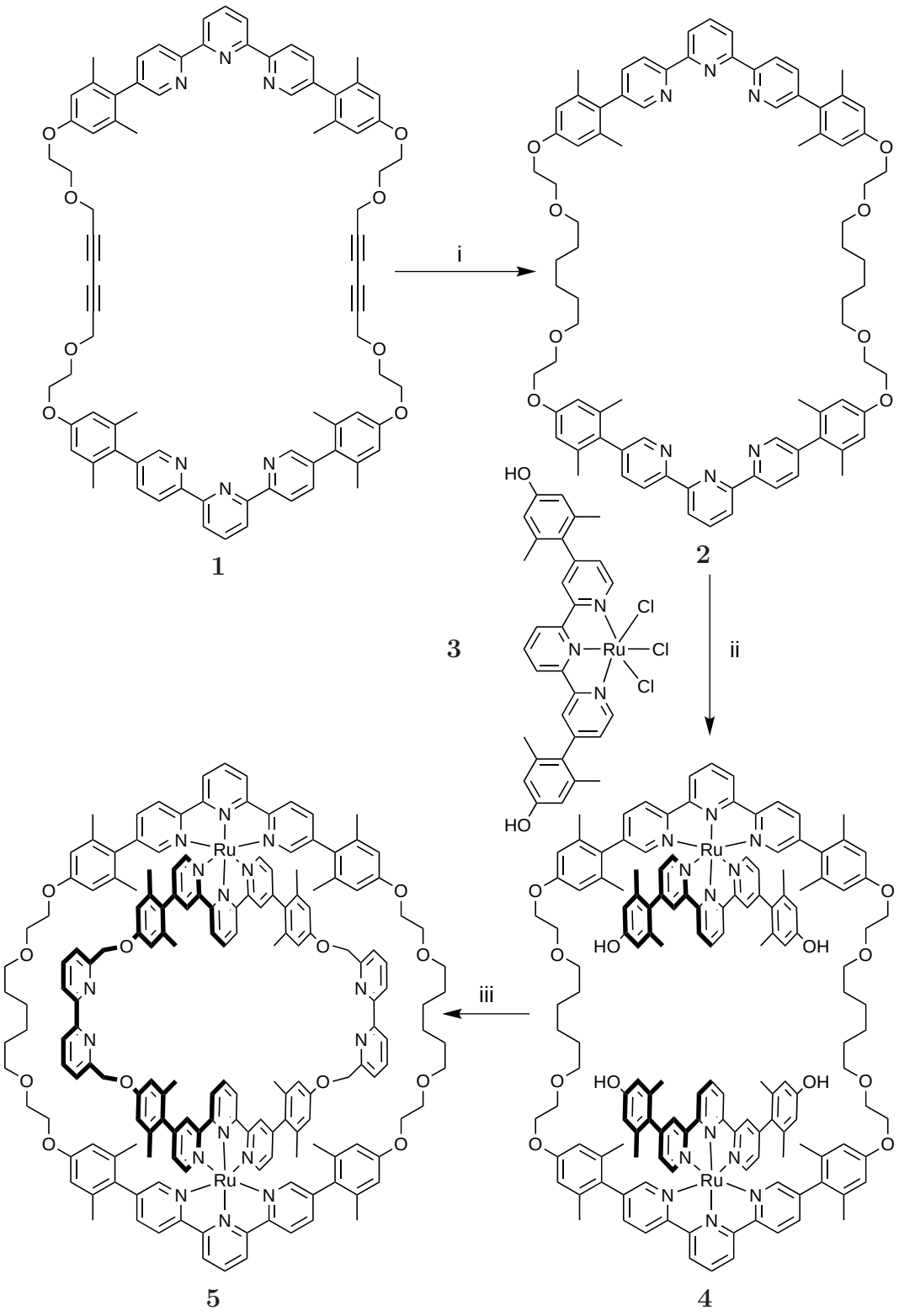

Scheme 2.1. Siegel's synthesis of a ring-in-ring complex. Reagents and conditions: i) **1**, H_2 80 psi, Pd/C (10%), ethanol/CH_2Cl_2 (1:1), 6 h, 91%; ii) **2**, **3**, CH_2Cl_2/EtOH/ethylene glycol (2:2:1), reflux, 12 h, 65%; iii) 6,6'-bisbromomethyl-2,2'-bipyridine, $CsCO_3$, acetonitrile, reflux, 72 h, 49%.

positions of the threaded divergent turn terpyridines and 6,6'-bisbromomethyl-2,2'-bipyridine.

2.2.3 Borromean Links by TM Directed Self Assembly Processes

Stoddart and co-workers exercised an intriguing example of self-assembly of Borromean links using an alternately convergent / divergent turn strategy in order to generate six crossing points.[3] These consisted of a zinc(II) anchor, which was coordinated to a tridentate and a bidentate ligand which were perpendicularly aligned. Each of the three identical macrocycles was formed by a reversible [2 + 2] multi-component reaction whilst being templated by Zn(II) ions.

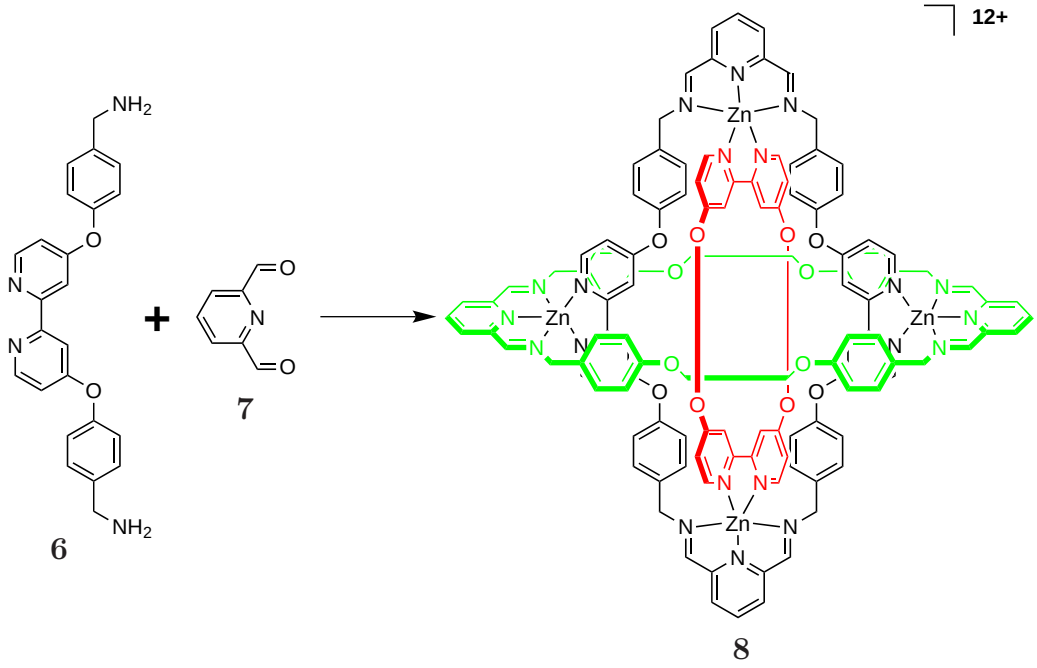

Scheme 2.2. The 18 component self-assembly of the first [3]Borromeate. Schematic representation of the Borromeate **8** with simplified red and green ring. Reagents and conditions: **6**, **7**, $Zn(OAc)_2$, MeOH / TFA, reflux, 3 d.

Stoddart and co-workers chose imine formation for macrocylisation, because it is reversible and thus the reaction could be run under thermodynamic control. This led to the desired Borromean link as it is the thermodynamic product, due to the stabilisation of the imine bonds by the zinc(II) anchor and the perfectly aligned π-stacking interactions of the bipyridine units with the phenyl

moieties. The self-assembly of the Borromean link was achieved by reacting the bis-amine ligand **6** with 2,6-diformylpyridine **7** in presence of $Zn(OAc)_2$ and TFA in methanol at reflux for three days. The reaction was followed by ^{1}H-NMR in CD_3OD, and showed a highly symmetrical species after 2 days which was identified as the desired Borromean link **8** using ESI-MS. Finally an X-ray crystal structure analysis confirmed the locked multi-ring structure and proved that the π-stacking interactions exist as intended in the design.

The dynamic covalent nature of the 2,6-bis-iminopyridine was shown in scrambling experiments using differently labelled (bromide / chloride) Borromean links.[8] Recently it was shown that, upon reduction of the imine bonds to secondary amines and subsequent demetallation using EDTA the Borromeate can be obtained, and that cleavage of any one of the rings lead to the whole assembly falling apart.[9]

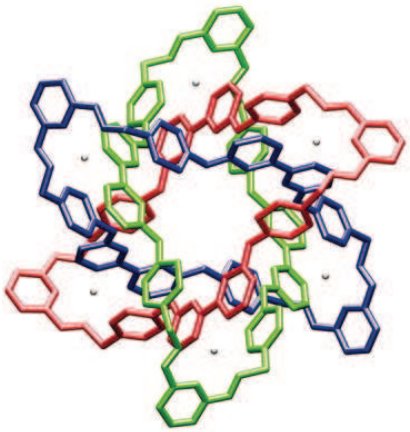

Figure 2.3. X-ray crystal structure of Borromean ring complex.[3]

2.3 Topological Analysis

The Borromean Link consists of three orthogonally aligned rings, which are interwoven so that no two of the rings are concatenated, giving a molecular entanglement. As there are $2^6 = 64$ (two possible arrangements of a crossing between two rings e.g. over or under; 6 crossing points) different configurations of the crossing points of three aligned rings, there are only two possible conformations of the 6 crossover points that represents the Borromean Link.

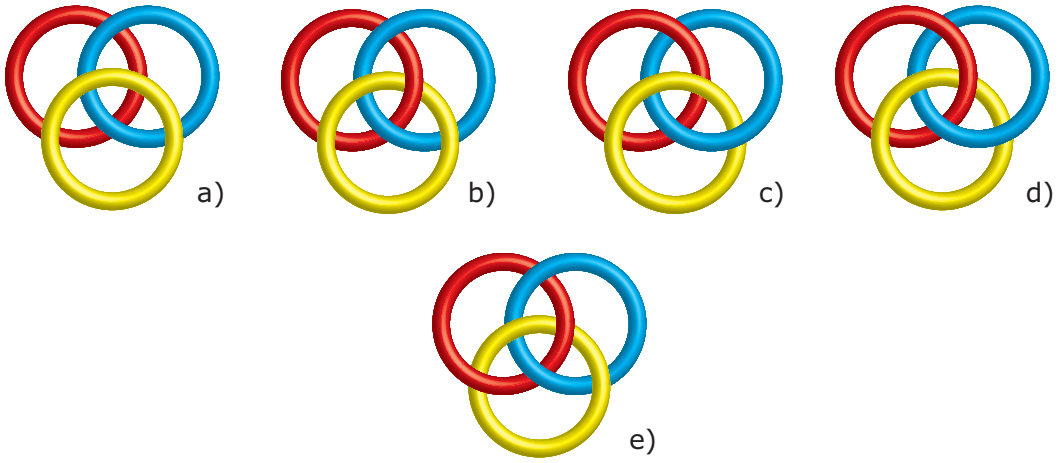

Figure 2.4. Alignments of three rings and their symmetry reduced link representatives (rings are identical but colored to visualise the crossover points). a) trivial link; b) Hopf link with trivial link; c) chain link; d) torus link; e) Borromean link.

The order and position of the ring-closure therefore has to be carefully weighed against the danger of creating a "false" connection (undesired orientation of the crossover point e.g. under instead of over), which would render the whole approach obsolete. Generally, the ring-closure reactions should occur in exo-positions, enabling unrestricted access for the reactants and/or catalysts to be used.

Consequently, the fusion of the last ring (yellow Figure 2.5) should preferably occur in the equatorial position, thus reducing the need for two metal template sites. This approach would require two identical yellow threads in the polar regions, implying that the last ring has to be closed via a symmetric coupling procedure. Disconnecting the red ring above and below the equatorial plane dissipates the assembly into three fragments, two identical "polar caps" (red convergent turn and yellow thread) and the remainder (blue ring with red threads),

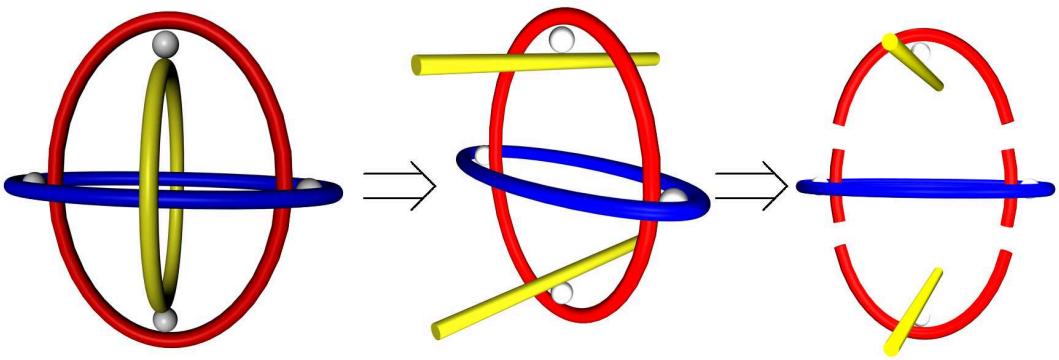

Figure 2.5. Borromean link assembly; first and second disconnection.

which will be the first ring to be established and represents the main scaffold on which the entire system will be built. Furthermore, special attention has to be paid towards the lengths of the counter-parts of the red and yellow ring. If these parts are too long, it could result in unwanted ring closures, like the formation of a catenane. Also twisting of the main scaffold could lead to the formation of a Solomon link (double crossover catenane). To avoid all these problems, the employed system should exhibit exceptional structural and geometrical stability.

2.4 Design of the Heterocircuit Borromean Link

The rational design of the heterocircuit Borromean link consists of four [3+1]-template sites, which align the three rings in an orthogonal manner and act as guiding motif for the synthesis (Scheme 2.6). Two of the four tridentate units (the fundamental constituents of the template) are located in the blue ring, whereas the remaining two tridentate ligands are situated in the red ring. The red ring is held in place by a 2-point ligation to the palladium(II) anchors coordinated to the blue ring. The yellow ring is fixed in its position by coordination to the two palladium(II) anchors of the red ring.

The palladium(II) [3+1]-template has proved to be stable under a small selection of reaction conditions, such as RCM, Mitsunobu alkylation of phenols, Williamson ether synthesis of alkyl bromides with phenols, amide formation of activated esters with primary benzylic amines and the CuAAC or "click"-reaction of terminal alkynes with azides. Preliminary studies, which were based on the

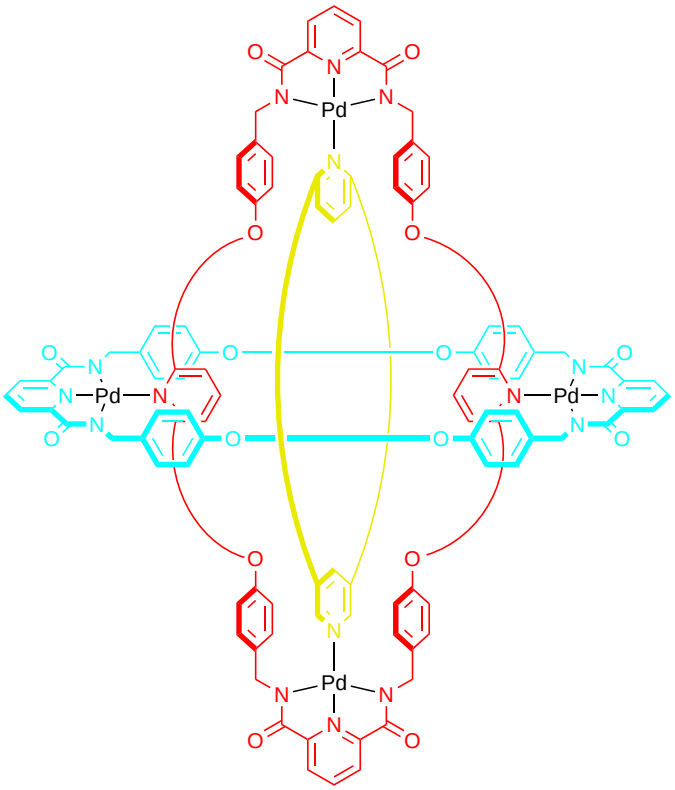

Figure 2.6. Simplified schematic representation of the envisaged Borromean link assembly and positions of the [3+1]-template assemblies therein.

pre-formation of the blue macrocycle, pre-metallation thereof, threading of the monodentate ligands and successive "click"-reaction with two capping fragments, failed due to the formation of inseparable exo-/endo-complex mixtures when threading the monodentate ligands through the cavity of the blue ring.* Further studies that were carried out showed (Scheme 2.3), that designing the blue ring as a "clamp" and establishing the the [3+1] template prior to the ring-closure fails due to the incompatibility of the alkyne residues with the RCM ring-closure procedure.

Therefore, a double "click" ring-closure of two complementary "half-ring" building blocks towards the main scaffold is devised (Scheme 2.7). Here, the main scaffold bears silyl protecting groups on the alkynes. This is necessary to prevent the premature reaction of the otherwise unprotected alkynes during the ring-closure reaction of the blue ring. After removal of the protecting group, the next successive fourfold "click"-reaction can be carried out to obtain the ring-

*These preliminary studies were carried out by Dr. D. Barney Walker.

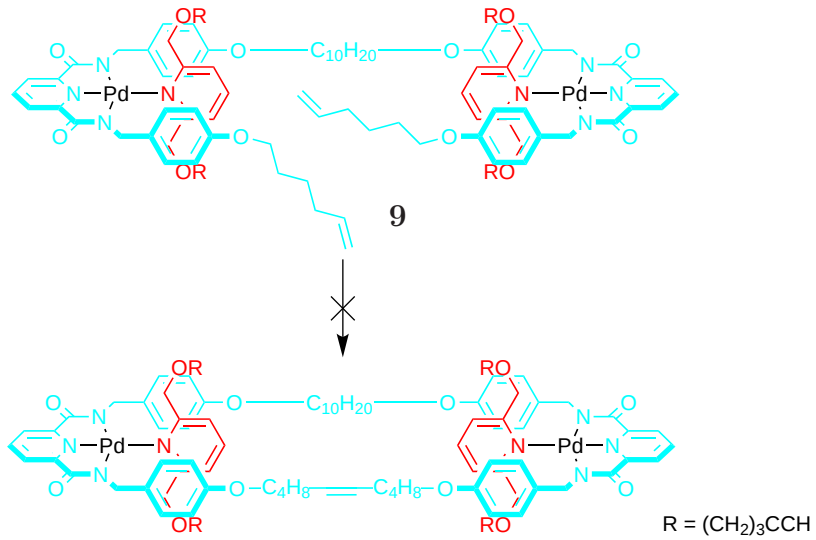

Scheme 2.3. Preliminary studies of Main Scaffold synthesis. Reagents and conditions: **9**, Grubbs' 1st. Generation catalyst, CH_2Cl_2, 1 mM, RT, 18 h.

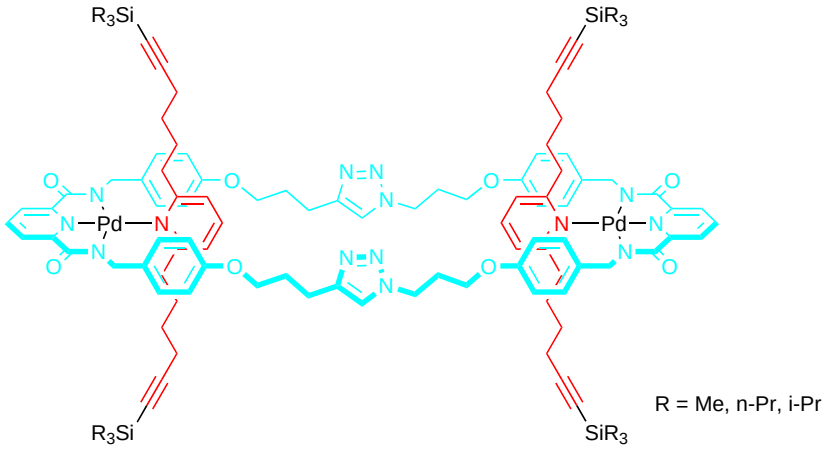

Figure 2.7. Envisaged design of the main scaffold.

in-ring complex. In this thesis, the synthesis of the main scaffold - the main precursor towards the synthesis of the Borromean link - is described.

2.5 Retrosynthesis of the Main Scaffold MS

The proposed retrosynthesis of the main scaffold (**MS**) is shown in Scheme 2.4. Here a double "click"-reaction of the the two complementary building blocks

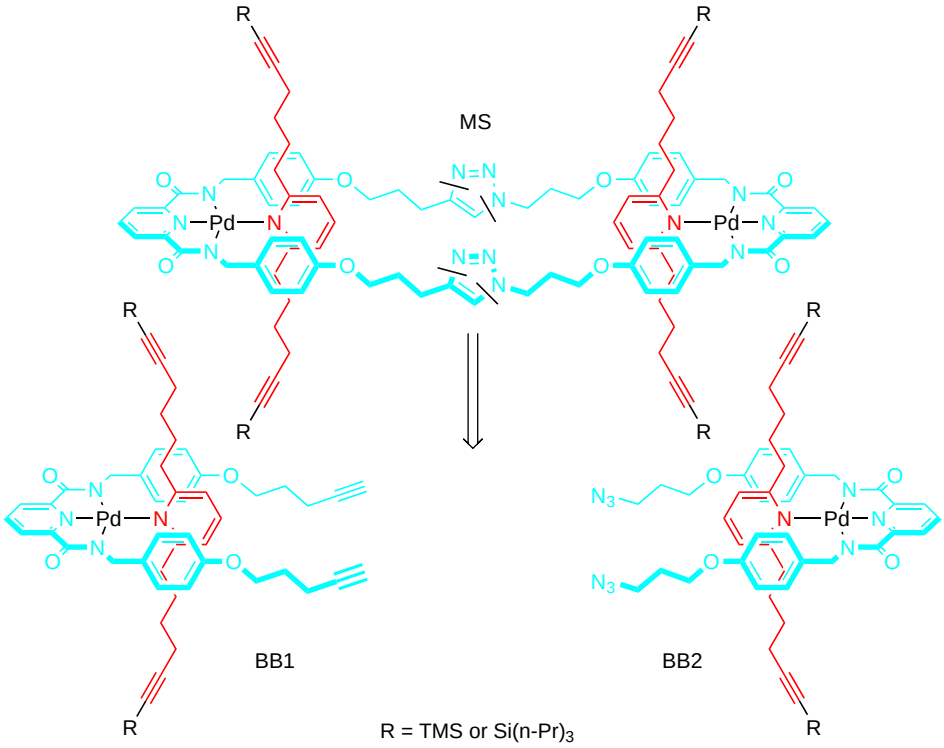

Scheme 2.4. Retrosynthesis of the proposed Main Scaffold **MS** and indicated disconnections.

BB1, containing two terminal alkynes, and **BB2**, containing two alkyl azides, should afford **MS** with its four alkyl silyl protected alkynes orthogonally aligned to the plane of the 56-member macrocycle.

The building blocks **BB1** and **BB2** differ only in their tridentate phenol ether substituents. Inserting palladium into the tridentate ligand that contains azides is expected to be straightforward; alkyl azides are stable under these conditions, as preliminary tests have shown. However, as palladium is known to activate terminal triple bonds and could therefore lead to decomposition of the substrate in the case of **BB1**, the phenol ether formation with an appropriate alkyne linker has to be performed after the metal was inserted into the tridentate ligand.

Subjecting the **BB1** assembly to retrosynthetic analysis (Scheme 2.5), the first disconnection is made at the phenolic positions, as it should be accessible

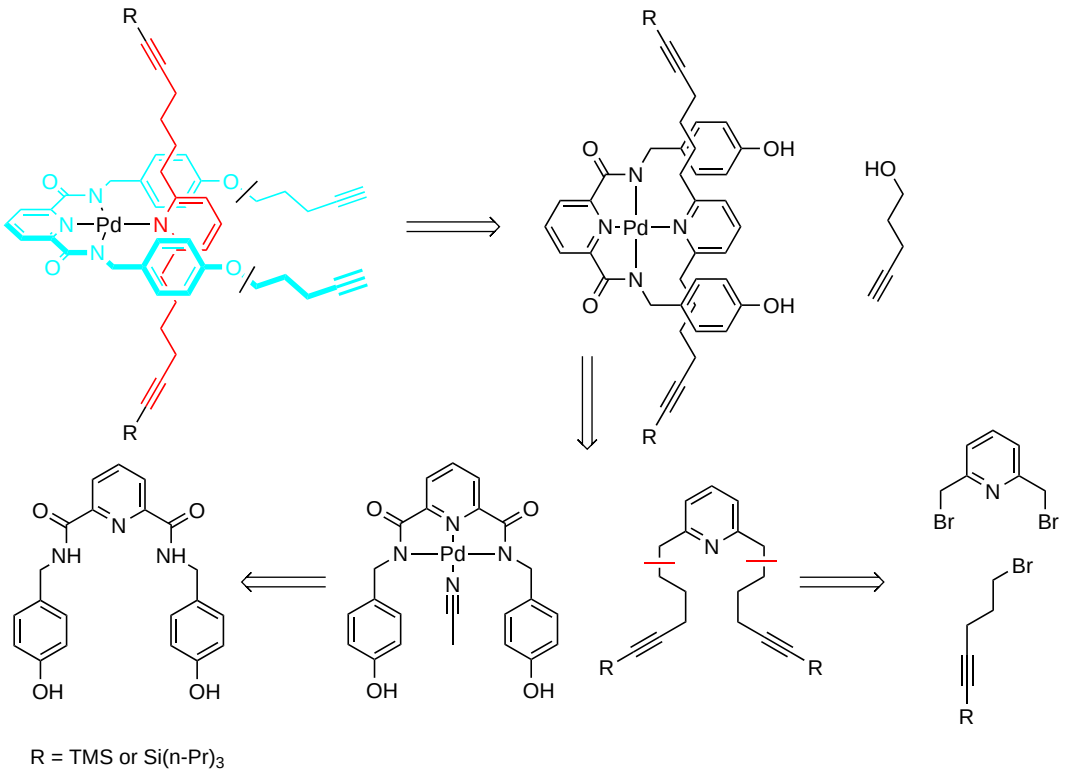

Scheme 2.5. Retrosynthesis of the proposed **BB1** and indicated disconnections.

from the monodentate bisphenol complex and pentynol in a Mitsunobu reaction. This complex can be obtained via ligand exchange reaction of the pre-metallated bisphenol U-shape with the 2,6-disubstituted pyridine monodentate ligand. The pre-metallated bisphenol U-shape is accessible by inserting the palladium(II) into the 2,6-di(4-hydroxybenzyl-N-amido)pyridine (**BPU**) tridentate ligand in the presence of MeCN. The monodentate ligand, with its short alkyl spacer between the aromatic core of the pyridine and alkyne moiety shall be obtained from a Wurtz coupling of the doubly lithiated 2,6-bis-(bromomethyl)-pyridine with a silyl-protected bromo-alkyne.

Undertaking a retrosynthetic analysis on the building block assembly **BB2**, the first retosynthetic step is the ligand exchange of the labile acetonitrile of the pre-metallated azide-containing tridentate ligand against the 2,6-disubstituted pyridine monodentate ligand. The pre-metallated bisazide tridenate ligand is derived from the free ligand by insertion of palladium(II) in the presence of MeCN. The bisazide U-shape in turn should be obtainable from the bisphenol U-shape by a Williamson phenol ether synthesis with an appropriate propylazide.

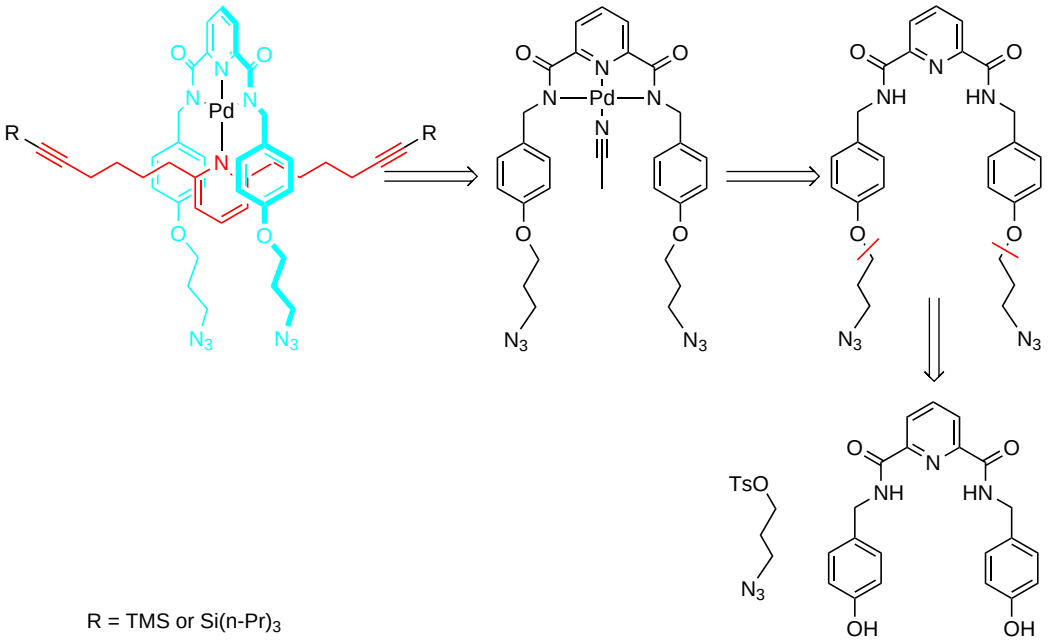

Scheme 2.6. Retrosynthesis of the proposed **BB2** and indicated disconnections.

2.6 Synthesis

2.6.1 Synthesis of the Monodentate Ligands

The first route towards the monodentate ligand **MDL1**(bearing different protecting groups), developed by Dr. José Berná-Cánovas, starts from the commercially available 4-pentyn-1-ol **10** (Scheme 2.7). The 4-pentyn-1-ol was treated with two equivalents of EtMgBr to deprotonate the alcohol, forming a stable bromo magnesium alcoholate, and the deprotonated alkyne.[10] Addition of the corresponding trialkylsilylchloride [$(n\text{-Pr})_3$SiCl, $(i\text{-Pr})_3$SiCl] leads to the desired trialkylsilane protected alkynes **11a** and **11b**. Subsequent conversion of the alcohol group into a bromide using standard Appel reaction conditions affords the products **12a/b**.

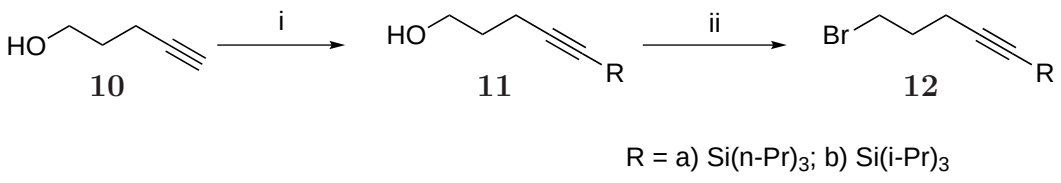

Scheme 2.7. Synthesis of silyl protected bromo pentyne derivatives. Reagents and conditions: i) a: EtMgBr, $(n\text{-Pr})_3$SiCl reflux, THF, 66%; b: EtMgBr, $(i\text{-Pr})_3$SiCl, THF, reflux, 70%; ii) CBr_4, PPh_3, Et_2O, a = 71%, b = 78%.

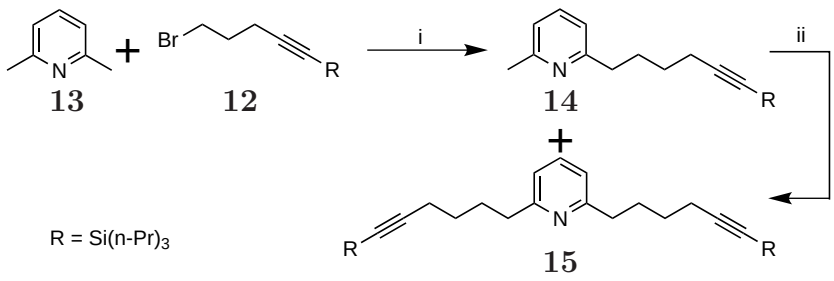

Scheme 2.8. Route towards the MDL1 **15**. Reagent and conditions: i) **13**, **12b**, *n*-BuLi, THF, $-50\,^{\circ}\mathrm{C}$, 34%.

Monodentate ligand (**15**) was synthesised from 2,6-lutidine, which was doubly deprotonated with *n*-BuLi and reacted with **12a** (Scheme 2.8). This reaction delivered predominantly the monosubstituted and some disubstituted product. However, the monosubstituted lutidine derivative could be resubmitted to the same reaction conditions to increase the yield.

Due to the relatively low yields and the difficult isolation of the desired products **15**, developing a new route towards a suitable alkyne-containing 2,6-disubstituted pyridine became necessary. Ideally a high yielding metal mediated cross coupling reaction with good to excellent tolerance towards silyl protected alkynes should be employed. A suitable candidate is the palladium-catalysed Negishi cross coupling reaction, which is capable of forming an sp^3-sp^2-carbon-carbon bond between an organozinc compound (sp^3-part) and a halogen substituted aromatic substrate (sp^2-part). This approach would necessitate the use of a 6-trialkylsilylhex-5-yn-1-bromide, to stay consistent with respect to the spacer length between the aromatic core and the alkyne units. However, the formation of the organozinc compound from 6-trialkylsilylhex-5-yn-1-bromide, would exclusively produce cyclopentylidenemethyl-trialkyl-silane, as was demonstrated by Negishi et al.[11] To circumvent these problems, the far less frequently employed sp^3-sp^3 Negishi cross-coupling procedure, developed by Organ et al.,[12] was tested for its ability to produce **MDL1** (**15**) from the commercially available 2,6-bis(bromomethyl)pyridine **17** and the zincate of **12b**.

This reaction failed to yield the desired product and therefore the decision to was made to use a spacer one carbon shorter in length. Hence a route towards the

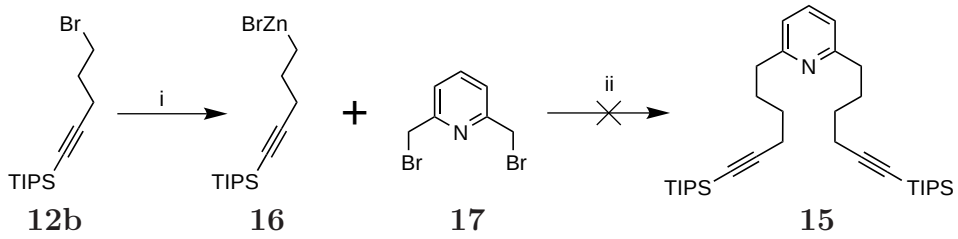

Scheme 2.9. Route towards MDL1 **15**. Reagent and conditions: i) **12b**, Zn dust, I_2, NMP, 80 °C; ii) **16**, **17**, PEPPSI, LiBr, NMP / THF, RT.

2,6-di(5-tri-*i*-propylsilylpent-4-ynyl)-pyridine **19** was developed (Scheme 2.10). Starting from the previously prepared 5-tri-*i*-propylsilylpent-4-yn-1-bromide **12b** and subjecting it to the zincation conditions, using zinc dust activated *in situ* with iodine at 80 °C, the reaction cleanly yielded the desired organozinc compound **16**. **16** was then reacted with with 2,6-dibromopyridine **18** and the PEPPSI catalyst, which predominantly forms the doubly substituted product, to afford the 2,6 substituted pyridine derivative **19** in good yield (81%).

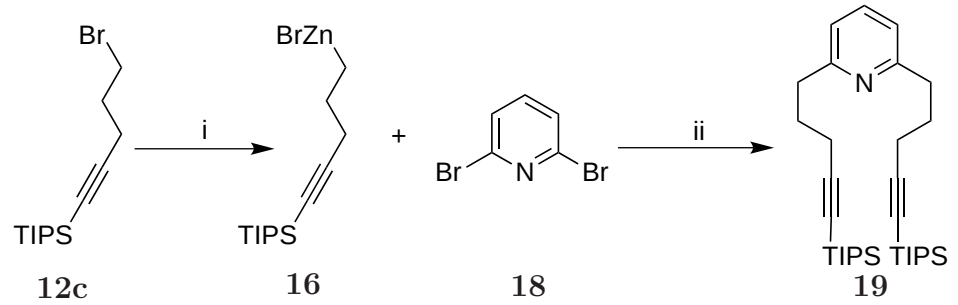

Scheme 2.10. PEPPSI-catalysed Negishi cross-coupling. Reagents and conditions: **12c**, Zn powder, NMP, 80 °C; ii) **16**, **18** , PEPPSI, LiBr, RT, NMP / THF, 81% (over 2 steps).

2.6.2 Synthesis of the Bisphenol U-Shape BPU

The synthesis of 2,6-di(4-hydroxybenzyl-N-amido)pyridine **22** was previously achieved by reacting 4-aminomethyl-phenol with the commercially available 2,6-pyridinedicarbonyl dichloride at −78 °C to afford the desired product in up to 99% yield (Scheme 2.11).[13]

However, as the phenol positions are unprotected, they are able to form mixed ester amide u-shapes that co-crystallise, hence the color of the obtained product

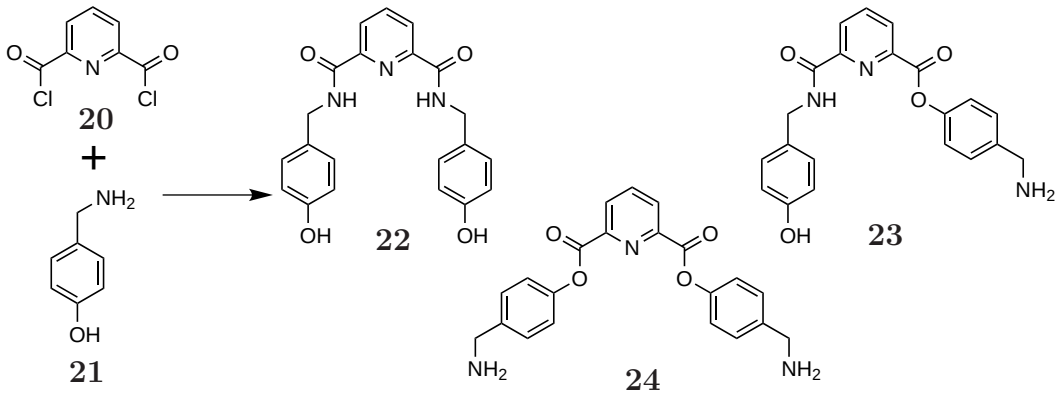

Scheme 2.11. Bisphenol U-Shape synthesis. Reagents and conditions: **20**, **21**, NEt_3, THF, $-78\,^{\circ}C$, 99%.

is increasingly brownish the more impurities are present. Using standard normal phase column chromatography to separate these impurities from the product proved to be impossible due to the very polar nature of all products. Usually **22** was subjected to a Williamson ether forming reaction, where, in the presence of base and nucleophiles, the ester bonds can be cleaved and therefore makes it possible to remove these impurities. Nonetheless, when palladium is to be inserted into **22**, synthesised with the above described method, the outcome is complete degradation of the substrate together with the formation of some palladium black. Therefore a new route for the synthesis of highly pure **22** was developed (Scheme 2.12).

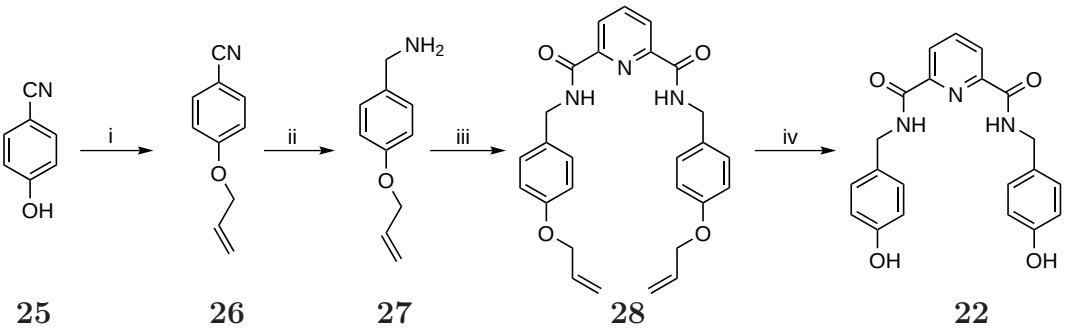

Scheme 2.12. Revised synthesis of Bisphenol U-Shape. Reagents and conditions: i) **25**, allyl bromide, K_2CO_3, DMF, 88%; ii) **26**, $LiAlH_4$, THF, 58%; **27**, pyridine-2,6-dicarboxylic acid chloride, CH_2Cl_2, 91%; iv) **28**, Pd/C, MeOH / H_2O, 88%.

It starts from the commercially available phenol **25**, which was converted into the allyl ether **26** and purified by fractionated distillation. This was followed by the reduction of the nitrile with $LiAlH_4$ to obtain the benzylic amine **27**. The

reaction product could be directly used for the next reaction step without further purification. Subsequent amide formation with the 2,6-pyridinedicarbonyl dichloride in CH_2Cl_2 with NEt_3 as base at 0 °C gives the desired product **28** in excellent yield. Finally, the reductive deallylation of the phenol using Pd/C and p-toluenesulfonic acid in water / methanol, affords the 2,6-(4-hydroxybenzyl-*N*-amido)-pyridine **BPU** as shiny white crystals with a melting point of 211 °C in contrast to the previously reported decomposition at 200 °C.[13] This constitutes the main precursor for the following synthesis of the building blocks and represents the core structure of any tridentate ligand that follows.

2.6.3 Synthesis of the Building Block BB1

The synthesis of **BB1** (**29**) poses a challenge due to the four incorporated alkynes in the presence of a palladium core. Therefore the synthesis sequence has to circumvent the presence of terminal alkynes when introducing the palladium(II) anchor into the tridentate ligand. When the palladium is coordinated to the tridentate, its ability to activate alkynes is inhibited. On the other hand, post coordinative manipulation of a palladium complex has to carefully avoid any reagents or byproducts that might reduce or oxidise the metal, or that can act as ligands. Further, the alkylation of the phenolic positions with a pentynyl substituent has to be carried out with the monodentate position blocked by a strongly coordinating ligand, to avoid complex decomposition.

In light of all these requirements, the synthesis started from the BPU **22** into which palladium was introduced as $Pd(OAc)_2$ (Scheme 2.13). Although BPU **22** and the palladium salt are not very soluble in MeCN, throughout the course of the reaction both starting materials get consumed visibly, culminating in a clear deep brown-red solution from which the product precipitates upon further stirring as dark yellow amorphous powder **30**. The pre-metallated U-shape is then subjected to a ligand exchange reaction, where the labile acetonitrile is displaced by the monodentate ligand **MDL1 15**, affording the desired product **31** in moderate yield (54%). To complete the synthesis of **BB1 29**, a Mitsunobu reaction on the phenolic positions of complex **31** was carried out. The reaction

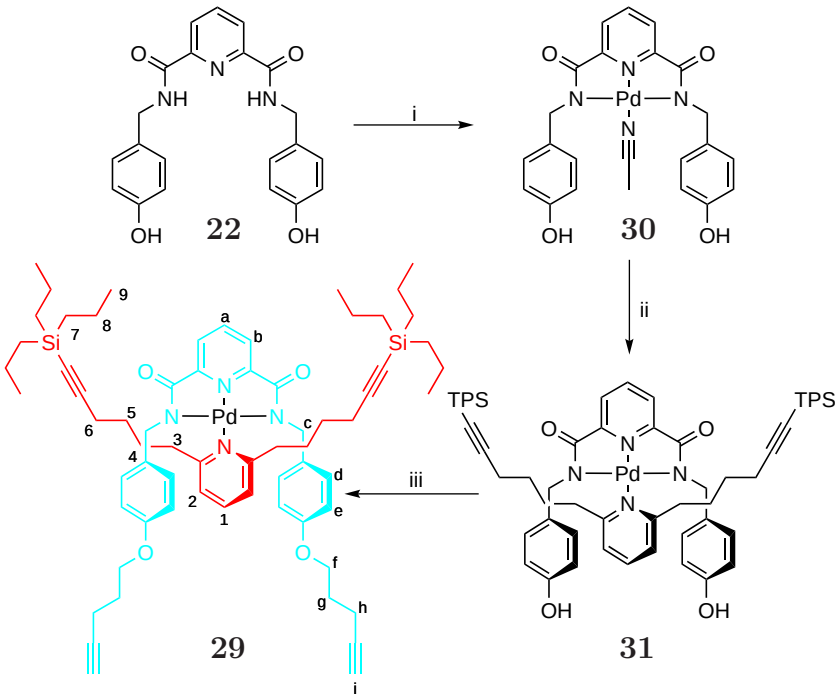

Scheme 2.13. Synthsis of BB1 **29** from **22** and MDL1 **15**. Reagents and conditions: i) **22**, $Pd(OAc)_2$, MeCN, 98%; ii) **15**, **30**, MeOH, 54%; iii) **31**, pent-4-yn-1-ol, DIAD, PPh_3, THF, 29%.

was conducted according to standard conditions of coupling primary alcohols to phenolic positions, using an 1.5 eq excess of PPh_3, DIAD and pent-4-yn-1-ol per coupling site. As triphenylphosphine is very bulky, it was hoped to avoid ligand exchange due to the steric demand of the phosphine which should not be able to be accommodated inside the cavity of the tridentate ligand. After 72 h the reaction mixture was purified by column chromatography, and the product was obtained as an amorphous yellow solid that still contained triphenylphosphine oxide ($OPPh_3$), which could not be removed by successive purification efforts. Fortunately, this product could be used for the later steps, as $OPPh_3$ is not known to inhibit the envisaged "click"-reaction. The low yield of the Mitsunobu reaction is one of the major drawbacks of this synthesis. So far, a large excess of phosphine and other reagents was avoided, leading to a lower conversion. Ligand exchange was observed to some extend, but not quantified due to the large amounts of by-products. Further, the product slowly degrades, even in the dark and under an atmosphere of nitrogen.

Figure 2.8 shows a stacked plot of the ^{1}H-NMR spectra of **MDL1 15** (Figure

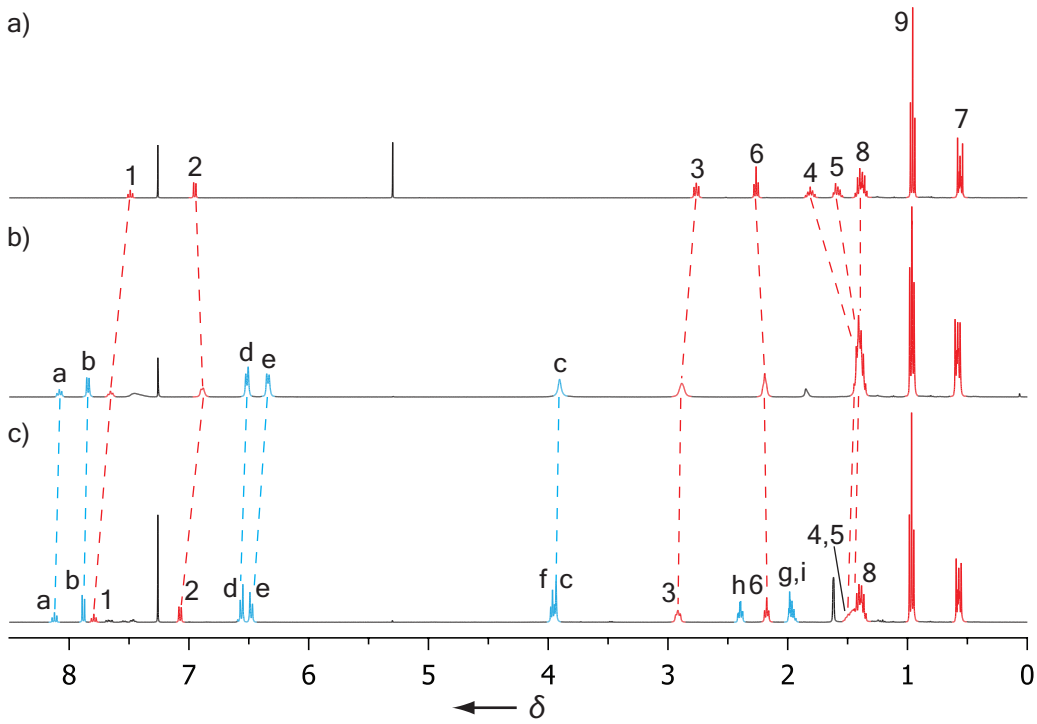

Figure 2.8. ^{1}H-NMR (400 MHz, $CDCl_3$, 300 K) of a) monodentate ligand **MDL1 15**; b) **31**; c) **BB1 29**. The assignment corresponds to the lettering shown in Figure 2.13

2.8a), the bisphenol complex **31** (Figure 2.8b) and **BB1 29** (Figure 2.8c). The spectrum of **31** shows π-stacking interactions between the 2,6-disubstituted pyridine of the monodentate ligand and the flanking phenol moieties of the tridentate ligand represented by the protons H_d and H_e. Monodentate ligand protons H_1 and H_3 exhibit a downfield shift upon complexation, whereas proton H_2 is shifted upfield. The monodentate protons H_{4-6} are shifted upfield, indicating a shielding effect caused by the flanking phenol moieties of the tridentate, which decreases with distance from the pyridine core. Upon alkylation, all protons in the aromatic region show downfield shifts and increased π-stacking. Due to the simplicity of the spectrum of **BB1 29** it is possible to infer a C_{2v} symmetry in solution.

2.6.4 Synthesis of the Building Block BB2

The synthesis of **BB2** (**34**) (Scheme 2.14) follows the outlined route in the retrosynthesis section. Starting from the common precursor **BPU 22**, a double Williamson ether forming reaction was used to alkylate the phenol positions. As

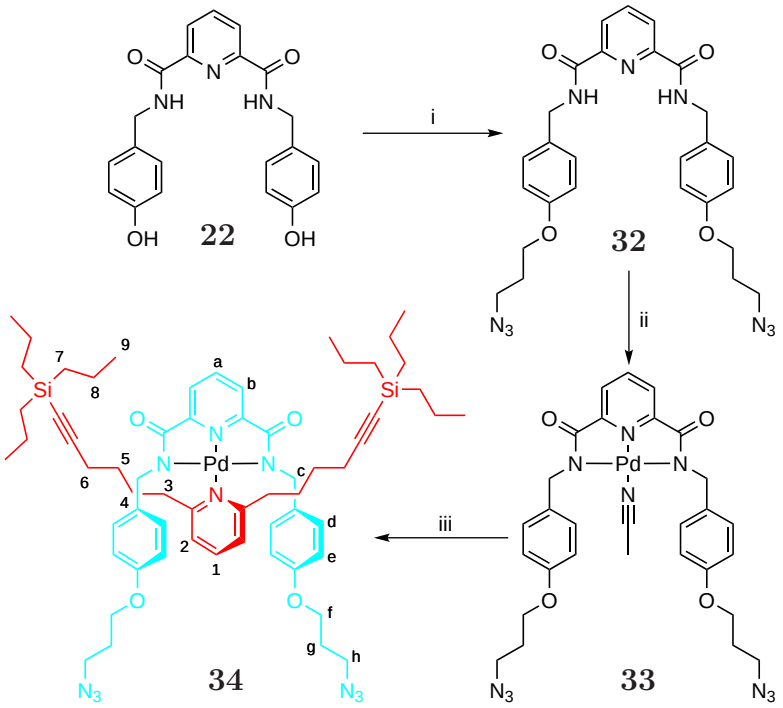

Scheme 2.14. Synthesis of **BB2** from main precursor **BPU** (**22**) and **MDL1** (**15**). Reagents and conditions: i) **22**, $TsO(CH_2)_3N_3$, K_2CO_3, 2-butanone, reflux, 85%; ii) **32**, $Pd(OAc)_2$, MeCN, 86%; iii) **33**, **15**, MeOH, 83%.

alkylating agent $TsO(CH_2)_3N_3$ was used, which was prepared according to literature procedure developed in the Leigh group.[14] This reaction afforded **32** in good yield (85%). Taking advantage of the rather large tosyl leaving group avoids the use of low molecular weight organic azides, as these compounds are known to be potentially explosive. Inserting the palladium metal into the tridentate ligand by simply stirring the two components in MeCN affords the product **33** as yellow-green powder upon precipitation with Et_2O in good yield (86%). Subsequent ligand exchange of the labile acetonitrile ligand with **MDL1** (**15**) leads to the desired **BB2 34** in very good yield (83%). Therefore the combined yield over three steps is 60%, using simple procedures, thus allowing facile acess to **34**.

The ^{1}H-NMR of **BB2** (**34**) is shown in Figure 2.9b, together with the spectra of its constituents **MDL1** (**15**) (Figure 2.9a) and **32** (Figure 2.9c) for comparison. **BB2** (**34**) clearly shows a C_{2v} symmetry, with strong π-stacking between the coordinated monodentate ligand **MDL1 15** and the aromatic protons H_d and H_e of the tridentate ligand **32**. Strong downfield shifts of the protons H_b ($\Delta\sigma$ = -0.53 ppm), H_c ($\Delta\sigma$ = -0.66 ppm) and H_e ($\Delta\sigma$ = -0.69 ppm) indicate a significant

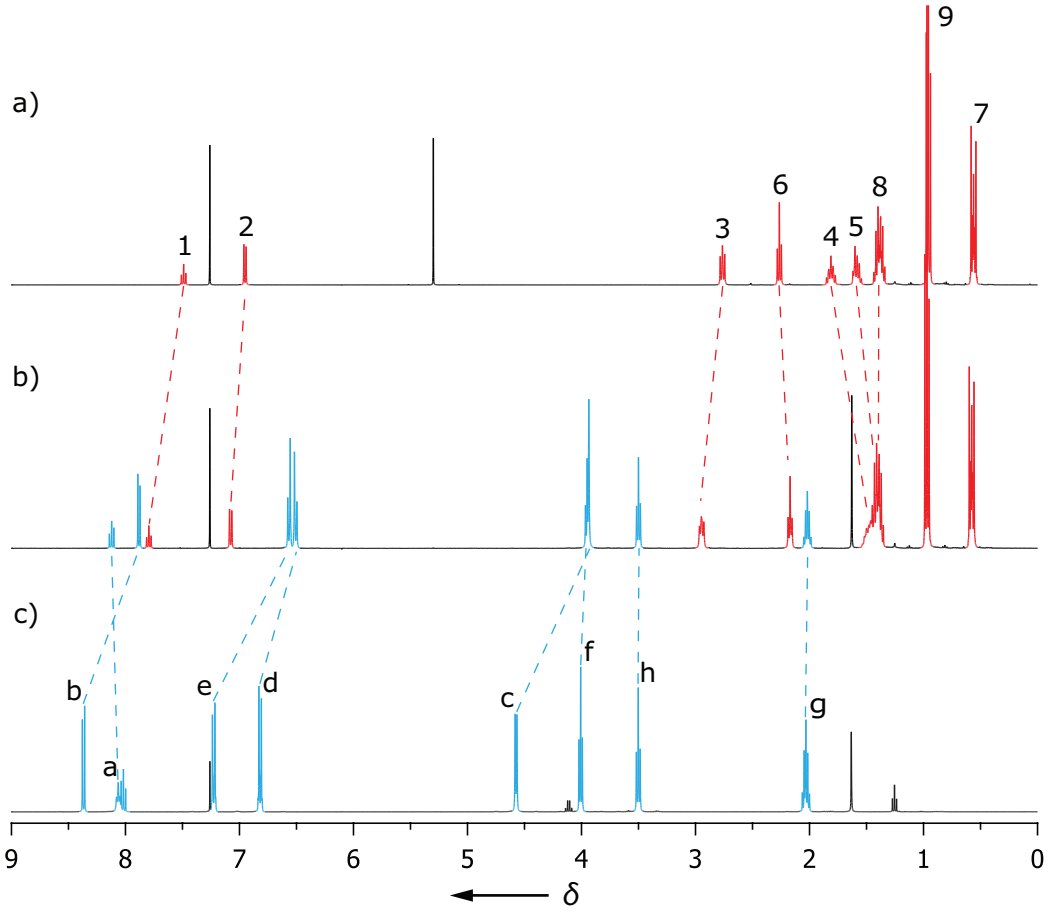

Figure 2.9. ^{1}H-NMR (400 MHz, $CDCl_3$, 300 K) of a) monodentate ligand **MDL1** (**15**); b) **BB2** (**34**); c) tridentate ligand **32**. The assignment corresponds to the lettering shown in Figure 2.14

metal to ligand backbonding. In contrast, the aromatic signals H_1 ($\Delta\sigma$ = 0.31 ppm), H_2 ($\Delta\sigma$ = 0.12 ppm) and the aliphatic proton H_3 ($\Delta\sigma$ = 0.19 ppm) of **MDL1** (**15**) are shifted downfield, indicating that these protons are experiencing the electron withdrawing effect of the central metal, without the benefit of metal to ligand backbonding. The rest of the protons H_{4-6} of the coordinated **MDL1** (**15**) show a shielding effect with decreasing intensity the further they are located from the pyridine core.

2.6.5 Synthesis of the Main Scaffold MS

The synthesis of the **MS** (**35**) was the central step of the synthesis and performed as a double "click" ring-closure reaction (Scheme 2.15). Generally macrocyclisations are difficult reactions, which are performed under high dilution to avoid

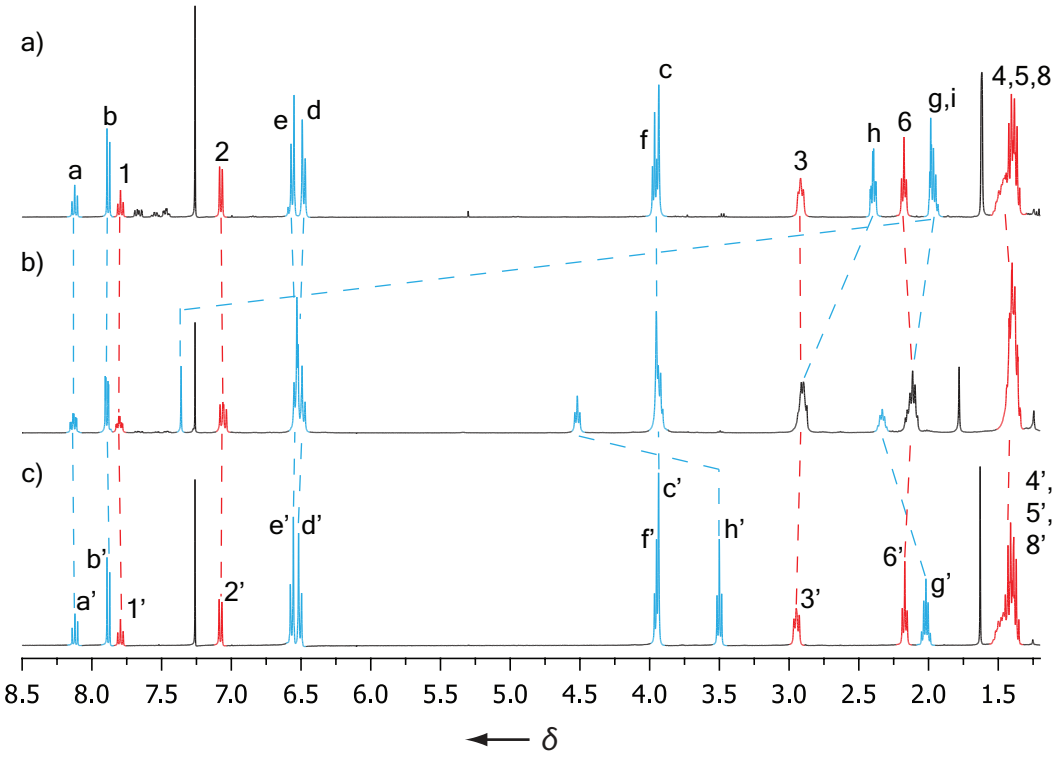

Figure 2.10. ^{1}H-NMR (400 MHz, $CDCl_3$, 300 K) of a) BB1 **29**; b) MS **35**; c) BB2 **34**. The assignment corresponds to the lettering shown in Figure 2.15.

polymerisation of the substrates used. This leads to long reaction times and often incomplete conversion. Further, when complementary recognition motifs are formed, this could lead to mechanically interlocked structures or to coordination polymers when metals are present.

The double click-reaction was performed at RT in CH_2Cl_2 at a 0.25 mM concentration with respect to the building blocks **BB1** and **BB2**, using $[Cu(MeCN)_4]PF_6$ as copper(I) source. As amine ligand for the copper, 11 eq. of DIPEA were used. The large excess of amine is used to prevent copper acetylide cluster formation and increase the reaction rate due to increased availability of the reactive copper acetylide intermediate. The catalyst load was 20 mol% at the start of the reaction and was maintained at approximately that level by adding 20 mol% increments each day. Meticulous exclusion of oxygen ensured that oxidation of the copper(I) species did not culminate in alkyne-alkyne homocoupling of **BB1** (**29**). After 5 days no further reaction occurred, as shown by TLC. After purification by column chromatography, the desired product **35** was isolated as a yellow varnish in 35% yield.

The ^{1}H-NMR spectra of **MS 35**, **BB1** and **BB2** are shown in Figure 2.10. The spectrum of **MS 35** (Figure 2.10b) exhibits strong downfield shifts for the protons adjacent to the formed triazole ring $H_{h'}$ ($\Delta\sigma$ = 0.95 ppm) and H_h ($\Delta\sigma$ = 0.56 ppm). As expected, proton H_i the former terminal alkyne proton, shows a downfield shift of 5.30 ppm, as it is now part of the electron deficient triazole unit. The rest of the spectrum of **MS 35** resembles a superposition of **BB1 29** and **BB2 34**, indicating that the structural features of the building blocks remain largely unchanged with retention of the C_{2v} symmetry in solution.

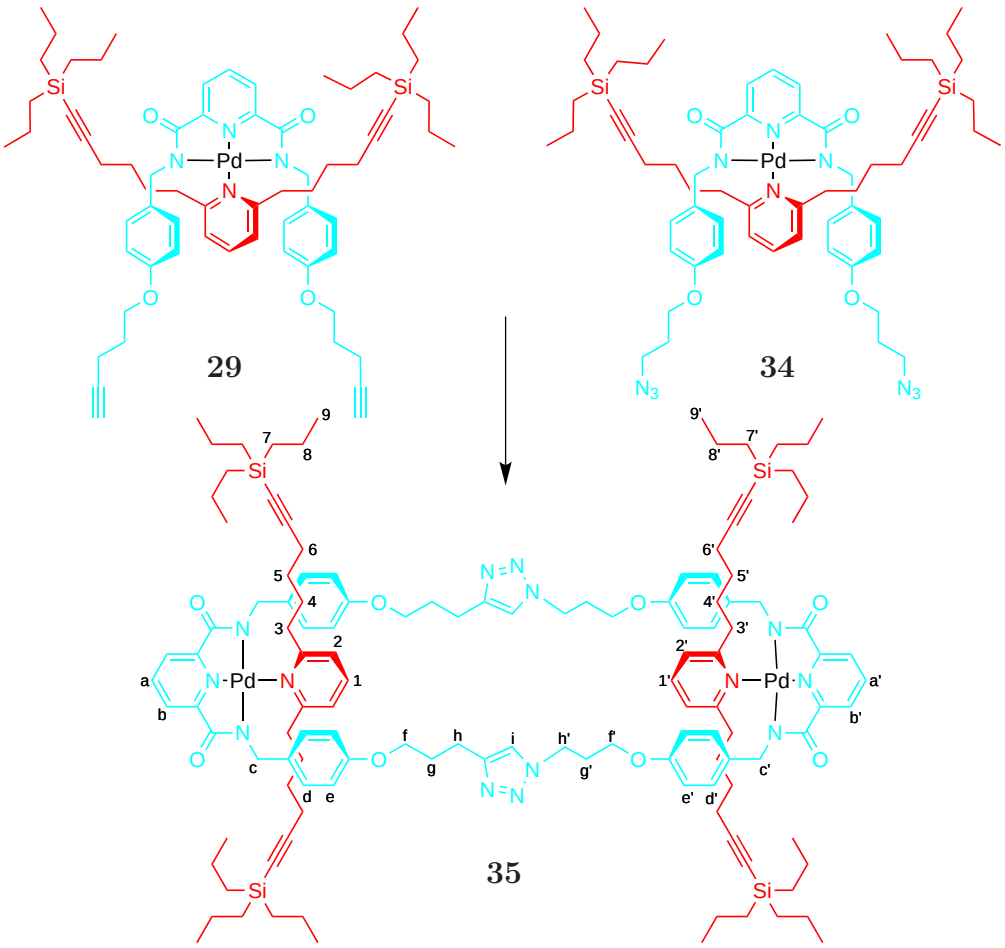

Scheme 2.15. Synthesis of MS from the main building blocks BB1 (**29**) and BB2 (**34**). Reagents and conditions: **BB1 29**, **BB2 34**, $[Cu(MeCN)_4]PF_6$, DIPEA, CH_2Cl_2, c = 0.25 mM, RT, 5 d, 35%.

2.7 Conclusions

The successful synthesis of the the Main Scaffold (**MS**) from its acyclilc building blocks **BB1** and **BB2** by a double "click" macrocyclisation marks the starting point towards a possible stepwise synthesis of a Borromean link. The revised monodentate ligand synthesis is efficient and simple in contrast to the initial strategy. The synthesis of **BB2** is high yielding and allows facile access to this important precursor. The challenging synthesis of a alkyne-containing palladium(II) templated building block **BB1**, was successfully implemented by introducing the alkyne funcionalities at a very late stage. Although the achieved yields in the Mitsunobu reaction were only moderate, further optimisation is possible as shown in later chapters. In conclusion, the double "click" ring-closure of two complementary building blocks gives access to the underlying framework of a stepwise Borromean link synthesis, without the need of threading the individual components.

2.8 Experimental

2.8.1 General

3-Azidopropyl tosylate was prepared according to literature procedure.[14]

2.8.2 Synthesis

5-Tri-n-propylsilylpent-4-yn-1-ol (11a)

A solution of 4-pentyn-1-ol (8.43 g, 95.3 mmol) in THF (250 mL) was prepared under an atmosphere of nitrogen, and a solution of ethylmagnesium bromide (2 M, 100 mL, 200 mmol) in THF was added. The mixture was then refluxed for 16 h, cooled to RT and a solution of tri-*n*-propylsilyl chloride (18.4 g, 95.3 mmol) in THF (50 mL) was added. The mixture was then refluxed another 16 h, cooled to RT and poured into a 1 M HCl solution, extracted with Et_2O and dried over $MgSO_4$. After filtration and concentration under reduced pressure, the crude was purified by distillation under high vacuum to give the desired product as colourless viscous oil (15.0 g, 66%).

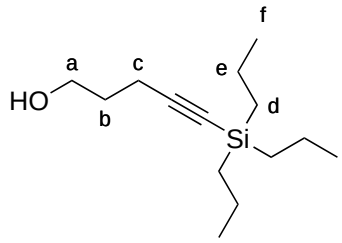

^{1}H-NMR (400 MHz, $CDCl_3$, 300 K): δ = 3.76 (t, 2H, J = 6.0 Hz, H_a), 2.35 (t, 2H, J = 6.8 Hz, H_c), 1.80-1.73 (m, 2H, H_b), 1.43-1.32 (m, 6H, H_e), 0.96 (t, 9H, J = 7.2 Hz, H_f), 0.59-0.54 (m, 6H, H_d).
^{13}C-NMR (100 MHz, $CDCl_3$, 300 K): δ = 107.5, 83.2, 62.0, 31.2, 18.2, 17.4, 16.6, 16.1.
HREI-MS: m/z = 240.19111 $[M]^+$ (calc. for $C_{14}H_{28}OSi$ 240.19149)

5-Tri-n-propylsilylpent-4-yn-1-bromide (12a)

A solution of 5-tripropylsilylpent-4-yn-1-ol (11.2 g, 46.5 mmol) in dry Et_2O (80 mL) was prepared, CBr_4 (19.3 g, 58.2 mmol) was added and the mixture

was cooled to 0 °C. After portion-wise addition of PPh_3 (14.0 g, 53.5 mmol), the cooling bath was removed, and the mixture allowed to stir for 16 h. The crude mixture was concentrated under reduced pressure and the residue dissolved in cold hexane, followed by filtration. The resulting solution was concentrated under reduced pressure and the crude was distilled under high vacuum. The resulting oil was passed through a plug of silica using hexane as eluent. The product was obtained after evaporation of the volatiles as a colourless oil (10 g, 71%)

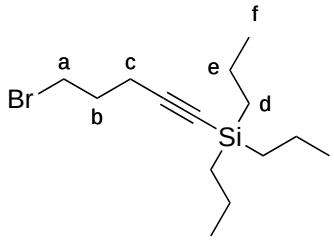

^{1}H-NMR (400 MHz, $CDCl_3$, 300 K): δ = 3.52 (t, 2H, J = 6.5 Hz, H_a), 2.42 (t, 2H, J = 6.7, H_c), 2.07-2.00 (m, 2H, H_b), 1.43-1.34 (m, 6H, H_e), 0.97 (t, 9H, J = 7.3, H_f), 0.59-0.55 (m, 6H, H_d).

^{13}C-NMR (100 MHz, $CDCl_3$, 300 K): δ = 106.11, 83.88, 32.38, 31.65, 18.74, 18.35, 17.64, 16.30.

HREI-MS: m/z = 302.10579 $[M]^+$

(calc. for $C_{14}H_{27}BrSi$ 302.10709)

5-Tri-i-propylsilylpent-4-yn-1-ol (11b)[10]

A solution of 4-pentyn-1-ol (8.43 g, 95.3 mmol) in THF (250 mL) was prepared under an atmosphere of nitrogen and a commercially available solution of ethylmagnesium bromide (2 M, 100 mL, 200 mmol) in THF was added. The mixture was then refluxed for 16 h, cooled to RT and a solution of tri-*i*-propylsilyl chloride (18.4 g, 95.3 mmol) in THF (50 mL) was added. The mixture was then refluxed 16 h, cooled to RT and poured into a 1 M HCl solution, extracted with Et_2O and dried over $MgSO_4$. After filtration and concentration under reduced pressure, the crude was purified by distillation under high vacuum to give the desired product as colourless viscous oil (16.1 g, 70%).

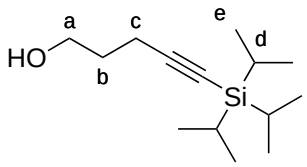

^{1}H-NMR (400 MHz, $CDCl_3$, 300 K): δ = 3.76 (t, 2H, J = 5.6 Hz, H_a), 2.36 (t, 2H, J = 6.8 Hz, H_c), 1.80-1.73 (m, 2H, H_b), 1.06-1.01 (m, 21H, $H_{d/e}$).

^{13}C-NMR (100 MHz, $CDCl_3$, 300 K): δ = 108.36, 81.16, 62.00, 31.55, 18.71, 16.67, 11.36.

LRESI-MS: m/z = 263 $[M + Na]^+$.

HRESI-MS: m/z = 263.18195 $[M + Na]^+$

(calc. for $C_{14}H_{28}NaOSi$ 263.18126)

5-Tri-i-propylsilylpent-4-yn-1-bromide (12b)

5-Tri-*i*-propylsilylpent-4-yn-1-ol (16.1 g, 66.9 mmol) was dissolved in dry Et_2O (150 mL) and CBr_4 (27.7 g, 83.6 mmol) added. The mixture was cooled to 0 °C and PPh_3 (21.3 g, 76.9 mmol) was added portion wise. Then, the cooling bath was removed and the reaction mixture was allowed to stir for 16 h. The reaction was quenched by addition of EtOH, concentrated under reduced pressure and distilled under high vacuum to obtain the desired product as a colourless viscous oil (16 g, 78%).

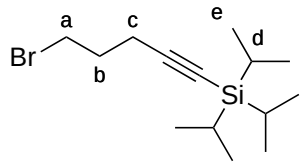

^{1}H-NMR (400 MHz, $CDCl_3$, 300 K): δ = 3.55 (t, 2H, J = 6.5 Hz, H_a), 2.45 (t, 2H, J = 6.7 Hz, H_c), 2.08-2.01 (m, 2H, H_b), 1.10-0.98 (m, 21H, $H_{d/e}$).

^{13}C-NMR (100 MHz, $CDCl_3$, 300 K): δ = 106.5, 81.6, 32.3, 31.5, 18.6, 18.6, 11.2.

HREI-MS: m/z = 302.10579 $[M]^+$

(calc. for $C_{14}H_{27}BrSi$ 302.10709)

2,6-Di(6-tri-n-propylsilylhex-5-ynyl)pyridine (15)

A solution of *n*-BuLi (5.30 mL, 13.2 mmol) in dry THF (5 mL) was cooled to −50 °C and a solution of 2,6-dimethylpyridine (0.6 mL, 0.55 g, 5.27 mmol) in dry THF (15 mL) was added. After 1 h, the cooling bath was removed for 30 min. The mixture was cooled to −40 °C and a solution of 5-tri-*n*-propylsilylpent-4-yn-1-bromide (4.00 g, 13.2 mmol) in dry THF (15 mL) was added. After 30 min, the cooling bath was removed and the resulting mixture was allowed to stir for 16 h. The reaction mixture was cooled to 0 °C and quenched by addition of NH_4Cl. The crude was diluted with EtOAc and dried over $MgSO_4$. After filtration, the crude mixture was concentrated under reduced pressure and the residue was purified by column chromatography (Hexane 95% / Et_2O 5%) to give the desired product as a colourless viscous oil (1 g, 34%).

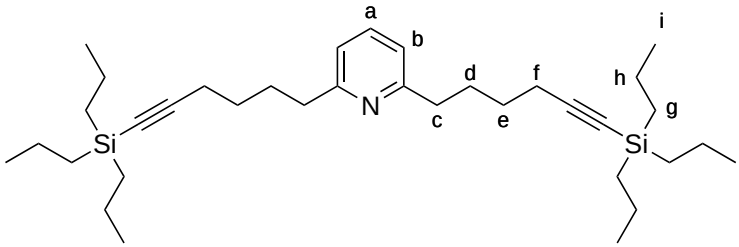

^{1}H-NMR (400 MHz, $CDCl_3$, 300 K): δ = 7.48 (t, 1H, J = 7.6 Hz, H_a), 6.95 (d, 2H, J = 7.6 Hz, H_b), 2.76 (t, 4H, J = 7.8 Hz, H_c), 2.26 (t, 1H, J = 7.1 Hz, H_f), 1.85-1.77 (m, 4H, H_d), 1.61-1.54 (m, 4H, H_e), 1.43-1.33 (m, 12H, H_h), 0.95 (t, 12H, J = 7.2 Hz, H_g), 0.58-0.54 (m, 18H, H_i).

^{13}C-NMR (100 MHz, $CDCl_3$, 300 K): δ = 161.4, 136.4, 119.6, 108.3, 82.3, 37.8, 29.1, 28.3, 19.7, 18.2, 17.5, 16.2.

LRESI-MS: m/z = 552 $[M + H]^+$.

HRESI-MS: m/z = 552.44326 $[M + H]^+$

(calc. for $C_{35}H_{62}NSi_2$ 552.44263)

2,6-di(5-tri-i-propylsilylpent-4-ynyl)-pyridine (19)

A dry Schlenk tube was charged with activated Zn powder (850 mg, 13.0 mmol) and I_2 (110 mg, 0.44 mmol) under an atmosphere of nitrogen and dry *N*-methyl-2-pyrrolidone (9 mL) was added. When the colour of the iodine vanished, 5-tri-*i*-

propylpent-4-yn-1-bromide (2.50 g, 8.70 mmol) was added, and the mixture was stirred for 4 h at 80 °C. The suspension was allowed to settle at RT. A dry Schlenk tube was charged with PEPPSI (102 mg, 0.15 mmol) and LiBr (1.40 g, 16.1 mmol) under an atmosphere of nitrogen. Dry THF (9 mL) and *N*-methyl-2-pyrrolidone (9 mL) were added. To this solution was added the previously prepared 5-tri-*i*-propylsilylpent-4-ynyl-zinc-bromide solution and the resulting mixture was stirred for 10 min. Then, 2,6-dibromopyridine was added, and the resulting solution was allowed to stir for 16 h. The crude mixture was diluted with Et_2O and washed with 1 M Na_3HEDTA solution (300 mL), water (300 mL) and brine. After concentrating under reduced pressure, the crude was purified by column chromatography (hexane 95% / Et_2O 5%) to obtain the desired product as a colourless viscous oil (1.15 g, 81%).

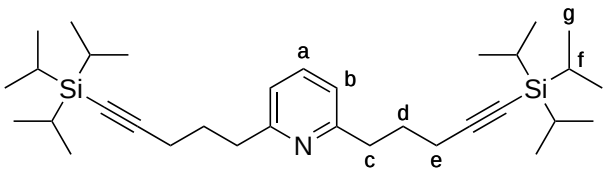

^{1}H-NMR (400 MHz, $CDCl_3$, 300 K): δ = 7.48 (t, 1H, J = 7.6 Hz, H_a), 6.97 (d, 2H, J = 7.6 Hz, H_b), 2.88 (t, 4H, J = 7.6 Hz, H_c), 2.28 (t, 4H, J = 6.9 Hz, H_e), 2.00-1.88 (m, 4H, H_d), 1.10-1.01 (m, 21H, $H_{f/g}$).

^{13}C-NMR (100 MHz, $CDCl_3$, 300 K): δ = 160.9, 136.5, 120.2, 108.7, 80.6, 37.2, 29.1, 19.4, 18.6, 11.3.

LRESI-MS: m/z = 524 $[M + H]^+$.

HRESI-MS: m/z = 524.40964 $[M + H]^+$

(calc. for $C_{33}H_{57}N_1Si_2$ 524.41023)

p-Allyloxybenzonitrile (26)

p-Hydroxybenzonitrile (79.8 g, 0.67 mol) was dissolved in DMF (250 mL), and potassium carbonate (278 g, 2.01 mol) and allyl bromide (162 g, 1.34 mol) were added at RT. The mixture was stirred for 24 h, poured into water, and then extracted with CH_2Cl_2 (3 x 150 mL). The extract was washed with water, dried over $MgSO_4$, and concentrated under reduced pressure. The pale yellow oil was

distilled under high vacuum to give *p*-(allyloxy)benzonitrile as colorless oil (94.8 g, 88%).

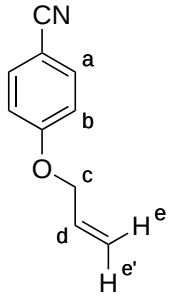

^{1}H-NMR (400 MHz, $CDCl_3$, 300 K): δ = 7.57 (d, 2H, J = 8.9 Hz, H_a), 6.96 (d, 2H, J = 8.9 Hz, H_b), 6.03 (m, 1H, H_d), 5.42 (dd, 1H, J = 15.8, 1.5 Hz, H_e), 5.32 (dd, 1H, J = 9.2, 1.3 Hz, $H_{e'}$), 4.58 (m, 2H, H_c).

^{13}C-NMR (100 MHz, $CDCl_3$, 300 K): δ = 161.85, 133.98, 132.09, 119.24, 118.50, 115.47, 104.02, 69.00.

LREI-MS: m/z = 159 $[M]^+$.

HREI-MS: m/z = 159.06865 $[M]^+$

(calc. for $C_{10}H_9NO$ 159.06896)

p-(Allyloxy)benzylamine (27)

A dry 2 L roundbottomed flask was charged with $LiAlH_4$ (33.1 g, 0.87 mol) and flushed with nitrogen. After addition of dry THF (0.7 L) the suspension was stirred for 20 min and a solution of *p*-(allyloxy)benzonitrile (55.7 g, 0.35 mol) in THF (300 mL) was added over 30 min and stirred for another 10 min. The suspension was refluxed for 24 h and then slowly quenched with THF / 1 M NaOH solution followed by filtration. The resulting solution was concentrated under reduced pressure until the total volume was around 250 mL, diluted with 500 mL water and extracted with EtOAc (3 x 200 mL). The combined organic fractions were dried over $MgSO_4$, filtered and concentrated under reduced pressure to yield the desired product as a pale yellow oil (33.5 g, 58%). This product was used without any further purification.

Pyridine-2,6-dicarboxylic acid bis-(4-allyloxy-benzylamide) (28)

4-(Allyloxy)-benzylamine (33.5 g, 205 mmol) and triethylamine (20.7 g, 205 mmol) were dissolved in dry CH_2Cl_2 (1 L) and cooled to 0 °C. A solution of 2,6-di(chlorocarbonyl)-pyridine in dry CH_2Cl_2 (500 mL) was added during 1 h at 0 °C. After 1 h of further stirring, the ice bath was removed and the reaction mixture allowed to warm to RT. After 18 h the solution was washed with 1M HCl (2 x 500 mL), sat. $NaHCO_3$ (2 x 500 mL), brine (2 x 500 mL) and dried over $MgSO_4$. After filtration the solution was concentrated under reduced pressure and the desired product was precipitated as a white crystalline solid by slow addition of Et_2O (34.2 g, 91%).

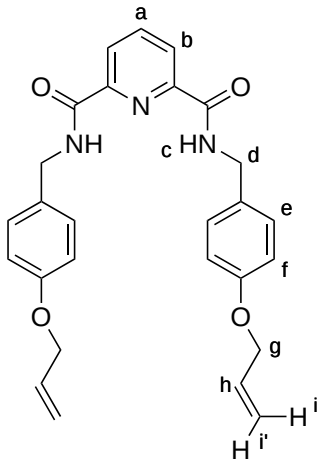

^{1}H-NMR (400 MHz, $CDCl_3$, 300 K): δ = 8.35 (d, 2H, J = 7.8 Hz, H_b), 8.14 (t, 2H, J = 6.0 Hz, H_c), 8.00 (t, 1H, J = 7.8 Hz, H_a), 7.18 (d, 4H, J = 8.6 Hz, H_f), 6.81 (d, 4H, J = 8.6 Hz, H_e), 6.02 (m, 2H, H_h), 5.39 (dd, 2H, J = 17.2, 1.6 Hz, H_i), 5.27 (dd, 2H, J = 10.5, 1.4 Hz, $H_{i'}$), 4.54 (d, 4H, J = 6.1 Hz, H_d), 4.48 (d, 4H, J = 5.3 Hz, H_g).

^{13}C-NMR (100 MHz, $CDCl_3$, 300 K): δ = 163.4, 157.9, 148.7, 138.9, 133.1, 130.2, 128.9, 125.2, 117.7, 114.8, 68.7, 42.8.

LRESI-MS: m/z = 457 $[M]^+$, 914 $[2M]^+$.

HRESI-MS: m/z = 475.24427 $[M + NH_4]^+$

(calc. for $C_{27}H_{31}N_4O_4$ 475.2340)

Pyridine-2,6-dicarboxylic acid bis-(4-hydroxy-benzylamide) (22)

Pyridine-2,6-dicarboxylic acid bis-(4-hydroxy-benzylamide) (32.7 g, 71.5 mmol) was suspended with Pd/C (4.43 g, 10% palladium loading), *p*-toluenesulfonic acid (4.43 g) in water (70 mL). Methanol (215 mL) was added under an atmosphere of nitrogen and this mixture was refluxed for 5 d. The suspension was diluted with methanol (250 mL) whilst hot, and then filtered through a plug of celite. The resulting solution was concentrated under reduced pressure and taken up in EtOAc, washed with water (3 x 250 mL) and dried over $MgSO_4$. After filtration, the product was precipitated on addition of Et_2O as a white crystalline powder (23.7 g, 88%).

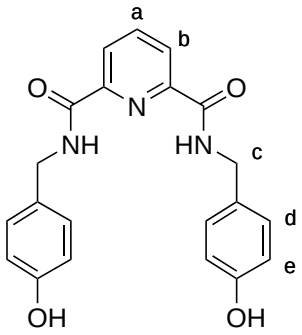

^{1}H-NMR (400 MHz, $CDCl_3$, 300 K): δ = 8.27 (d, 2H, J = 7.6 Hz, H_b), 8.12 (t, 1H, J = 7.8 Hz, H_a), 7.15 (d, 4H, J = 8.5 Hz, H_e), 6.71 (d, 4H, J = 8.5 Hz, H_d), 4.50 (s, 4H, H_c).

^{13}C-NMR (100 MHz, $CDCl_3$, 300 K): δ = 165.7, 157.7, 150.3, 140.4, 130.7, 129.9, 125.8, 116.2, 43.6.

LRESI-MS: m/z = 377 $[M]^+$.

HRESI-MS: m/z = 395.1716 $[M + NH_4]^+$ (calc. for $C_{21}H_{23}N_4O_4$ 395.1714)

mp = 211 °C.

Pyridine-2,6-dicarboxylic acid bis-[4-(3-azido-propoxy)-benzylamide] (32)

Pyridine-2,6-dicarboxylic acid bis-(4-hydroxy-benzylamide) (5 g, 13.3 mmol), 3-azidopropyl tosylate[14] (10.2 g, 39.8 mmol) and potassium carbonate (18 g, 0.13 mol) were suspended in 2-butanone (200 mL) and refluxed for 18 h. The suspension was allowed to cool to RT, diluted with CH_2Cl_2 (150 mL) and filtered.

The yellowish solution was concentrated under reduced pressure and the resulting residue purified by column chromatography. Upon evaporation of the solvent, the product was obtained as an off-white amorphous solid (6.14 g, 85%).

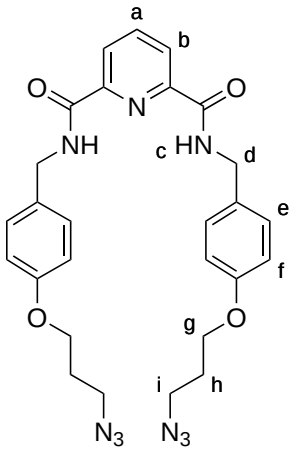

^{1}H-NMR (400 MHz, $CDCl_3$, 300 K): δ = 8.38 (d, 2H, J = 7.8 Hz, H_b), 8.03 (t, 1H, J = 7.8 Hz, H_a), 7.98 (t, 2H, J = 6.0 Hz, H_c), 7.25 (d, 4H, J = 8.8 Hz, H_f), 6.84 (d, 4H, J = 8.7 Hz, H_e), 4.59 (d, 4H, J = 6.2 Hz, H_d), 4.02 (t, 4H, J = 5.9 Hz, H_g), 3.50 (t, 4H, J = 6.6 Hz, H_i), 2.04 (m, 4H, H_h).
^{13}C-NMR (100 MHz, $CDCl_3$, 300 K): δ = 163.76, 157.87, 148.61, 138.73, 130.36, 128.87, 124.96, 114.31, 64.39, 48.11, 42.71, 28.63.
LRESI-MS: m/z = 544 $[M]^+$, 566 [M + Na].
HRESI-MS: m/z = 561.2679 $[M + NH_4]^+$
(calc. for $C_{27}H_{33}N_{10}O_4$ 561.2681)

{κ^3-2,6-bis-[4-(3-azido-propoxy)-benzylamide]-pyridino}(acetonitrile) palladium(II) (33)

2,6-*Bis*-(4-(3-azido-propoxy)-benzylamide)-pyridine (202 mg, 0.37 mmol) and palladium acetate (123 mg, 0.55 mmol) were dissolved in acetonitrile (8 mL) and stirred for 18 h. After that time Et_2O (50 mL) was added and the mixture was cooled to 0 °C and stirred 1 h. The desired yellow green crystalline product was filtered off, washed with Et_2O and dried under high vacuum (220 mg, 86%). This product was used without any further purification.

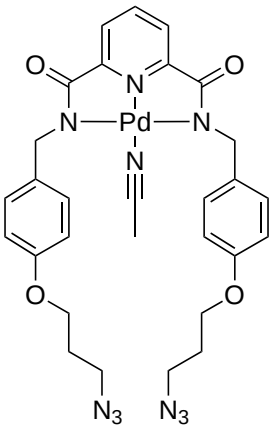

{κ^3-2,6-Bis-[4-(3-azido-propoxy)-benzylamide]-pyridino}(2,6-di(6-tri-n-propylsilyl-hex-5-ynyl)-pyridine) palladium(II) (34)

{κ^3-2,6-bis-[4-(3-azido-propoxy)-benzylamide]-pyridino}(acetonitrile) palladium(II) (220 mg, 0.32 mmol) and 2,6-di(6-tri-*n*-propylsilyl-hex-5-ynyl)-pyridine (265 mg, 0.48 mmol) were dissolved in methanol (20 mL) and stirred for 18 h. The reaction was monitored by TLC (4 % MeOH in CH_2Cl_2) and upon completion the solution was concentrated under reduced pressure to yield a yellow residue. The crude mixture was dissolved in CH_2Cl_2 and filtered through a plug of silica, where the product stays on the silica whilst the excess of ligand was washed out with CH_2Cl_2. The desired product was eluted using 4 % methanol in CH_2Cl_2 and obtained as a deep yellow amorphous solid upon concentration under reduced pressure (320 mg, 83%).

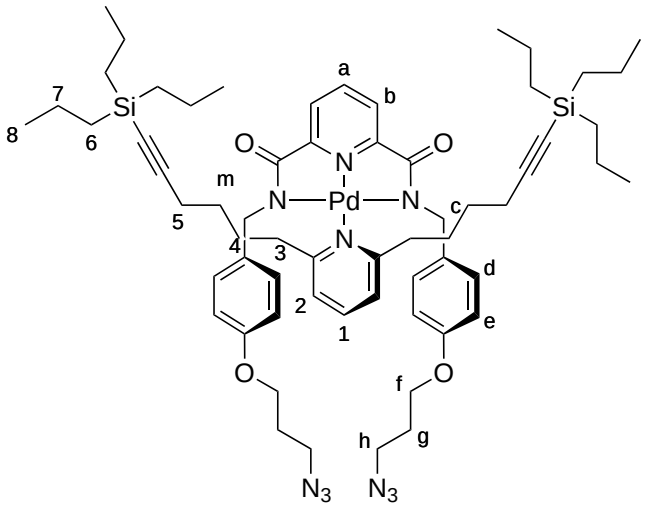

^{1}H-NMR (400 MHz, $CDCl_3$, 300 K): δ = 8.12 (t, 1H, J = 7.8 Hz, H_a), 7.85 (d, 2H, J = 7.8 Hz, H_b), 7.79 (t, 1H, J = 7.8 Hz, H_1), 7.07 (d, 2H, J = 7.8 Hz, H_2), 6.56 (d, 4H, J = 8.7 Hz, H_e), 6.51 (d, 4H, J = 8.7 Hz, H_d), 3.93-3.96 (m, 8H, $H_{c/f}$), 3.50 (t, 4H, J = 6.6 Hz, H_h), 2.95 (t, 4H, J = 7.6 Hz, H_3), 2.17 (t, 4H, J = 6.9 Hz, H_6), 2.02 (m, 4H, H_g), 1.35-1.53 (m, 20H, $H_{4/5/8}$), 0.97 (t, 18H, J = 7.2 Hz, H_9), 0.55-0.60 (m, 12H, H_7).

^{13}C-NMR (100 MHz, $CDCl_3$, 300 K): δ = 171.2, 163.5, 157.3, 152.8, 140.5, 138.8, 133.5, 128.5, 124.8, 120.8,113.9, 107.5, 82.9, 64.4, 48.9, 48.2, 38.0, 28.8, 28.4, 26.5, 19.7, 18.2, 17.5, 16.2.

LRESI-MS: m/z = 1199 $[M + H]^+$, 1221 $[M + Na]^+$.

HRESI-MS: m/z = 1199.5792 $[M + H]^+$

(calc. for $C_{62}H_{89}N_{10}O_4PdSi_2$ 1199.5656)

{κ^3-2,6-Bis[4-hydroxy-benzylamide]-pyridino}(acetonitrile) palladium(II) (30)

2,6-Bis(4-hydroxy-benzylamide)-pyridine (500 mg, 1.32 mmol) was dissolved in acetonitrile (25 mL) and $Pd(OAc)_2$ (357 mg, 1.59 mmol) was added. The solution was stirred for 18 h, diluted with Et_2O and cooled to 0 °C. The precipitate was filtered off, washed with Et_2O and dried under reduced pressure to give the desired product as a yellow crystalline powder (683 mg, 98%). This product was used straight away, without any further purification.

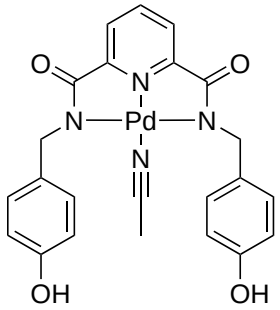

{κ^3-2,6-Bis-[4-hydroxy-benzylamide]-pyridino}(2,6-di(6-tripropylsilyl-hex-5-ynyl)-pyridine) palladium(II) (31)

A 100 mL flask was charged with {κ^3-2,6-bis-[4-hydroxy-benzylamide]-pyridino} (acetonitrile) palladium(II) (229 mg, 438 mol), 2,6-di(6-tripropylsilyl-hex-5-ynyl)-

pyridine (242 mg, 438 mol) and dissolved in CH_2Cl_2 / acetone 1:1 (50 mL). The solution was stirred for 18 h, concentrated under reduced pressure and purified via flash column chromatography using CH_2Cl_2 / acetone 1:1. The product was obtained as a yellow amorphous solid after evaporation of the solvent (225 mg, 54%).

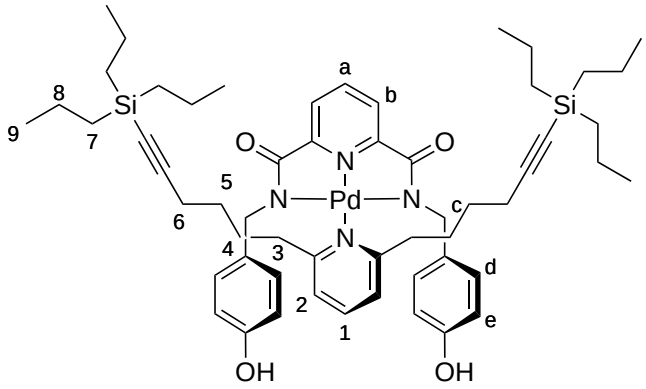

^{1}H-NMR (400 MHz, $CDCl_3$, 300 K): δ = 8.33 (t, 1H, J = 7.9 Hz, H_a), 7.96 (t, 1H, J = 7.8 Hz, H_1), 7.87 (d, 2H, J = 7.9 Hz, H_b), 7.22 (d, 2H, J = 7.9 Hz, H_2), 6.49 (d, 4H, J = 8.5 Hz, H_e), 6.37 (d, 4H, J = 8.5 Hz, H_d), 3.93 (s, 4H, H_c), 2.95 (t, 4H, J = 8.0 Hz, H_3), 2.25 (t, 4H, J = 6.9 Hz, H_6), 1.66-1.56 (m, 4H, H_4), 1.50-1.33 (m, 4H, $H_{5/8}$), 0.96 (t, 18H, J = 7.3 Hz, H_9), 0.57-0.53 (m, 12H, H_7).
^{13}C-NMR (100 MHz, $CDCl_3$, 300 K): δ = 171.5, 163.7, 156.1, 153.2, 141.5, 139.5, 131.4, 128.7, 125.3, 121.3, 115.2, 108.2, 83.1, 49.3, 38.2, 28.8, 26.7, 19.9, 18.4, 17.8, 16.5.
LRESI-MS: m/z = 1033 $[M + H]^+$.
HRESI-MS: m/z = 1033.46977 $[M + H]^+$
(calc. for $C_{56}H_{79}N_4O_4PdSi_2$ 1033.46876).

{κ^3-2,6-Bis-[4-(3-ynyl-propoxy)-benzylamide]-pyridino}(2,6-di(6-tri-n-propylsilyl-hex-5-ynyl)-pyridine) palladium(II) (29)

A dry flask was charged with {κ^3-2,6-bis-[4-hydroxy-benzylamide]-pyridino}(2,6-di(6-tripropylsilyl-hex-5-ynyl)-pyridine) palladium(II) (225 mg, 0.24 mmol), PPh_3 (193 mg, 0.956 mmol), dry THF (4 mL) and was cooled to 0 °C. After 10 min, 4-pentyn-1-ol (80 mg, 0.956 mmol) and after additional 5 min DIAD (193 mg, 0.956 mmol) were added. The reaction mixture was allowed to stir for 72 h. The

crude was concentrated under reduced pressure and filtered through a plug of silica, washing out the unreacted starting materials with Et_2O and the product using CH_2Cl_2 / MeOH 3 %. The product was finally purified by column chromatography (CH_2Cl_2 85% / Acetone 14% / MeOH 1%) and obtained as a yellow amorphous solid (83 mg, 29%).

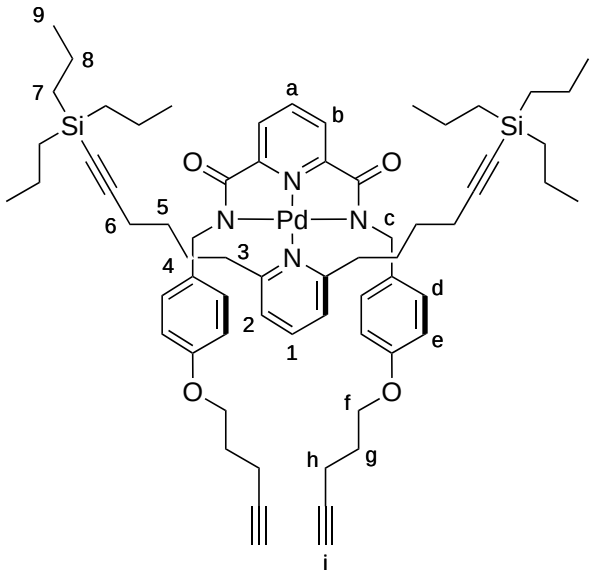

^{1}H-NMR (400 MHz, $CDCl_3$, 300 K): δ = 8.00 (t, 1H, J = 7.8 Hz, H_a), 7.76 (d, 2H, J = 7.8 Hz, H_b), 7.67 (t, 1H, J = 7.8 Hz, H_1), 6.95 (d, 2H, J = 7.8 Hz, H_2), 6.44 (d, 4H, J = 8.6 Hz, H_d), 6.36 (d, 4H, J = 8.5 Hz, H_e), 3.85-3.81 (m, 8H, $H_{c/f}$), 2.79 (t, 4H, J = 7.1 Hz, H_3), 2.29-2.25 (m, 4H, H_h), 2.05 (t, 4H, J = 6.8 Hz, H_6), 1.99-1.93 (m, 6h, $H_{g/i}$), 1.53-1.34 (m, 20H, $H_{4/5/8}$), 1.22 (t, 18H, J = 7.2 Hz, H_9), 0.47-0.42 (m, 12H, H_7).

^{13}C-NMR (100 MHz, $CDCl_3$, 300 K): δ = 171.2, 163.4, 157.5, 152.7, 140.4, 138.8, 133.3, 128.5, 124.8, 120.9, 113.8, 107.7, 82.8, 66.9, 64.1, 49.2, 38.1, 30.3, 29.3, 28.6, 26.7, 22.3, 19.7, 18.2, 17.5, 16.1.

LRESI-MS: m/z = 1165 $[M + H]^+$.

HRESI-MS: m/z = 1165.56103 $[M + H]^+$

(calc. for $C_{66}H_{91}N_4O_4PdSi_2$ 1165.56192).

Main Scaffold (35)

A dry flask was charged with BB1 (73 mg, 60 μmol) and BB2 (71 mg, 60 μmol) under an atmosphere of nitrogen, and CH_2Cl_2 (250 mL) was added. To this so-

lution, [Cu (MeCN)$_4$] PF$_6$ (8.0 mg, 20 μmol) and DIPEA (50 μL, 0.24 mmol) were added, and the solution was allowed to stir for 48 h. The reaction was monitored each 24 h by TLC, and if not completed, another batch of catalyst and base was added ([Cu (MeCN)$_4$] PF$_6$ = 4 mg; DIPEA = 25 μL]). When no more starting material was observed, the crude was washed with 1 M Na$_4$EDTA solution (250 mL), brine (250 mL) and dried over MgSO$_4$. After filtration and concentration under reduced pressure, the crude was purified by column chromatography (CHCl$_3$ 99% / MeOH 1% to CHCl$_3$ 97% / MeOH 3%). The product was obtained as a yellow amorphous solid (50 mg, 35%).

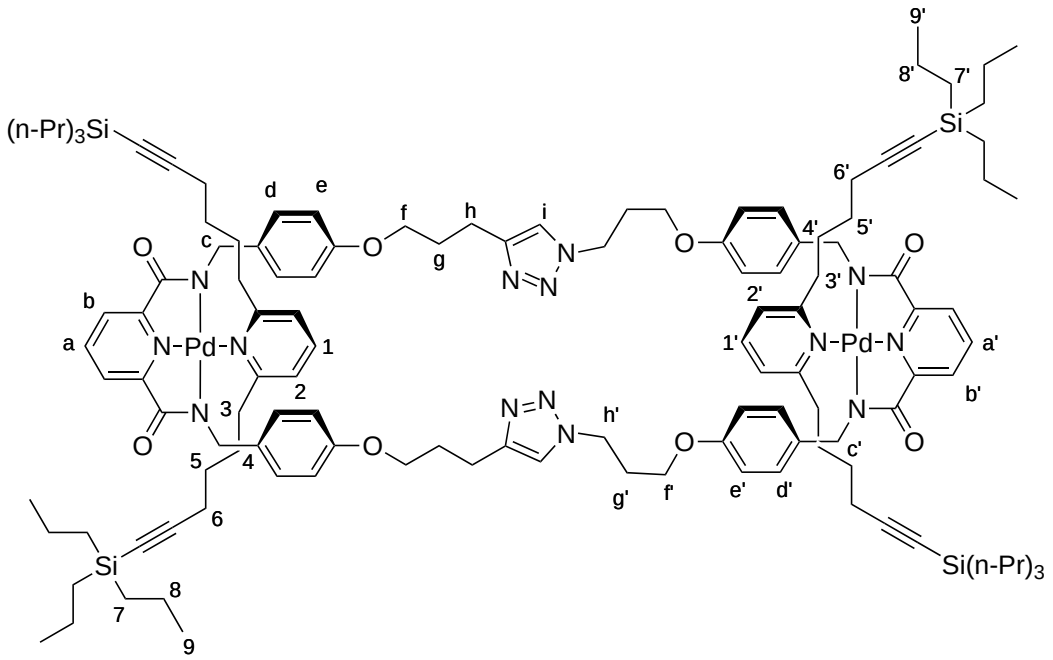

^{1}H-NMR (400 MHz, CDCl$_3$, 300 K): δ = 8.09-8.04 (m, 2H, H$_{a/a'}$), 7.84-7.81 (m, 4H, H$_{b/b'}$), 7.76-7.71 (m, 2H, H$_{j/j'}$), 7.29 (s, 2H, H$_i$), 7.01-6.97 (m, 4H, H$_{k/k'}$), 6.48-6.40 (m, 2H, H$_{d/d'/e/e'}$), 4.45 (t, 4H, J = 7.1 Hz, H$_{h'}$), 3.88-3.84 (m, 16H, H$_{f/f'/c/c'}$), 2.85-2.81 (m, 12H, H$_{h/l/l'}$), 2.30-2.23 (m, 4H, H$_{g'}$), 2.10-2.01 (m, 12H, H$_{g/o/o'}$), 1.37-1.28 (m, 40H, H$_{m/m'/n/n'/q/q'}$), 0.89 (t, 36H, J = 7.2 Hz, H$_{r/r'}$), 0.52-0.48 (m, 12H, H$_{q/q'}$).

^{13}C-NMR (100 MHz, CDCl$_3$, 300 K): δ = 171.2, 171.2, 163.4, 163.3, 157.5, 157.0, 152.7, 147.4, 140.4, 138.9, 138.8, 133.7, 133.3, 128.5, 124.8, 120.9, 120.8, 113.8, 113.7, 107.7, 82.8, 82.7, 66.9, 64.1, 49.2, 49.1, 47.0, 38.1, 30.3, 29.3, 28.6, 26.7, 22.3, 19.7, 18.2, 17.5, 16.1.

LR-ESI: m/z = 2365 $[M]^+$

HR-FAB (3-NOBA): 2366.12678 $[M + H]^+$

(calc. for $C_128H_178N_14O_8Pd_2Si_4$ 2366.11365)

References

[1] J. C. Loren, M. Yoshizawa, R. F. Haldimann, A. Linden, J. S. Siegel, *Angew. Chem., Int. Ed. Engl.* **2003**, *42*, 5702–5705.

[2] C. Mao, W. Sun, N. C. Seeman, *Nature* **1997**, *386*, 137–138.

[3] K. S. Chichak, S. J. Cantrill, A. R. Pease, S.-H. Chiu, G. W. V. Cave, J. L. Atwood, J. F. Stoddart, *Science* **2004**, *304*, 1308–1312.

[4] H. Wu, S. Brittain, J. Anderson, B. Grzybowski, S. Whitesides, G. M. Whitesides, *J. Am. Chem. Soc.* **2000**, *122*, 12691–12699.

[5] H. Qiu, J. C. Dewan, N. C. Seeman, *J. Mol. Biol.* **1997**, *267*, 881–898.

[6] A. Rich, A. Nordheim, A. Wang, *Annu. Rev. Biochem.* **1984**, *53*, 791–846.

[7] M. Schmittel, A. Ganz, D. Fenske, *Org. Lett.* **2002**, *4*, 2289–2292.

[8] K. S. Chichak, S. J. Cantrill, J. F. Stoddart, *Chem.Commun.* **2005**, 3391–3393.

[9] A. J. Peters, K. S. Chichak, S. J. Cantrill, J. F. Stoddart, *Chem. Commun.* **2005**, 3394–3396.

[10] M. E. Layton, C. A. Morales, M. D. Shair, *J. Am. Chem. Soc.* **2002**, *124*, 773–775.

[11] G. Wu, F. E. Cederbaum, E.-I. Negishi, *Tetrahedron Lett.* **1990**, *31*, 493–496.

[12] M. G. Organ, S. Avola, I. Dubovyk, N. Hadei, E. A. B. Kantchev, C. J. O'Brien, C. Valente, *Chem.–Eur.J.* **2006**, *12*, 4749–4755.

[13] J. D. Crowley, D. A. Leigh, P. J. Lusby, R. T. McBurney, L.-E. Perret-Aebi, C. Petzold, A. M. Z. Slawin, M. D. Symes, *J. Am. Chem. Soc.* **2007**, *129*, 15085–15090.

[14] V. Aucagne, K. D. Hänni, D. A. Leigh, P. J. Lusby, D. B. Walker, *J. Am. Chem. Soc.* **2006**, *128*, 2186–2187.

Chapter 3

Palladium(II)-Templated Synthesis of a [3]Catenane

Acknowledgements and Declaration

Dr. David Schultz supplied the precursor to **41** and Raul Garcia Rodriguez undertook the synthesis of compounds **34-38**. The project was designed and coordinated by the Author.

Synopsis

In this chapter, the highly convergent palladium(II)-template directed synthesis of a [3]catenane is reported, alongside its conceptual design, retrosynthetic analysis and characterisation. The [3]catenane was synthesised from two complementary building blocks, both of which consist of a tridentate ligand (bearing the functional groups for the final ring-closure step) monodentate ligand (preformed macrocycle) assembly, held together by a palladuim(II) anchor. The final cyclisation reaction was conducted as a one pot in situ deprotection and Cu(I)-catalysed azide-alkyne 1,3-dipolar cycloaddition.

3.1 Introduction

3.1.1 Topological Analysis

The [3]catenane as a topological target is accessible in many ways, three of which are shown in Figure 3.1 (the depicted [3]catenane is the simplest representative with two identical rings catenated by a large ring). These synthetic strategies represent the commonly used approaches for the ultimate assembly step that leads to the desired structure.

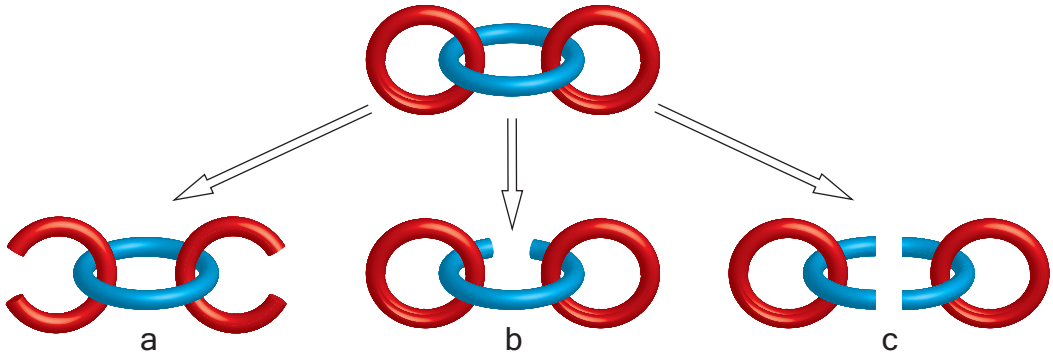

Figure 3.1. Possible routes towards a [3]catenane via a) as double clipping; b) as "clamp"-fusion; c) double ring fusion.

In Figure 3.1a, the double clipping approach, the central ring (cyan) holds two threaded macrocycle precursors in place. To afford the [3]catenane, these macrocycle precursors will be clipped around the central macrocycle to yield the final assembly.

A different approach is depicted in Figure 3.1b, where two preformed macrocycles (red) are threaded by a clamp-like central macrocycle precursor (cyan), which prearranges the constituents and enables a single site ring-closure to the [3]catenane.

The third option (Figure 3.1c), represents a double ring fusion of two complementary parts with the macrocycles held in place by the threaded "half" central rings. Here, as well as in the double clipping approach, two successive bond formations have to take place. However, when the first bond formation has succeeded, the prearranged ensemble will favorably act like the approach presented in Figure 3.1b. This route may appear the least favorable, due to the ring closure

of the more complex central ring, but it can also offer a higher degree of versatility when an asymmetric ringclosure is performed.

In the presented work, a double ring fusion approach has been chosen.

3.1.2 [3]Catenanes from Double Clipping Strategies

The first example of a [3]catenane derived from the previously defined double clipping strategy was published by Schill in 1981.[1]

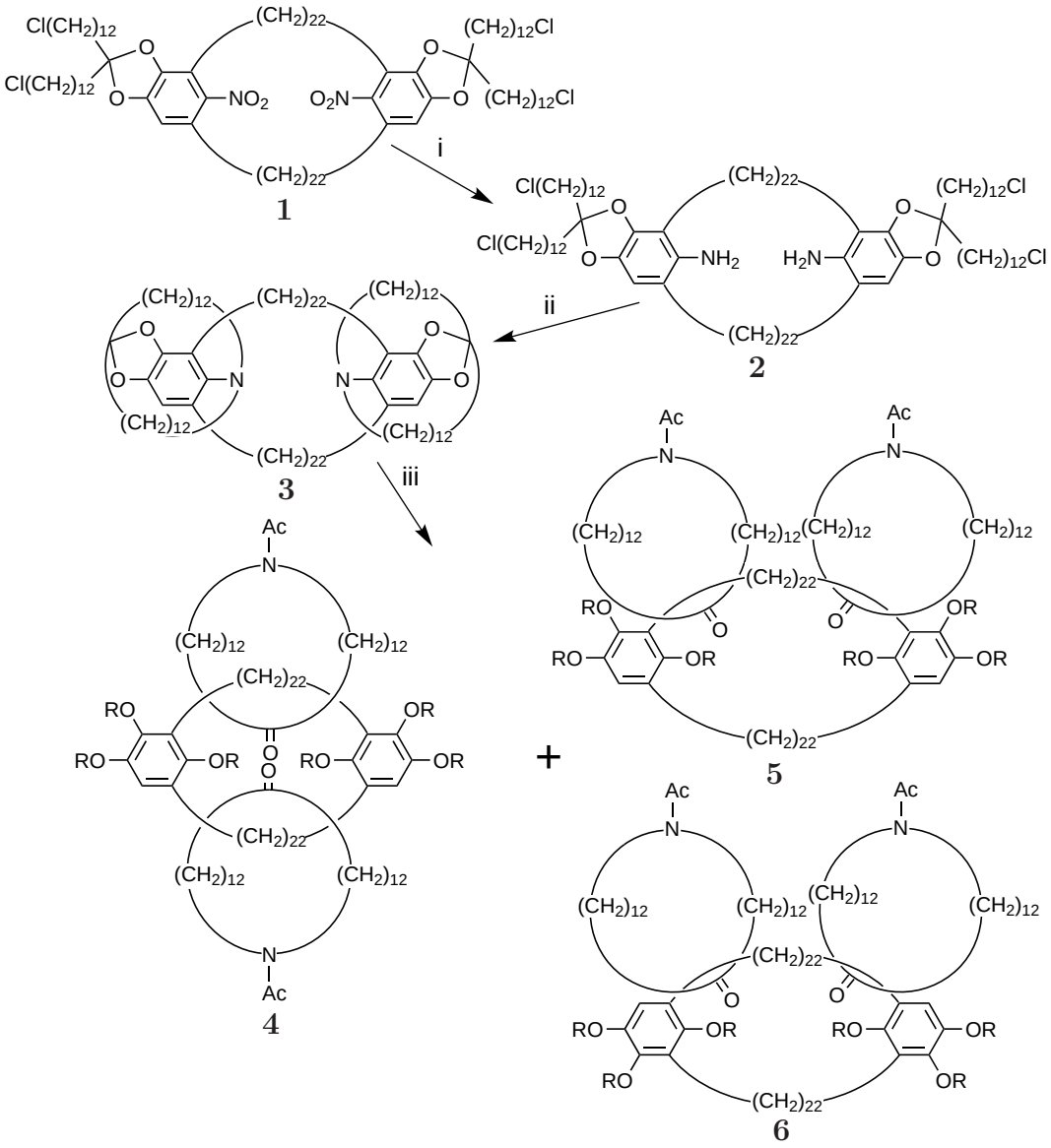

Scheme 3.1. Schill's [3]catenane *via* double clipping approach. Reaction steps: i) reduction; ii) substitution; iii) cleavage.

Schill's approach did not comprise the use of a templating strategy in a

supramolecular sense; it was solely a sequence of bond forming and bond cleaving reactions, which very elegantly led to the desired mechanically interlocked structure. Macrocycle **1**, containing two nitro substituents, was reduced to give the bisamine macrocycle **2**. The amine functionalities were reacted with the terminal chloride bearing acetal tethers to form the doubly attached macrocycle precursors on the central ring **3**. Cleavage of all macrocyclic attachment points led to the [3]catenane in three distinct co-conformers, the symmetric co-conformer **4**, and two co-conformers where the two macrocycles are trapped on one side of the asymmetric central ring **5** and **6**.

Almost twenty years later, Vögtle and co-workers published the successful synthesis of two [3]catenanes.[2] The catenanes were obtained via hydrogen-bonding templated cyclisation around two bisamide recognition motifs incorporated into the central ring. In the year 2003, Leigh and co-workers presented a [3]catenane, on which they were able to exercise unidirectional movement of both rings around the central ring by a blocking path mechanism.[3] Vögtle and Leigh's ways of obtaining [3]catenanes are double clipping approaches; here only Leigh's work will be presented as representative for amide-based [3]catenanes.

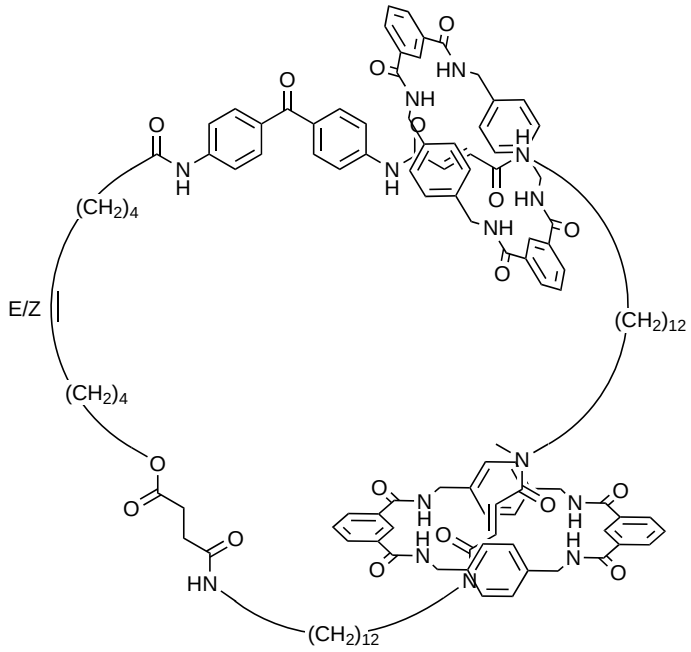

Figure 3.2. Leigh's [3]catenane from a double clipping approach.

The synthesis of the [3]catenane (Figure 3.2) commenced from the open form

of the central ring, which was closed using RCM. The obtained macrocycle has four different recognition motifs (itemised clockwise), a secondary amide fumaramide group, a bis-N-methylated fumaramide moiety, a succinic amide ester and benzophenone amide functionality. The first two recognition motifs are capable of templating the [2+2] macrocyclistion reaction of isophthaloyl dichloride and p-xylylenediamine to give [2]catenane and [3]catenane in 50% and 21% yield respectively. Recently, a metal-templated double clipping approach was realised

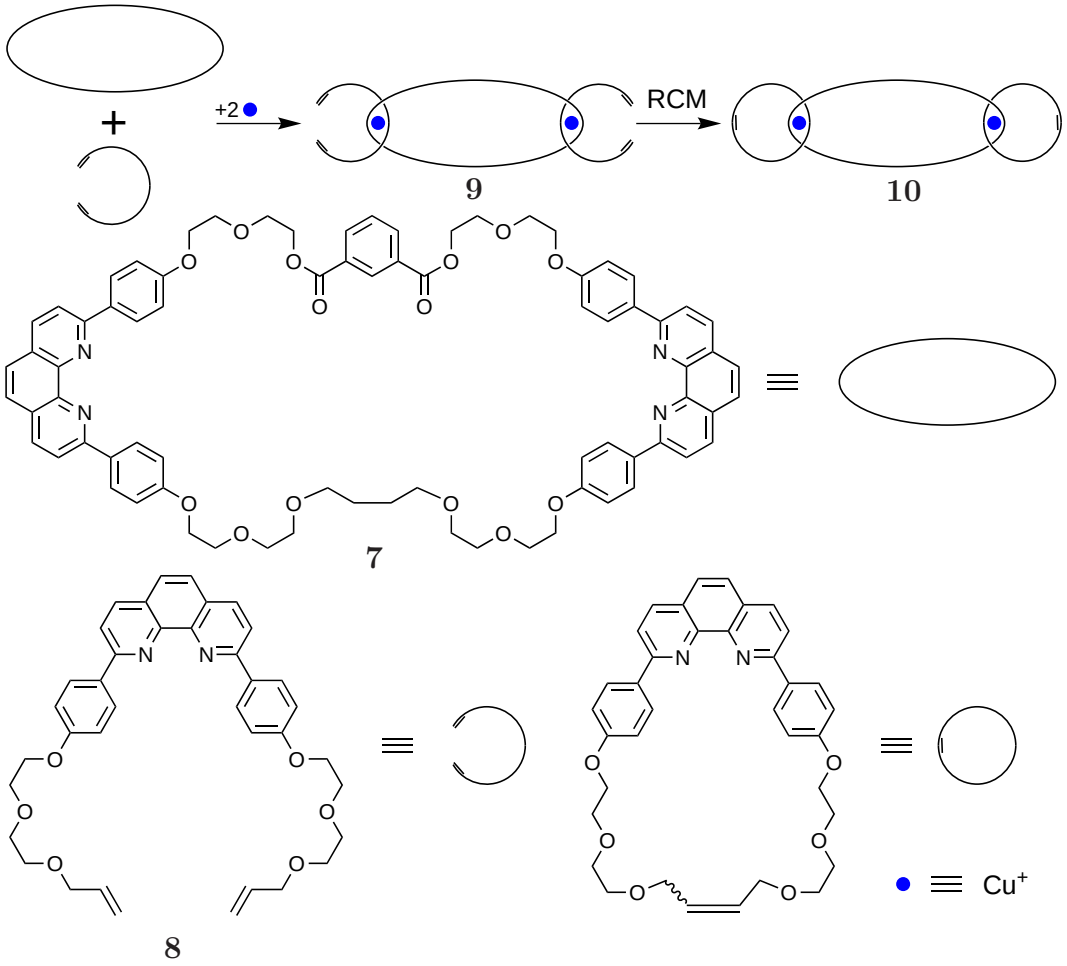

Scheme 3.2. Schematic representation of Mayer's [3]catenane synthesis using RCM as cyclisation step.

by Mayer and co-workers.[4] Here, Mayer used Sauvage's template methodology, to generate the crossover points. This was achieved by coordinating two 1,10-phenantroline macrocycle precursors **8** with two Cu(I) anchors inside the cavity of a preformed central macrocycle **7** containing two 1,10-phenantroline units, which gave the [3]catenane precursor **9**. Employing RCM as macrocyclisation

step to clip the two macrocycles around the central ring afforded the [3]catenane **10** in 71% yield. Upon demetallation of **10** with KCN the [3]catenand could be obtained.

Stoddart and co-workers also published a successful [3]catenane synthesis relying on the double clipping approach.[5,6] However, these efforts were clearly outperformed by the "clamp" precursor strategy (see next section).

3.1.3 [3]Catenanes from Clamp Precursor Assemblies

The first precedent of a successful application of the "clamp" precursor strategy was published by Stoddart and co-workers in 1991.[7]

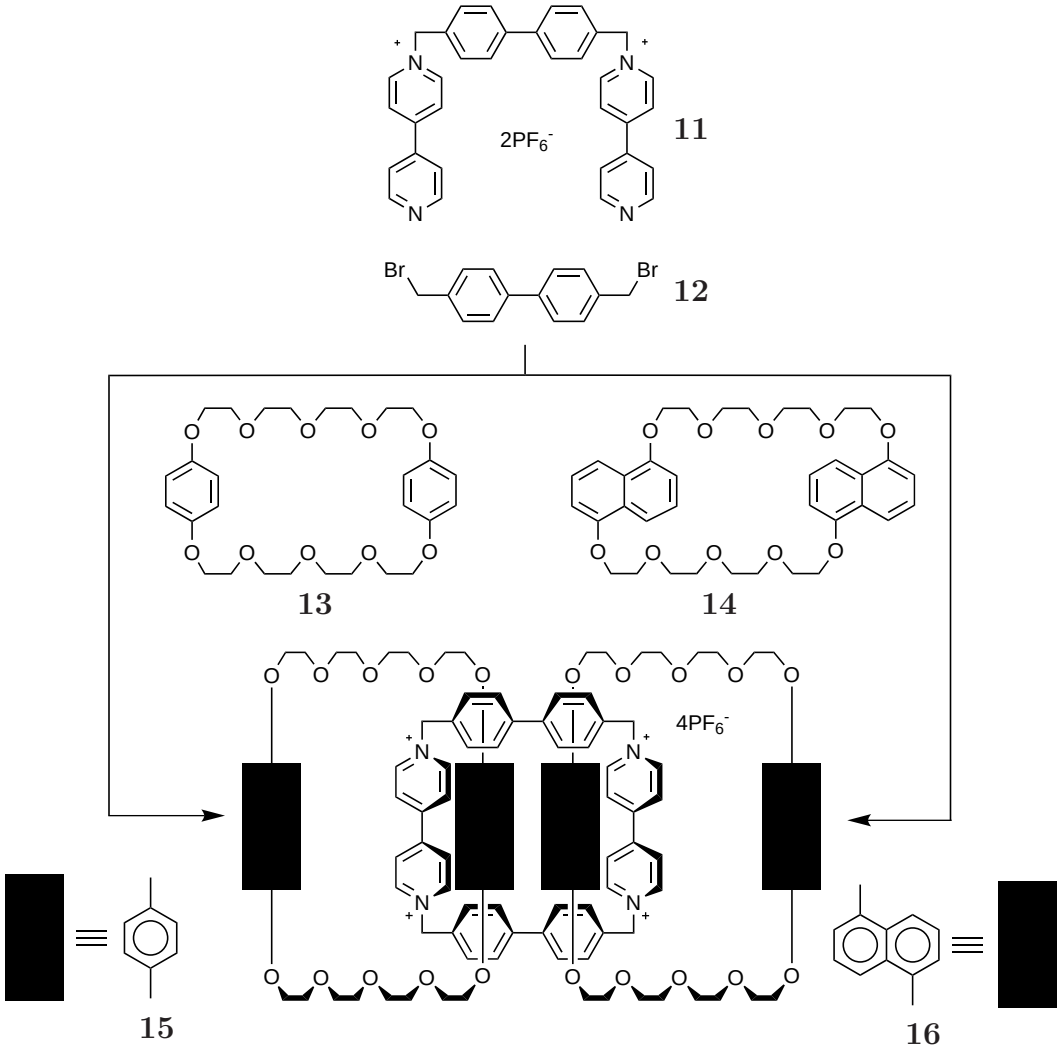

Scheme 3.3. Stoddart's self assembly [3]catenane synthesis.

The formation of the [3]catenane was accomplished by employing a self-assembly approach (Scheme 3.3), where the dicationic "clamp"-like macrocycle precursor **11** was reacted with 4,4'-bis-bromomethyl-biphenyl **12** in the presence of excess macrocycle **13** or **14**. This reaction yielded 20% in the presence of macrocycle **13** which led to [3]catenane **15** and 31% for the variant using macrocycle **14** leading to catenane **16**. In the following years, Stoddart and co-workers optimised the reaction conditions and found that applying high pressure benefitted the catenation process in accordance with Le Châtelier's prin-

ciple.[8] Furthermore, by varying the preformed macrocycles, Stoddart and co-workers were able to obtain a series of similar [3]catenanes from this approach and ultimately a precursor towards the higher [5]- and [7]catenanes.[5,6,8–10] Despite Stoddart's success in developing synthetic strategies towards [3]- and higher [n]catenanes using the "clamp" precursor approach, there is only one example of a metal-templated variant, which was presented by Sauvage and co-workers.[11] Here (Scheme 3.4), the well established copper(I) template, consisting of two dif-

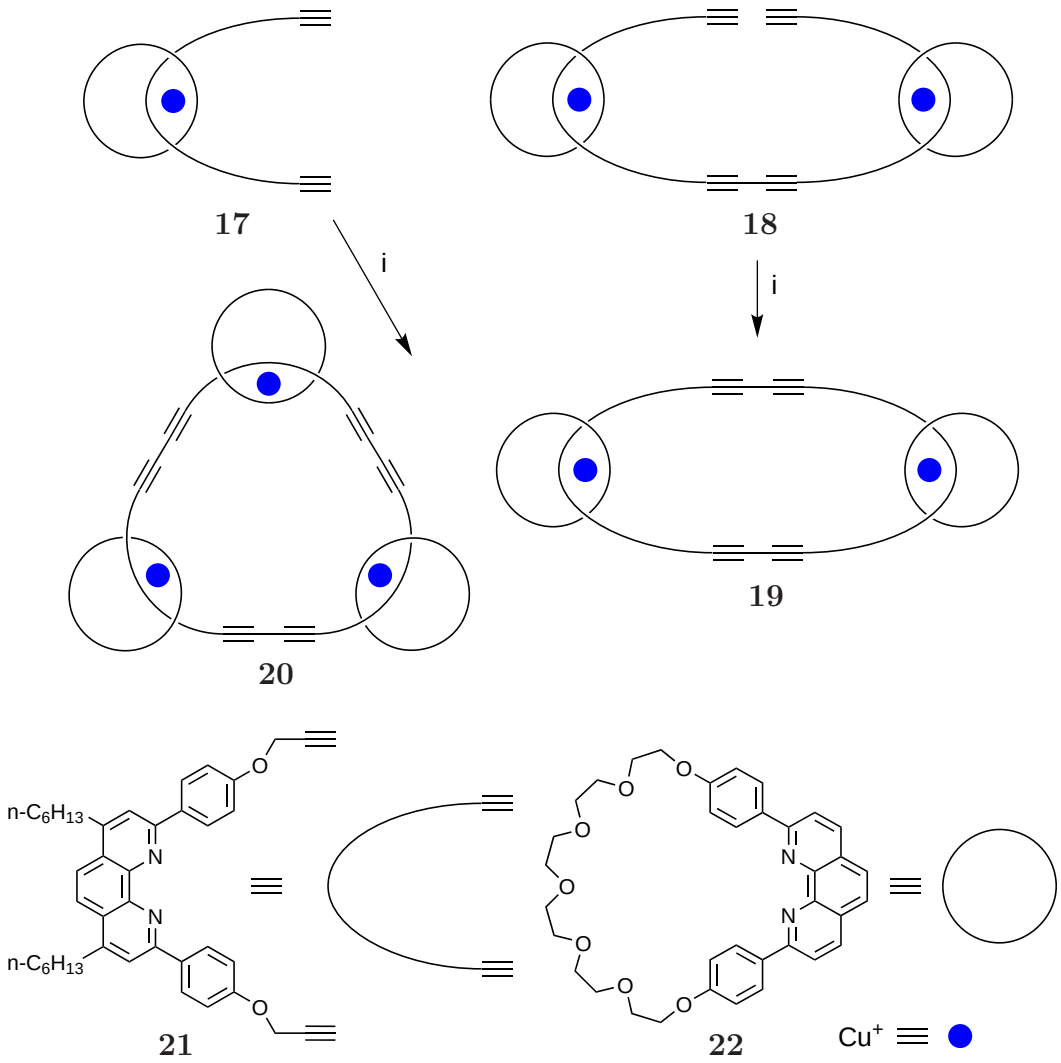

Scheme 3.4. Sauvage's TM templated synthesis of a [3]catenane via "clamp" closure approach. Reaction step: i) oxidative Glaser alkyne-alkyne coupling.

ferent 1,10-phenanthroline ligands coordinated to a copper(I) anchor, was used to prearrange the preformed macrocycles **22** and the "clamp" **18**. Subsequent oxidative Glaser alkyne-alkyne coupling furnished the desired [3]catenane **19** in

48% yield. In comparison to this approach, the double ring fusion of the central ring is shown as well. This reaction yield [3]catenane **19** in 40% yield and some [4]catenane **20** (6%).

3.1.4 [3]Catenanes from Double Ring Fusion Pathways

In 1969, Schill and Zürcher announced the first successful synthesis of a [3]catenane, which was obtained via a directed synthesis, that consisted of a sequence of covalent bond formations and cleavages.[12] In a wider sense, this strategy constitutes a double ring fusion approach. Schill started the synthesis (Scheme 3.5)

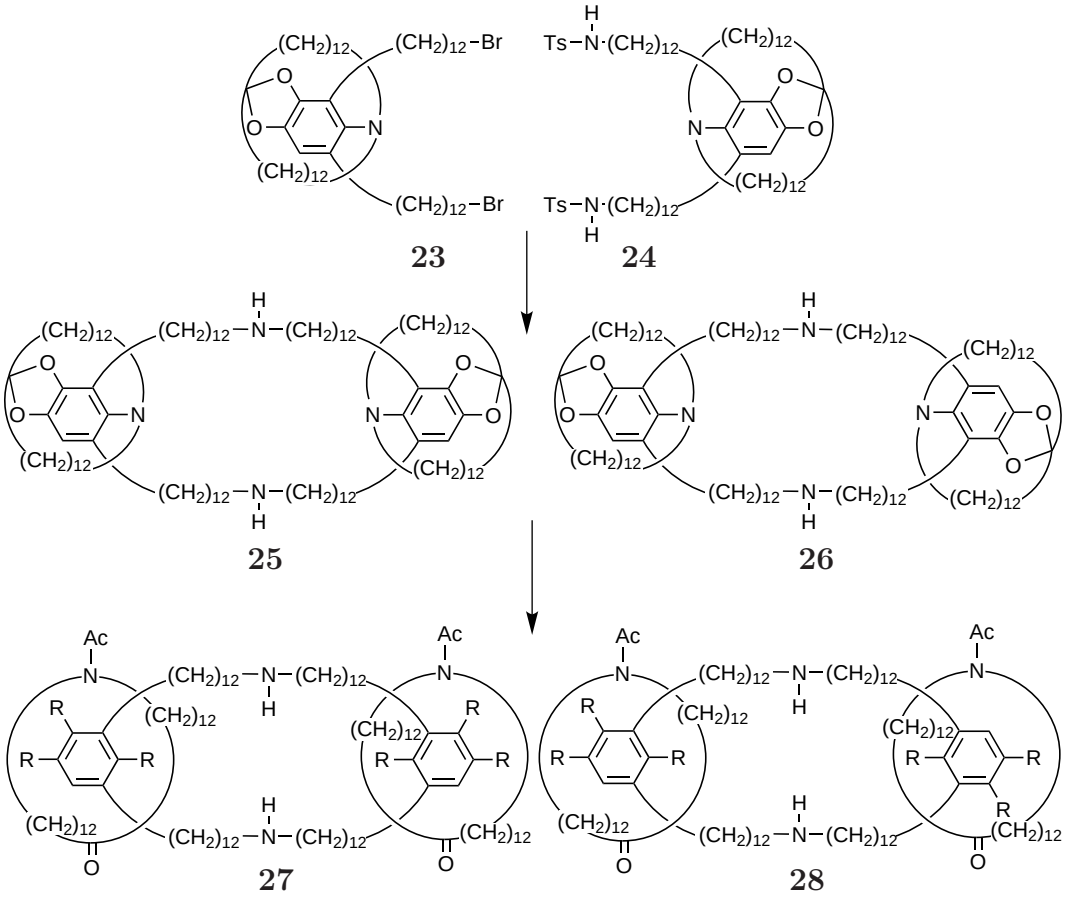

Scheme 3.5. First [3]catenane synthesis by Schill using a double ring fusion approach.[12]

from the common macrocycle thread precursor **23** and converted the bromide to the secondary p-toluenesulfonamide, thus giving access to **24**. Reacting **23** and **24** under high dilution conditions afforded a mixture of **25** and **26**, which upon

cleavage of the acetal and sec. aniline afforded [3]catenanes **27** and **28** in an remarkable combined 32% yield.

With the introduction of the copper(I) - 1,10-phenanthroline metal template system, Sauvage and co-workers were able to synthesise a [3]catenane in very poor yield, using the double ring fusion approach and Williamson ether synthesis as ring-closure reaction.[13] However, one year later, Sauvage was able to drastically improve the ring-closure efficiency using an oxidative coupling of terminal alkynes and was able to produce the [3]cantenane in 58% yield.[14] Recently, Schuster and Megiatto reported their synthesis of a [3]catenane, using the now widely established copper(I)-catalysed 1,3-dipolar cycloaddition of azides to alkynes (CuAAC or "click" chemistry).[15]

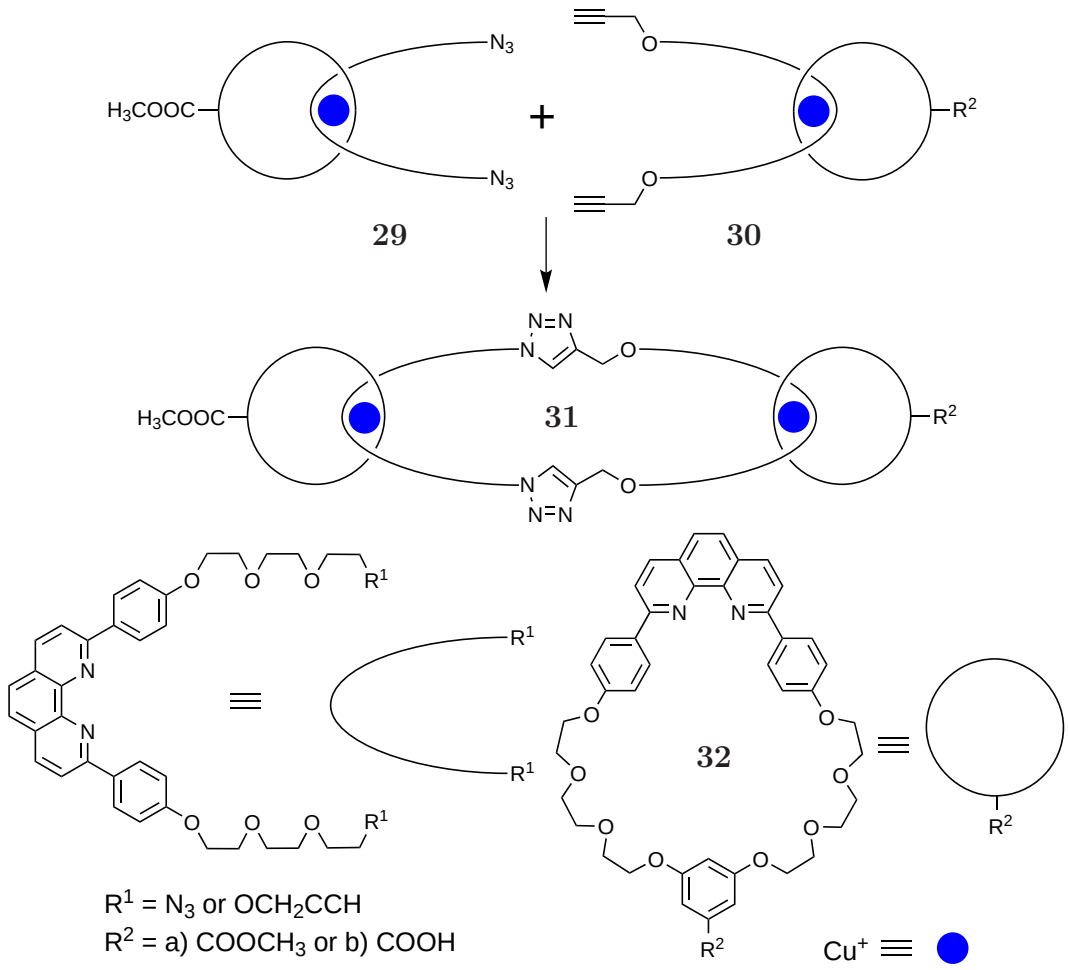

Scheme 3.6. Schuster's [3]catenane from an assymmetric double ring closure using CuAAC chemistry.[15]

Here (Scheme 3.6), Schuster used Sauvage's template to prearrange the pre-

formed macrocycles and the threads, holding the complementary reactive groups (azide **29** and terminal alkyne **30a/b**) together. These complexes were subsequently subjected to CuAAC conditions to afford the [3]catenanes **31a** and **31b** in yields of 65% and 70% respectively. Furthermore, with [3]catenane **31b** Schuster established the first example of a totally hetero-circuit system, where no ring is the same.

In addition to the aforementioned double ring fusion examples, there are further examples of [3] catenane syntheses using crown-ether secondary amine templates Fukazawa[16] and Loeb.[17] Finally, Beer and Lankshear reported the use of chloride anion templation to generate [2]catenanes and [3]catenane as minor by-product.[18]

3.2 Retrosynthesis

The envisaged [3]-catenane and its retrosynthetic analysis is shown in Scheme 3.7. It features two TM complex sites, which align the monodentate macrocycles orthogonally to the plane defined by the three donor nitrogens of the tridentate ligands of the central macrocycle.

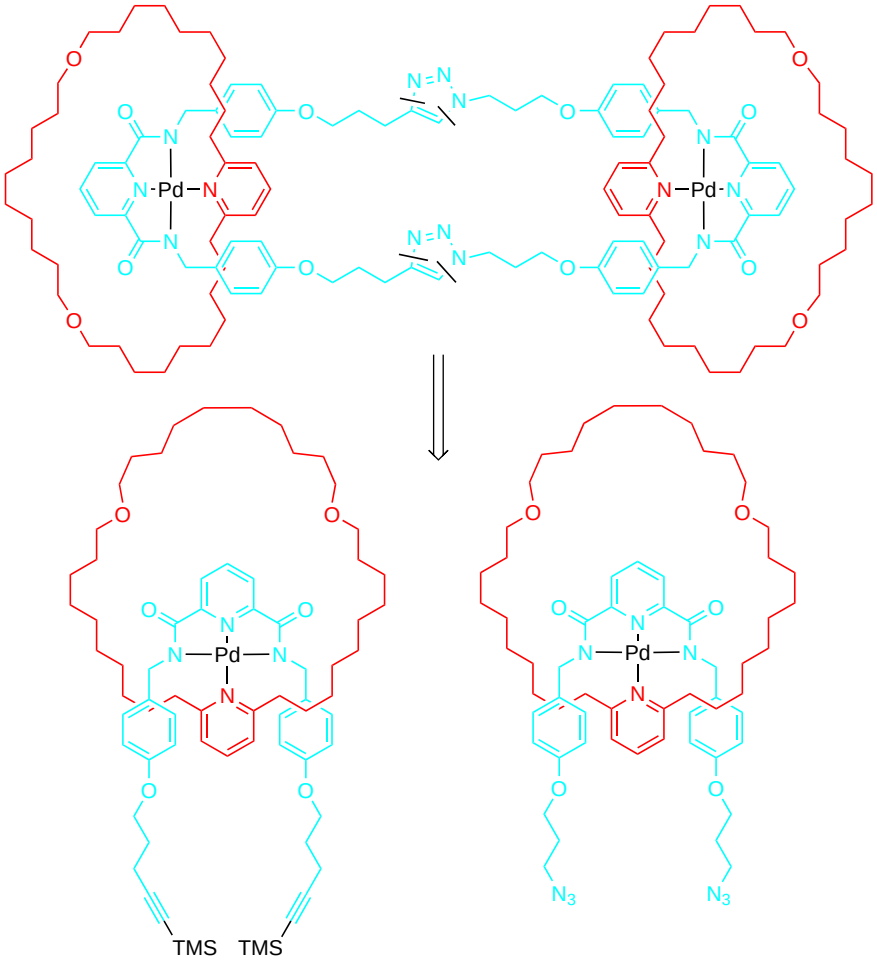

Scheme 3.7. Retrosynthetic analysis of the proposed [3]-catenane, first disconnections and resulting building blocks **BBa** (left) and **BBb** (right).

The terminal macrocycles consist of a long bisether alkyl loop, fused to a 2,6-disubstituted pyridine. This design was chosen to guarantee good solubility in a wide range of solvents and to avoid ^{1}H-NMR signal congestion in the region of the aromatics. Exercising retrosynthetic analysis on the [3]-catenane leads to the first disconnections of the triazole units yielding the two complementary building blocks. Both building blocks share the same structural features, such as macrocycle and tridentate moiety, which only differ in the functional groups

attached to the phenol positions. Here, the building block on the left, containing the TMS protected terminal alkyne units, shall be referred to as **BBa**. The building block on the right, bearing the azide units, should be referred to as **BBb**. As previous findings suggest, the alkynes should be protected with a easy to remove protecting group such as TMS. This should increase stability and shelf life of this compound. However, this strategy requires the TMS-group to be removed prior to the double click reaction or *in situ*.

Carrying out a retrosynthetic analysis on **BBa-TMS** (Scheme 3.8), the first disconnection is made at the phenolic positions, as neither terminal nor protected alkynes should be present when introducing the TM. This disconnection gives rise to the macrocycle bisphenol tridentate complex, which should be easily obtainable via ligand exchange reaction of the labile acetonitrile ligand of the pre-metallated U-shape and the corresponding macrocycle.

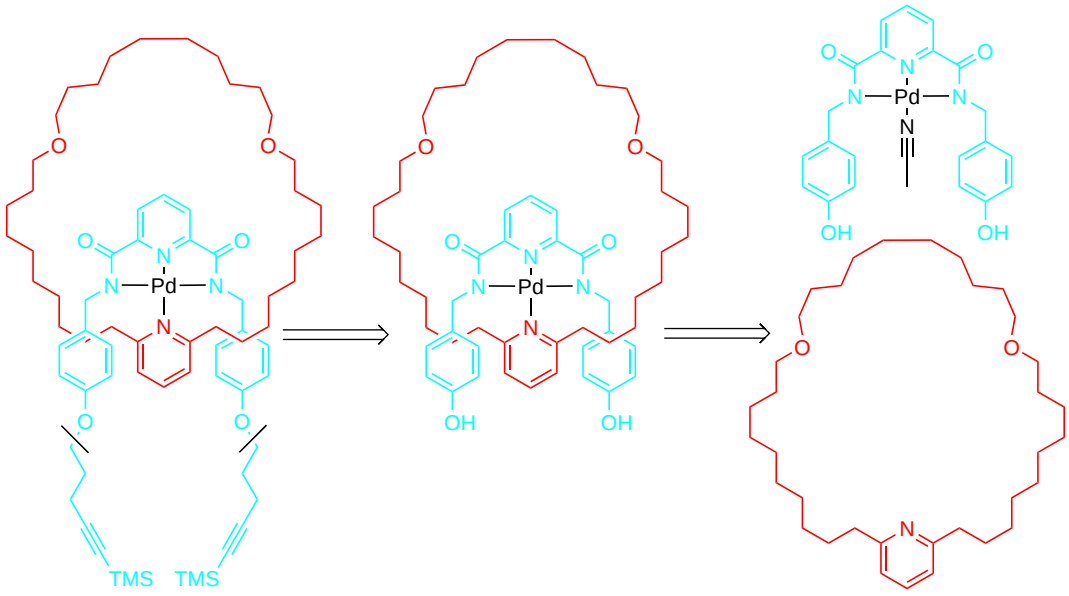

Scheme 3.8. Retrosynthetic analysis of the envisaged **BBa-TMS**, with indicated disconnections and resulting subcomponents (pre-metallated bisphenol U-shape and macrocycle **M1**).

BBb (Scheme 3.9) with its bisazide-containing tridentate ligand, should be obtained from a ligand exchange reaction of the pre-metallated palladium bisazide tridentate ligand and the corresponding macrocycle.

The macrocycle **M1** consists of a long alkyl diether loop that is attached to the pyridine in the 2 and 6 position. Performing the retrosynthetic analysis on

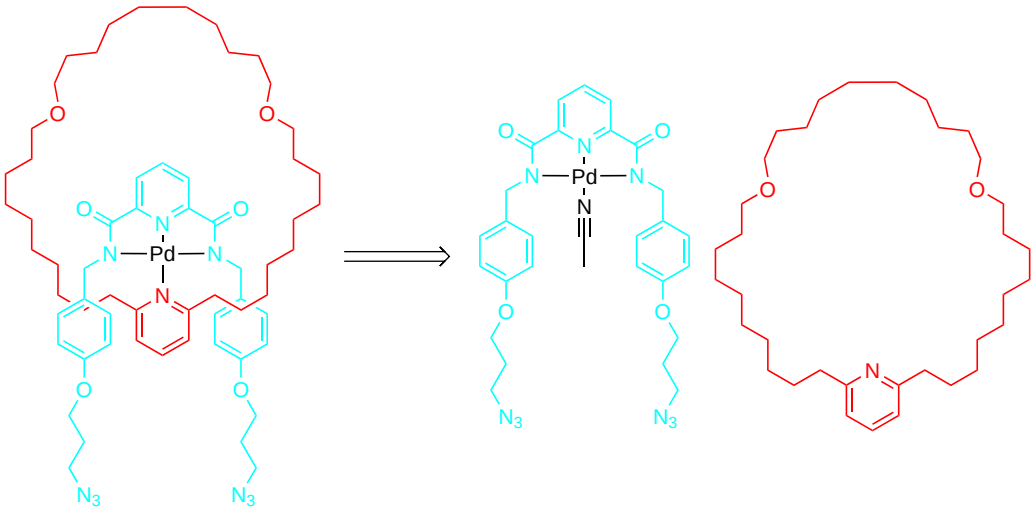

Scheme 3.9. Retrosynthetic analysis of the proposed **BBb** and resulting subcomponents (pre-metallated bisazide U-shape and macrocycle **M1**).

macrocycle **M1** (Scheme 3.10), FGI leads to the alkene macrocycle.

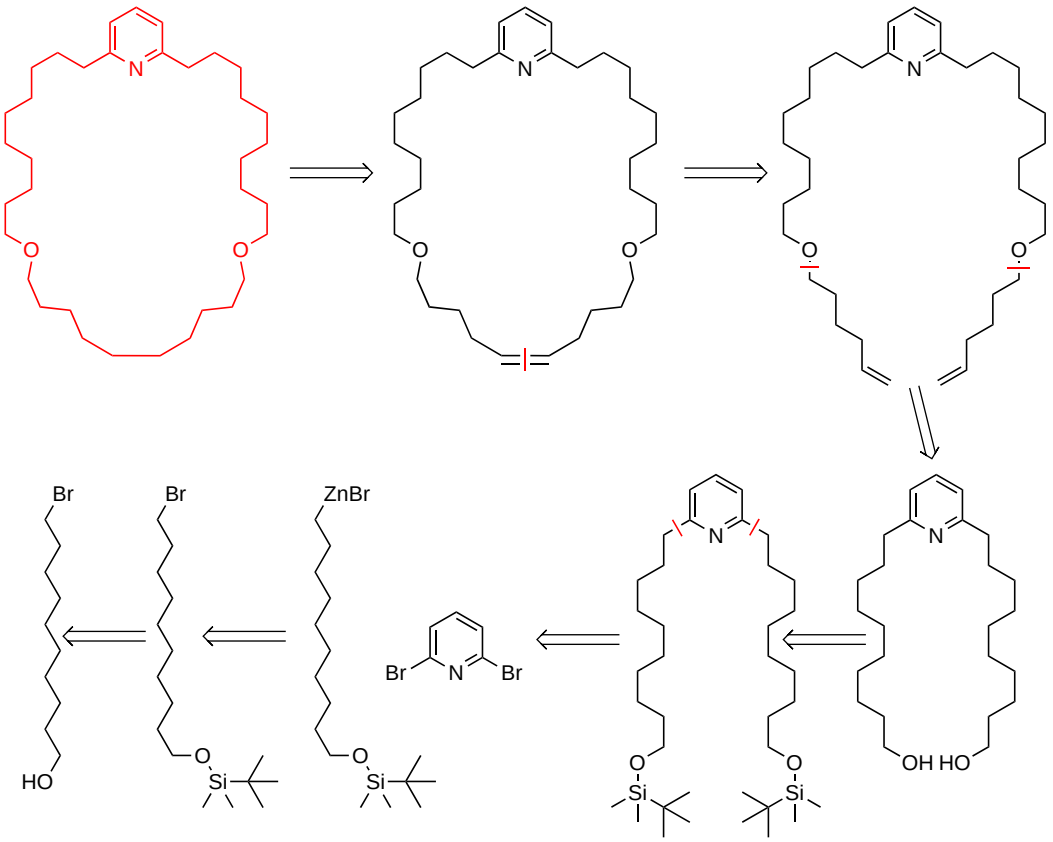

Scheme 3.10. Retrosynthetic analysis of the proposed monodentate macrocycle M1 and indicated disconnections.

Disconnecting the macrocycle at the middle of the chain generates the bisalkene

open form, which can be closed using RCM under high dilution conditions. The bisalkene can be obtained from the diol via Williamson ether synthesis of the diol-containing pyridine with the appropriate hexene derivative. The diol is obtained from the TBDMS-protected species, which is necessary for the Negishi coupling, which does not tolerate free alcohols at either position of the cross-coupling substrates. The zincate should be easily obtainable from the primary bromide. The OTBDMS protected bromodecanol can be prepared according to a literature procedure[19] and 2,6-dibromo pyridine is a commercially available substance.

3.3 Synthesis

3.3.1 Synthesis of M1

The synthesis of the macrocycle started from the commercially available 10-bromo-1-decanol **33**, which was reacted with TBDMSCl in the presence of imidazole to obtain **34** in moderate yield.[19] **34** was then converted into the zincate **35** by reacting the bromide with zinc dust, which was *in situ* activated by the addition of 5 mol% iodine, at 80 °C in DMF. The subsequent cross coupling was was achieved by addition of $[Pd(PPh_3)_4]$ as catalyst together with the coupling partner 2,6-dibromo pyridine and produced the desired product **36** in good yield. The TBDMS-protected monodentate ligand was then treated with TBAF, to obtain the diol species **37** in quantitative yield.

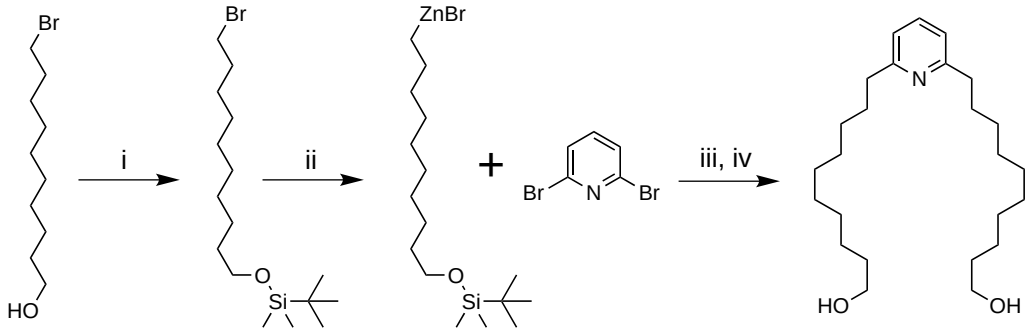

33 **34** **35** **37**

Scheme 3.11. Synthesis of the macrocycle precursor. Reagents and conditions: i) 1-bromo-10-decanol, TBDMSCl, imidazole, CH_2Cl_2, 54%; ii) **34**, Zn dust, I_2, DMF, 80 °C, 4h; iii) **35**, 2,6-dibromo pyridine, $[Pd(PPh_3)_4]$, DMF, 80 °C, 75%; iv) **36**, TBAF, THF, RT, quant.

To obtain the RCM precursor **38**, diol **37** was treated with NaH in DMF and subsequently reacted with 1-tosyl-hex-5-ene. The bisalkene **38** was then subjected to RCM under high dilution, using Grubbs' $^{1st.}$ generation catalyst, to afford the macrocycle **39** as a cis/trans mixture in good yield (73%). This mixture was then hydrogenated using Pd/C in THF and produced the desired macrocycle **40** in quantitative yield. The ^{1}H-NMR of macrocycle **M1** (**40**) is given in Figure 3.3 together with its assignment.

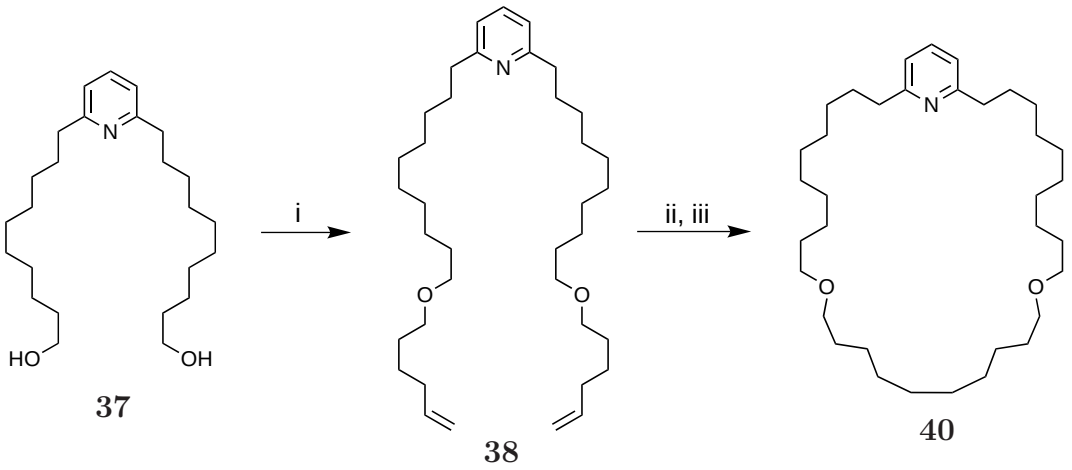

Scheme 3.12. Synthesis of the macrocycle. Reagents and conditions: i) **37**, 1-tosyl-hex-5-ene, NaH, 15-crown-5, DMF, 40%; ii) **38**, Grubbs' 1st. generation catalyst, Toluene, 73%; iii) **39**, Pd/C (10% palladium load), H_2, THF, quant.

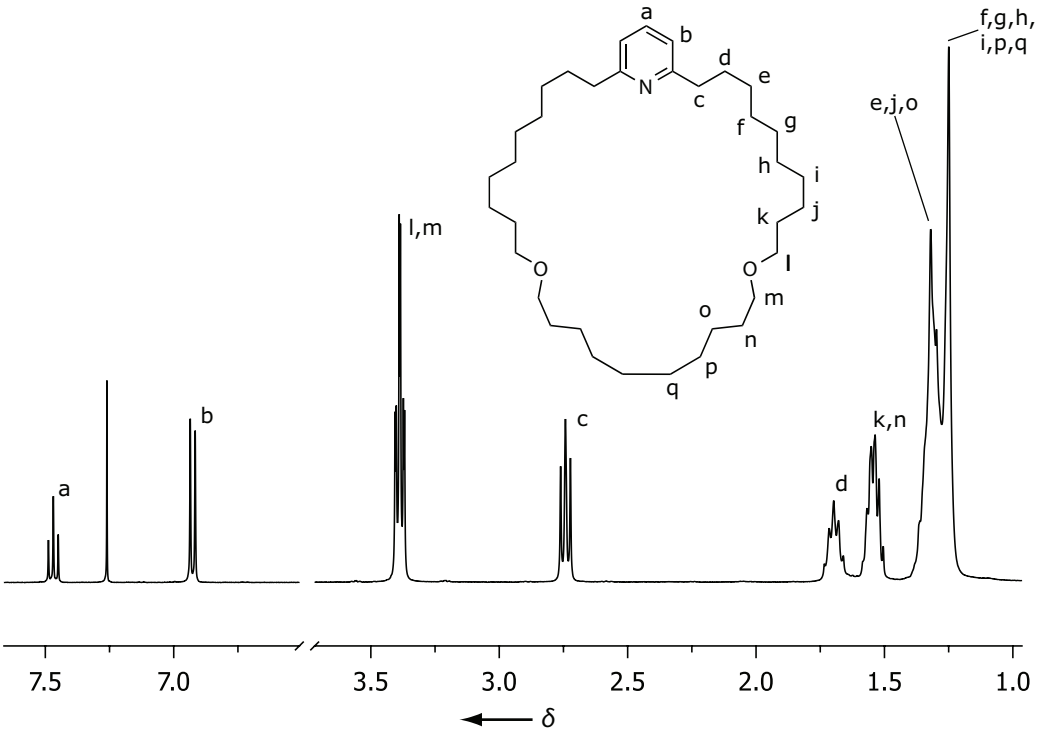

Figure 3.3. ^{1}H-NMR (400 MHz, $CDCl_3$, 300 K) of macrocycle **M1** (**40**).

3.3.2 Synthesis of BBa

The synthesis of the alkyne containing building block M1PdtAl-TMS **43** commenced from the pre-metallated bisphenol U-shape **41**, which was already presented in Chapter 2 (Compound **30**).

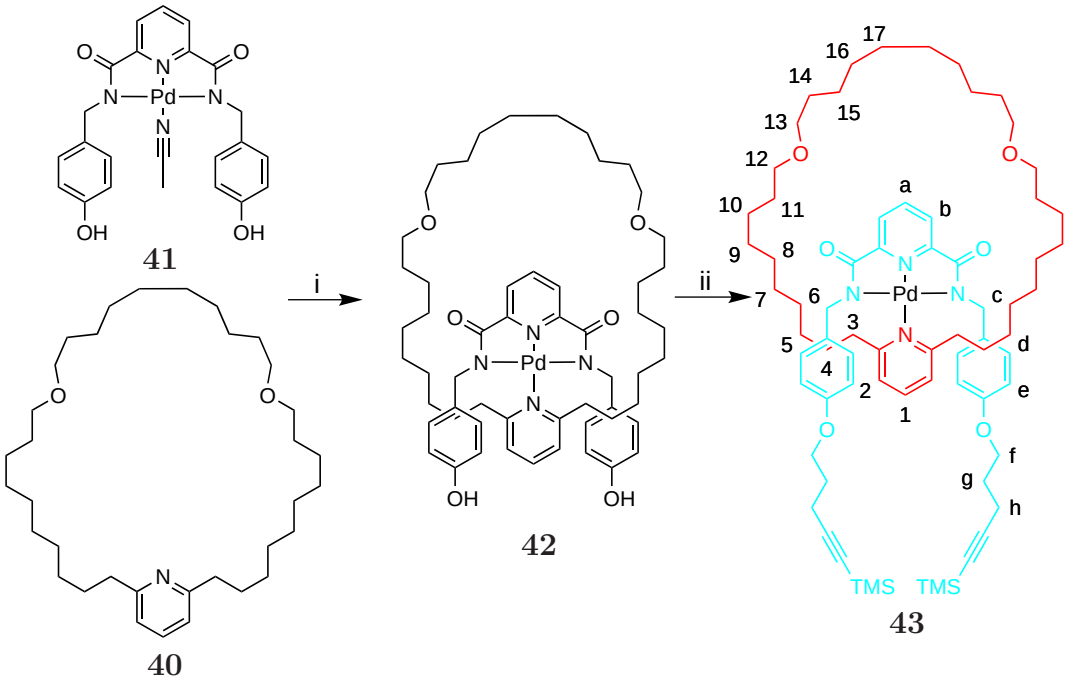

Scheme 3.13. Synthesis of **BBa-TMS 43**. Reagents and conditions: i) **41**, **40**, CH_2Cl_2/DMF, 80%; ii) **42**, PCy_3, DIAD, 5-TMS-4-pentyn-1-ol, THF, 41%.

Ligand exchange of the labile acetonitrile ligand with macrocycle **40** afforded the bisphenol macrocycle complex **42** in good yield. The double alkylation of the phenolic positions was achieved using an optimised Mitsunobu protocol. This comprised the sequential formation of the phosphonium ylid with tricyclohexylphosphine and DIAD at 0 °C in THF, followed by the addition of the primary TMS-protected alkynyl alcohol to form the alkylating oxyphosphonium species. The resulting mixture was then added to **42** and produced **BBa-TMS** (**43**) in moderate yield.

The ^{1}H-NMR of **43** is shown in Figure 3.4c, spectra of the uncoordinated macrocycle (Figure 3.4a) and the bisphenol complex **42** (Figure 3.4b) are shown for comparison. Upon complexation **42**, the proton signals H_1 and H_2 of the aromatic pyridine experience a downfield shift of 0.27 ppm and 0.09 ppm respec-

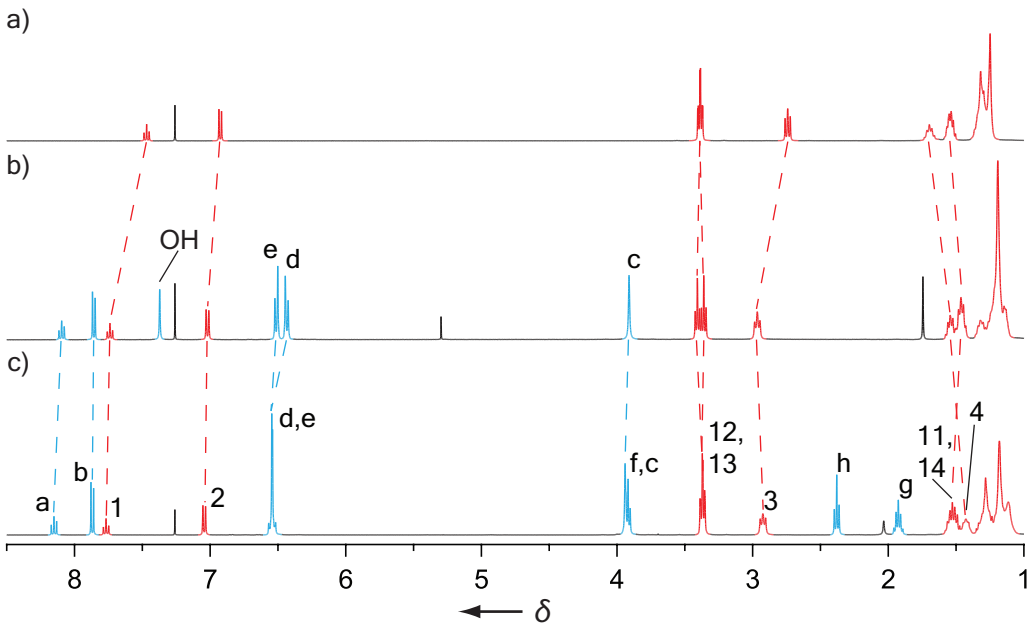

Figure 3.4. ^{1}H-NMR (400 MHz, $CDCl_3$, 300 K) of a) macrocycle **40**; macrocycle tridentate complex **42**; c) M1PdtAl-TMS **43**. The assignment corresponds to the lettering shown in 3.13.

tively. This coincides with the coordination to a TM, which withdraws electron density predominantly from the ortho and para positions. H_3 is also affected by the reduced electron density and shows a downfield shift of 0.22 ppm. At position H_4, an upfield shift of 0.16 ppm can be observed. This is possibly due to the protons facing and contacting the d_{z^2}-orbital of the palladium, and thus experiencing additional shielding effects. The spectrum of **43** shows just small changes, with the exception of the aromatic protons H_d and H_e, which exhibit a significant increase of π-stacking interactions. The simplicity of the spectrum of **43** suggests a C_{2v} symmetry in solution.

3.3.3 Synthesis of BBb

The synthesis of the azide-containing building block **BBb** (**45**) started from the pre-metallated bisazide U-shape **44**, which was introduced in chapter 2 (compound **33**). Here, **44** was reacted with macrocycle **M1** (**40**) in a ligand exchange reaction to obtain the desired **BBb** (**45**) in excellent yield.

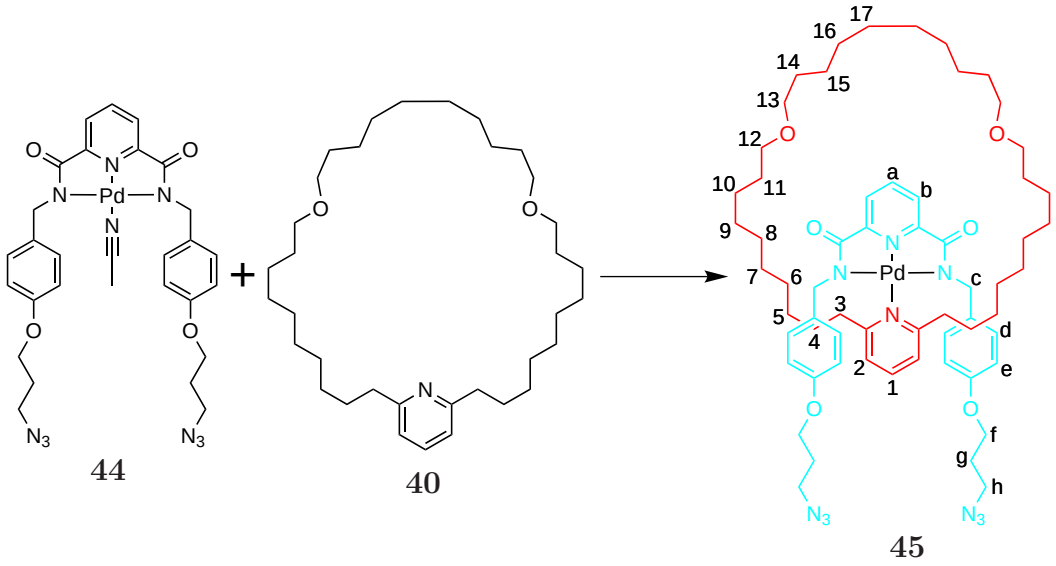

Scheme 3.14. Synthesis of the **BBb**. Reagents and Conditions: **44**, **40**, CH_2Cl_2, 94%.

The ^{1}H-NMR of **BBb** (**45**) is shown in Figure 3.5b alongside with the spectra of **40** (Figure 3.5a) and the bisazide tridentate ligand (Figure 3.5c). Comparing the chemical shifts of the macrocycle **M1** (**40**) with the corresponding signals in **BBb**, one can note the close similarity to the signal pattern of the macrocycle in **BBa-TMS**. Again, the para and ortho positions are experiencing the strongest electron withdrawing effect from the TM with 0.31 ppm for proton H_1 and 0.21 ppm for proton H_3. Proton H_4 exhibits an increased shielding effect and shifts upfield by 0.21 ppm. Comparing the unmetallated tridentate ligand with the ready assembled **BBb** (**45**), most of the protons show significant upfield shifts, except proton H_a, which shifts downfield by 0.14 ppm. Protons H_e and H_d show strong π-interactions of phenyl positions with the "sandwiched" electron deficient 2,6-disubstituted pyridine. As with **43**, the simplicity of the spectrum suggests a C_{2v} in solution.

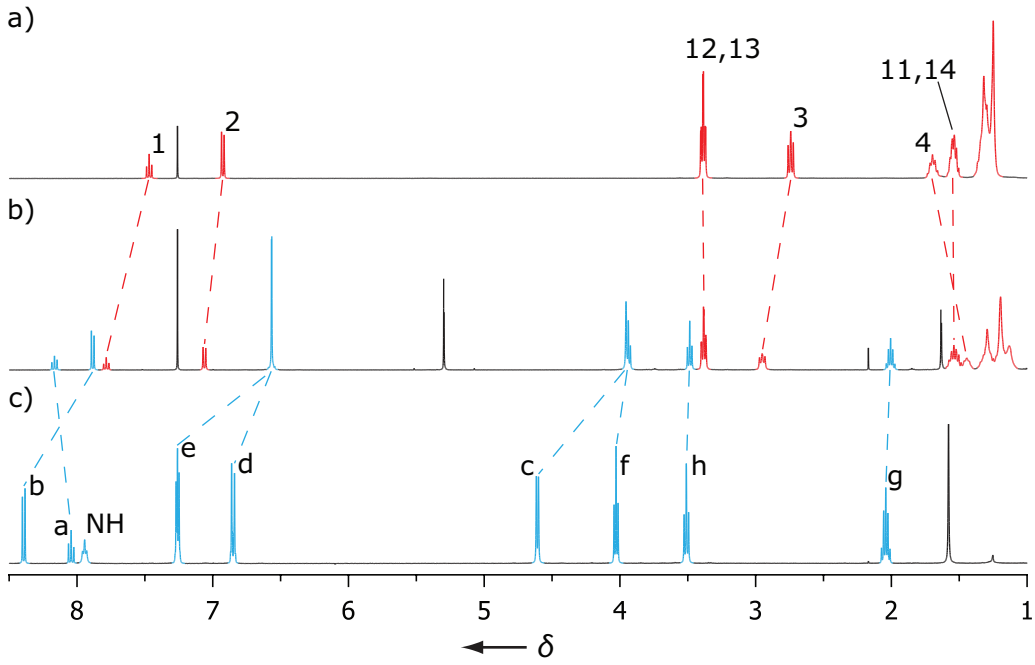

Figure 3.5. ^{1}H-NMR (400 MHz, $CDCl_3$, 300 K) of a) macrocycle **40**; b) BBb (**45**); c) bisazide tridentate ligand. The assignment corresponds to the lettering shown in Figure 3.14.

3.3.4 Synthesis of the [3]Catenane via Double-Click Ring-Closure

The synthesis of the [3]-catenane **46** is based on the findings from the synthesis towards the Borromean links presented in Chapter 2. The ring-closure was envisaged to be performed as a one pot double-click reaction together with an *in situ* deprotection of the TMS protecting groups attached to the terminal alkynes, using a silver(I) salt.[20] To improve the performance of the click-reaction, the use of an additional copper stabilising ligand was advised. In this reaction, the tetradentate ligand TBTA was used, as it has been reported to accelerate the triazole formation and to stabilise the copper(I) cation against oxidation.[21]

The click-components **43** and **45** were dissolved in equal amounts of dry and degassed CH_2Cl_2 and MeOH. These solutions were added to a performed TBTA $[Cu(MeCN)_4]PF_6$ complex solution in CH_2Cl_2. Addition of the silver(I) salt started off the reaction, which was allowed to stir for two days. The crude mixture showed significant formation of silver black, therefore an additional batch of silver(I) salt and copper(I) salt were added after one day. The reaction itself pro-

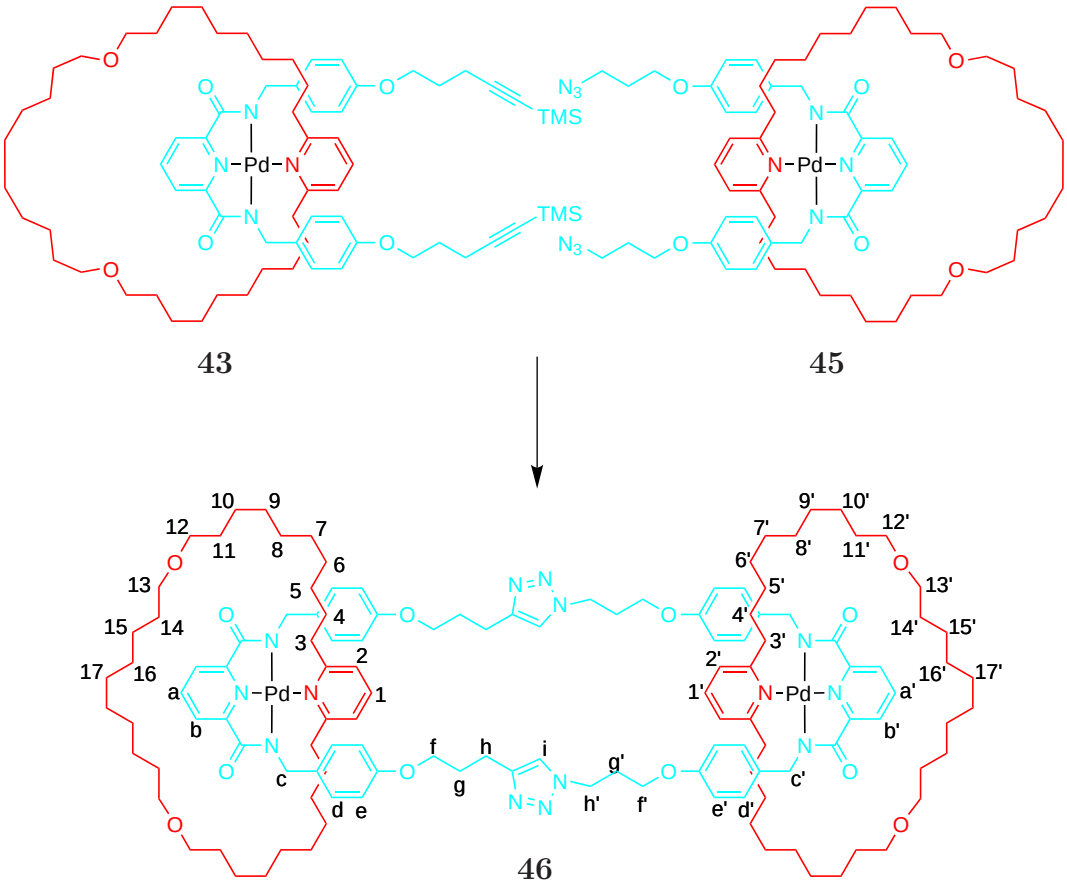

Scheme 3.15. Synthesis of [3]catenane by in situ deprotection and successive "click"-reaction as one pot strategy. Reagents and Conditions: **43**, CNrefMK302, $[Cu(MeCN)_4]PF_6$, TBTA, $AgBF_4$, CH_2Cl_2, MeOH, c = 5 mM, 2 d, 18 %.

gressed extremely sluggish and after 2 days no more conversion could be detected by TLC. After purification by column chromatography on silica, the product **46** was obtained in 18% yield.

The ^{1}H-NMR of [3]catenane (**46**) is shown in Figure 3.6b, the spectra of **BBa-TMS** (**43**) (Figure 3.6a) and **BBb** (**45**) (Figure 3.6c) are shown for comparison. Comparing the signals of the [3]catenane with the signals from the building blocks, one can note that the macrocycle signals are almost unaffected, with the exception of protons H_3, $H_{3'}$, H_4 and $H_{4'}$ which experience a slight upfield shift. This could be the consequence of the restricted movement of the phenyl groups due to the ring-closure. Strong downfield shifts of protons H_h ($\Delta\sigma \approx 0.5$ ppm) and $H_{h'}$ ($\Delta\sigma = 1.0$ ppm), which are adjacent to the formed triazole ring, indicate the successful formation of the double click-product. The electron-withdrawing effect of the triazole unit lessen with distance from its core, so that the β-protons on

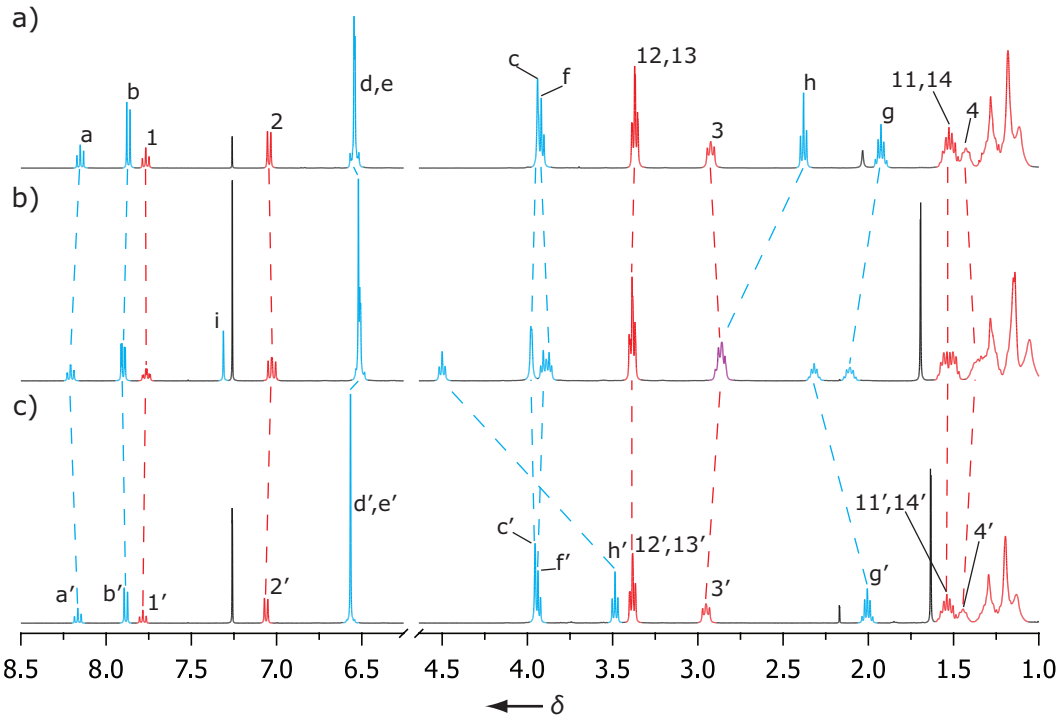

Figure 3.6. ^{1}H-NMR (400 MHz, $CDCl_3$, 300 K) of a)M1PdtAl-TMS **43**; b) [3]catenane; c) M1PdtAz **45**. The assignment corresponds to the numbering shown in Figure 3.15. Blue signals correspond to the central ring, red signals to the catenated macrocycles and the violet signal constitutes an overlap between the two.

position H_g and $H_{g'}$ are much less affected and show downfield shifts of $\Delta\sigma = 0.30$ ppm and $\Delta\sigma = 0.17$ ppm respectively. The remaining signals only experience minor changes in comparison to the starting materials. The remainder of the macrocycle signals are superimposed, indicating that the ring-closure does not affect the complex integrity. Due to the simplicity of the spectrum, it is possible to conclude a C_{2v} symmetry in solution.

3.4 Conclusions

It was demonstrated, that the palladium [3+1] template is able to withstand a variety of reaction conditions and allowed the late manipulation of the building block precursors to introduce the necessary alkyne residues. The employed one-pot deprotection and click-protocol produced the desired [3]catenane and showcased, that the palladium tridentate monodentate assembly was chemically and structurally stable under these conditions. The presented [3]catenane is the first oligocatenane produced with an TM other then Cu(I). Despite the moderate yield of the double Mitsunobu reaction and the rather low yield for the double click-cyclistaion, further optimisation of the reaction conditions (i.e. temperature, concentration, catalyst load, copper source, catalyst ligand and solvent composition) is possible.

3.5 Experimental

3.5.1 Synthesis

10-bromodecane-1-oxy-dimethyl-t-butylsilane (34)[19]

A dry flask was charged with 1-bromo-10-decanol (6.73 g, 24.6 mmol), imidazole (2.00 g, 29.5 mmol), *t*-butyldimethylsilyl chloride (4.09 g, 27.1 mmol), CH_2Cl_2 (70 mL) and stirred for 18 h. The reaction mixture was washed with 1M HCl, saturated $NaHCO_3$ solution, brine and dried over Na_2SO_4. The resulting solution was concentrated in vacuo, taken up in hexane, absorbed on a plug of silica and eluted (10% Et_2O in hexane). Evaporation of the solvent afforded the desired product as colourless oil (7.93 g, 54%).

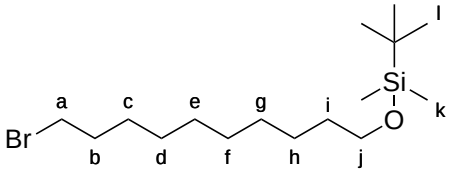

^{1}H-NMR (400 MHz, $CDCl_3$, 300 K): δ = 3.55 (t, 2H, J = 6.6 Hz, H_j), 3.36 (t, 2H, J = 6.9 Hz, H_a), 1.86 - 1.74 (m, 2H, H_b), 1.50 - 1.42 (m, 2H, H_i), 1.37 (p, 2H, J = 7.2 Hz, H_c), 1.30 - 1.20 (m, 10H, $H_{d/e/f/g/h}$), 0.90 - 0.80 (m, 9H, H_l), 0.05 - (-0.03) (m, 6H, H_k).
^{13}C-NMR (100 MHz, $CDCl_3$, 300 K): δ = 63.37, 34.00, 32.98, 32.96, 29.64(2x), 29.51, 28.88, 28.30, 26.10, 25.90, 18.47, -5.15.
LREI-MS: m/z = 351 $[M + H]^+$.
HREI-MS: m/z = 350.16484 $[M]^+$
(calc. for $C_{16}H_{35}O_1BrSi$ 350.16460).

2,6-bis(11-t-butyldimethylsilyl-10-oxodecyl)-pyridine (36)

A dry Schlenk tube was charged with activated Zn dust (260 mg, 4 mmol) and set under Nitrogen. DMF (2 mL) was added and the suspension stirred for 5 min. Then Iodine (50 mg, 200 μmol) was added and the solution was stirred until the colour of the Iodine vanished. To this solution, the bromide **34** (1.19 g, 2 mmol) was added, and the reaction mixture was heated to 80 °C for 4 h. $[Pd(PPh_3)_4]$

(77 mg, 66 μmol) and 2,6-dibromo pyridine (156 mg, 66 μmol) were added and the solution was stirred further 2 h at 80 °C. The reaction mixture was allowed to cool to RT, diluted with Et_2O (100 mL) and washed with 1M Na_4EDTA solution, dilute NH_3 solution, water, Brine and dried over $NaSO_4$. The resulting solution was concentrated in vacuo and purified via column chromatography (3% EtOAc in hexane) to afford the product as colourless oil (310 mg, 75%).

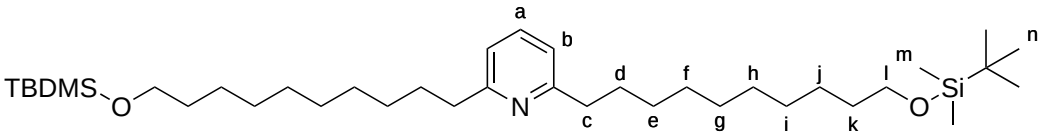

^{1}H-NMR (400 MHz, $CDCl_3$, 300 K): δ = 7.43 (t, 1H, J = 7.7 Hz, H_a), 6.89 (d, 2H, J = 7.7 Hz, H_b), 3.55 (t, 4H, J = 6.7 Hz, H_l), 2.75 - 2.64 (m, 4H, H_c), 1.71 - 1.58 (m, 4H, H_d), 1.45 (p, 4H, J = 6.8 Hz, H_k), 1.36 - 1.16 (m, 24H, $H_{e/f/g/h/i/j}$), 0.85 (t, 18H, J = 2.8 Hz, H_n), 0.00 (t, 12H, J = 3.1 Hz, H_m).
^{13}C-NMR (100 MHz, $CDCl_3$, 300 K): δ = 162.04, 136.49, 119.70, 63.50, 38.77, 33.03, 30.41, 29.75, 29.67(2x), 29.61, 29.58, 26.13, 25.94, 18.53, -5.11.
LRESI-MS: m/z = 620 $[M + H]^+$.

2,6-Bis-(10-hydroxydecyl)-pyridine (37)

36 (200 mg, 322 μmol) was dissolved in dry THF (6.5 mL) and TBAF 1M in THF (774 μL, 774μmol) was added. The solution was stirred for 2 h at RT. The rection was quenched upon addition of water (1 ml). The product precipitated out of solution, was isolated by filtration and washed with water and Et_2O. Drying under HV afforded the desired product as an amorphous white solid (125 mg, 99%).

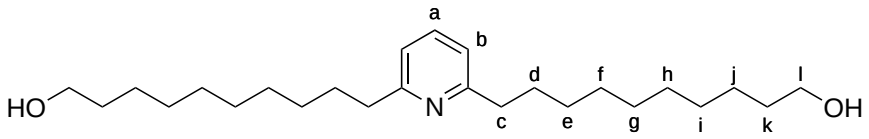

^{1}H-NMR (400 MHz, $CDCl_3$, 300 K): δ = 7.47 (t, 1H, J = 7.7 Hz, H_a), 6.93 (d, 2H, J = 7.7 Hz, H_b), 3.63 (t, 4H, J = 6.7 Hz, H_l), 2.73 (m, 4H, H_c), 1.68 (p, 4H, J = 7.7 Hz, H_d), 1.55 (m, 4H, H_k), 1.30 (m, 24H, $H_{e/f/g/h/i/j}$).
^{13}C-NMR (100 MHz, $CDCl_3$, 300 K): δ = 161.84, 136.37, 119.58, 62.98, 38.52,

32.76, 30.21, 29.52, 29.45, 29.43, 29.38, 29.36, 25.69.

HREI-MS: m/z = 392.35289 $[M + H]^+$

(calc. for $C_{25}H_{46}O_2N$ 392.35340).

2,6-Bis-(10-(hex-5-enyloxy)-decyl)-pyridine (38)

A dry Schlenk tube was charged with 2,6-Bis-(10-hydroxydecyl)-pyridine **37** (150 mg, 384 μmol) and dry DMF (4 mL) was added. NaH 60% in oil suspension (46 mg, 1.15 mmol) was added and the solution was stirred for 1 h. To this solution hex-5-enyl-1-tosylate (620 mg, 2.43 mmol) and 15-crown-5 (84 mg, 76 μL, 384μmol) were added and the solution stirred for 4 d at 70 °C. The reaction mixture was poured into water and extracted 4 times with EtOAc. The combined extracts were washed with water and brine, dried over $MgSO_4$ and concentrated in vacuo. The resulting residue was purified by column chromatography (5% EtOAc in hexane) to afford the product as off white waxy solid (85 mg, 40%).

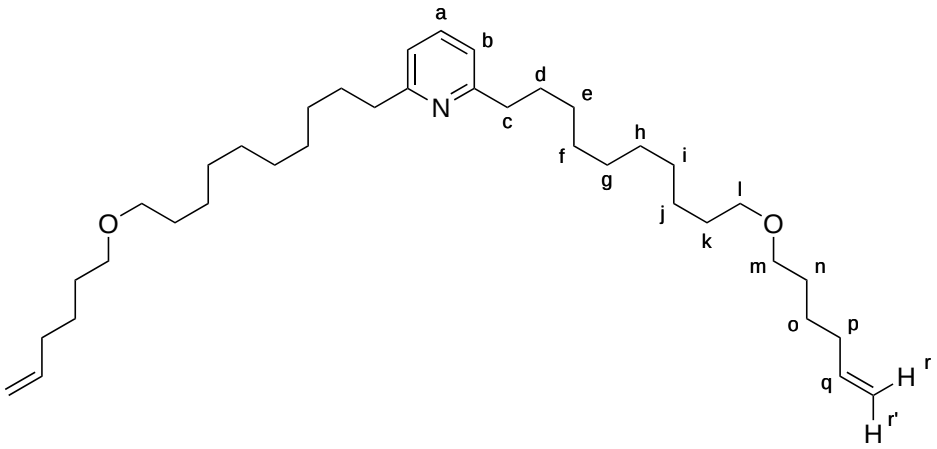

^{1}H-NMR (400 MHz, $CDCl_3$, 300 K): δ = 7.47 (t, 1H, J = 7.7 Hz, H_a), 6.93 (d, 2H, J = 7.7 Hz, H_b), 5.80 (m, 2H, H_q), 5.00 (dd, 2H, J = 17.1, 3.6, H_r), 4.94 (dd, 2H, J = 10.2, 2.2, $H_{r'}$), 3.39 (q, 8H, J = 6.5 Hz, $H_{l/m}$), 2.78-2.69 (m, 4H, H_c), 2.11-2.02 (m, 4H, H_p), 1.74-1.63 (m, 4H, H_d), 1.63-1.50 (m, 8H, $H_{k/n}$), 1.49-1.39 (m, 4H, H_o), 1.39-1.16 (m, 24H, $H_{e/f/g/h/i/j}$.

^{13}C-NMR (100 MHz, $CDCl_3$, 300 K): δ = 162.03, 138.97, 136.49, 119.70, 114.59, 71.13, 70.83, 38.77, 33.73, 30.41, 29.90, 29.72, 29.66, 29.63, 29.61, 29.37, 26.32, 25.63.

LRESI-MS: m/z = 556 $[M + H]^+$

2,6-(10,21-dioxo-[16]tritriaconteno)-pyridine (39)

A dry flask was charged with 2,6-Bis-(10-(hex-5-enyloxy)-decyl)-pyridine **38** (372 mg, 669 umol) and dry toluene (1 L) was added under an atmosphere of nitrogen. Upon addition of Grubbs' 1st. generation catalyst (82 mg, 100 μmol), the solution was stirred for 24 h and 2 h open to air. The reaction mixture was concentrated in vacuo and purified by column chromatography using a gradient (Et_2O 5% to 10% in hexane) to obtain the product as white amorphous solid (258 mg, 73%).

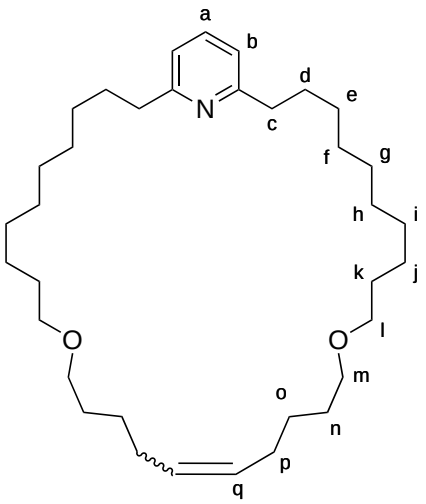

^{1}H-NMR (400 MHz, $CDCl_3$, 300 K): δ = 7.49–7.44 (m, 1H, H_a), 6.94–6.90 (m, 2H, H_b), 5.42–5.39 (m, 2H, H_q), 5.38–5.39 (m, 2H, H_q), 3.41–3.35 (m, 4H, $H_{l/m}$), 2.74 (t, 4H, J = 7.6 Hz, H_c), 2.15–2.02 (m, 4H, H_p), 1.75–1.50 (m, 16H, $H_{d/k/n/o}$), 1.37–1.18 (m, 24H, $H_{e/f/g/h/i/j}$).

^{13}C-NMR (100 MHz, $CDCl_3$, 300 K): δ = 161.82, 161.76, 136.29, 136.26, 130.17, 129.75, 119.79, 119.72, 70.98, 70.86, 69.98, 69.86, 38.45, 38.27, 30.10, 29.94, 29.76, 29.70, 29.61, 29.51, 29.45, 29.40, 29.38, 29.37, 29.33, 29.10, 28.95, 28.86, 26.19, 26.16, 23.72. (Signal overlap in the region of 29.7-29.4 ppm.)

LRESI-MS: m/z = 528 $[M + H]^+$

HRESI-MS: m/z = 528.47661 $[M]^+$

(calc. for $C_{35}H_{62}NO_2$ 528.47751).

2,6-(10,21-dioxo-tritriacontano)-pyridine (40)

A dry flask was charged with **39** (258 mg, 448 μmol), Pd/C (10% palladium load, 26 mg) and flushed with nitrogen. Anhydrous THF was added and hydrogen was flushed through the suspension for 4 h whilst stirring vigorously. The reaction was monitored by TLC (Et_2O 15% in hexane). The reaction mixture was filtered through a plug of celite and concentrated in vacuo to obtain the desired product as white amorphous solid (258 mg, 99%).

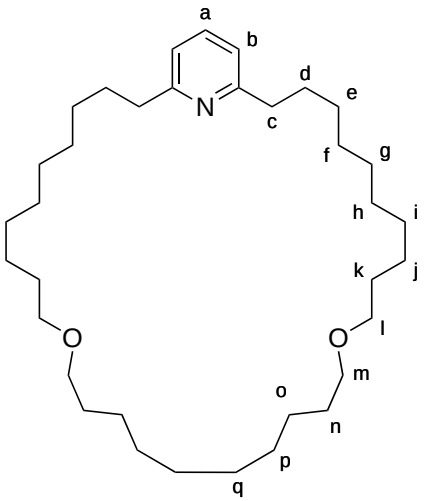

^{1}H-NMR (400 MHz, $CDCl_3$, 300 K): δ = 7.47 (t, 1H, J = 7.6 Hz, H_a), 6.93 (d, 2H, J = 7.7 Hz, H_b), 3.41–3.62 (m, 8H, $H_{l/m}$), 2.78-2.70 (m, 4H, H_c), 1.75-1.63 (m, 4H, H_d), 1.60-1.48 (m, 8H, $H_{k/n}$), 1.40-1.20 (m, 36H, $H_{e/f/g/h/i/j/o/p/q}$).
^{13}C-NMR (100 MHz, $CDCl_3$, 300 K): δ = 162.00, 136.45, 119.83, 70.89, 70.83, 38.65, 30.26, 29.84, 29.70, 29.55, 29.49(2x), 29.47(2x), 29.29, 29.26, 26.31, 26.08.
HREI-MS: m/z = 530.49441 $[M + H]^+$
(calc. for $C_{35}H_{64}NO_2$ 530.49425).

{κ^3-2,6-bis-[4-(3-azido-propoxy)-benzylamide]-pyridino}{2,6-(10,21-dioxo-tritriacontano)-pyridino} palladium(II)
(45)

A flask was charged with {κ^3-2,6-bis-[4-(3-azido-propoxy)-benzylamide]-pyridino} {acetonitrile} palladium(II) (143 mg, 207 μmol), 2,6-(10,21-dioxo-tritriacontano)-pyridine **40** (100 mg, 188 μmol), dissolved in CH_2Cl_2 (10 mL) and let stir

for 18 h. The reaction mixture was concentrated in vacuo and purified by column chromatography (MeOH 3% in CH_2Cl_2) to afford the desired product as amorphous yellow-orange solid (210 mg, 94%).

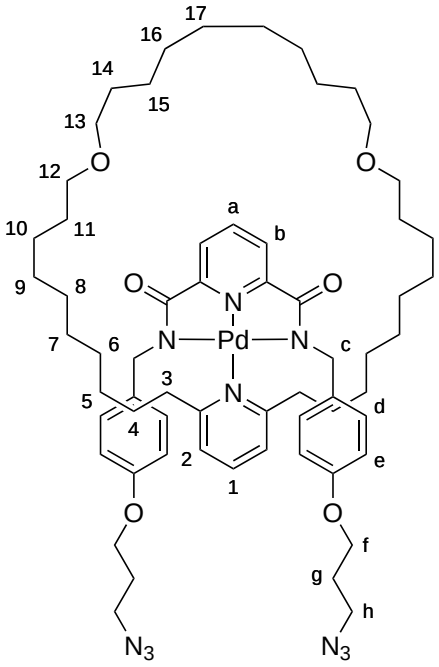

^{1}H-NMR (400 MHz, $CDCl_3$, 300 K): δ = 8.17 (t, 1H, J = 7.8 Hz, H_a), 7.88 (d, 2H, J = 7.8 Hz, H_b), 7.78 (t, 1H, J = 7.8 Hz, H_1), 7.06 (d, 2H, J = 7.8 Hz, H_2), 6.57 (m, 8H, $H_{d/e}$), 3.96–3.92 (m, 8H, $H_{c/f}$), 3.49 (t, 4H, J = 6.6 Hz, H_h), 3.38 (m, 8H, $H_{12/13}$), 2.95 (t, 4H, H_3), 2.01 (p, 4H, J = 6.3 Hz, H_g), 1.63–1.48 (m, 8H, $H_{11/14}$), 1.53–1.39 (m, 4H, H_4), 1.38–1.06 (m, 36H, $H_{5/6/7/8/9/10/15/16/17}$)

^{13}C-NMR (100 MHz, $CDCl_3$, 300 K): δ = 171.41, 164.18, 157.46, 152.90, 140.82, 138.92, 133.74, 128.71, 125.01, 121.52, 114.14, 71.22, 71.09, 64.59, 49.28, 48.39, 38.95, 30.09, 30.03, 29.74, 29.57, 29.42, 29.28, 29.19, 28.98(2x), 28.82, 27.60, 26.45, 26.27.

HRESI-MS: m/z = 1177.6318 $[M + H]^+$ (calc. for $C_{62}H_{90}N_{10}O_6Pd$ 1177.6173).

{κ^3-2,6-Bis[4-hydroxy-benzylamide]-pyridino}{2,6-(10,21-dioxo-tritriacontano)-pyridino}palladium(II)

(42)

{κ^3-2,6-Bis[4-hydroxy-benzylamide]-pyridino}{acetonitrile} palladium(II) (100 mg, 191 μmol) and 2,6-(10,21-dioxo-tritriacontano)-pyridine **40** (96 mg, 182 μmol)

were dissolved in a mixture of CH_2Cl_2 and DMF (2 mL: 1 mL) and stirred for 24 h. The reaction mixture was concentrated in vacuo and purified by column chromatography (20% THF in CH_2Cl_2). Removal of the volatiles yielded the desired product as yellow amorphous solid (148 mg, 80%).

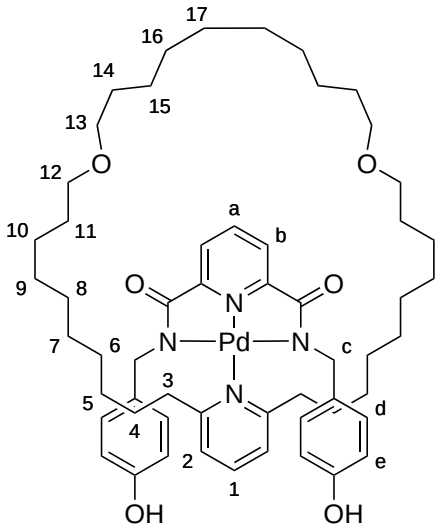

^{1}H-NMR (400 MHz, $CDCl_3$, 300 K): δ = 8.10 (t, 1H, J = 7.8 Hz, H_a), 7.86 (d, 2H, J = 7.8 Hz, H_b), 7.74 (t, 1H, J = 7.8 Hz, H_1), 7.43 (s, 2H, H_{OH}), 7.02 (d, 2H, J = 7.8 Hz, H_2), 6.51 (d, 4H, J = 8.5 Hz, H_e), 6.43 (d, 4H, J = 8.5 Hz, H_d), 3.91 (s, 4H, H_c), 3.46 3.30 (m, 8H, $H_{12/13}$), 2.96 (t, 4H, J = 7.8 Hz, H_3), 1.59 1.40 (m, 12H, $H_{4/11/14}$), 1.37 1.09 (m, 36H, $H_{5/6/7/8/9/10/15/16/17}$).
^{13}C-NMR (100 MHz, $CDCl_3$, 300 K): δ = 171.28, 164.01, 155.43, 153.00, 140.70, 138.89, 132.08, 128.71, 124.92, 121.47, 115.25, 71.30, 71.11, 49.46, 38.93, 29.61, 29.49, 29.41, 28.98, 28.77(2x), 28.76, 28.55, 28.53, 27.53, 26.18, 25.79.
HRESI-MS: m/z = 1011.5266 $[M + H]^+$
(calc. for $C_{56}H_{81}N_4O_6Pd$ 1011.5205).

{κ^3-2,6-Bis-[4-(5-trimethylsilyl-3-ynyl-propoxy)-benzylamide]-pyridino}{2,6-(10,21-dioxo-tritriacontano)-pyridino}palladium(II)
(43)

A dry Schlenk tube was charged with tricyclohexyl phosphine (373 mg, 1,33 mmol) and set under nitrogen. Dry THF (1.3 mL) was added and the solution was cooled to 0 °C. DIAD (269 mg, 275 μL, 1.33 mmol) was added the solution

allowed to stir at 0 °C for 30 min. 5-trimethylsilyl-pent-4-yn-1-ol (208 mg, 251 μL, 1.33 mmol) was added, the solution stirred for 20 min at 0 °C and 30 min at RT. The reaction mixture was then added to the bisphenol complex **42** (135 mg, 133 μmol) and the resulting solution was allowed to stir for 18 h. Concentration in vacuo and purification by gradient column chromatography (*i*-PrOH 1% to 4% in CH_2Cl_2) afforded the desired product as yellow amorphous solid (68 mg, 41%).

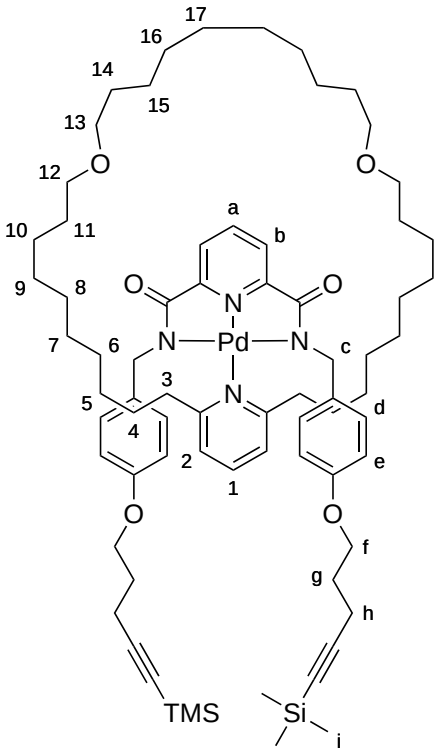

^{1}H-NMR (400 MHz, $CDCl_3$, 300 K): δ = 8.16 (t, 1H, J = 7.8 Hz, H_a), 7.88 (d, 2H, J = 7.8 Hz, H_b), 7.78 (t, 1H, J = 7.8 Hz, H_1), 7.06 (d, 2H, J = 7.8 Hz, H_2), 6.58-6.52 (m, 8H, $H_{d/e}$), 3.97-3.90 (m, 8H, $H_{c/f}$), 3.41–3.62 (m, 8H, $H_{12/13}$), 2.97-2.90 (m, 4H, H_3), 2.39 (t, 4H, J = 7.1 Hz, H_h), 1.94 (p, 4H, J = 6.6 Hz, H_g), 1.60-1.47 (m, 8H, $H_{11/14}$), 1.47-1.38 (m, 4H, H_4), 1.37-1.07 (m, 36H, $H_{5/6/7/8/9/10/15/16/17}$), 0.13 (s, 18H, H_i).

^{13}C-NMR (100 MHz, $CDCl_3$, 300 K): δ = 171.22, 164.04, 157.49, 152.75, 140.62, 138.71, 133.30, 128.50, 124.81, 121.30, 113.97, 106.23, 85.02, 71.05, 70.92, 66.22, 49.09, 38.74, 29.91, 29.86, 29.58, 29.40, 29.24, 29.11, 29.01, 28.81, 28.65, 28.39, 27.41, 26.28, 26.08, 16.59, 0.11.

HRESI-MS: m/z = 1309.6946 $[M + Na]^+$

(calc. for $C_{72}H_{108}N_4O_6PdSi_2Na$ 1309.6757).

[3]catenane (46)

A dry Schlenk tube was charged with TBTA (3.1 mg, 5.9 μmol), $[Cu(MeCN)_4]PF_6$ (2.2 mg, 5.9 μmol), flushed with nitrogen and CH_2Cl_2 (2 mL) was added. Dry degassed solutions of *bis*-azide **45** (69.5 mg, 59 μmol) in CH_2Cl_2 (3 mL), *bis*-TMS alkyne **43** (76 mg, 58.9 μmol) in CH_2Cl_2 (3 mL) and $AgBF_4$ (1.1 mg, 5.9 μmol) were added. The resulting reaction mixture was allowed to stir for 2 d. Upon removal of the volatiles and purification by column chromatography (EtOH 5% in CH_2Cl_2) the product was obtained as yellow amorphous solid (24 mg, 18%).

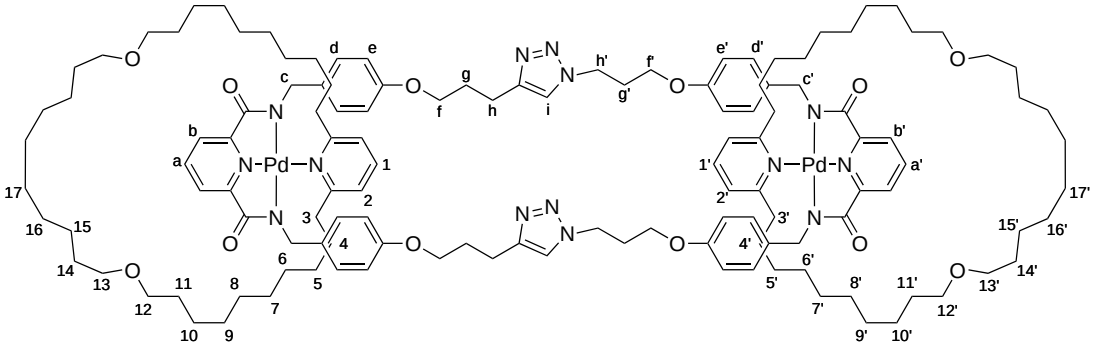

^{1}H-NMR (400 MHz, $CDCl_3$, 300 K): δ = 8.23-8.18 (m, 2H, $H_{a/a'}$), 7.92-7.87 (m, 4H, $H_{b/b'}$), 7.79-7.73 (m, 2H, $H_{1/1'}$), 7.31 (s, 2H, H_i), 7.06-6.99 (m, 4H, $H_{2/2'}$), 6.54-6.47 (m, 16H, $H_{d/d'/e/e'}$), 4.50 (t, 4H, J = 6.9 Hz, $H_{h'}$), 4.00-3.98 (m, 8H, $H_{c/c'}$), 3.93-3.85 (m, 8H, $H_{f/f'}$), 3.41-3.35 (m, 16H, $H_{12/12'/13/13'}$), 2.91-2.82 (m, 12H, $H_{h/3/3'}$), 2.36-2.27 (m, 4H, $H_{g'}$), 2.16-2.06 (m, 4H, H_g), 1.60-1.45 (m, 16H, $H_{11/11'/14/14'}$), 1.42-0.99 (m, 80H, $H_{4/4'/5/5'/6/6'/7/7'/8/8'/9/9'/10/10'/15/15'/16/16'/17/17'}$).
^{13}C-NMR (100 MHz, $CDCl_3$, 300 K): δ = 171.47, 171.44, 164.23, 164.18, 157.62, 157.18, 152.89, 152.84, 147.53, 140.98, 140.96, 139.12, 139.04, 134.13, 133.65, 128.88, 128.80, 125.08, 125.05, 121.61, 121.52, 121.12, 114.07, 114.05, 71.30, 71.28, 71.09, 67.00, 64.19, 49.39, 49.34, 47.12, 39.03, 30.31, 30.18, 29.99, 29.73, 29.72, 29.67, 29.63, 29.52, 29.50, 29.36, 29.29, 29.23, 28.78, 28.76, 27.91, 27.86, 26.45, 26.34, 26.33, 22.46.(53 signals observed; 62 signals expected. Multiple signal overlaps due to the pseudo C_{2h} symmetry.)
HRESI-MS: m/z = 2344.2151 $[M + Na]^+$
(calc. for $C_{128}H_{182}N_{14}O_{12}Pd_2Na$)

References

[1] G. Schill, K. Rissler, H. Fritz, W. Vetter, *Angew. Chem., Int. Ed. Engl.* **1981**, *20*, 187–189.

[2] O. Safarowsky, E. Vogel, F. Vögtle, *Eur. J. Org. Chem.* **2000**, 499–505.

[3] D. A. Leigh, J. K. Y. Wong, F. Dehez, F. Zerbetto, *Nature* **2003**, *424*, 174–179.

[4] M. Gupta, S. Kang, M. F. Mayer, *Tetrahedron Lett.* **2008**, *49*, 2946–2950.

[5] P. R. Ashton, C. L. Brown, E. J. T. Chrystal, K. P. Parry, M. Pietraszkiewicz, N. Spencer, J. F. Stoddart, *Angew. Chem., Int. Ed. Engl.* **1991**, *30*, 1042–1045.

[6] D. B. Amabilino, P. R. Ashton, A. S. Reder, N. Spencer, J. F. Stoddart, *Angew. Chem., Int. Ed. Engl.* **1994**, *33*, 433–437.

[7] P. R. Ashton, C. L. Brown, E. J. T. Chrystal, T. T. Goodnow, A. E. Kaifer, K. P. Parry, A. M. Z. Slawin, N. Spencer, J. F. Stoddart, D. J. Williams, *Angew. Chem., Int. Ed. Engl.* **1991**, *30*, 1039–1042.

[8] P. R. Ashton, S. E. Boyd, C. G. Claessens, R. E. Gillard, S. Menzer, J. F. Stoddart, M. S. Tolley, A. J. P. White, D. J. Williams, *Chem.–Eur. J.* **1997**, *3*, 788–798.

[9] D. B. Amabilino, P. R. Ashton, V. Balzani, S. E. Boyd, A. Credi, J. Y. Lee, S. Menzer, J. F. Stoddart, M. Venturi, D. J. Williams, *J. Am. Chem. Soc.* **1998**, *120*, 4295–4307.

[10] D. B. Amabilino, P. R. Ashton, A. S. Reder, N. Spencer, J. F. Stoddart, *Angew. Chem., Int. Ed. Engl.* **1994**, *33*, 1286–1290.

[11] J. M. Kern, J. P. Sauvage, J. L. Weidmann, *Tetrahedron* **1996**, *52*, 10921–10934.

[12] G. Schill, C. Zürcher, *Angew. Chem., Int. Ed. Engl.* **1969**, *8*, 988.

[13] J.-P. Sauvage, J. Weiss, *J. Am. Chem. Soc.* **1985**, *107*, 6108–6110.

[14] C. O. Dietrich-Buchecker, A. Khemiss, J.-P. Sauvage, *J. Chem. Soc., Chem. Commun.* **1986**, 1376–1378.

[15] J. D. Megiatto, Jr., D. I. Schuster, *Chem.–Eur. J.* **2009**, *15*, 5444–5448.

[16] H. Iwamoto, K. Itoh, H. Nagamiya, Y. Fukazawa, *Tetrahedron Lett.* **2003**, *44*, 5773–5776.

[17] A. L. Hubbard, G. J. E. Davidson, R. H. Patel, J. A. Wisner, S. J. Loeb, *Chem.Commun.* **2004**, 138–139.

[18] M. D. Lankshear, P. D. Beer, *Acc. Chem. Res.* **2007**, *40*, 657–668.

[19] C. Goulaouicdubois, A. Guggisberg, M. Hesse, *Tetrahedron* **1995**, *51*, 12035–12046.

[20] V. Aucagne, D. A. Leigh, *Org. Lett.* **2006**, *8*, 4505–4507.

[21] T. R. Chan, R. Hilgraf, K. B. Sharpless, V. Fokin, *Org. Lett.* **2004**, *6*, 2853–2855.

Chapter 4

Synthesis Towards Linear [2n+3]-catenanes

Acknowledgements and Declaration

Dr. Kevin Hänni supplied the macrocycle **15**. The project was designed and realised by the Author.

Synopsis

This chapter presents the synthesis and use of a comprehensive click building block library based on the palladium(II) [3+1] template methodology presented throughout this thesis. The building blocks, a selection of "capping" macrocycle-containing and acyclic click counterparts, were designed to generate mechanically interlocked architectures such as [2]-, [3]- and [n]catenanes. The modularity of this approach is exhibited by the ease of creating this diverse library from a small selection of subcomponents. The synthesis of a [2]catenane and [3]catenane showcase the potential of this methodology. The synthesis of higher [n]catenanes with n>3 is discussed and a precursor compound towards these elusive targets is presented.

4.1 Introduction

With the exception of Stoddart's higher linear and sidechain [n]catenanes (3<n<7), which were obtained via high pressure assisted self-assembly processes and do not rely on TM templation, there are no examples of these difficult synthetic targets present in the current literature.[1,2]

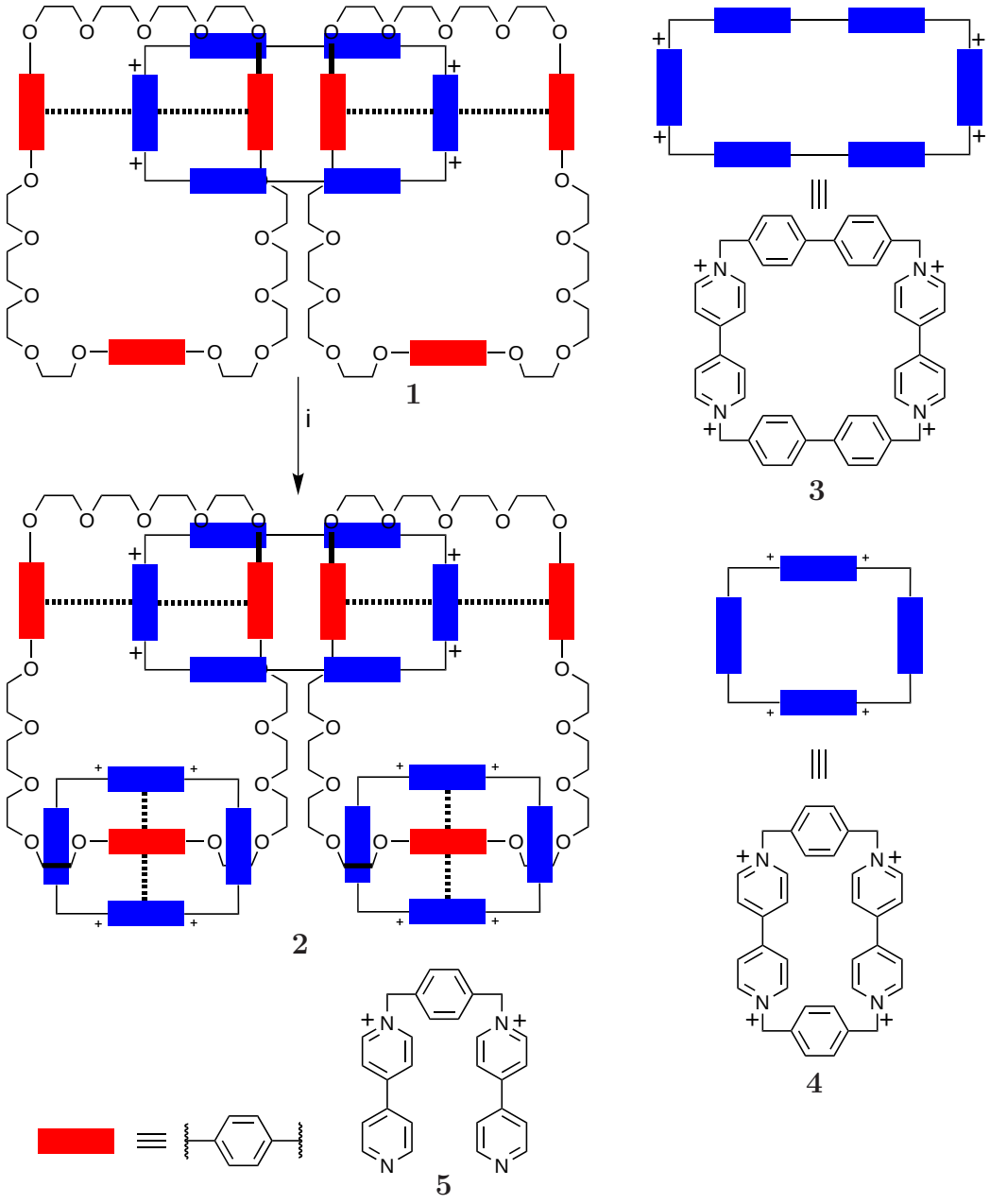

Scheme 4.1. Stoddart's [5]catenane synthesis. Reagents and conditions: i) 1. **1**, **5**, 1,4-*Bis*-bromomethyl-benzene, **1**, MeCN; 2. NH_4PF_6, H_2O, [4]catenane (31%), [5]catenane (5%).

However, there are some examples of necklace [n]catenanes (with 3<n<5),[3–5] but these structures were mainly constructed by self assembly processes. Although Sauvage and co-workers have reportedly been investigating linear polycatenanes for more than 25 years they have not been able to isolate them and obtain unambiguous proof of their existence.[6,7] Therefore, to generate these structures by the means of TM template directed synthesis would be a novelty. Stoddart's synthesis of Olympiadanes commenced from the [3]catenane, which was synthesised using a 3-station polyethylenglycol macrocycle (Figure 4.1) and the *bis*-bipyridinium clamp precursor of **3** together with 1,4-*bis*-bromomethyl-benzene in a self assembly process to obtain **1** in a very poor yield of 6%. Subsequent reaction of **1** with **5** and 1,4-*Bis*-bromomethyl-benzene afforded a mixture of [4]- and [5]catenane in 31% and 5% respectively.[1,2] This yield was tremendously improved by substituting the benzene-1,4-diol station in the 3-station macrocycle with 1,5-dihydroxynaphthalene and applying high pressure. As a consequence, Stoddart and co-workers were able to improve the yield of the catenated species and obtained the linear [5]catenane and sidechain [6]- and [7]catenane as products in 30%, 28% and 26% yield respectively.[8]

4.1.1 Topological Analysis

Linear oligo catenanes are very difficult synthetic targets and can theoretically be obtained via a multitude of synthetic strategies. Therefore a topological analysis was carried out on a linear [7]catenane ([2n+3]catenane with n = 2) Figure 4.1a, to identify ways to access this target in a modular and convergent manner, using a non-threading building block based strategy.

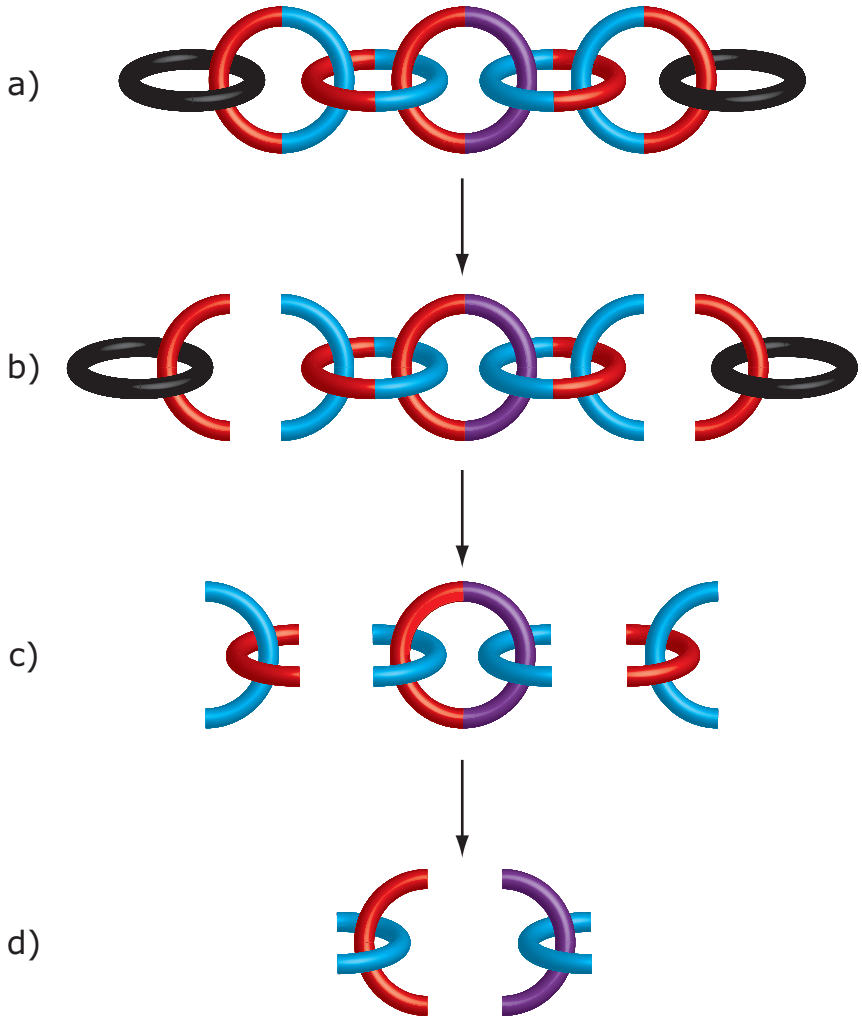

Figure 4.1. Topological analysis of a representative [2n+3]catenane with n = 2.

The [7]catenane shown (Figure 4.1a) consists of five fused rings (depicted in two different colours e.g. red and cyan or purple) and the black "capping"-macrocycles at either end of the chain. Embedded in its structure are six crossover points that orthogonally align the rings, establishing a C_{2v} symmetry throughout the linear chain. Dissecting the terminal fused rings (Figure 4.1b) leads

to a [3]catenane assembly with two blue threads in the terminal regions and two terminal "capping"-fragments consisting of a black macrocycle and a red thread. Further deconstruction of the [3]catenane assembly (Figure 4.1c) yields the "chain-lock" (depicted as red and purple fused ring) holding two identical blue threads in place and the repeating unit, represented as red and blue threads, which are orthogonally aligned in a "handshake" or convergent turn–convergent turn configuration. Finally, cleaving the "chain-lock" (Figure 4.1d) produces two complementary assemblies, one purple and blue thread "handshake" assembly and one red and blue thread assembly, that is identical to the repeating unit of Figure 4.1c.

Figure 4.2. Building blocks and their sub-components.

As a result of this topological analysis, three distinct building blocks were identified (Figure 4.2). To complete the library a fourth building block is introduced, which could be used to generate a [3]catenane. These four differnent building blocks consist of four different subcomponents in total and therefore giving rise to a highly convergent synthetic strategy.

4.2 Retrosynthsesis

In this section, the retrosynthetic analysis of a [2]-, [3]- and [5]catenane will be discussed. These catenanes are based on the palladium [3+1] template chemistry, presented throughout this thesis. The desired synthetic strategy should be highly convergent and modular, so that it permits facile replacement of key components without the need to redesign the entire synthetic strategy. Therefore, a selection of building blocks (TM template assemblies of monodentate and tridentate coordinated to a palladium(II) anchor), consisting of a restricted number of subcomponents, will form the backbone of the synthetic strategy. Due to the complexity of catenane synthesis in general, the discussion starts with the smallest representative ([2]catenane) and progresses towards the most complex ([5]catenane) via the [3]catenane. The envisaged [2]catenane is shown in Figure 4.3. It

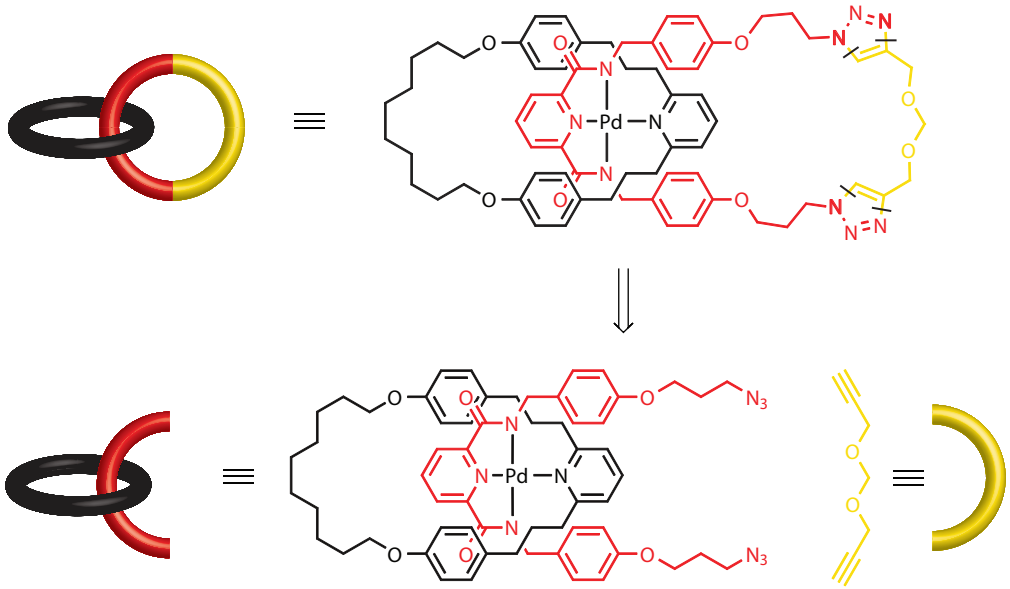

Figure 4.3. Retrosynthetic analysis of the envisaged [2]catenane, first disconnections, resulting building block and complementary "click"-component.

features a preformed 29-member monodentate macrocycle (black ring), which is held in place by the palladium anchor, and a tridentate double "click"-fused 36-member macrocycle (red and yellow fused ring). Disconnecting the triazole units gives rise to the **BB1**, consisting of a monodentate macrocycle and tridentate *bis*-azide convergent turn, and a formaldehyde dipropargyl acetal unit (yellow), which a known compound in the literature.[9] Dissecting **BB1** (Figure 4.4) affords

the pre-metallated *bis*-azide tridentate ligand, bearing a labile DMF ligand, and the macrocycle, which has been described in a recent publication by Leigh.[10] The proposed retrosynthesis of the [3]catenane is shown in Figure 4.5. The

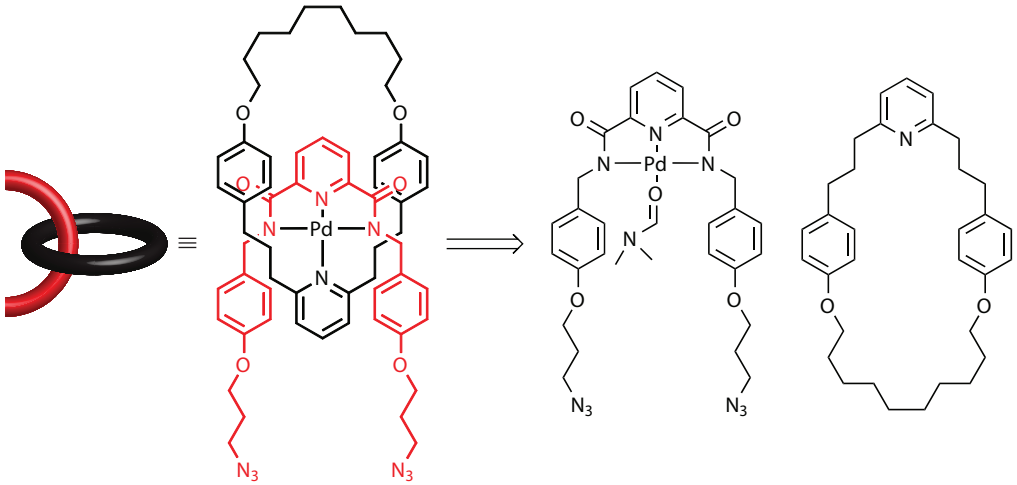

Figure 4.4. Retrosynthetic analysis of **BB1**.

catenane, a product of a double click ring-closure, consists of two monodentate macrocycles and a 56-member central ring. Disconnecting the triazoles yields two complementary building blocks **BB1** (black macrocycle and red thread) and **BB2** (black macrocycle and violet thread). **BB2** consists of the previously introduced monodentate macrocycle and the TMS-protected *bis*-alkyne tridentate ligand, which are coordinated to the palladium(II) anchor. As mentioned in the previous chapters, the TMS-protection of the alkynes was introduced to increase the stability and shelf life of the alkyne residues on the tridentate ligands, as they have a tendency to degrade. As a consequence, deprotection of the TMS-alkynes prior to the ring-forming reaction or *in situ* is required.

The retrosynthetic analysis of **BB2** is shown in Figure 4.6, where two indicated disconnections at the phenolic positions yield the macrocycle *bis*-phenol complex. This complex is easily obtainable by ligand exchange reaction of the pre-metallated U-shape, bearing a labile DMF ligand, with the pyridine macrocycle.

The retrosynthesis of the proposed [5]catenane is depicted in Figure 4.7. Dissecting the two outer two toned rings (red and cyan), yields the "capping" building block **BB1** and the central ring (violet and red), bearing two cyan convergent

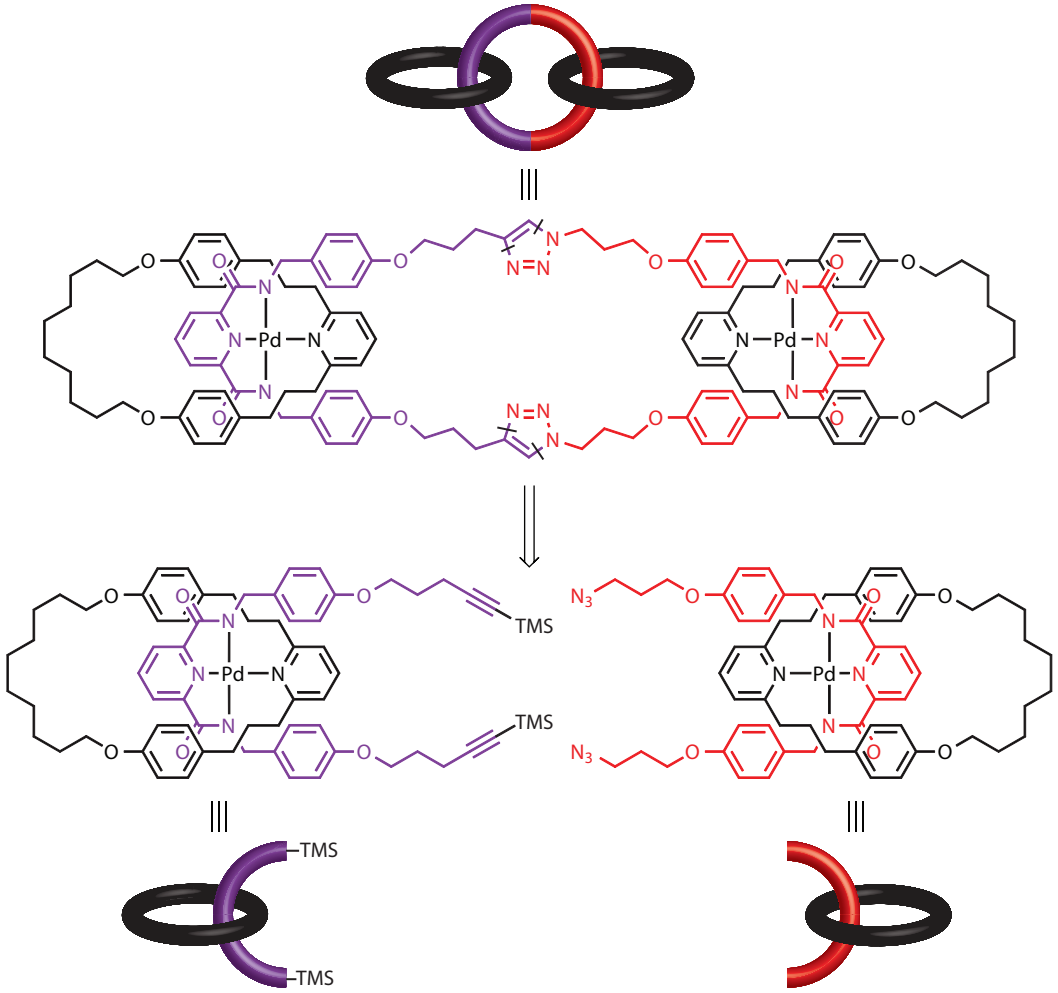

Figure 4.5. Retrosynthetic analysis of the envisaged [3]catenane, first disconnections and resulting building blocks.

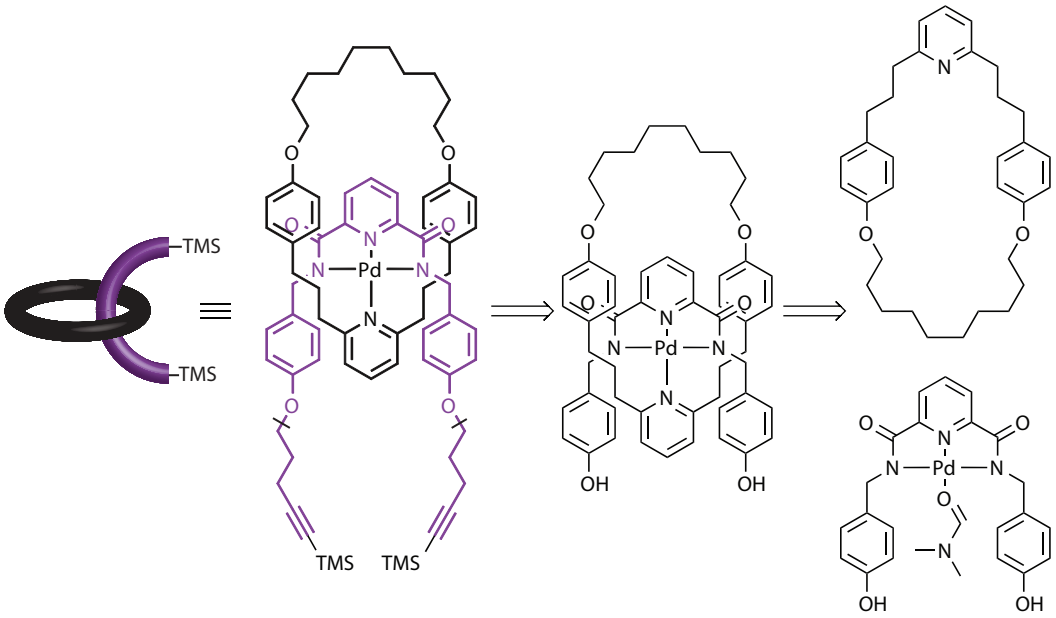

Figure 4.6. Retrosynthetic analysis of building block **BB2** with indicated disconnections.

turns. Protection of the alkynes of the monodentate ligands leads to the TIPS protected "chain-lock". Disconnection of the triazole units affords two complementary building blocks **BB3** (tetraalkyne complex) and **BB4** (*bis*-azide-*bis*-alkyne complex).

The proposed retrosynthesis of **BB3** is given in Scheme 4.8. As with all alkyne containing tridentate ligands, diconnections at the phenolic positions give rise to the *bis*-phenol U-shape monodentate complex, which is readily prepared via ligand exchange reaction of the pre-metallated U-shape and the TIPS-protected monodentate pyridine ligand.

BB4 (Figure 4.9) is composed of a *bis*-azide tridentate and TIPS-protected *bis*-alkyne monodentate ligand held in place by the palladium anchor and should be obtained by ligand displacement of the labile DMF of the premetallated *bis*-azide U-shape with the TIPS-protected pyridine monodentate ligand.

Subjecting the remaining TIPS-protected *bis*-alkyne pyridine monodentate ligand to a retrosynthetic analysis (Figure 4.10), the disconnections adjacent to the aromatic core of the pyridine produce the 2,6-dibromo pyridine and the corresponding zincate. Functional group interconversion of the bromo-zincate gives rise to the bromide, which in turn can be obtained from the corresponding alcohol.

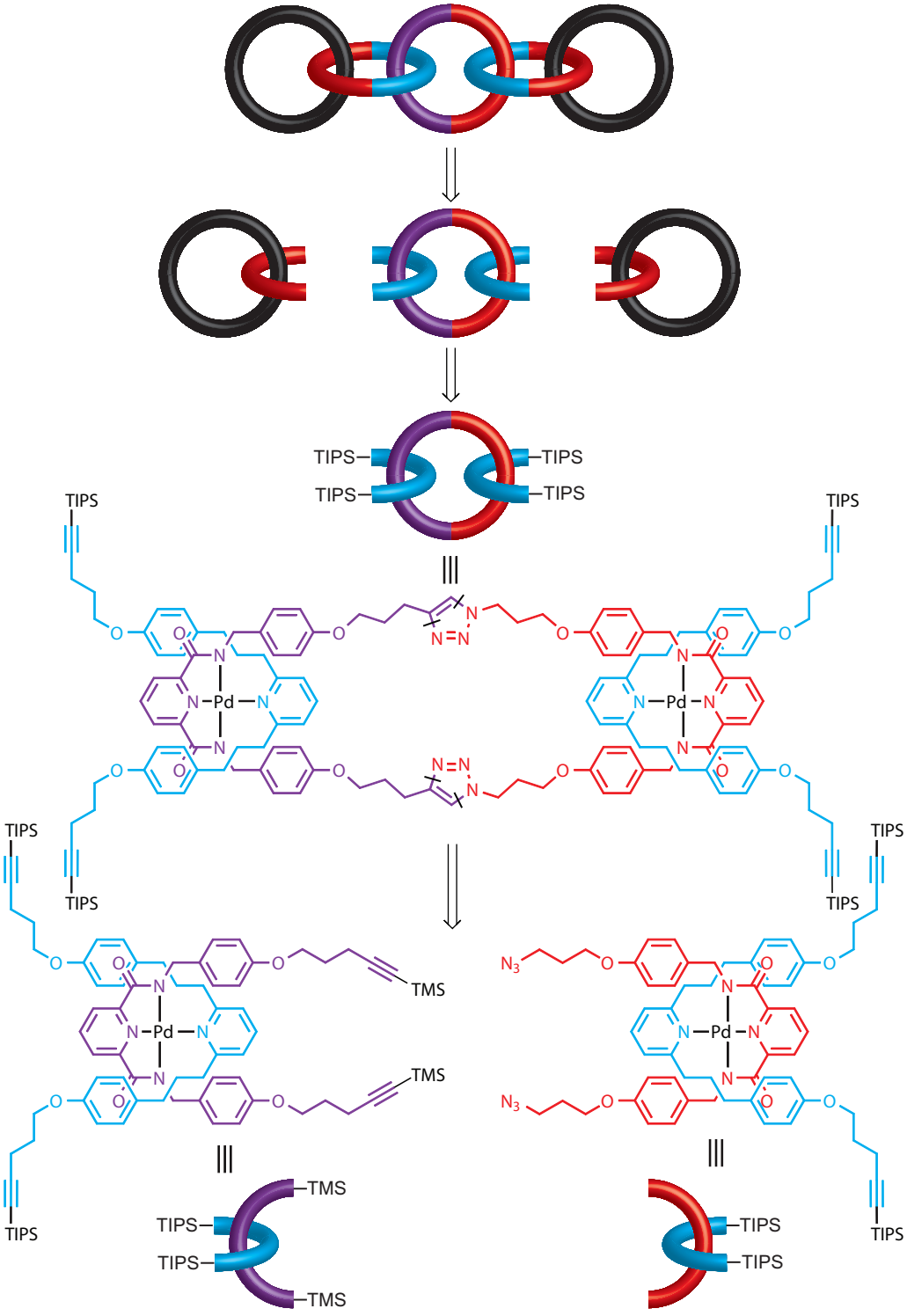

Figure 4.7. Retrosynthetic analysis of the proposed [5]catenane and resulting building blocks.

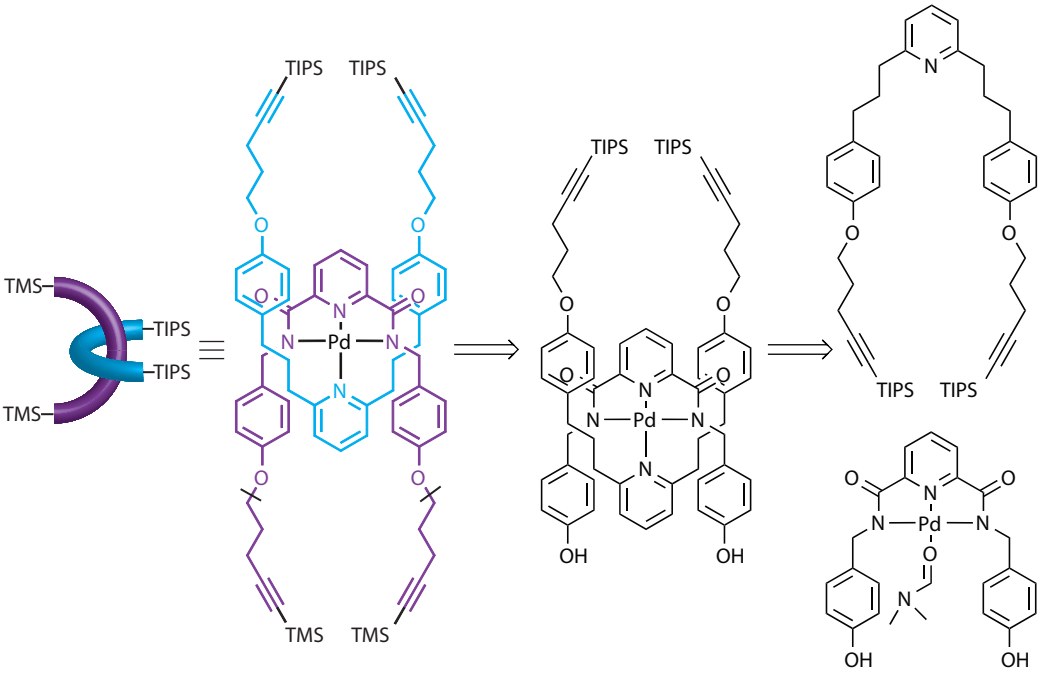

Figure 4.8. Retrosynthetic analysis of Building Block **BB3** and indicated disconnections.

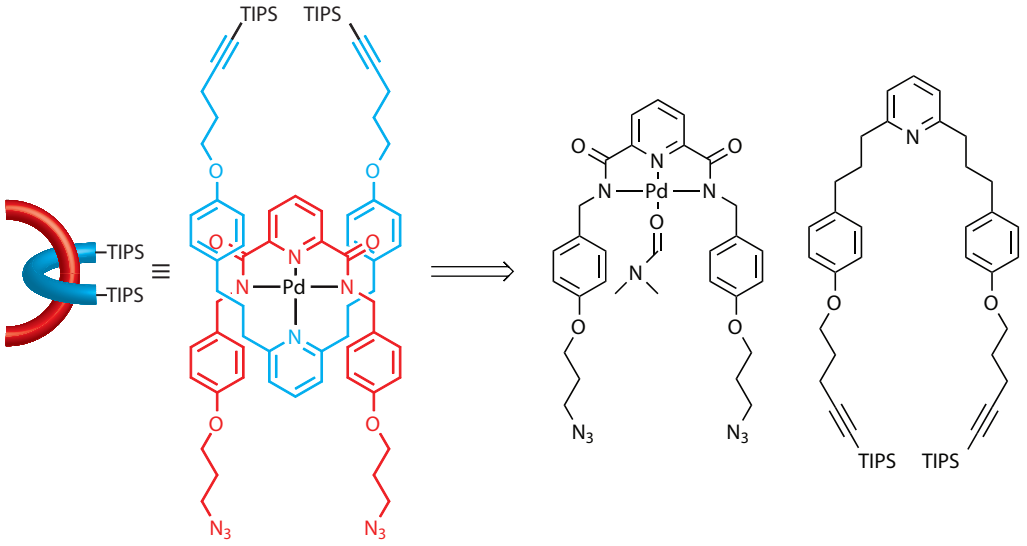

Figure 4.9. Retrosynthetic analysis of **BB4**.

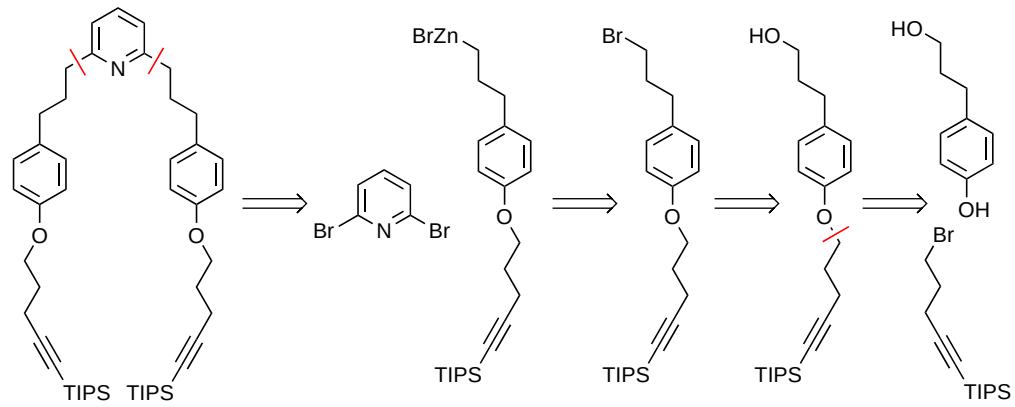

Figure 4.10. Retrosynthetic analysis of TIPS-protected *bis*-alkyne pyridine monodentate ligand and indicated disconnections.

The final disconnection at the phenolic position affords the commercially available 3-(*p*-hydroxy-phenyl)-propan-1-ol and the previously introduced 1-bromopent-4-yne-5-tri-*i*-propylsilane.

4.3 Synthesis

4.3.1 Synthesis of the Monodentate Ligands

The synthesis of the TIPS-protected *bis*-alkyne pyridine monodentate ligand **12** commenced from the commercially available p-hydroxy-phenyl-propan-1-ol **7**, which was reacted together with 1-bromo-pent-4-yne-5-tri-*i*-propylsilane **6** under standard Williamson ether forming conditions to afford **8** in very good yield (86%). Subsequent transformation of the alcohol to the bromide, using PPh_3 and CBr_4 in Cl_2CH_2, produced the desired product **9** in excellent yield (94%). Reacting the bromide **9** with activated zinc dust, cleanly generated the bromozincate **11** which was used in a Negishi cross-coupling reaction with 2,6-dibromopyridine **10** as coupling partner and PEPPSI as catalyst. This reaction exclusively produces the disubstituted product **12** (only traces of the monocoupled product could be observed) in good yield (71%).

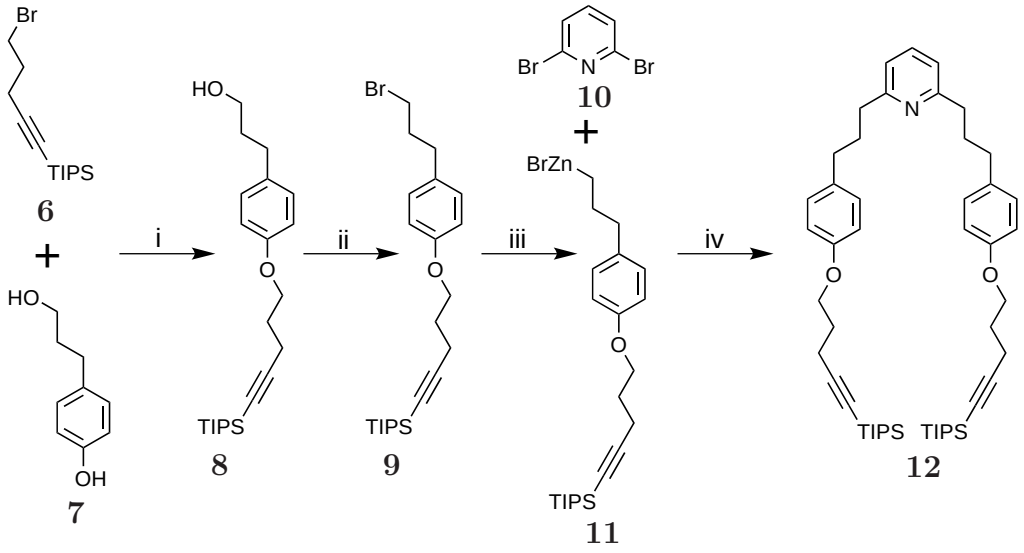

Scheme 4.2. Synthesis of monodentate ligand **12**. Reagents and conditions: i) **7**, **6**, K_2CO_3, DMF, 80 °C, 86%; ii) **8**, PPh_3, CBr_4, Cl_2CH_2, 0 °C, 94%; iii) **9**, Zn, I_2, NMP, 80 °C, 4h, quant.; iv) **11**, **10**, PEPPSI, LiBr, NMP, RT, 71%.

4.3.2 Synthesis of BB1

The synthesis of **BB1** commenced from the previously introduced *bis*-azide U-shape (compound **13** Chapter 2), which was pre-metallated using palladium(II) acetate in DMF, to produce the desired product as DMF complex in excellent yield (95%). The DMF U-shape complex **14** was then subjected to a ligand exchange reaction with the macrocycle **15** and afforded the **BB1** (**16**) after column chromatography in very good yield (85%).

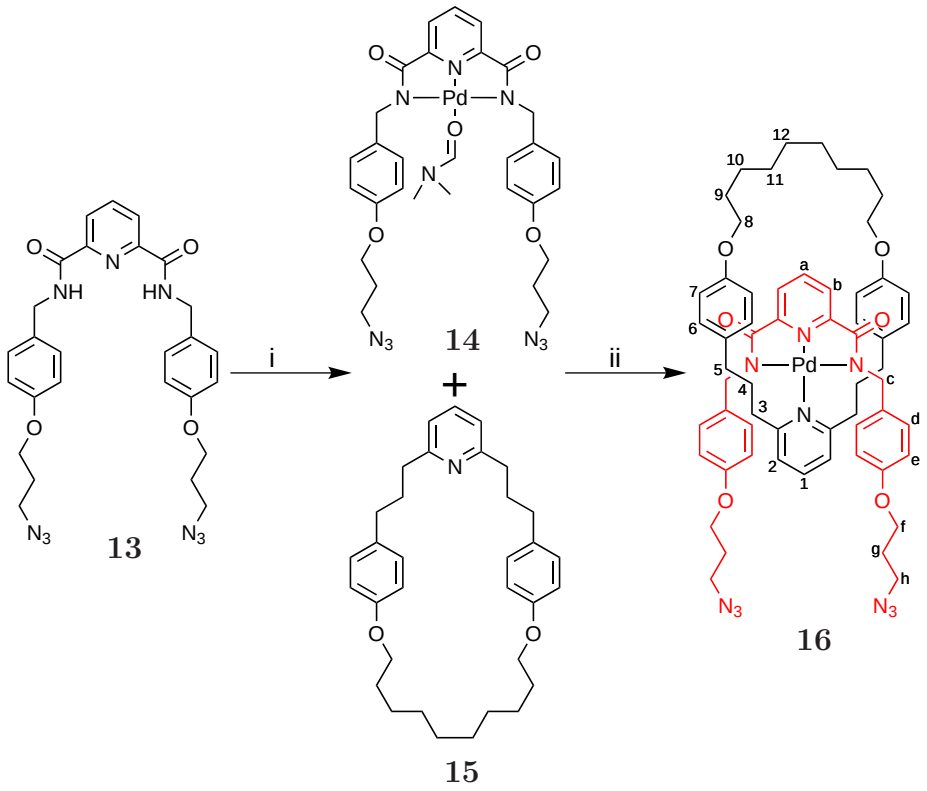

Scheme 4.3. Synthesis of **BB1**. Reagents and conditions: i) **13**, $PdOAc_2$, DMF, RT, 95%; ii) **14**, **15**, CH_2Cl_2, 85%.

The ^{1}H-NMR of **BB1** (**16**) is shown in Figure 4.11b alongside with the free macrocycle monodentate ligand **15** (Figure 4.11a) and the *bis*-azide U-shape **13** (Figure 4.11c). Upon complexation, the monodentate macrocycle **15** protons of the aromatic pyridine core shift downfield by 0.21 ppm for H_1 and 0.04 ppm for H_2. The protons at the positions H_6 and H_7 of the phenyl moieties experience upfield shifts of 0.27 ppm and 0.52 ppm respectively, which could be attributed to the π-stacking interactions between the U-shape pyridine and the phenyl cores. The protons H_3 and H_5 of the C_3 spacer between the pyridine and the phenyl positions

experience only modest upfield shifts and show significant line broadening, which might be caused by their proximity to the d_{z^2} orbital of the palladium(II) anchor. The protons at position H_4 are shifted upfield by 0.31 and show line broadening, which could be the result of facing and contacting d_{z^2}-orbital. The protons of the aliphatic chain H_{8-12}, show upfield shifts for the phenoxy adjacent position H_8, no shift for position H_9 and downfield shifts for positions H_{10-12}. Upon complexation, the tridentate ligand proton at position H_a experiences a small downfield shift, whereas proton H_b exhibits a strong upfield shift of 0.62 ppm. Phenyl positions H_e and H_d show signs of π-stacking interactions and upfield shifts of 0.38 ppm and 0.65 ppm respectively. The protons attached to position H_c are significantly shifted upfield by 0.92 ppm. The remaining protons on positions H_{f-h} exhibit no change in their chemical shifts and signal shape. The the absence of diastereotopic proton signals suggest that the symmetry in solution is C_{2v}.

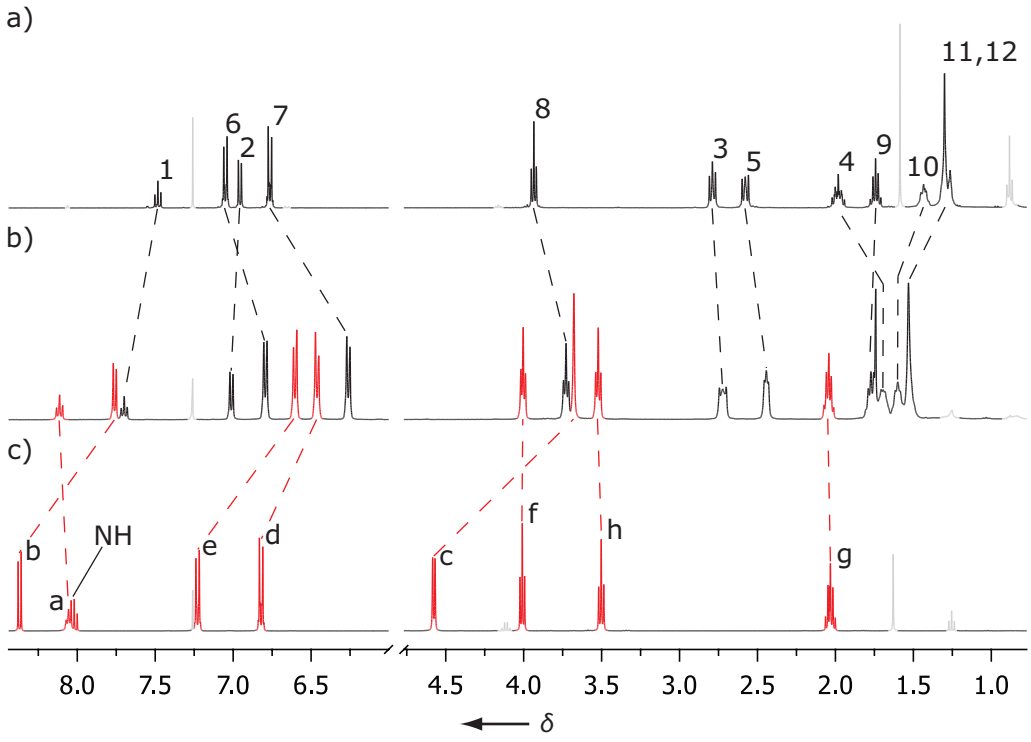

Figure 4.11. ^{1}H-NMR (400 MHz, $CDCl_3$, 300 K) of a) macrocycle **15**; b) **BB1 16**; c) *bis*-azide U-shape **13**. The assignment corresponds to the lettering shown in scheme 4.3.

4.3.3 Synthesis of BB2

The synthesis of **BB2** started from the *bis*-phenol U-shape **17** (compound **22** Chapter 2), which was pre-metallated using palladium(II) acetate in DMF and produced compound **18** in good yield. Subsequent ligand exchange of the labile DMF ligand of **18** with the macrocycle **15** afforded the corresponding macrocycle U-shape complex **19** in good yield. Further elaboration of complex **19**, employing the previously presented (chapter 3) optimised Mitsunobu reaction conditions, furnished the desired product **BB2** (**20**) as yellow amorphous solid in moderate yield.

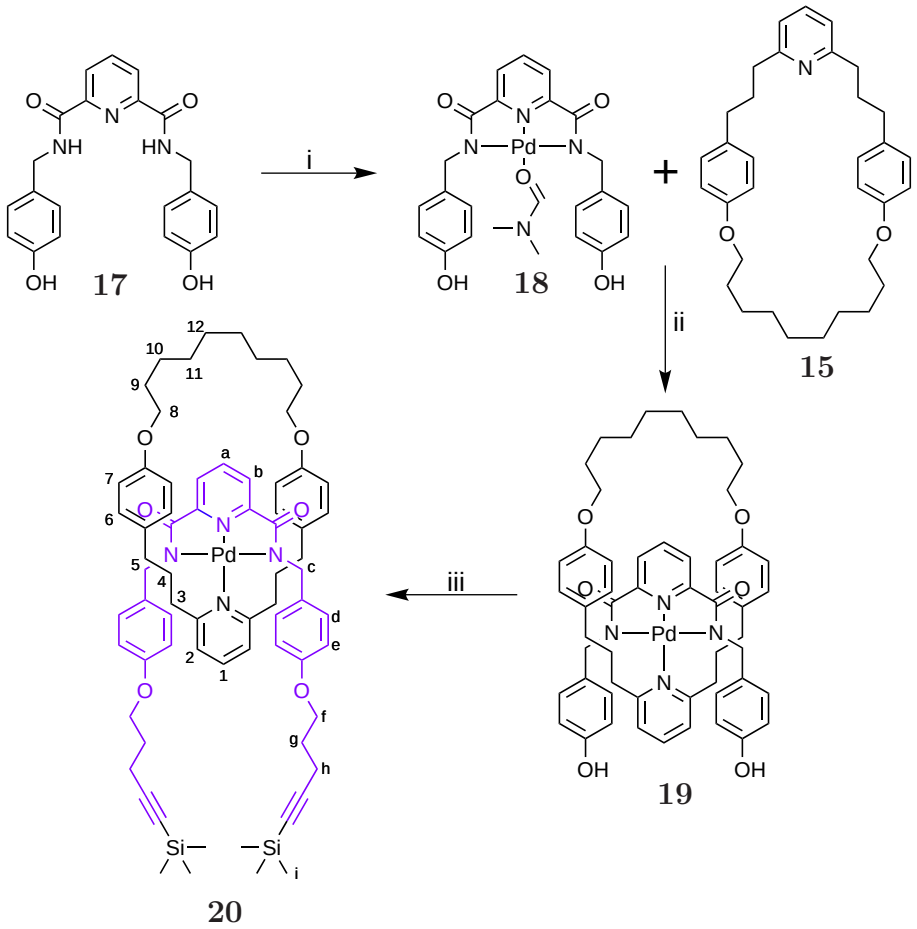

Scheme 4.4. Synthesis of **BB2**. Reagents and conditions: i) **17**, $Pd(OAc)_2$, DMF, RT, 80%; ii) **18**, **15**, $CHCl_3$/DMF, RT, 76%; iii) PCy_3, DIAD, 5-trimethylsilyl-4-pentyn-1-ol, **19**, THF, 0 °C → RT, 62%.

The ^{1}H,^{1}H-COSY and NOESY spectra of **BB2** are shown in figures 4.12 and 4.13 respectively. In the COSY spectrum, the C_3 chain between the aromatic pyridine core and the phenyl units of the monodentate macrocycle (positions 3-

5) can clearly be seen, although the protons of position H_4 are overlapped by the residual water peak. The other C_3 chain of the tridentate ligand, between the phenoxy position and the alkyne residues, exhibits cross-peaks of positions H_f and H_h with position H_g, which is consistent with the β-position of H_g from either the phenoxy or alkyne position. The C_{10} alkyl chain of the monodentate macrocycle can be identified from position H_8, the α-position to the phenoxy residue, which shows a cross-peak with the proton signal of position H_9. The protons at position H_{10}, show cross-peaks with $H_{11/12}$ (which overlap and solely show as broad singlet) and H_9. Positions H_d and H_e of the tridentate ligand show a significant roofing effect and are flanked by proton signals H_6 and H_7 of the monodentate ligand, where the roofing effect is almost absent. In the NOESY spectrum, weak through space contacts between the proton of position H_a and H_b with $H_{11/12}$ indicate that the alkyl loop fully engulfs the pyridine moiety of the tridentate ligand. The simplicity of the spectrum suggests a C_{2v} symmetry in solution.

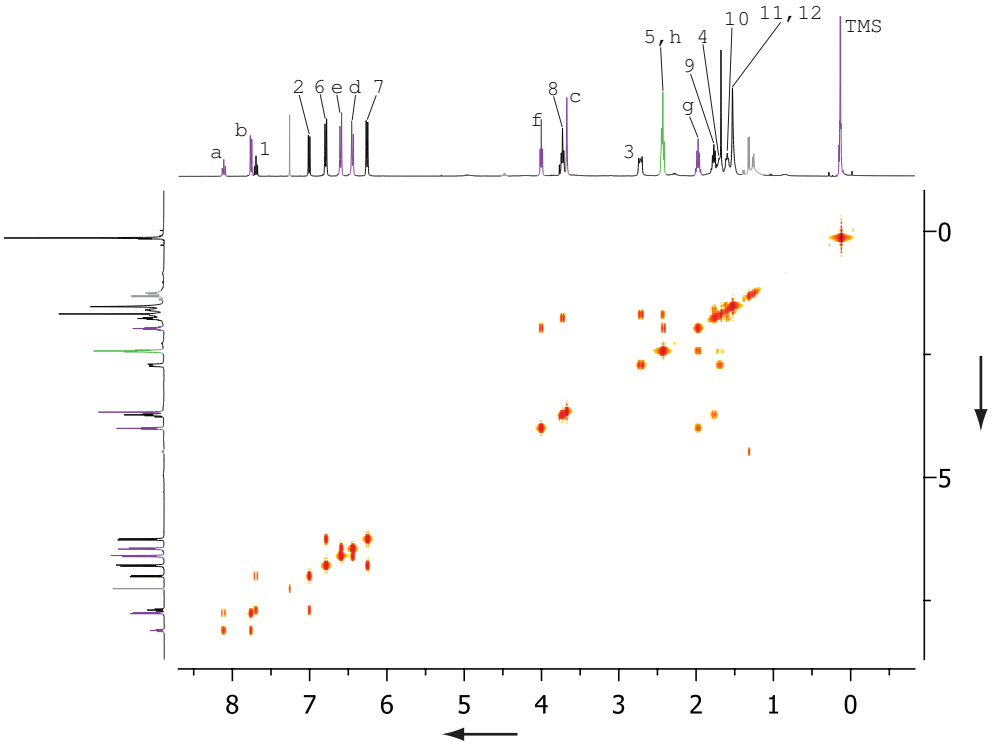

Figure 4.12. ^{1}H,^{1}H-COSY (400 MHz, $CDCl_3$, 300 K) of **BB2 20**. The assignment corresponds to the lettering of **20** in scheme 4.4. Non overlapping residual solvent and/or impurity signals are coloured in light gray and overlapping compound signals are colored in green.

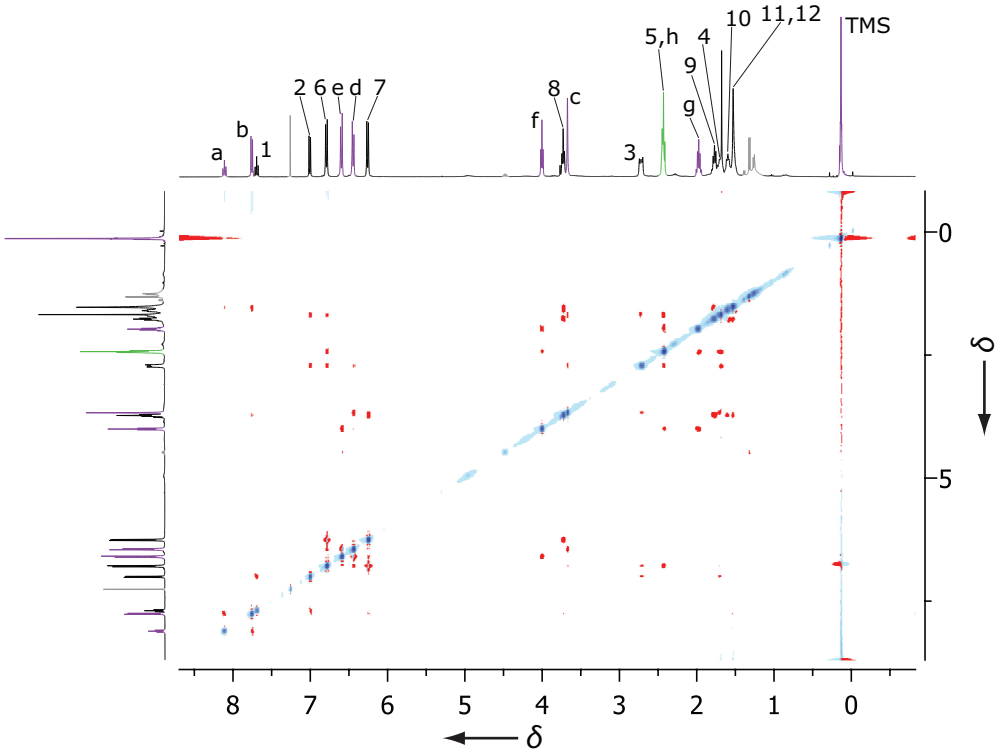

Figure 4.13. NOESY (400 MHz, $CDCl_3$, 300 K) of **BB2 20**. The assignment corresponds to the lettering of **20** in scheme 4.4.

4.3.4 Synthesis of BB3

The synthesis of **BB3** started with a ligand exchange reaction of the pre-metallated U-shape **18** with the TIPS-protected monodentate ligand **12** to obtain the *bis*-phenol U-shape monodentate complex in very good yield (Scheme 4.5). The phenol positions of the tridentate ligand were alkylated with 5-trimethylsilyl-4-pentyn-1-ol, using the optimised Mitsunobu protocol, and delivered the desired product **22** in moderate yield. The tetraalkyne complex is relatively unstable and should be used within two days, or be repurified prior to use.

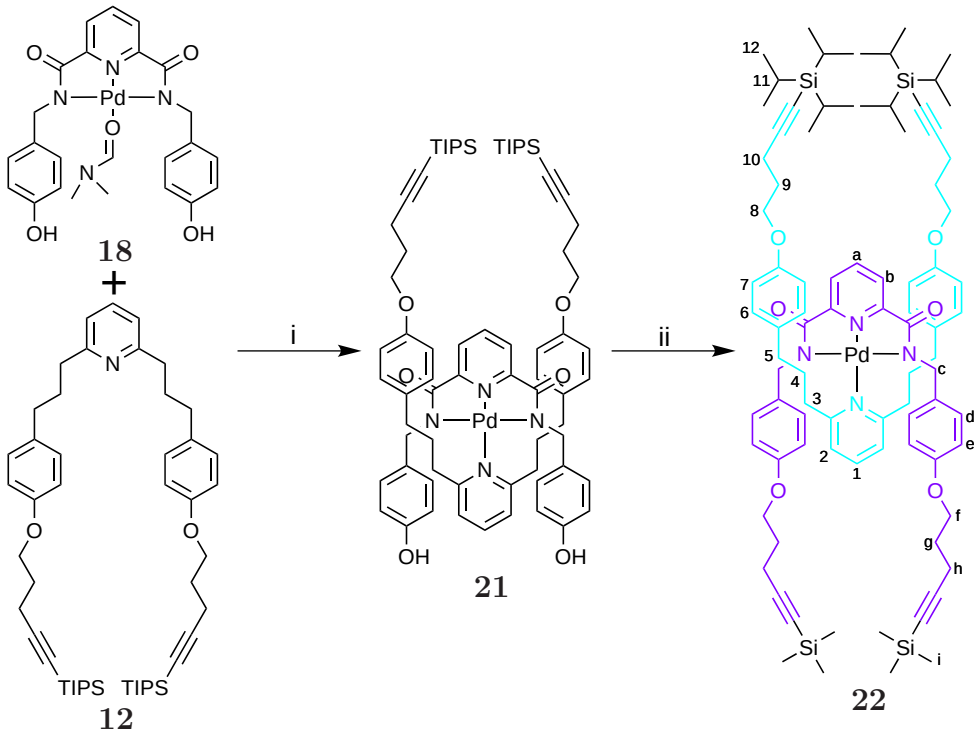

Scheme 4.5. Synthesis of BB3. Reagents and conditions: i) **18**, **12**, CH_2Cl_2/DMF, RT, 95%; ii)PCy_3, DIAD, 5-trimethylsilyl-4-pentyn-1-ol, **21**, THF, RT, 57%.

To confirm the successful isolation of **22** a series of NMR experiments were carried out, two of which are shown in figures 4.14 and 4.15. The ^{1}H-NMR showed overlapping signals at 7.01 ppm, 3.89 ppm and 2.46-2.36 ppm. The signal at 7.01 ppm exhibited COSY cross-peaks with positions H_1 and H_7, as well as ROESY cross-peaks with positions $H_{3/4/5}$, and was determined as an overlap of the proton signals of positions H_2 and H_6. The overlapping signal at 3.89 ppm only exhibited one COSY cross-peak with position H_g, but five ROESY cross-peaks with H_g (strong), H_h (weak), H_3 (intermediate), H_e (strong) and H_d (strong).

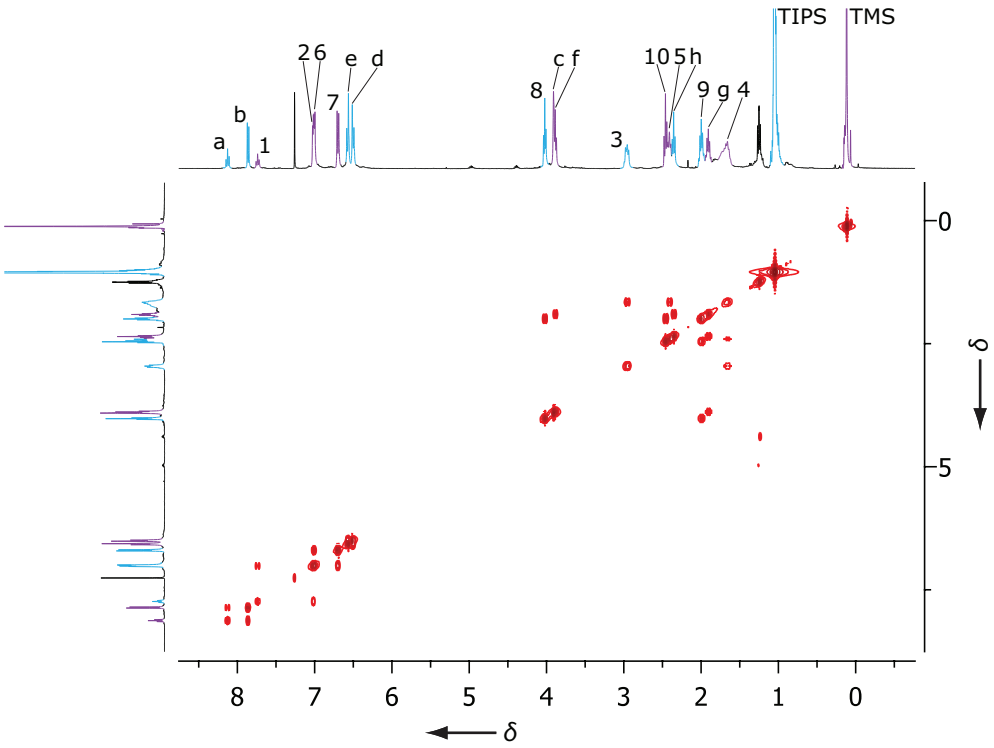

Figure 4.14. ^{1}H,^{1}H-COSY (400 MHz, $CDCl_3$, 300 K) of **BB3 22**. The assignment corresponds to the lettering and coloring of **22** in scheme 4.5. Residual solvent and/or impurities are colored in black.

Due to the different centers of gravity of the cross-peaks, the assignment could be determined as positions H_c and H_f. Finally the signals in the region of 2.46-2.36 ppm could be determined as H_h, H_5, and H_{10}, as all of these signals are part of one of the side-chains and therefore exhibit COSY and ROESY contacts to the surrounding framework. Interestingly, no long-range contact between positions H_a or H_b of the tridentate ligands pyridine unit and the alkylalkyne side-chain of the monodentate ligand could be observed, indicating a greater degree of freedom in contrast to **BB2**, with its restricted geometry. As with **BB1** and **BB2**, the simplicity and absence of diastereotopic signal splitting, the symmetry in solution can be determined as C_{2v}.

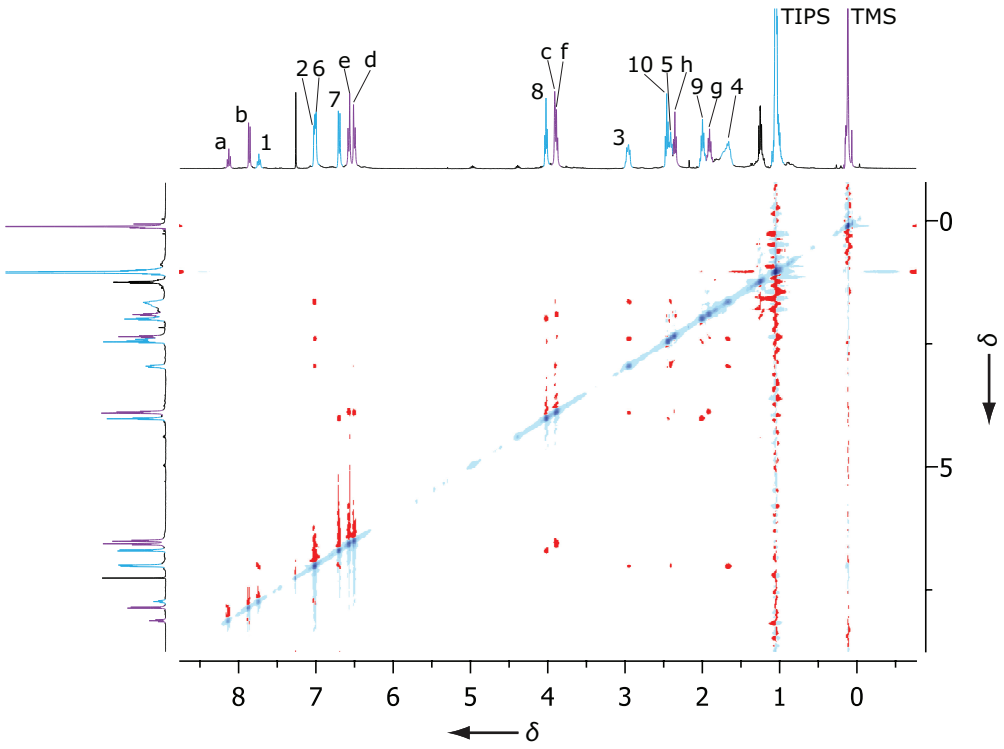

Figure 4.15. ROESY (400 MHz, $CDCl_3$, 300 K) of **BB3 22**. The assignment corresponds to the lettering of **22** in scheme 4.5.Residual solvent and/or impurities are colored in black.

4.3.5 Synthesis of BB4

BB4 was synthesised via a ligand exchange reaction of the *bis*-azide tridentate palladium(II) DMF complex **14** with the TIPS-protected *bis*-alkyne pyridine monodentate ligand **12** (Scheme 4.6). This reaction cleanly delivered the desired product **23** in excellent yield. The ^{1}H-NMR of the building block **BB4** is shown

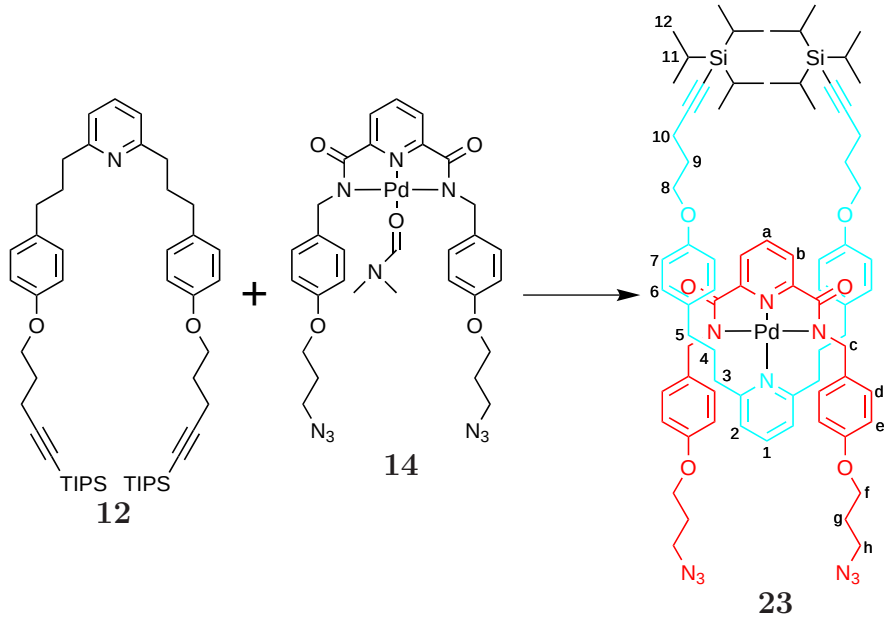

Scheme 4.6. Synthesis of BB4. Reagents and conditions: **12**, **14**, DMF/CH_2Cl_2 (1:1), RT, 93%.

in Figure 4.16b, in addition to its constituents monodentate ligand **12** (Figure 4.16a) and the tridentate ligand **13** (Figure 4.16c). Upon complexation, the protons located in position H_1, H_2 and H_3 shift downfield ($\Delta_{H1} = 0.27$ ppm, $\Delta_{H2} = 0.09$ ppm, $\Delta_{H3} = 0.18$ ppm), which can be attributed to the complexation to the palladium anchor. The remaining protons of the monodentate ligand experience upfield shifts. The tridentate ligand proton H_a is shifted downfield by 0.1 ppm, which coincides with the complex formation and the corresponding reduction of electron-density at the para and ortho position. Metal to ligand backbonding apparently affects protons H_b and H_c, which are shifted upfield by 0.52 ppm and 0.67 ppm respectively. Protons H_d and H_e experience π-stacking interactions and are shifted upfield by 0.32 ppm and 0.68 ppm. The signals of the side-chain protons H_{f-h} are slightly shifted upfield.

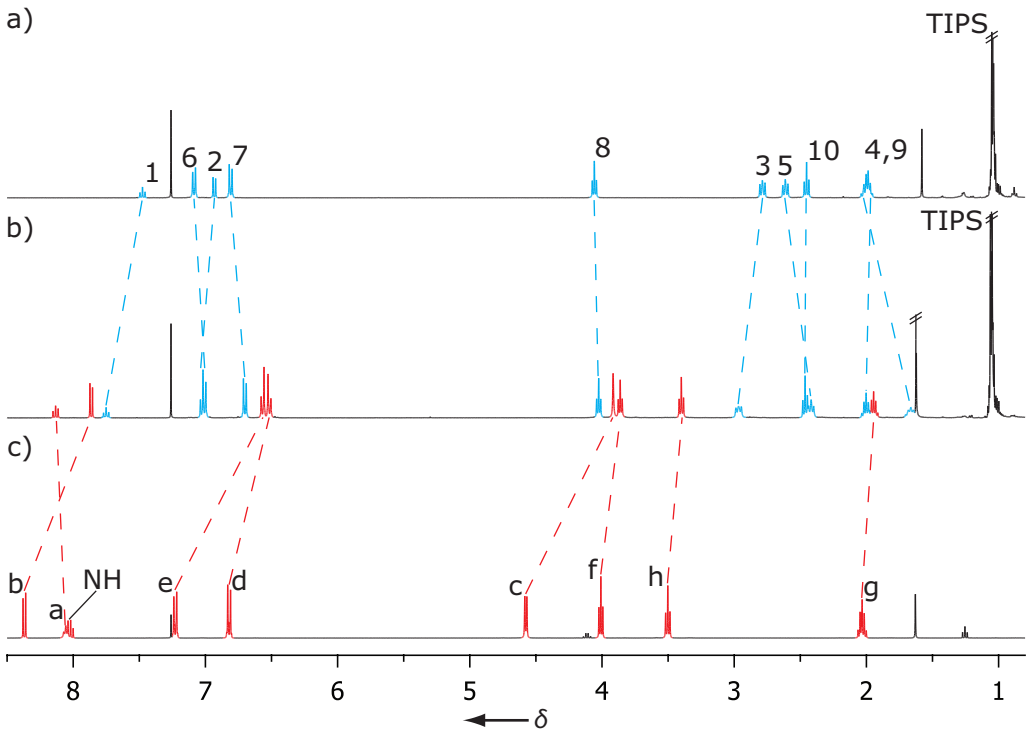

Figure 4.16. ^{1}H-NMR (400 MHz, $CDCl_3$, 300 K) of a) monodentate ligand **12**; b) **BB4 23**; c) pre-metallated tridentate ligand complex **14**. The assignment corresponds to the lettering shown in Scheme 4.6.

4.3.6 Synthesis of the [2]catenane

The synthesis of the [2]catenane was performed on a small scale only. The purpose of this exercise was to develop and optimise reversed phase LC-MS methods for a larger screening of reaction conditions for the double click ring-closure reaction. The reaction was performed at high dilution at 50 °C with a two fold excess of *bis*-alkyne **24** to boost the yield. However, these results are part of ongoing work and therefore they should be treated as preliminary.

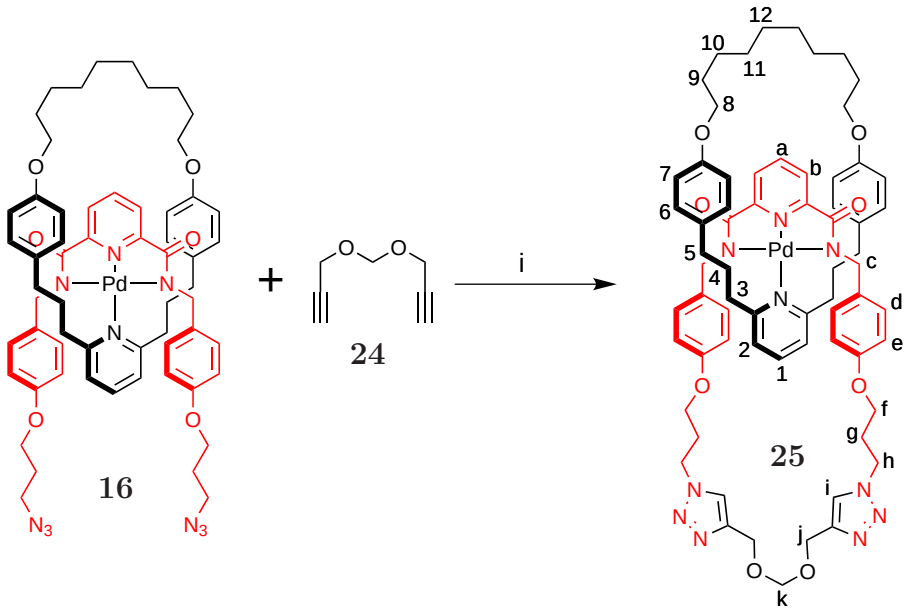

Scheme 4.7. Synthesis of a [2]catenane via double click ring-closure. Reagents and conditions: i) **16**, **24**, $[Cu(MeCN)_4]PF_6$, TBTA, 1,2-dichlorethane/1-propanol (95:5), 50 °C, 7d, estimated yield 50%.

The LC-MS UV and TIC trace of the crude reaction mixture after 7 days is given in Figure 4.17. The signal at 6.147 min corresponds to the [2]catenane, which can be confirmed by the mass spectrum (see inset) that corresponds to the calculated isotope pattern for the [2]catenane. The signal at 11.476 corresponds to **16** and is separated from the productby 5 minutes, showing that with the formation of the two triazole units the product becomes significantly more polar. Isolation of the peak at 6.147 min by preparative HPLC and successive NMR analysis revealed a highly symmetrical species, which could be identified as the desired product.

The ^{1}H-NMR of [2]catenane **25** is given in Figure 4.18b together with **24**

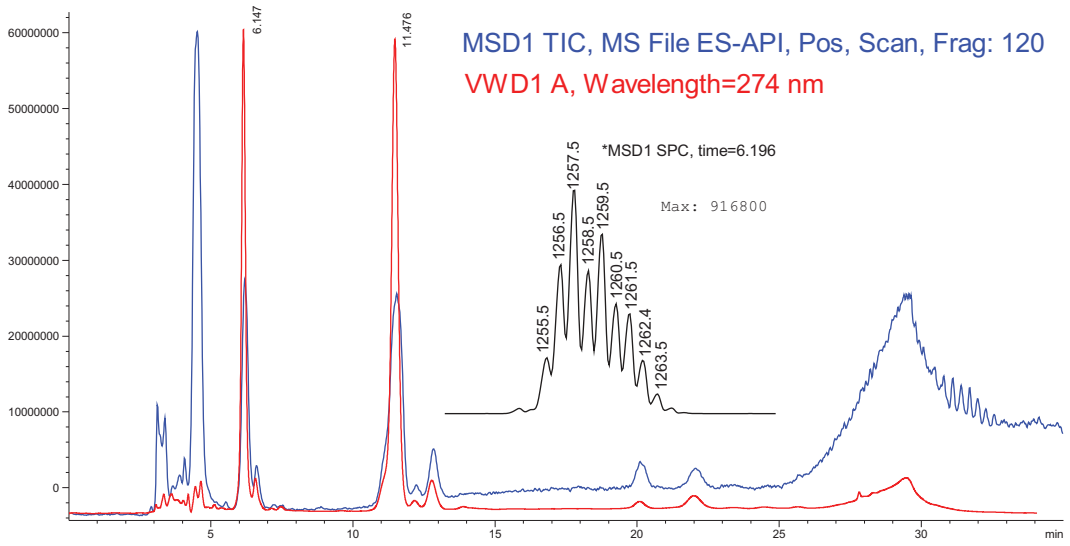

Figure 4.17. LC-MS trace of the crude mixture of the [2]catenane (6.147 min) and **16** (11.476 min) after 7 d reaction time. The LRESI-MS spectrum of the peak at 6.147 min is shown as inset. Supelco-Ascentis© C-18 4.6x250mm; 0.7 mL/min; isocratic MeOH/CH_2Cl_2/H_2O (60:30:10).

(Figure 4.18a) and **16** (Figure 4.18c). Comparing the spectrum of **25** with its precursor compound **16** the most prominent changes are shown by the protons adjacent to the formed triazole ring (H_h, H_g). The singals of H_h and H_g show downfield shifts of 1.20 ppm and 0.38 ppm respectively, which can be attributed to the triazole ring. Proton H_f however, shows a small upfield shift of 0.09 ppm. The signals of H_i and H_j shift downfield by 5.18 ppm and 0.44 ppm respectively, which is due to the triazole formation as H_i is now part of the electron-deficient triazole and H_j adjacent to it. The rest of the proton signals exhibit little or no change, confirming that the overall structure of the complex remains the same. Due to the absence of signal splitting and therefore the absence of diastereotopic environments, the symmetry in solution can be determined as C_{2v}.

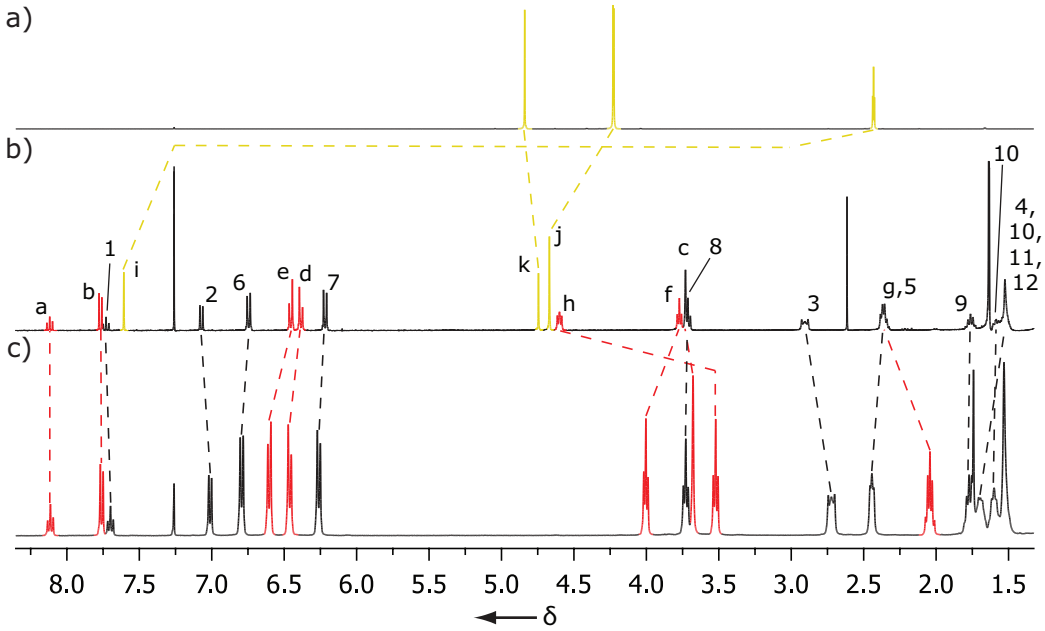

Figure 4.18. ^{1}H-NMR (400 MHz, $CDCl_3$, 300 K): a:) **24**; b) **25**; c) **16**. Proton signals of the tridentate ligand are colored in red and signals from **24** in yellow.

4.3.7 Synthesis of the [3]catenane

The synthesis of the [3]catenane **26** was conducted similarly to the [2]catenane and represents ongoing work (Scheme 4.8). The increased complexity of this

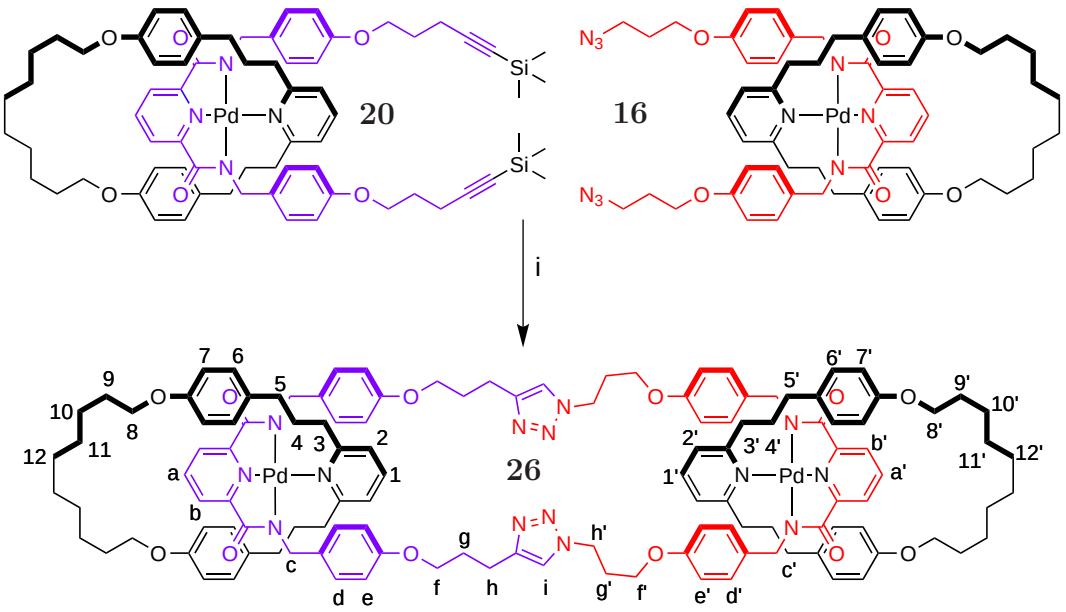

Scheme 4.8. Synthesis of the [3]catenane **26**. Reagents and conditions: i) **16**, **20**, $[Cu(MeCN)_4]PF_6$, TBTA, 1,2-dichloroethane/1-propanol (95:5), 50 °C, 7d, estimated yield 35%.

target enables the study of the double click-reaction between two palladium-containing building blocks and to gain further insight into this reaction, as so far only modest yields were achieved. The reaction was carried out under high dilution conditions to avoid potential polymerisation. Furthermore, the TMS-protected alkynes were deprotected *in situ* using TBAF as an additive to the reaction. As catalyst, the combination of TBTA and $[Cu(MeCN)]_4PF_6$ was used, as it so far delivered reliable and reproducible results. In the LC-MS UV trace (Figure 4.19, red line), four larger peaks are identifiable, where the peak at 13.705 min corresponds to the fully deprotected **20**, 14.011 min to **16**, 14.852 min to the [3]catenane and 15.617 min tentatively assigned as to the mono click product. The peak at 14.852 min was isolated using preparative reversed phase HPLC with an isocratic method and subjected to NMR analysis, which confirmed the formation of a highly symmetric compound that can be identified as the desired [3]catenane. However, full characterisation is pending and therefore these results

have to be considered as preliminary.

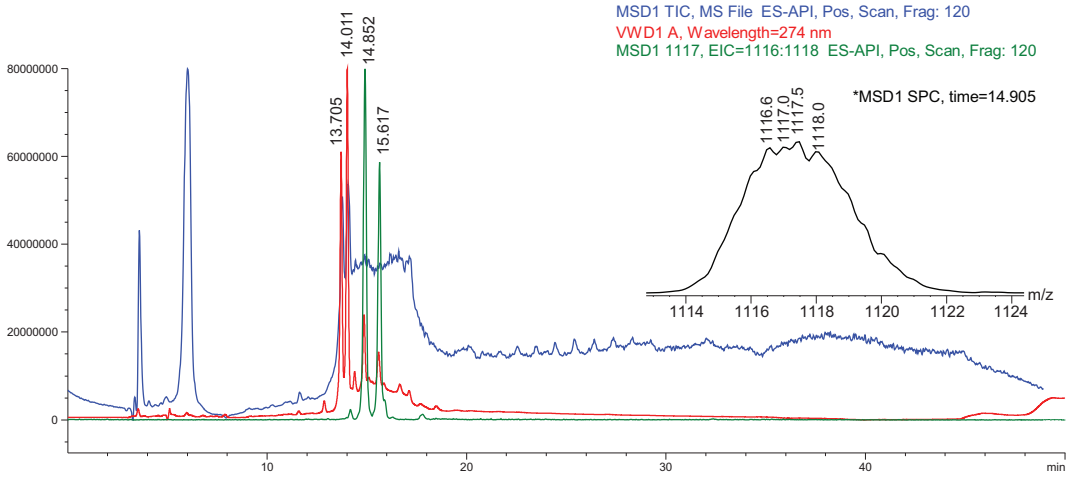

Figure 4.19. LC-MS trace of the crude mixture of the [3]catenane (14.852 min), deprotected **20** (13.705 min), **16** (14.011 min) and possible mono click product (15.617 min) after 5 d reaction time. The LRESI-MS spectrum of the peak at 14.852 min is shown as inset. Supelco-Ascentis© C-18 4.6x250mm; 0.7 mL/min.

The ^{1}H-NMR of the [3]catenane **26** is shown in Figure 4.20b alongside with its precursor compounds **20** (Figure 4.20a) and **16** (Figure 4.20c). Most of the signals of the two precursor compounds experience only minor shifts and are superimposed, creating groups of signals, which are indistinguishable. However, the signals in close proximity to the triazole ring formed show the same pattern as all the presented examples beforehand. The large downfield shift (>1 ppm) for the nitrogen connected proton $H_{h'}$, medium downfield shift for $H_{g'}$ ($\approx$ 0.5 ppm) and small downfield shifts for H_g ($\approx$ 0.2 ppm) and H_h ($\approx$ 0.3 ppm) are a common signature for all double click macrocyclisation products presented in this thesis. H_f and $H_{f'}$ show upfield shifts and invert their relative positions. The absence of split signals due to diastereotopic environments allows the conclusion that the symmetry in solution is C_{2v}.

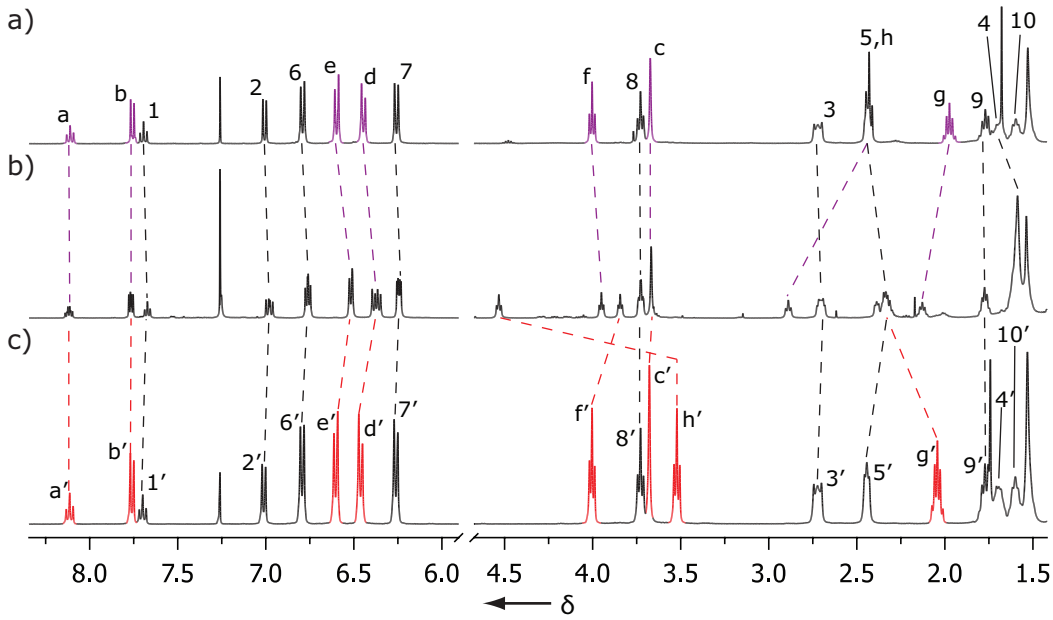

Figure 4.20. ^{1}H-NMR (400 MHz, $CDCl_3$, 300 K): a:) **20**; c) **16**; (500 MHz, $CDCl_3$, 298 K): b) **26**. Please note that the spectra are recorded using different field strengths and are therefore for a qualitative comparison only. The colour code and numbering corresponds to Scheme 4.8.

4.3.8 Synthesis of the Chain Lock

The chain lock was synthesised from the building blocks **22** and **23** under high dilution conditions with TBTA and $[Cu(MeCN)_4]PF_6$ as catalyst combination. For the *in situ* deprotection KF in MeOH was used. The purification of the product proved to be rather difficult. Analysis by NMR after the first column chromatography showed significant amounts of TBTA in the product fractions obtained, which could not be removed by repeated purification efforts.

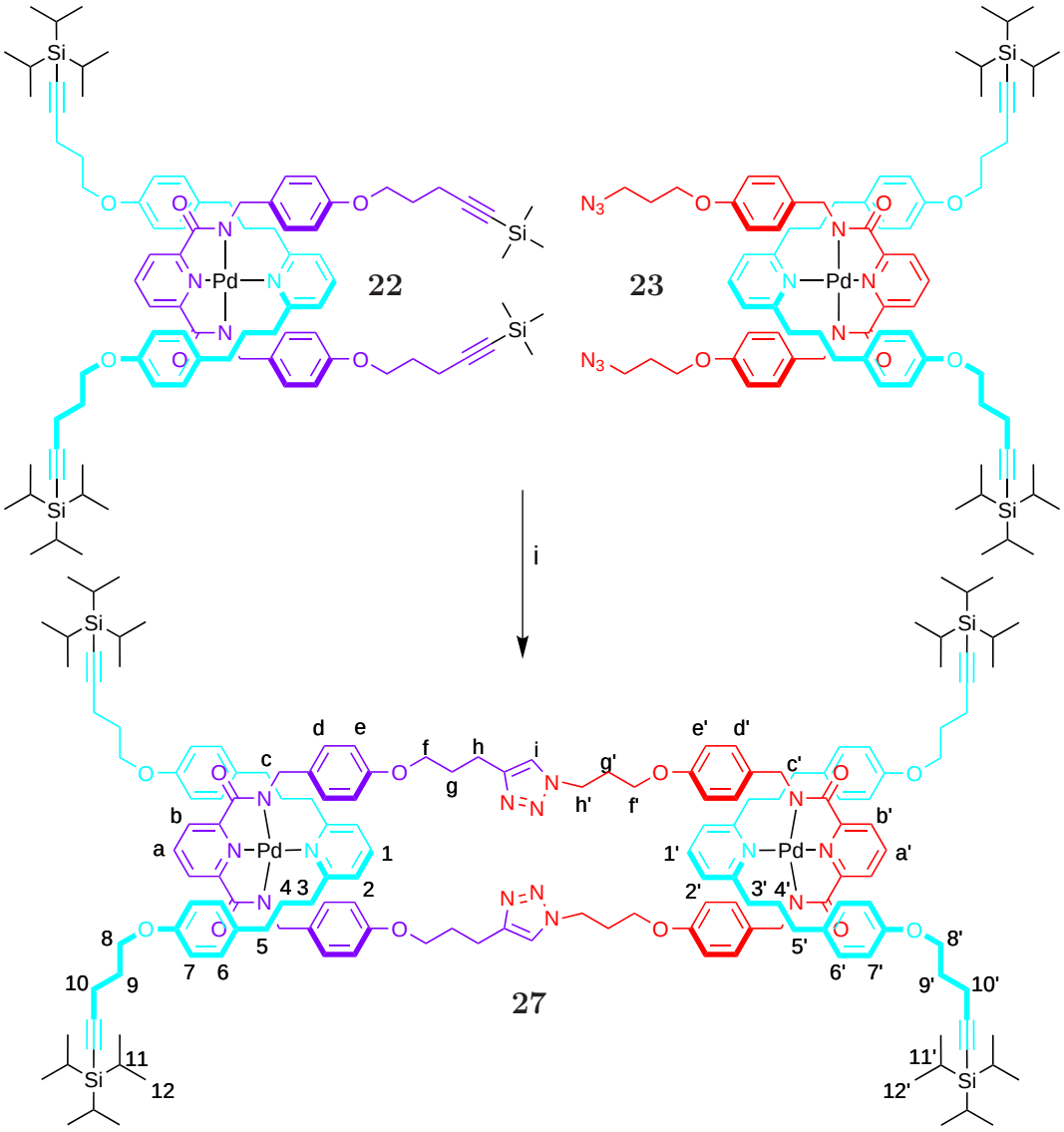

Figure 4.21. Synthesis of **27**. Reagents and conditions: i) **22**, **23**, CH_2Cl_2/MeOH (1:1), TBTA, $[Cu(MeCN)_4]PF_6$, KF, 23%.

Further, the possibility of traces of copper(I) sequestered in the cavity of the macrocycle binding the observed TBTA could not be excluded. Attempts

to oxidise the Cu(I) to Cu(II) which has a much lower affinity to the triazoles ligands resulted in complete decomposition. Attempts to purify the partially purified product mixture by size exclusion chromatography over Sephadex LH-60 (lipophilic sephadex with an exclusion limit of 10000 Da) was not successful but showed the possibility that with a higher exclusion limit separation would be possible. Therefore an attempt was made with a 120x2.5 cm column filled with BioBeads S-X1 (BioRad, size exclusion limit 14000 Da), and the product mixture was successfully separated. The mass recovery after pre-purification and size exclusion was 23%. However, this product showed signs of rapid degradation. Furthermore, the subsequent deprotection proved to be rather difficult. Although the totally deprotected species could be observed by mass spectrometry, the isolation as pure compound was not possible. As a consequence of these findings, this route was abandoned. The ^{1}H-NMR of the chain lock **27** is shown in Figure

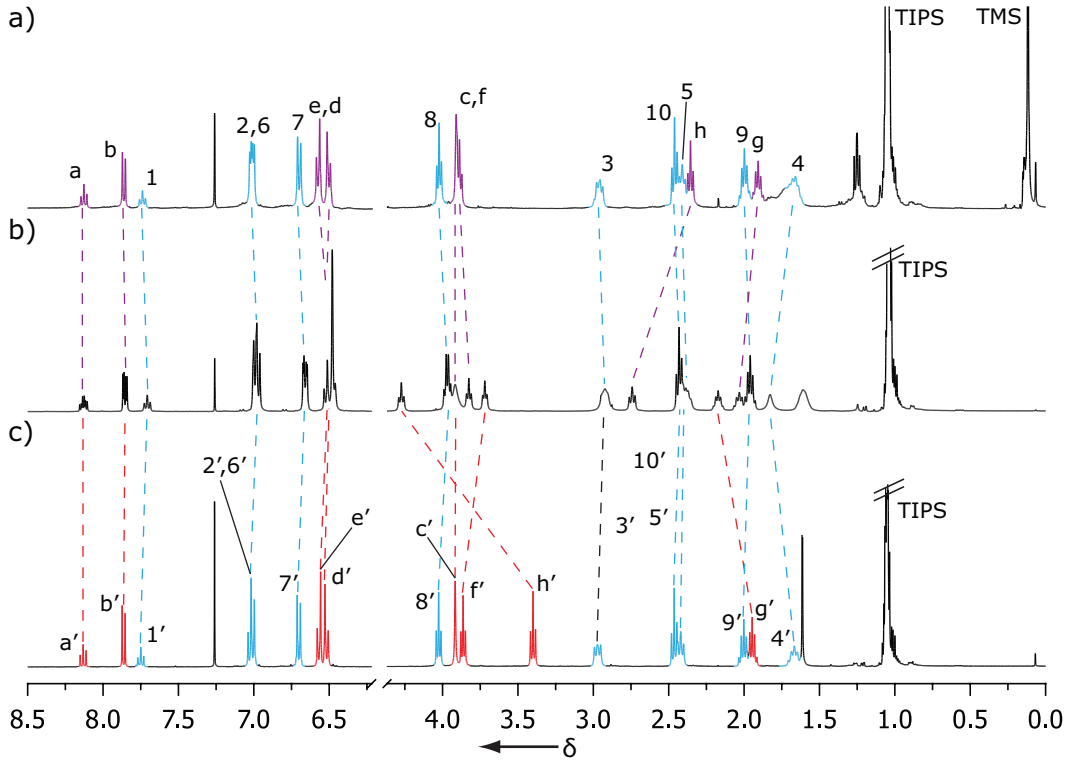

Figure 4.22. ^{1}H-NMR (400 MHz, $CDCl_3$, 300 K) of a) **22**; b) chain link **27**; c) **23**. The colour code and numbering corresponds to Figure 4.8.

4.22b accompanied by the spectra of **22** (Figure 4.22a) and **23** (Figure 4.22c) for comparison. The spectrum of **27** is mostly a superposition of the spectra of **22** and **23** with the exception of the protons attached to the triazole ring. As

expected, the proton $H_{h'}$ shows the strongest shift downfield (0.67 ppm) followed by H_h (0.38 ppm) and $H_{g'}$ (0.27 ppm). Due to the simplicity of the spectrum and the absence of signal splitting caused by diastereotopic environments a C_{2v} symmetry in solution is plausible.

4.4 Conclusions

The click building block library presented in this chapter has been used successfully to generate complicated interlocked structures, such as a [2]catenane, a [3]catenane and a "chain-lock" for higher [n]catenanes. The synthesis of the building blocks is highly modular and, due to the advantages of the [3+1] palladium template, easily expandable. The optimised conditions to generate a *bis*-alkyne containing tridentate ligand, now yield up to 60% doubly alkylated product from the *bis*-phenol precursor complex and the optimised purification thereof now makes the product accessible without by-product traces. Two *in situ* deprotection methodologies have been established to generate the free alkynes during the click reaction. However, the unresolved stability problems of the tetraalkyne-containing compounds, be it **22** or **27** raise questions if the [5]catenane can be obtained via this route. However, all *bis*-alkyne-containing compounds were perfectly stable without special storage conditions. This would lead to the conclusion, that the higher catenanes would probably be accessible via a sequence of double click reaction starting from **20** and **23**, forming the [2]catenane with two functional handles which can be elaborated further.

4.5 Experimental

4.5.1 General

Compounds (**15**)[10] and (**24**)[9] were prepared according to literature procedure.

4.5.2 Synthesis

3-((5-tri-i-propylsilyl-4-yn-pentoxy)4-phenyl)-propan-1-ol (8)

A dry flask was charged with 3-(*p*-hydroxy-phenyl)-propan-1-ol (2.10 g, 13.8 mmol), 5-tri-*i*-propylsilyl-pent-4-yn-1-bromide (4.60 g, 16.5 mmol), K_2CO_3 (5.72 g, 41.4 mmol), DMF (10 mL). The resulting suspension was allowed to stir for 18 h at 80 °C. The reaction mixture was then partitioned between 1M HCl solution and EtOAc and the organic phase was washed with brine, water and dried over $MgSO_4$. Upon concentration in vacuo, the crude mixture was purified via column chromatography (EtOH/Cl_2Cl_2 (0.2:99.8)) to yield the desired product as colourless viscous oil (4.46 g, 86%).

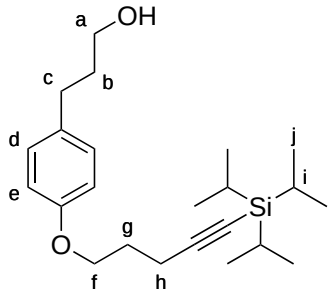

^{1}H-NMR (400 MHz, $CDCl_3$, 300 K): δ = 7.10 (d, 2H, J = 8.5 Hz, H_d), 6.83 (d, 2H, J = 8.6 Hz, H_e), 4.07 (t, 2H, J = 6.3 Hz, H_f), 3.67 (t, 2H, J = 6.4 Hz, H_a), 2.69-2.60 (m, 2H, H_c), 2.46 (t, 2H, J = 6.9 Hz, H_h), 1.99 (p, 2H, J = 6.6 Hz, H_g), 1.91-1.82 (m, 2H, H_b), 1.13-0.95 (m, 21H, $H_{i/j}$).

^{13}C-NMR (100 MHz, $CDCl_3$, 300 K): δ = 157.30, 133.94, 129.40, 114.60, 107.99, 81.04, 77.48, 77.16, 76.84, 66.52, 62.41, 34.57, 31.27, 28.76, 18.75, 16.77, 11.37.

HREI-MS: m/z = 375.27227 $[M + H]^+$

(calc. for $C_{23}H_{39}O_2Si$ 375.27248).

3-[(5-tri-i-propylsilyl-4-yn-pentoxy)4-phenyl]-propyl bromide (9)

A dry Schlenk flask was charged with 3-[(5-tri-*i*-propylsilyl-4-yn-pentoxy)4-phenyl]-propan-1-ol (4.46 g, 11.9 mmol), CBr_4 (5.10 g, 15.4 mmol), set under an inert gas atmosphere and dry CH_2Cl_2 (60 mL) was added. The solution was cooled to 0 °C and a solution of triphenylphoshine (4.04 g, 15.4 mmol) in CH_2Cl_2 (60 mL) was added dropwise over a period of 30 min. The solution was allowed to stir at RT for 2 h and the reaction quenched upon addition of EtOH (2 mL). The reaction mixture was concentrated in vacuo, taken up in hexane, filtered and absorbed on a plug of silica. The plug was washed with hexane followed by hexane/Et_2O (95:5) to elute the product. Upon evaporation of the volatiles the product was obtained as colourless oil (4.9 g, 94%).

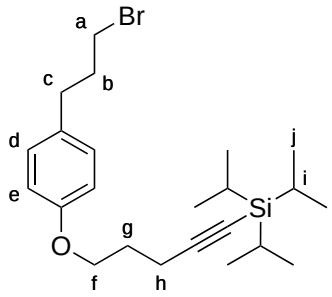

^{1}H-NMR (400 MHz, $CDCl_3$, 300 K): δ = 7.10 (d, 2H, J = 8.6 Hz, H_d), 6.84 (d, 2H, J = 8.6 Hz, H_e), 4.07 (t, 2H, J = 6.2 Hz, H_f), 3.39 (t, 2H, J = 6.6 Hz, H_a), 2.72 (t, 2H, J = 7.3 Hz, H_c), 2.46 (t, 2H, J = 6.9 Hz, H_h), 2.19–2.05 (m, 2H, H_b), 2.00 (p, 2H, J = 6.6 Hz, H_g), 1.10–0.94 (m, 21H, $H_{i/j}$).
^{13}C-NMR (100 MHz, $CDCl_3$, 300 K): δ = 157.52, 132.65, 129.58, 114.67, 107.95, 81.07, 66.51, 34.51, 33.32, 33.15, 28.74, 18.75, 16.77, 11.37.
LREI-MS: m/z = 437 $[M + H]^+$

2,6-bis{3-[(5-tri-i-propylsilyl-4-yn-pentoxy)4-phenyl]-propyl}pyridine (12)

A dry Schlenk tube was charged with Zn dust (2.19 g, 33.6 mmol), set under nitrogen and extra dry 1-methyl-2-pyrrolidone (12 mL). Iodine (426 mg, 1.68 mmol) was added and the solution was stirred until all iodine was consumed. Upon addition of the 5-tri-*i*-propylsilyl-4-yn-pentoxy-4-phenyl-propyl-1-bromide (4.9 g, 11.2 mmol) the solution was allowed to stir for 4 h at 80 °C. The heat

source was removed and the solution was allowed to settle. The supernatant was transferred to a Schlenk tube containing a solution of 2,6-dibromo pyridine (796 mg, 3.36 mmol), PEPPSI catalyst (114 mg, 168 mmol), LiBr (1.94 g, 22.4 mmol) in extra dry 1-methyl-2-pyrrolidone (12 mL) under inert gas atmosphere. The rection mixture was stirred for 3 h at RT and the reaction quenched upon adition of water (2 mL). The crude mixture was partitioned between Et_2O and 1M Na_4EDTA soution and separated. The organic phase was washed twice with dilute NH_3 solution, Brine and water, dried over Na_2SO_4 and concentrated in vacuo. The residue was purified via column chromatography (Et_2O/Hexane (10:90)) and upon removal of the volatiles, the product was obtained as a colorless viscous oil (1.89 g, 71%).

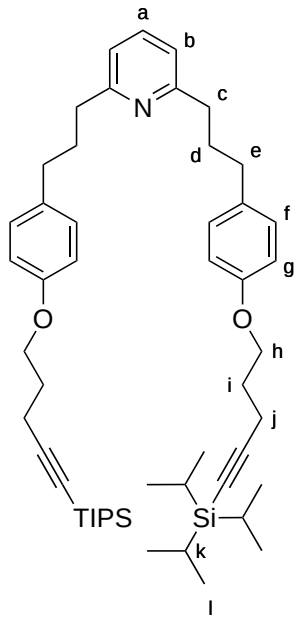

^{1}H-NMR (400 MHz, $CDCl_3$, 300 K): δ = 7.48 (t, 1H, J = 7.7 Hz, H_a), 7.09 (d, 4H, J = 8.5 Hz, H_f), 6.93 (d, 2H, J = 7.7 Hz, H_b), 6.81 (d, 4H, J = 8.6 Hz, H_g), 4.06 (t, 4H, J = 6.2 Hz, H_h), 2.79 (m, 4H, H_c), 2.61 (m, 4H, H_e), 2.45 (t, 4H, J = 6.9 Hz, H_j), 2.04–1.95 (m, 8H, $H_{d/i}$), 1.07–0.96 (m, 42H, $H_{k/l}$).

^{13}C-NMR (100 MHz, $CDCl_3$, 300 K): δ = 161.45, 157.05, 136.42, 134.36, 129.30, 119.78, 114.34, 107.88, 80.85, 66.37, 38.01, 34.69, 32.03, 28.64, 18.60, 16.63, 11.22.

LRESI-MS: m/z = 792 $[M + H]^+$

HRESI-MS: m/z = 792.5573 $[M + H]^+$

(calc. for $C_{51}H_{78}NO_2Si_2$792.5566).

{κ^3-2,6-bis-[4-(3-azido-propoxy)-benzylamide]-pyridino}(N,N-dimethylformamide) palladium(II)

(14)

2,6-*Bis*-(4-(3-azido-propoxy)-benzylamide)-pyridine (570 mg, 1.05 mmol), $Pd(OAc)_2$ (258 mg, 1.15 mmol) and K_2CO_3 (725 mg, 5.25 mmol) were suspended in DMF (10 mL) and the reaction mixture was allowed to stir at 80 °C for 1 h. The reaction mixture was allowed to cool to RT, diluted with Et_2O and absorbed on a plug of silica. The plug was washed with $MeOH/CH_2Cl_2$ (3:97) and then $MeOH/CH_2Cl_2$ (15:85) to elute the product. Removal of the volatiles yielded the desired product as yellow/orange amorphous solid (669 mg, 88%). This product was used straight away without any further purification.

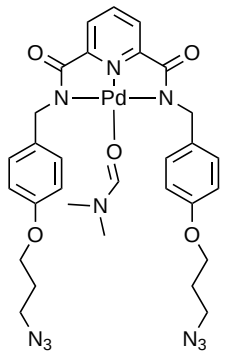

BB1 (BB1)

A flask was charged with {κ^3-2,6-*bis*-[4-(3-azido-propoxy)-benzylamide]-pyridino} (*N,N*-dimethylformamide) palladium(II) (46 mg, 63 μmol), **15**[10] (31.0 mg, 63.0 μmol) and CH_2Cl_2 (2 mL). The resulting solution was allowed to stir for 18 h. The mixture was then concentrated in vacuo and purified by column chromatography ($EtOH/CH_2Cl_2$ (1.5:98.5)). After removal of the volatiles under reduced pressure, the product was obtained as yellow amorphous solid (62 mg, 85%).

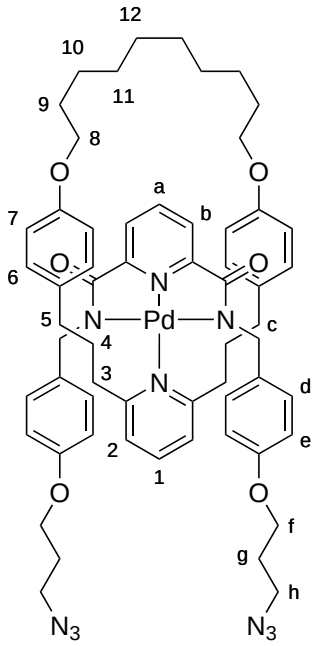

^{1}H-NMR (400 MHz, $CDCl_3$, 300 K): δ = 8.11 (t, 1H, J = 7.8 Hz, H_a), 7.76 (d, 2H, J = 7.8 Hz, H_b), 7.70 (t, 1H, J = 7.7 Hz, H_1), 7.01 (d, 2H, J = 7.7 Hz, H_2), 6.79 (d, 4H, J = 8.3 Hz, H_6), 6.60 (d, 4H, J = 8.4 Hz, H_e), 6.46 (d, 4H, J = 8.4 Hz, H_d), 6.26 (d, 4H, J = 8.3 Hz, H_7), 4.00 (t, 4H, J = 5.9 Hz, H_f), 3.73 (t, 4H, J = 6.6 Hz, H_8), 3.67 (s, 4H, H_c), 3.52 (t, 4H, J = 6.5 Hz, H_h), 2.76–2.68 (m, 4H, H_3), 2.48–2.41 (m, 4H, H_5), 2.04 (p, 4H, J = 6.2 Hz, H_g), 1.80–1.72 (m, 4H, H_9), 1.72–1.64 (m, 4H, H_4), 1.64–1.56 (m, 4H, H_{10}), 1.56–1.46 (m, 8H, $H_{11/12}$).
^{13}C-NMR (100 MHz, $CDCl_3$, 300 K): δ = 170.83, 163.94, 157.18, 156.91, 151.95, 139.50, 138.64, 133.93, 131.94, 129.73, 128.84, 124.10, 122.06, 113.85, 113.31, 67.16, 64.54, 49.09, 48.21, 38.46, 34.45, 30.48, 28.94, 28.80, 28.76, 28.59, 25.74.
HRESI-MS: pattern matched.

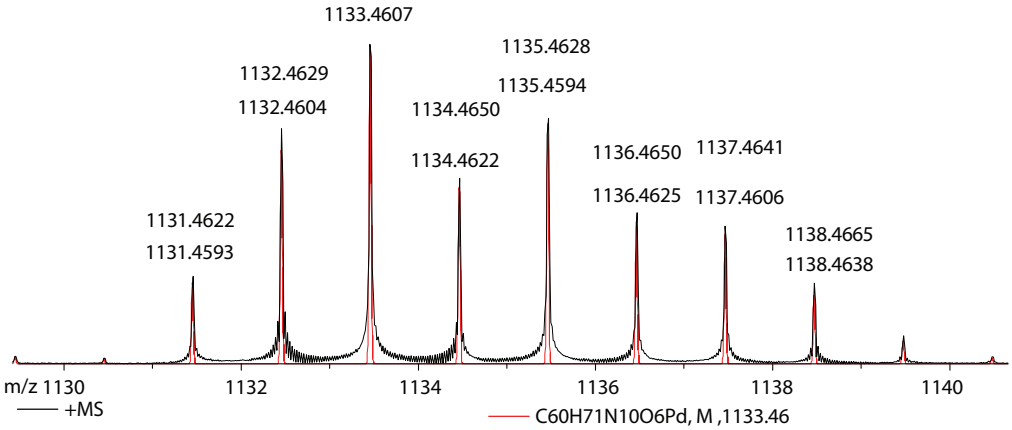

BB4 (BB4)

A flask was charged with {κ^3-2,6-*bis*-[4-(3-azido-propoxy)-benzylamide]-pyridino} (*N,N*-dimethylformamide) palladium(II) (425 mg, 589 mmol), 2,6-*bis*(3-((5-tri-*i*-propylsilyl-4-yn-pentoxy)4-phenyl)-propyl)pyridine (467 mg, 589 mmol) and DMF/CH_2Cl_2 (1:1, 5 mL). The solution was allowed to stir for 18 h, concentrated in vacuo and purified by column chromatography (gradient EtOH/CH_2Cl_2 (1:99) → EtOH/ CH_2Cl_2 (3:97)). Removal of the volatiles yielded the desired product as a yellow amorphous solid (795 mg, 93%).

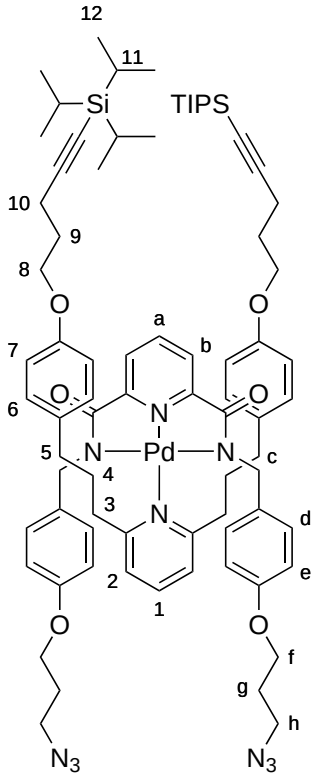

^{1}H-NMR (400 MHz, $CDCl_3$, 300 K): δ = 8.13 (t, 1H, J = 7.8 Hz, H_a), 7.86 (d, 2H, J = 7.8 Hz, H_b), 7.75 (t, 1H, J = 7.8 Hz, H_1), 7.05–6.97 (m, 6H, $H_{2/6}$), 6.70 (d, 4H, J = 8.6 Hz, H_7), 6.57 (d, 4H, J = 8.7 Hz, H_e), 6.52 (d, 4H, J = 8.7 Hz, H_d), 4.03 (t, 4H, J = 6.2 Hz, H_8), 3.92 (s, 4H, H_c), 3.86 (t, 4H, J = 6.0 Hz, H_f), 3.40 (t, 4H, J = 6.6 Hz, H_h), 3.01–2.93 (m, 4H, H_c), 2.49–2.39 (m, 8H, $H_{10/5}$), 2.04–1.91 (m, 8H, $H_{g/9}$), 1.71–1.59 (m, 4H, H_4), 1.09–0.96 (m, 42H, $H_{11/12}$).

^{13}C-NMR (100 MHz, $CDCl_3$, 300 K): δ = 171.16, 163.60, 157.30, 157.16, 152.61, 140.26, 138.85, 133.64, 133.29, 129.21, 128.61, 124.68, 121.11, 114.21, 113.91, 107.92, 80.82, 66.30, 64.50, 49.05, 48.16, 38.56, 34.80, 29.93, 28.75 (2 peak over-

lap), 18.61, 16.68, 11.22.

HRESI-MS: m/z = pattern matched.

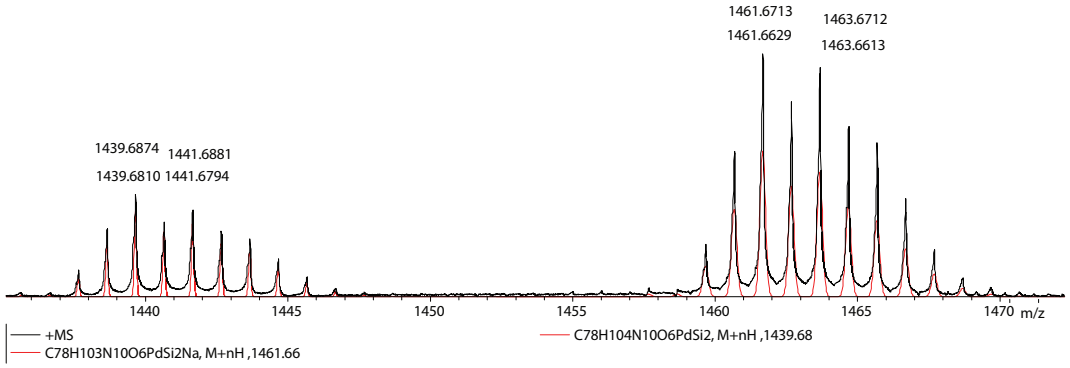

{κ^3-2,6-Bis[4-hydroxy-benzylamide]-pyridino}(N,N-dimethylamide) palladium(II) (18)

2,6-*Bis*(4-hydroxy-benzylamide)-pyridine (1.97 mg, 5.22 mmol) was dissolved in DMF (25 mL) and $Pd(OAc)_2$ (1.19 mg, 5.30 mmol) was added. The solution was stirred for 18 h, and the product precipitated with water. The suspenstion was then filtered through a plug of celite where the product was retained. The plug was washed repeatedly with water until the solution stayed colorless. The product was then eluted with DMF/$CHCl_3$ (1:1). Upon removal of the volatiles afforded the desired product as a yellow amorphous solid (2.34 g, 80%). This product was used straight away, without any further purification.

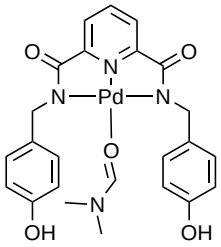

{κ^3-2,6-bis-[4-hydroxy-benzylamide]-pyridino}(6,17-dioxa-1(2,6)-pyridina-5,18(1,4)dibenzenacyclohencosaphane) palladium(II) (19)

A dry flask was charged with {κ^3-2,6-*Bis*[4-hydroxy-benzylamide]-pyridino}(*N*,*N*-dimethylformamid) palladium(II) (269 mg, 485 μmol), **15**[10] (205 mg, 422 μmol) and $CHCl_3$/DMF (5:3, 8 mL). The resulting suspension was stirred for 18 h,

loaded on a plug of silica and eluted with EtOH/CH_2Cl_2 (15:85). Removal of the volatiles afforded the crude mixture, which was purified by column chromatography (5% EtOH/CH_2Cl_2). The product was obtained as bright yellow amorphous solid (76%).

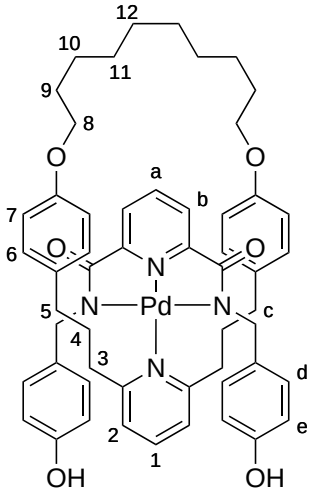

^{1}H-NMR (400 MHz, $(CD_3)_2SO$, 300 K): δ = 9.09 (s, 2H,H_{OH}), 8.32 (t, 1H, J = 7.8 Hz, H_a), 7.88 (t, 1H, J = 7.8 Hz, H_1), 7.65 (d, 2H, J = 7.8 Hz, H_b), 7.20 (d, 2H, J = 7.8 Hz, H_2), 6.76 (d, 4H, J = 8.5 Hz, H_6), 6.45 (d, 4H, J = 8.5 Hz, H_e), 6.22–6.14 (m, 8H, $H_{d/7}$), 3.67 (t, 4H, J = 6.8 Hz, H_8), 3.45 (s, 4H, H_c), 2.78–2.57 (m, 4H, H_3), 2.52–2.30 (m, 4H, H_5), 1.74–1.61 (m, 8H, $H_{9/4}$), 1.55–1.41 (m, 12H, $H_{10/11/12}$).

^{13}C-NMR (100 MHz, $(CD_3)_2SO$, 300 K): δ = 170.04, 162.87, 156.47, 155.61, 151.59, 140.45, 139.47, 131.79, 131.33, 129.49, 128.17, 123.63, 122.23, 114.48, 112.98, 66.61, 48.34, 37.68, 33.87, 29.29, 28.50, 28.34, 28.09, 25.21.

HRESI-MS: pattern matched.

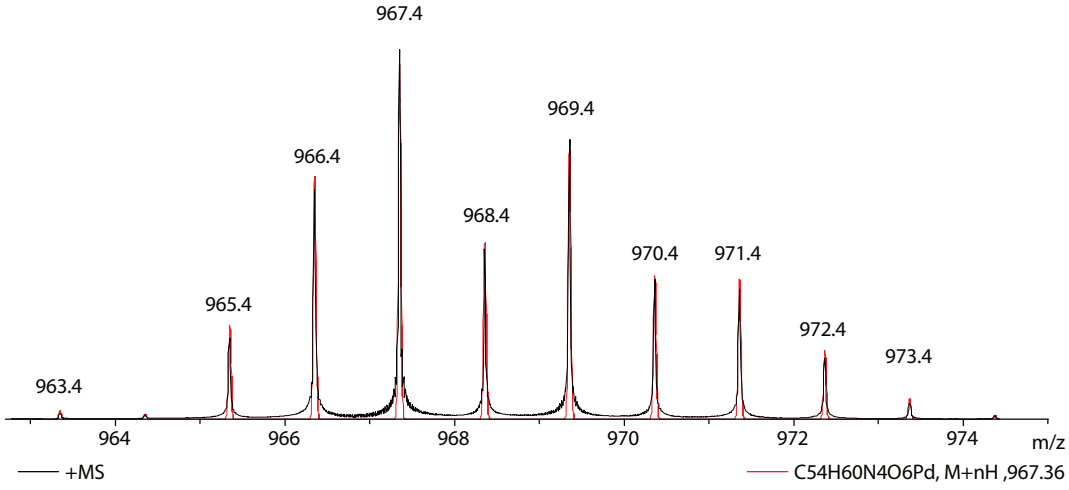

BB2 (22)

A dry Schlenk tube was charged with commercially available 1M tricyclohexyl phosphine solution (2.06 mL, 2.06 mmol), dry THF (8 mL) and cooled to 0 °C. Freshly distilled DIAD (405 μL, 2.06 mmol) was added dropwise until a slight yellow colour remained and the solution was allowed to stir for 20 min. 5-Trimethylsilyl-pent-4-yn-1-ol (321 μL, 2.06 mmol) was then added and the solution was stired for forther 30 min at 0 °C. The rection mixture was then added to a Schlenk tube charged with **21** (200 mg, 206 μmol) and the resulting solution was allowed to stir 18 h at RT. The crude mixture was then concentrated in vacuo, taken up in MeOH/water (95:5) and loaded on a plug of activated charcoal (10 cm height). The plug was washed with MeOH, then with CH_2Cl_2 to extract the product. Concentration in vacuo and column chromatography of the crude mixture (gradient EtOH/CH_2Cl_2 (0.2:99.5) → EtOH/CH_2Cl_2 (1.5:98.5)) afforded the product as yellow amorphous solid (157.5 mg, 62%).

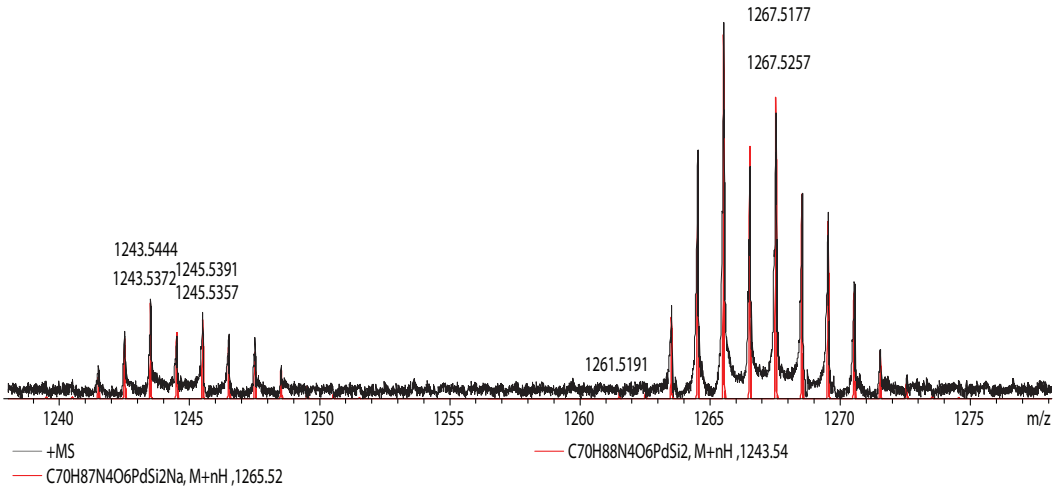

^{1}H-NMR (400 MHz, $(CD_3)_2SO$, 300 K): δ = 8.11 (t, 1H J = 7.8 Hz, H_a), 7.76 (d, 2H J = 7.8 Hz, H_b), 7.69 (t, 1H J = 7.7 Hz, H_1), 7.01 (d, 4H J = 7.8 Hz, H_2), 6.79 (d, 4H J = 8.4 Hz, H_6), 6.60 (d, 4H J = 8.6 Hz, H_e), 6.45 (d, 4H J = 8.5 Hz, H_d), 6.26 (d, 4H J = 8.4 Hz, H_7), 4.00 (t, 4H J = 6.2 Hz, H_f), 3.73 (t, 4H J = 6.7 Hz, H_8), 3.67 (s, 4H, H_c), 2.81-2.64 (m, 4H, H_3), 2.47–2.41 (m, 8H, $H_{h/5}$), 1.97 (p, 4H, J = 6.6 Hz, H_g), 1.82-1.64 (m, 8H, $H_{4/9}$), 1.64-1.56 (m, 4H, H_{10}), 1.61-1.46 (m, 8H, $H_{11/12}$), 0.18-0.05 (m, 36H, H_i).

^{13}C-NMR (100 MHz, $(CD_3)_2SO$, 300 K): δ = 170.98, 164.12, 157.53, 157.08,

152.15, 139.65, 138.77, 133.86, 132.08, 129.90, 128.97, 124.26, 122.17, 114.07, 113.48, 106.39, 85.27, 67.33, 66.55, 49.24, 38.62, 34.65, 30.59, 29.11, 28.94, 28.76, 28.47, 25.91, 16.73, 0.28.

HRESI-MS: pattern matched.

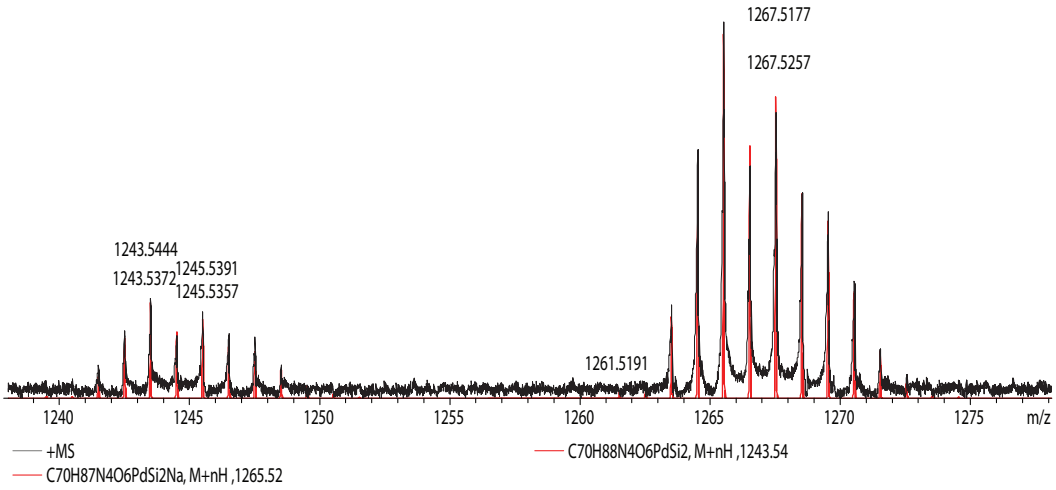

{κ^3-2,6-bis-[4-hydroxy-benzylamide]-pyridino}(2,6-bis(3-((5-tri-i-propylsilyl-4-yn-pentoxy)4-phenyl)-propyl)pyridino) palladium(II)

(21)

A flask was charged with {κ^3-2,6-*bis*[4-hydroxy-benzylamide]-pyridino}(dimethylformamide) palladium(II) (282 mg, 366 μmol), 2,6-*bis*(3-((5-tri-*i*-propylsilyl-4-yn-pentoxy)4-phenyl)-propyl)pyridine (366 mg, 462 μmol) and CH_2Cl_2/DMF (4:1, 5 mL). The solution was allowed to stir for 1 d, concentrated in vacuo and purified by column chromatography (MeOH/CH_2Cl_2 (5:95)). Upon evaporation of the volatiles the product was obtained as yellow amorphous solid (560 mg, 95%).

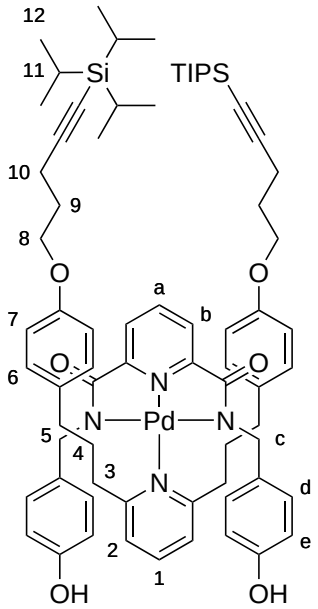

^{1}H-NMR (400 MHz, $(CD_3)_2SO$, 300 K): δ = 9.19 (s, 2H, H_{OH}), 8.31 (t, 1H, J = 7.8 Hz, H_a), 7.94 (t, 1H, J = 7.8 Hz, H_1), 7.76 (d, 2H, J = 7.8 Hz, H_b), 7.19 (d, 2H, J = 7.8 Hz, H_2), 7.01 (d, 4H, J = 8.5 Hz, H_6), 6.58 (d, 4H, J = 8.5 Hz, H_7), 6.48 (d, 4H, J = 8.4 Hz, H_e), 6.30 (d, 4H, J = 8.4 Hz, H_d), 3.94 (t, 4H, J = 6.2 Hz, H_8), 3.68 (s, 4H, H_c), 2.88–2.79 (m, 4H, H_3), 2.43 (t, 4H, J = 6.9 Hz, H_{10}), 2.33 (t, 4H, J = 7.1 Hz, H_5), 1.88 (p, 4H, J = 6.5 Hz, H_9), 1.68–1.57 (m, 4H, H_4), 1.04–0.99 (m, 42H, $H_{11/12}$).

^{13}C-NMR (100 MHz, $(CD_3)_2SO$, 300 K): δ = 170.21, 162.65, 156.48, 155.91, 151.81, 141.52, 139.75, 133.26, 131.22, 129.37, 128.10, 124.38, 121.72, 114.58, 114.49, 113.79, 108.76, 80.13, 65.70, 38.00, 34.33, 29.76, 28.14, 18.52, 15.96, 10.72.

LRESI-MS: m/z = 1273 $[M + H]^+$.

HRESI-MS: m/z = 1273.58541 $[M + H]^+$

(calc. for $C_{72}H_{95}N_4O_6PdSi_2$ 1273.58305).

BB3 (22)

A dry Schlenk tube was charged with commercially available 1M tricyclohexyl phosphine solution (5.24 mL, 5.24 mmol), dry THF (6 mL) and cooled to 0 °C. Freshly distilled DIAD (1.03 mL, 5.24 mmol) was added dropwise until a slight yellow colour remained and the solution was allowed to stir for 20 min. 5-Trimethylsilyl-pent-4yn-1-ol (0.95 mL, 5.24 mmol) was then added and the solu-

tion was stired for forther 30 min at 0 °C. The rection mixture was then added to a Schlenk tube charged with MK429 (668 mg, 524 μmol) and the resulting solution was allowed to stir 18 h at RT. The crude mixture was then concentrated in vacuo, taken up in MeOH/water (95:5) and loaded on a plug of activated charcoal (10 cm height). The plug was washed with MeOH, then with CH_2Cl_2 to extract the product. Concentration in vacuo and column chromatography of the crude mixture (gradient MeOH/CH_2Cl_2 (0.5:99.5) $\rightarrow$ MeOH/CH_2Cl_2 (1.5:98.5)) afforded the product as yellow amorphous solid (466 mg, 57%).

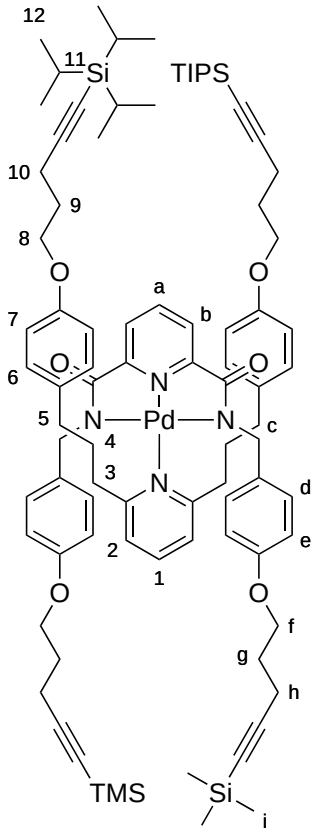

^{1}H-NMR (400 MHz, $CDCl_3$, 300 K): δ = 8.13 (t, 1H, J = 7.8Hz, H_a), 7.86 (d, 2H, J =7.8 Hz, H_b), 7.74 (t, 1H, J =7.8 Hz, H_1), 7.04–6.96 (m, 6H, $H_{2/6}$), 6.70 (d, 4H, J = 8.3 Hz, H_7), 6.57 (d, 4H, J = 8.5 Hz, H_e), 6.50 (d, 4H, J = 8.5 Hz, H_d), 4.02 (t, 4H, J = 6.1 Hz, H_8), 3.93–3.85 (m, 8H, $H_{c/f}$), 3.01–2.97 (m, 4H, H_3), 2.49–2.29 (m, 12H, $H_{h/5/10}$), 2.00 (p, 4H, J = 6.5 Hz, H_9), 1.91 (p, 4H, J =6.6 Hz, H_g), 1.72–1.58 (m, 4H, H_4), 1.10–0.95 (m, 42H, $H_{11/12}$), 0.12 (s, 18H, H_i).

^{13}C-NMR (100 MHz, $CDCl_3$, 300 K): δ = 171.13, 163.63, 157.55, 157.11, 152.63,

140.24, 138.79, 133.36, 133.31, 129.25, 128.58, 124.66, 121.06, 114.22, 113.96, 107.92, 106.13, 85.13, 80.80, 66.34, 66.27, 49.06, 38.54, 34.85, 30.07, 28.76, 28.27, 18.61, 16.69, 16.54, 11.21, 0.08.

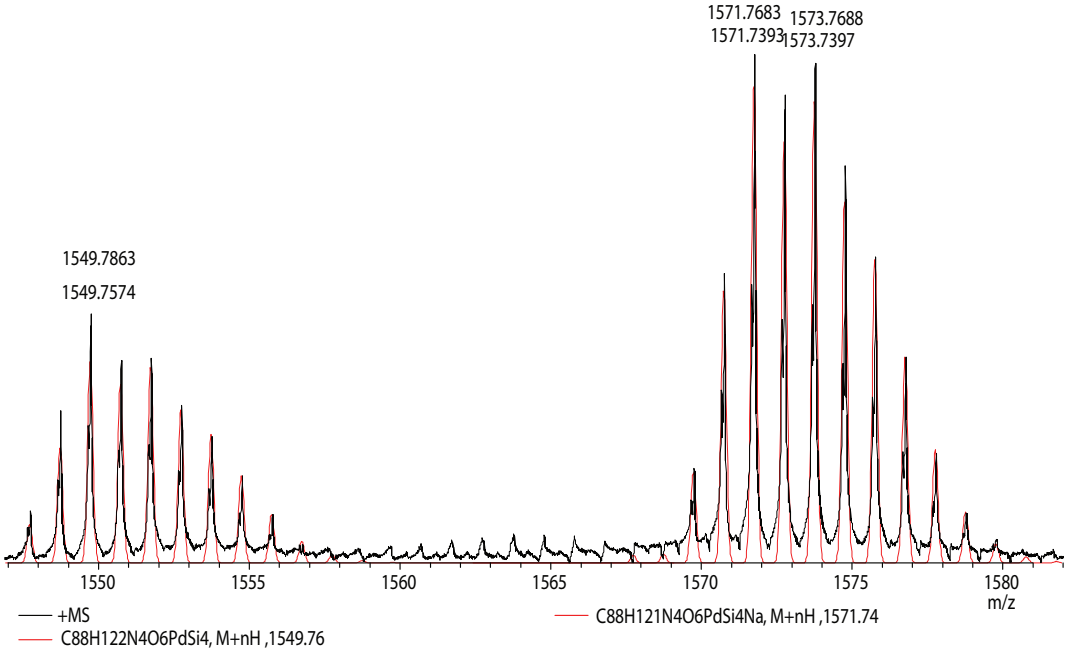

[2]catenane 25

Three degassed solutions were made: Solution A: *bis*-azide 12.2 mg (10.7 μmol) /10 mL (1,2-dichloroethane/1-propanol 95:5)

Solution B: dipropargyl formaldehydeacetal 12.4 mg (100 μ)mol /10 mL (1,2-dichloroethane/1-propanol 95:5)

Solution C: $[Cu(MeCN)_4]PF_6$ 1.5 mg (4 μmol) and TBTA 6.36 mg (12 μmol) / 2 mL (1,2-dichloroethane/1-propanol 95:5)

A dry and capped vial was flushed with nitrogen and loaded with Solution A (3 mL), Solution B (0.6 mL) and Solution C (0.1 mL). This mixture was allowed to stir for 7 d. Then the reaction mixture was partitioned between CH_2Cl_2 (20 mL) and 1 M Na_4EDTA (20 mL). The organic phase was washed two more times with 1 M Na_4EDTA (20 mL) and was dried over $NaSO_4$. Evaporation of the volatiles yielded a orange yellowish residue, which was dissolved in DMSO, filtered through a 0.45 μm syringe filter and purified by reversed phase HPLC chromatography (Ascentis C-18 21.2x250, isocratic 60% MeOH / 30% CH_2Cl_2/

10% H_2O). The product was obtained by evaporation of the volatiles under reduced pressure as a yellow varnish. Estimated yield is 50% based on mass recovery of 1.9 mg.

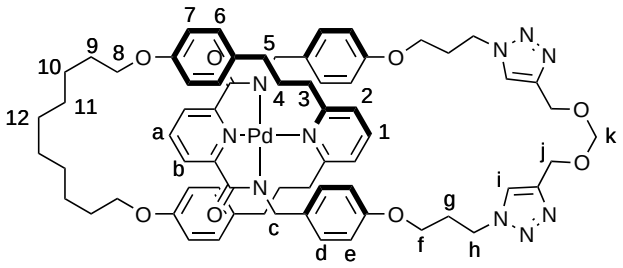

^{1}H-NMR (400 MHz, $CDCl_3$, 300 K): δ = 8.12 (t, 1H, J = 7.8 Hz, H_a), 7.77 (d, 1H, J = 7.8 Hz, H_b), 7.73 (t, 1H, J = 7.8 Hz, H_1), 7.61 (s, 2H, H_i), 7.07 (d, 2H, J = 7.8 Hz, H_2), 6.74 (d, 4H, J = 8.5 Hz, H_6), 6.45 (d, 4H, J = 8.7 Hz, H_e), 6.38 (d, 4H, J = 8.8 Hz, H_d), 6.22 (d, 4H, J = 8.6 Hz, H_7), 4.74 (s, 2H, H_k), 4.67 (s, 4H, H_j), 4.63-4.57 (m, 4H, H_h), 3.77 (t, 4H, J = 5.7 Hz, H_f), 3.75-3.68 (m, 8H, $H_{c/8}$), 2.94-2.87 (m, 4H, H_3), 2.40-2.31 (m, 8H, $H_{g/5}$), 1.81-1.72 (m, 4H, H_9), 1.62-1.48 (m, 16H, $H_{4/10/11/12}$).

^{13}C-NMR (125 MHz, $CDCl_3$, 298 K): δ = 171.13, 163.94, 157.13, 156.99, 152.14, 144.62, 139.77, 139.00, 134.35, 132.14, 129.94, 129.13, 124.31, 123.42, 122.15, 113.87, 133.46, 94.02, 67.38, 63.50, 60.83, 49.57, 46.75, 38.76, 34.57, 30.10, 29.85, 29.68, 29.01, 28.79, 25.96.

[3]catenane (26)

Solution A: *bis*-azide 12.2 mg (10.7 μmol) /10 mL (1,2-dichloroethane/1-propanol 95:5) Solution B: *bis*-alkyne 10.4 mg (8.4 μ)mol /10 mL (1,2-dichloroethane/1-propanol 95:5) Solution C: $[Cu(MeCN)_4]PF_6$ 1.5 mg (4 μmol) and TBTA 6.36 mg (12 μmol) / 2 mL (1,2-dichloroethane/1-propanol 95:5)

A dry and capped vial was flushed with nitrogen and loaded with Solution A (2 mL), Solution B (2.3 mL), Solution C (0.1 mL) and 1 M TBAF in THF (2 μL). The mixture was allowed to stir for 7 d; each 24 h another portion (0.2 mL) of freshly prepared Solution C was added. Then the reaction mixture was partitioned between CH_2Cl_2 (20 mL) and 1 M Na_4EDTA (20 mL). The organic phase was washed two more times with 1 M Na_4EDTA (20 mL) and was dried

over $NaSO_4$. Evaporation of the volatiles yielded a orange yellowish residue, which was dissolved in DMSO, filtered through a 0.45 μm syringe filter and purified by reversed phase HPLC chromatography (Ascentis C-18 21.2x250, isocratic 60% MeOH / 30% CH_2Cl_2/ 10% H_2O). After evaporation of the volatiles, the product was obtained as a yellow varnish. Estimated yield is 35% based on mass recovery of 1.6 mg.

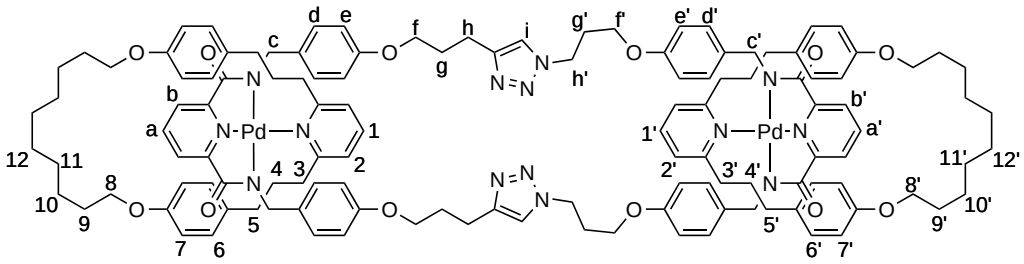

^{1}H-NMR (500 MHz, $CDCl_3$, 298 K): δ = 8.15-8.09 (m, 2H, $H_{a/a'}$), 7.80–7.72 (m, 4H, $H_{b/b'}$), 7.67 (t, 2H, J = 7.7 Hz, $H_{1/1'}$), 7.25 (s, 2H, H_i), 7.01-6.94 (m, 4H, $H_{2/2'}$), 6.80-6.72 (m, 8H, $H_{6/6'}$), 6.52 (d, 8H, J = 8.0 Hz, $H_{e/e'}$), 6.42-6.32 (m, 8H, $H_{d/d'}$), 6.28-6.20 (m, 8H, $H_{7/7'}$), 4.53 (t, 4H, J = 6.4 Hz, $H_{h'}$), 3.95 (t, 4H, J = 6.0 Hz, H_f), 3.84 (t, 4H, J = 5.6 Hz, $H_{f'}$), 3.75-3.69 (m, 8H, $H_{8/8'}$), 3.67 (s, 8H, $H_{c/c'}$), 2.89 (t, 4H, J = 7.2 Hz, H_h), 2.74-2.66 (m, 8H, $H_{3/3'}$), 2.37-2.29 (m, 12H, $H_{g'/5/5'}$), 2.15-2.10 (m, 4H, H_g), 1.81-1.74 (m, 8H, $H_{9/9'}$), 1.68-1.46 (m, 32H, $H_{4/4'/10/10'/11/11'/12/12'}$).

^{13}C-NMR (125 MHz, $CDCl_3$, 298 K): δ = 171.04, 171.01, 163.89 (2x), 157.50, 157.15, 152.19, 152.15, 139.75, 139.70, 139.08 (2x), 134.38, 133.95, 132.08, 132.04, 129.92 (2x), 129.16, 129.13, 124.32, 124.28, 122.29, 122.20, 121.44, 114.13, 114.02, 113.49 (2x), 67.37 (2x), 66.88, 64.01, 49.28, 49.20, 46.77, 38.55, 38.53, 34.70, 34.63, 30.38 (2x), 30.26 (2x), 29.85 (2x), 29.14 (2x), 29.00 (2x), 28.79 (2x), 25.96 (2x), 22.15. (56 signals expected; 55 signals observed. Significant overlap due to pseudo C_{2h} symmetry.)

chain lock (27)

A dry Schlenk tube was charged with **22** (62 mg, 40 μmol), **23** (57 mg, 40 μmol) and MeOH/CH_2Cl_2 (1:1, 40 mL) under an atmosphere of nitrogen. A solution of TBTA (4.25 mg, 8 μmol) and $[Cu(MeCN)_4]PF_6$ (2.95 mg, 8μmol)

in $MeOH/CH_2Cl_2$ (1:1, 1 mL) which was prepared under inertgas atmosphere, was added. Then a degassed solution of 0.1 M KF in MeOH (900 μL) was added and the resulting solution was stirred for 3 d. The reaction mixture was diluted with CH_2Cl_2 and washed with 1M Na_4EDTA solution and water, dried over Na_2SO_4. After removal of the volatiles, the crude mixture was purified by column chromatography ($MeOH/CH_2Cl_2$ (5:95)). Further purification by size exclusion chromatography over BioBeads S-X1 with CH_2Cl_2 eluent afforded the desired product after evaporation of the volatiles as yellow varnish (26.3 mg, 23%).

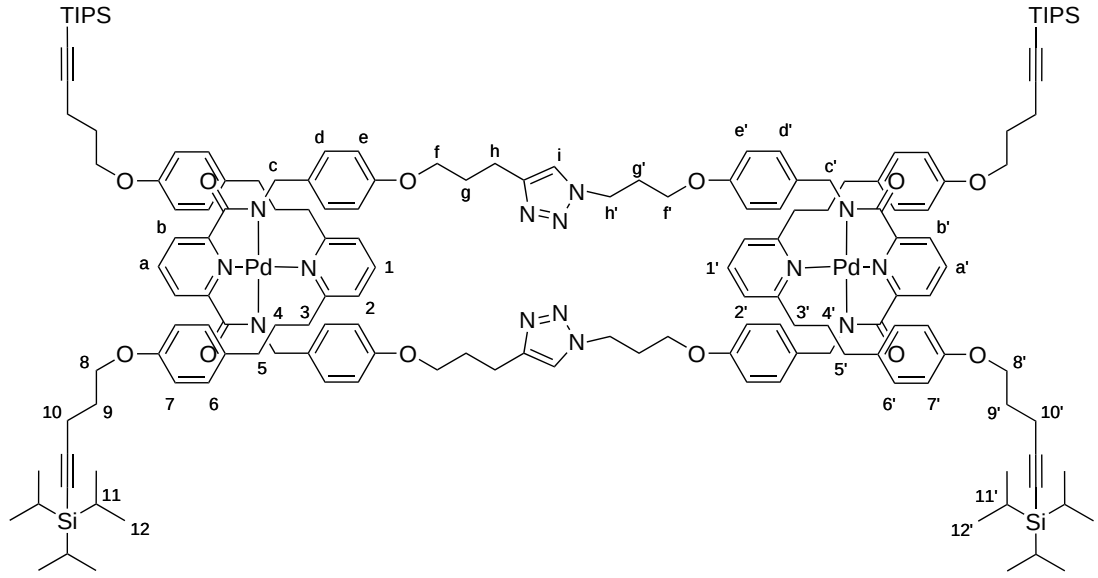

^{1}H-NMR (400 MHz, $CDCl_3$, 300 K): δ = 8.16–8.09 (m, 2H, Ha/a'), 7.88–7.83 (m, 4H, Hb/b'), 7.70 (t, 2H, J = 7.8 Hz, H1/1'), 7.02–6.95 (m, 14H, H2/2'/6/6'/i), 6.86–6.63 (m, 8H, H7/7'), 6.54–6.45 (m, 16H, Hd/d'/e/e'), 4.27 (t, 4H, J = 6.8 Hz, Hh'), 4.00–3.87 (m, 16H, Hc/c'/8/8'), 3.83 (t, 4H, J = 6.2 Hz, Hf), 3.72 (t, 4H, J = 5.7 Hz, Hf'), 2.97–2.87 (m, 8H, H3/3'), 2.74 (t, 4H, J = 7.6Hz, Hh), 2.46–2.33 (m, 16H, H5/5'/10/10'), 2.21–2.13 (m, 4H, Hg'), 2.08–1.91 (m, 12H, Hg/9/9'), 1.66–1.55 (m, 8H, H4/4'), 1.08–0.95 (m, 84H, H11/11'/12/12').

^{13}C-NMR (100 MHz, $CDCl_3$, 300 K): δ = 171.14, 163.47, 163.38, 157.47, 157.11, 157.07, 157.04, 152.55, 152.52, 147.08, 140.23, 140.21, 139.04, 138.96, 133.86, 133.43, 133.33, 133.22, 129.28, 129.23, 128.69, 128.63, 124.64, 124.62, 121.20, 121.17, 120.99, 114.20, 114.16, 113.82, 113.80, 107.83, 107.82, 80.96, 80.92, 66.86, 66.28, 66.25, 64.08, 49.16, 49.05, 46.72, 38.53, 34.78, 34.73, 29.96, 29.85, 29.67,

28.93, 28.72, 28.70, 22.06, 18.61, 16.69, 16.67, 11.20.

LRESI-MS: m/z = 1424 $[M + 2H]^{2+}$.

References

[1] D. B. Amabilino, P. R. Ashton, A. S. Reder, N. Spencer, J. F. Stoddart, *Angew. Chem., Int. Ed. Engl.* **1994**, *33*, 1286–1290.

[2] D. B. Amabilino, P. R. Ashton, A. S. Reder, N. Spencer, J. F. Stoddart, *Angew. Chem., Int. Ed. Engl.* **1994**, *33*, 433–437.

[3] S.-G. Roh, K.-M. Park, G.-J. Park, S. Sakamoto, K. Yamaguchi, K. Kim, *Angew. Chem., Int. Ed.* **1999**, *38*, 638–641.

[4] D. M. Whang, K.-M. Park, J. Heo, P. Ashton, K. Kim, *J. Am. Chem. Soc.* **1998**, *120*, 4899–4900.

[5] S.-H. Chiu, S. J. Rowan, S. J. Cantrill, L. Ridvan, P. R. Ashton, R. L. Garrell, J. F. Stoddart, *Tetrahedron* **2002**, *58*, 807–814.

[6] C. O. Dietrich-Buchecker, A. Khemiss, J.-P. Sauvage, *J. Chem. Soc., Chem. Commun.* **1986**, 1376–1378.

[7] J. M. Kern, J. P. Sauvage, J. L. Weidmann, *Tetrahedron* **1996**, *52*, 10921–10934.

[8] D. B. Amabilino, P. R. Ashton, V. Balzani, S. E. Boyd, A. Credi, J. Y. Lee, S. Menzer, J. F. Stoddart, M. Venturi, D. J. Williams, *J. Am. Chem. Soc.* **1998**, *120*, 4295–4307.

[9] N. R. El-Brollosy, P. T. Jörgensen, B. Dahan, A. M. Boel, E. B. Pedersen, C. Nielsen, *J. Med. Chem.* **2002**, *45*, 5721–5726.

[10] V. Aucagne, J. Berná, J. D. Crowley, S. M. Goldup, K. D. Hänni, D. A. Leigh, P. J. Lusby, V. E. Ronaldson, A. M. Z. Slawin, A. Viterisi, D. B. Walker, *J. Am. Chem. Soc.* **2007**, *129*, 11950–11963.